Universitá Degli Studi Di Napoli
"Federico II"

Scuola Politecnica e delle Scienze di Base
Area Didattica di Scienze Matematiche Fisiche e Naturali
Corso di Dottorato in Matematica e Applicazioni

Ciclo XXXV

PH.D Thesis by

Giuliana Massa

Recent Hydrodynamic Stability Results for Single and Double Porosity Materials

Contents

Acknowledgement

First of all, I would like to express my sincere gratitude to my supervisor and *mentor* Professor Florinda Capone, for being a thoughtful guide during my PhD study. Through her teaching and guidance, she conveyed me her passion for the world of research and our mathematical discussions have been crucial and fundamental for my scientific and personal growth. She always believed in my abilities and for that I will be forever thankful.
I would like to thank Professor Roberta De Luca, she has been a constant presence since my master thesis and her advice and support have been essential during these three years.
I would like to thank also Professor Vincenzo Sciacca and Professor Giuseppe Alì for reviewing this thesis.
I also thank all my *colleagues* with whom I shared this journey. My oldest colleagues, Jacopo and Giuseppe, are more than just colleagues, they became my dear friends and have been by my side in good and bad moments during these years. Thank to Fabiana, Grazia and Chiara, with whom I shared happy and anxious moments. I have to acknowledge Alba and Ludovica. Our daily "journeys" gave me the opportunity to get to know two wonderful women and I feel lucky to be able to call them my friends.
I am and will always be grateful to my family: my parents Dino and Maria, my brother Michele and my friend Marta. They have been a constant support during all of my life. I would like to particularly address my parents, they are my rock, they made me the person I am today and advise me with love and care every day, I wouldn't be here if it wasn't for them.
I thank my fiance Paco. Through his infinite love, he daily support me in everything I do and he was actually the first person to encourage me to start the PhD. I truly love him with every single cell of my body.

Introduction

This doctoral thesis deals with recent stability results for the onset of thermal *convection in single and double porosity materials*, obtained through linear and nonlinear stability analyses of the basic steady solution.
The onset of thermal convection for clear fluids and fluids saturating a porous medium is a well known problem and it has been widely analysed by many researchers, in the past as nowadays. When a horizontal layer of fluid (eventually saturating a porous material) is heated from below, a thermal boundary layer of less dense and hot fluid develops and grows with time. At a certain point, this boundary layer becomes unstable and breaks up, leading convective motions in the fluid above.
The model describing *fluid motions in porous media* is a reaction-diffusion dynamical system of P.D.Es and it is well suited for many applications in different fields, such as geophysics (geothermal reservoirs, geological storage of carbon dioxide), astrophysics (for example pore water convection within carbonaceous chondrite parent bodies), engineering and industrial processes (water treatment process, nuclear waste disposal, chemical reactor engineering, and the storage of heat-generating materials such as grain and coal) (see [1] and reference therein). These applications constitute a driving force for researchers to develop mathematical models in this area.
However, due to the growing need for *man-made materials* — e.g. ceramics, high porosity metallic foams — for heat transfer problems, since the 90s bi-disperse porous media have attracted the interest of many researchers, in particular chemical engineers, physicists and mathematicians. Bi-disperse porous media are *dual porosity materials* with a large number of practical applications in industrial field (in order to design heat pipes and computer chips [2], to understanding landslides or for the treatment of nuclear waste), in geophysics (the stockpiled pieces of coal stockpiled are small, but the coal itself contains small pores, moreover self-heating is a characteristic of these piles, hence the analysis and the understanding of heat transfer in this kind of materials is essential to avoid self-combustion [3]), biological and medical field (for instance engineered tissues for tissue regeneration, while brain,

bones, tumors are natural examples of dual porosity materials). Moreover, it was demonstrated by Nield and Kuznetsov in [4] that convection occurs at *higher* Rayleigh numbers in a dual porosity material with respect to an equivalent single porosity medium, so the heat transfer due to the convective fluid motion is delayed, for this reason dual porosity materials are better suited for insulation problems and thermal management problems (such as cooling of data centers).

In the modelling process for the derivation of the governing equations describing a *physical phenomenon* there is always room for improvement. With the aim of *improving* the mathematical model describing bi-disperse convection to obtain even more realistic mathematical models useful for designing man-made materials and engineered systems, great attention in this thesis is devoted to anisotropic bi-disperse porous materials — for which macro-permeability and micro-permeability are symmetric second-order tensors — since anisotropy is a powerful tool to optimise heat transfer.
In particular, most of this thesis is dedicated to the analysis of the onset of convection in rotating horizontal layers of bi-disperse porous media heated from below. A driving force behind the analysis of fluid flows in rotating porous materials is constituted by the applications of this kind of problems, such as physiological processes in human body subject to rotating trajectories, geophysical problems, cooling of electronic equipment in rotating radars and rotors, biomechanics, solidification and centrifugal casting of metals. Keeping in mind these applications, the interactions between anisotropy, inertial effects, high porosities and Coriolis effects are analysed, in order to determine how these physical aspects affect the onset of convection and the type of arising convective cells.
Later on, bi-disperse double-diffusive convection (which involves two diffusing components — heat and mass — interacting with each other and is relevant for chemical processes and engineering applications, e.g. nuclear waste disposal) is studied: the model describing the onset of convection in a horizontal layer of bi-disperse porous medium saturated by a binary fluid mixture is investigated, taking into account the Coriolis effect and, alternatively, anisotropy and Soret effects.

The final Chapters of this thesis are devoted to the description of new stability results related to porous convection problems.
In particular, the thermodynamic consistency of the Oberbeck-Boussinesq approximation is deeply discussed and, to the best of our knowledge, the Darcy-Bénard problem for an extended-quasi-thermal-incompressible fluid is studied for the first time. A more realistic constitutive equation for the fluid density is employed — in the body force term due to gravity — in order to

obtain more thermodynamically consistent instability results.
Finally, we perform linear instability and weakly nonlinear stability analyses of the throughflow solution for a horizontal layer of fluid-saturated porous medium heated from below and subject to a downward vertical net mass flow: we refer to this physical set-up as the Sutton Problem. The goal is to study the effect of the throughflow on the onset of convective instabilities and to determine for which values of the strength of the throughflow a transition from supercritical to subcritical instability happens.

In the following, we will give a more precise description of the organization of this thesis.

Plan of the Thesis

The present thesis is divided into three parts and is organized as follows. The First Part (Chapters 1 and 2) is devoted to the introductory theories and the research context concerned with convection problems. The Second Part (Chapters 3 – 7) deals with new stability results obtained for convection in bi-disperse porous media. Finally, in the Third Part (Chapters 8 and 9), recent results related to convection problems in single porosity media are presented.

Since all the mathematical models described in this thesis have been subjected to linear instability and nonlinear stability analyses of their respective stationary basic solutions, **Chapter 1** describes the theoretical foundation of linear instability analysis and nonlinear stability analysis theory.

Chapter 2 is devoted to the description of the *research context* concerned with thermal convection in single and double porosity materials. *In primis*, the historical background of convection problems, in clear fluids and in fluid-saturated porous media, is described. *In secundis*, bi-disperse porous media are portrayed from a physical point view and the early refined mathematical models governing the evolutionary behaviour of the thermal conduction solution in bi-disperse porous media are described. In particular, most of this thesis concerns with the analysis of thermal convection in a rotating horizontal layer of a bi-disperse porous medium heated from below, so the theoretical significance and the practical applications of this kind of problems are outlined.

In **Chapter 3**, thermal convection in a *horizontally isotropic* bi-disperse porous medium uniformly heated from below is analysed. The combined effects of uniform vertical rotation and Brinkman law on the stability of the steady state in a BDPM are investigated. Linear and nonlinear stability analysis of the conduction solution is performed, and the coincidence between linear instability and nonlinear stability thresholds in the L^2-norm is obtained.

Chapter 4 addresses the onset of thermal convection in a uniformly rotating and horizontally isotropic bi-disperse porous medium, taking into account *inertia effects*, hence considering the Vadasz term. Via linear instability analysis of the conduction solution, it is proved that the Vadasz term allows the onset of convection via an oscillatory state but does not directly affect convection via a stationary motion.

In **Chapter 5**, the onset of thermal convection in *fully anisotropic* rotating bidisperse porous media is investigated. The *optimal result* concerning the coincidence between linear and nonlinear thresholds — with respect the energy norm — is obtained.

Chapter 6 is devoted to the analysis of the onset of convection in a rotating layer of bi-disperse porous medium saturated by a *binary fluid mixture*. Unlike the diffusion of heat, the diffusion of salt can take place only through the fluid phase, so an additional physical effect has to be considered: the *Soret effect*, that is the mass flux created by a temperature gradient. Linear stability analysis of the conduction solution is performed in order to determine the instability thresholds for the onset of convection via a steady state (stationary convection) and via an oscillatory state (oscillatory convection). Nonlinear stability analysis is performed to obtain the global stability threshold with respect to the L^2-norm.

With the aim to *improve* the results found in Chapter 3 and to further analyse the onset of bi-disperse double-diffusive convection, in **Chapter 7** a rotating horizontal layer heated from below of anisotropic Brinkman bi-disperse porous medium filled by an incompressible fluid binary mixture is considered. Via linear instability analysis of the basic solution, we found that convection can set in through stationary or oscillatory motions and the critical Rayleigh numbers for the onset of *stationary secondary flow* (steady convection) and *overstability* (oscillatory convection) are determined.

In **Chapter 8** the *thermodynamic consistency* of the Oberbeck-Boussinesq approximation is discussed in detail and, to the best of our knowledge, the Darcy-Bénard problem for an *extended-quasi-thermal-incompressible fluid* is studied for the first time. Therefore, the linear analysis of the Darcy-Bénard problem is performed in the class of extended-quasi-thermal-incompressible fluids, introducing a factor β which describes the compressibility of the fluid and plays an essential role in the instability results. In particular, in the Oberbeck-Boussinesq approximation, a more realistic constitutive equation for the fluid density is employed in order to obtain more thermodynamic consistent instability results. Via linear instability analysis of the conduction solution, the critical Rayleigh-Darcy number for the onset of convection is determined as a function of a dimensionless parameter $\widehat{\beta}$ proportional to the compressibility factor β, proving that $\widehat{\beta}$ enhances the onset of convective motions.

The aim of **Chapter 9** is to analyse the effect of a *downward vertical net mass flow* on the type of instability occurring in a horizontal porous layer saturated by a fluid heated from below. The validity of the principle of exchange of stabilities is proved, hence the linear instability analysis of the basic steady flow is performed to determine the critical Rayleigh number for the onset of steady convective instabilities. A weakly nonlinear stability analysis is performed to determine disturbances that lead to subcritical instability. A user-written code based on the shooting method — that takes advantage of the Newton-Raphson scheme and of the fourth-order Runge-Kutta method — is employed to solve the boundary value problems we face in both the analyses.

Nomenclature

c	specific heat
d	depth of the layer
T_L	lower temperature
T_U	upper temperature
C_L	lower salt concentration
C_U	upper salt concentration
μ	dynamic fluid viscosity
$\tilde{\mu}$	effective viscosity
ν	kinematic fluid viscosity
ϱ_F	fluid density
α	thermal expansion coefficient
α_C	chemical expansion coefficient
ζ	interaction coefficient
h	thermal interaction coefficient
$\mathbf{v}$	seepage velocity (u, v, w)
C	concentration
P	pressure
$\mathbf{G}$	opposite pressure gradient
T	temperature
t	time
K	permeability
k	thermal conductivity
$\mathbf{i}, \mathbf{j}, \mathbf{k}$	unit vectors
φ	macropores porosity
ϵ	micropores porosity
S_T	Soret coefficient
β	compressibility factor

Nomenclature

$\mathbf{u}$	perturbation velocity
θ	perturbation temperature
π	perturbation pressure
γ	perturbation concentration
ψ	stream function
ϵ_1	fraction of volume occupied by the fluid
a	wavenumber
Ra	Rayleigh number
$\mathcal{C}$	concentration Rayleigh number
$\mathcal{S}$	Soret number
$\mathcal{T}$	Taylor number
Da	Darcy number
J	Vadasz number
Le	Lewis number
Pe	Péclet number
$\mathcal{H}$	space of kinematically admissible solutions

Subscripts

f	macropores related
p	micropores related
F	fluid related
sol	solid matrix related
m	porous medium related
C	concentration related

Part I

Chapter 1

Preliminaries on Stability Theory

In convection problems, the instability threshold, above which convective flows arise, is related to the critical value of the Rayleigh number, the dimensionless control parameter of the system. Therefore, the critical Rayleigh number is determined in order to *predict* the onset of convective fluid motions. In general, the prediction of the evolution in time of a physical phenomenon is crucial for real world applications and is achieved through a qualitative analysis of the mathematical model describing the evolutionary behaviour of the phenomenon, when the explicit solution of the model cannot be determined [5].
Since the critical Rayleigh number for the onset of convection is found through the stability analysis of the thermal basic solution, this Chapter is devoted to the description of the fundamental theory regarding linear instability analysis and nonlinear stability analysis of the basic solution a dynamical system.

1.1 Dynamical Systems and Stability Definitions

Let $\mathcal{F}$ be a phenomenon taking place on a domain $\Omega \subset \mathbb{R}^3$ and let $u_i(\mathbf{x}, t)$, with $i = 1, \dots, n$ $(n < \infty)$, $(\mathbf{x}, t) \in \Omega \times (0, T)$, be the relevant quantities describing the *state* of $\mathcal{F}$. The vector $\mathbf{u}$ with components u_i is the *state vector*.
If it is possible to determine - usually experimentally - a function

$$\mathbf{F}(\mathbf{x}, t, \mathbf{u}, \frac{\partial u_i}{\partial x_r}, \frac{\partial^2 u_j}{\partial x_r \partial x_s}, \dots) \qquad i, j = 1, \dots, n;\ r, s = 1, 2, 3$$

which describes the evolutionary behaviour in time of $\mathbf{u}$, then the phenomenon $\mathcal{F}$ is modelled by a P.D.E.

$$\frac{\partial \mathbf{u}}{\partial t} = \mathbf{F} \qquad \text{in } \Omega \times (0, T) \tag{1.1}$$

whose initial and boundary conditions are

$$\begin{aligned} \mathbf{u}(\mathbf{x}, 0) &= \mathbf{u}_0(\mathbf{x}) \qquad \mathbf{x} \in \Omega \\ A(\mathbf{u}, \nabla \mathbf{u}) &= \hat{\mathbf{u}} \qquad \text{on } \partial\Omega \times [0, T] \end{aligned} \tag{1.2}$$

respectively, where A is an assigned operator and $\hat{\mathbf{u}}(\mathbf{x}, t)$ is prescribed.
The problem (1.1)-(1.2) is called initial-boundary value problem (i.b.v.p) and is the **evolution equation** of $\mathcal{F}$. The space of functions X defined on Ω satisfying the prescribed boundary conditions is called the *state space* of the evolution equation. According to a classical definition of Hadamard, the problem (1.1)-(1.2) is *well-posed* in X if (see [5, 6])

- there globally exists a solution,
- the solution is unique,
- the solution continuously depends on the data.

Let (X, d) and $S(\mathbf{x}, r)$ be a metric space and the open ball with radius r centered in $\mathbf{x}$, respectively. Let us introduce the following definitions.

Definition 1.1.1. *A dynamical system on the metric space (X, d) is a mapping*

$$\mathbf{v} : (\mathbf{v}_0, t) \in X \times \mathbb{R}^+ \to \mathbf{v}(\mathbf{v}_0, t) \in X$$

such that $\mathbf{v}(\mathbf{v}_0, 0) = \mathbf{v}_0$

A solution $\mathbf{u}(\mathbf{u}_0, t)$ with $\mathbf{u}(\mathbf{u}_0, 0) = \mathbf{u}_0$ to the problem (1.1)-(1.2) is a dynamical system.

Definition 1.1.2. *A motion of initial data $\mathbf{v}_0$ is a dynamical system $\mathbf{v}$ defined as:*

$$\mathbf{v}(\mathbf{v}_0, \cdot) : t \in \mathbb{R}^+ \to \mathbf{v}(\mathbf{v}_0, t) \in X,$$

such that $\mathbf{v}(\mathbf{v}_0, 0) = \mathbf{v}_0$.

Definition 1.1.3. *If $\mathbf{v}(\mathbf{v}_0, t) = \mathbf{v}_0$ $\forall t \in \mathbb{R}^+$, the motion $\mathbf{v}(\mathbf{v}_0, \cdot)$ is stationary and $\mathbf{v}_0$ is an equilibrium point.*

Definition 1.1.4. *A motion* $\mathbf{v}(\mathbf{v}_0, \cdot)$ *depends continuously on the initial data if and only if*

$$\forall T, \epsilon > 0,\ \exists \delta(\epsilon, T) > 0 \,:\, d(\mathbf{v}_1, \mathbf{v}_0) < \delta \implies d(\mathbf{v}(\mathbf{v}_1, t), \mathbf{v}(\mathbf{v}_0, t)) < \epsilon,\ \forall t \in [0, T],$$

or equivalently if

$$\forall T, \epsilon > 0,\ \exists \delta(\epsilon, T) > 0 \,:\, \mathbf{v}_1 \in S(\mathbf{v}_0, \delta) \implies \mathbf{v}(\mathbf{v}_1, t) \in S(\mathbf{v}(\mathbf{v}_0, t), \epsilon),\ \forall t \in [0, T].$$

Definition 1.1.5. *A motion* $\mathbf{v}(\mathbf{v}_0, \cdot)$ *is Lyapunov stable (with respect to perturbations of the initial data) if and only if*

$$\forall \epsilon > 0,\ \exists \delta(\epsilon) > 0 \,:\, d(\mathbf{v}_1, \mathbf{v}_0) < \delta \implies d(\mathbf{v}(\mathbf{v}_1, t), \mathbf{v}(\mathbf{v}_0, t)) < \epsilon,\ \forall t > 0,$$

or equivalently if

$$\forall \epsilon > 0,\ \exists \delta(\epsilon) > 0 \,:\, \mathbf{v}_1 \in S(\mathbf{v}_0, \delta) \implies \mathbf{v}(\mathbf{v}_1, t) \in S(\mathbf{v}(\mathbf{v}_0, t), \epsilon),\ \forall t > 0.$$

If the dynamical system $\mathbf{v}$ is linear (i.e. $\mathbf{v}$ is a linear operator of X on X, $\forall t \in \mathbb{R}^+$), the stability of every motion is determined by the stability of the basic solution.
Introducing a generic *perturbation* at time t to the assigned basic motion $\mathbf{v}(\mathbf{v}_0, \cdot)$:

$$\mathbf{u}(\mathbf{u}_0, t) = \mathbf{v}(\mathbf{v}_1, t) - \mathbf{v}(\mathbf{v}_0, t),$$

the stability analysis of the basic motion is equivalent to the stability analysis of the null solution of the associated perturbed system. Therefore, $\|\cdot\|$ being the norm associated to the metric d, one obtains the following definition.

Definition 1.1.6. *A motion* $\mathbf{v}(\mathbf{v}_0, \cdot)$ *is stable with respect to perturbations of the initial data if and only if*

$$\forall \epsilon > 0,\ \exists \delta(\epsilon) > 0 \,:\, \|\mathbf{u}_0\| < \delta \implies \|\mathbf{u}(\mathbf{u}_0, t)\| < \epsilon,\ \forall t > 0,$$

or equivalently if

$$\forall \epsilon > 0,\ \exists \delta(\epsilon) > 0 \,:\, \mathbf{u}_0 \in S(0, \delta) \implies \mathbf{u}(\mathbf{u}_0, t) \in S(0, \epsilon),\ \forall t > 0.$$

1.2 Lyapunov direct method

In the following Section, let us outline the *direct method* to study the stability for an equilibrium point of a dynamical system.

Definition 1.2.1. *A function $V : X \to \mathbb{R}$ is a Lyapunov function on a subset $I \subset X$ if V is continuous on I and non-increasing with respect to time t along the solutions of a dynamical system $\mathbf{v}$ with initial data in I.*

Let $\mathcal{F}_r$ $(r > 0)$ be the set of functions $\varphi : [0, r) \to [0, \infty)$ continuous, strictly increasing and such that $\varphi(0) = 0$.

Definition 1.2.2. *Let $\mathbf{u}$ be a dynamical system on X and let $\boldsymbol{O}$ be an equilibrium point. If there exists for some $r > 0$ a Lyapunov function V on $S(\boldsymbol{O}, r)$ such that*

- $V(\boldsymbol{O}) = 0$,
- $\exists f \in \mathcal{F}_r$ *such that* $V(\mathbf{u}) \geq f(\|\mathbf{u}\|)$, *for* $\mathbf{u} \in S(\boldsymbol{O}, r)$,

then $\boldsymbol{O}$ is stable. Moreover, if

- $\exists g \in \mathcal{F}_r$ *such that* $\dot{V}(\mathbf{u}) \leq -g(\|\mathbf{u}\|)$, $\forall \mathbf{u} \in S(\boldsymbol{O}, r)$,

then $\boldsymbol{O}$ is asymptotically stable.

If the Lyapunov function V is positive definite $(V(\mathbf{O}) = 0, V(\mathbf{u}) > 0$ for $\mathbf{u} \neq \mathbf{0})$ and there exists a positive constant c such that, along the solutions of the system,

$$\dot{V} \leq -cV$$

i.e.

$$V \leq V(\mathbf{u}_0)e^{-ct}$$

then the equilibrium point is *asymptotically exponentially stable* with respect to the measure V.

Since the above definitions are given with respect to an assigned metric d, the stability of a dynamic system is strictly dependent on the choice of the *adopted norm* [5].

Remark 1.2.1. *On a linear finite dimensional space X (like $\mathbb{R}^n$) all norms are equivalent. Hence, the stability of the basic solution does not depend on the chosen norm. A phenomenon with an infinite number of degrees of freedom is modelled by a P.D.E. defined in a normed linear infinite dimensional space (where all possible norms are not equivalent). Therefore, in this case the stability is topologically dependent.*

In the following Section, we will investigate how a *proper choice* of the norm connects the linear and nonlinear stability analyses of the basic steady solution of a dynamical system [7, 8].

1.3 Linear and Nonlinear Stability

Let $\mathcal{H}$ be a Hilbert space and let us consider in $\mathcal{H}$ a initial value problem

$$\begin{cases} \mathbf{u}_t + L\mathbf{u} + N(\mathbf{u}) = 0 \\ \mathbf{u}(\mathbf{x}, 0) = \mathbf{u}_0(\mathbf{x}) \end{cases} \tag{1.3}$$

where L is a linear operator (possibly unbounded), while N is a nonlinear operator such that $N(\mathbf{0}) = 0$, hence (1.3) admits the null solution.
Let us assume that

1. L is an operator with compact resolvent, i.e. L is densely defined and closed, such that $(L - \lambda I)^{-1}$ is compact for some $\lambda \in \mathbb{C}$;

2. the bilinear form associated with L is defined on a space $\mathcal{H}'$ compactly embedded in $\mathcal{H}$;

3. the nonlinear operator N verifies the condition
$$(N(\mathbf{u}), \mathbf{u}) \geq 0, \quad \forall \mathbf{u} \in D(N).$$

Theorem 1.3.1. *Let L be a operator satisfying the assumption 1. Then the spectrum of L is composed of at most a denumerable number of eigenvalues* $\{\sigma_n\}_{n\in\mathbb{N}}$ *with finite multiplicities (both algebraic and geometric) and they cluster at infinity. Moreover, the eigenvalues of L are such that*

$$Re(\sigma_1) \leq Re(\sigma_2) \leq \cdots \leq Re(\sigma_n) \leq \ldots$$

Definition 1.3.1. *The null solution of system* (1.3) *is linearly stable if and only if*
$$Re(\sigma_1) > 0.$$

Definition 1.3.2. *The null solution of system* (1.3) *is nonlinearly stable is and only if* $\forall \epsilon > 0 \; \exists \delta = \delta_\epsilon$ *such that*

$$\|\boldsymbol{u}_0\| < \delta \implies \|\boldsymbol{u}\| < \epsilon$$

and $\exists \gamma$*, with* $0 < \gamma \leq \infty$*, such that*

$$\|\boldsymbol{u}_0\| < \gamma \implies \lim_{t\to\infty} \|\boldsymbol{u}(\boldsymbol{x}, t)\| = 0.$$

In particular, if $\gamma = \infty$*, the null solution is unconditionally nonlinearly stable.*

In general, L is not a symmetric operator, hence it can be decomposed as $L = L_1 + L_2$, with L_1 e L_2 such that

- $D(L_2) \supset D(L_1) = D(L)$;
- L_1 is symmetric with compact resolvent;
- L_2 is skew-symmetric and bounded in $\mathcal{H}'$.

L_1 satisfies theorem 1.3.1, hence its eigenvalues $\{\lambda_n\}_{n\in\mathbb{N}}$ are such that

$$\lambda_1 \leq \lambda_2 \leq \cdots \leq \lambda_n \leq \ldots$$

Let $L_1[\Phi,\Phi]$, $\Phi \in \mathcal{H}'$, be the bilinear form associated with L_1:

$$(L_1\Phi, \Phi) = L_1[\Phi, \Phi], \quad \forall \Phi \in D(L_1).$$

Under the above conditions, the following theorems hold, see [7].

Theorem 1.3.2. *Let $\overline{\Phi}$ be a normalized eigenfunction associated with the eigenvalue λ_1, then*

$$\lambda_1 = L_1[\overline{\Phi}, \overline{\Phi}] = \min_{\Phi\in\mathcal{H}'} \frac{L_1[\Phi, \Phi]}{\|\Phi\|^2}.$$

Theorem 1.3.3. *Assuming*

$$\lambda_1 > 0,$$

the null solution (1.3) *is nonlinearly stable.*

We can conclude that the linear instability analysis deals with studying the eigenvalue problem associated to L. The nonlinear stability analysis is reduced to studying the eigenvalue problem associated to the symmetric part L_1 of L. When $L_2 = 0$, i.e. the linear operator L - with compact resolvent - is symmetric, the linear instability analysis a priori implies the nonlinear stability of the basic solution, i.e. the linear analysis furnishes a *necessary and sufficient* condition for the onset of instability.

1.4 Principle of Exchange of Stabilities

A steady fluid flow (or a solution to a partial differential equation) is asymptotically stable or unstable according as whether small superposed disturbances decay to zero or grow with time. The **principle of exchange of stabilities** is said to hold if all non-decaying disturbances are non-oscillatory in time [9].

According to what is explained in the previous Section, let us consider the linearised version of (1.3), i.e. $\mathbf{u}_t + L\mathbf{u} = 0$. If L is autonomous, it is possible to look for solution $\mathbf{u}(\mathbf{x}, t) = e^{-\sigma t}\hat{\mathbf{u}}(\mathbf{x})$, so $\sigma \in \mathbb{C}$ is the growth rate of the system. Using this kind of solution, it follows $-\sigma e^{-\sigma t}\hat{\mathbf{u}}(\mathbf{x}) + e^{-\sigma t}L\hat{\mathbf{u}}(\mathbf{x}) = 0$, i.e. $(L - \sigma I)^{-1}\hat{\mathbf{u}}(\mathbf{x}) = 0$. Solution $\mathbf{u}$ is stable - decays exponentially to zero - if $Re(\sigma) > 0$.
Depending on the nature of the growth rate σ, the thermal convection can arise via steady motions (steady convection) or oscillatory motions (oscillatory convection). States of marginal stability - which separates the stable state and the unstable one - are *stationary* if characterized by $\sigma = 0$, i.e. $Re(\sigma) = Im(\sigma) = 0$, *oscillatory* if are characterized by $Re(\sigma) = 0$ i.e. $\sigma = i\ Im(\sigma)$. In the first case, the amplitude of a generic perturbation grow (or is damped) aperiodically, so the transition from stability to instability takes place via a marginal state via a stationary pattern of motions. When the growth rate is purely imaginary, the perturbations are characterized by oscillations of increasing (or decreasing) amplitude, this means that the instability occurs through oscillatory motions with frequency $Im(\sigma)$.
According to [10], the **strong form** of the principle of exchange of stabilities holds if $\sigma \in \mathbb{R}$. In this case, the marginal states are characterized by $\sigma = 0$ and convection cannot occur through oscillatory motions. The **weak form** of the principle of exchange of stabilities holds when from $Im(\sigma) \neq 0$ it follows $Re(\sigma) < 0$.

Chapter 2

Convection in Porous Media

2.1 Historical Background of Convection Problems in Clear Fluids and Porous Media

The first attempt to experimentally analyse the onset of thermal convection in a horizontal layer of viscous incompressible clear fluid heated from below is attributable in 1900 to the physicist Henry Bénard, in the paper [11]. Since the horizontal layer is uniformly heated from below, the fluid at bottom of the layer is lighter then the fluid at the top, due to thermal expansion, hence the temperature gradient maintained across the fluid layer is qualified as adverse. The physical situation just described is of potential instability, since the temperature and density gradients in the horizontal layer lead to an unstable arrangement, and the resulting physical-mathematical problem is known in literature as Bénard Problem. Because of the instability, the fluid will rearrange itself in order to tend to the equilibrium, but this rearrangement is delayed by the fluid viscosity, therefore the adverse temperature gradient has to reach a critical value for instability to arise. Moreover, in his experiments, Bénard observed that, once instability occurs, the fluid organizes itself into a regular pattern of cells, called convection cells or periodicity cells (see Figure 2.1).
The first refined mathematical analysis describing the Bénard Problem was proposed in 1916 by the physicist John William Strutt (Lord Rayleigh), in the paper [12]. Considering a horizontal layer of thickness d of incompressible fluid in a reference frame $Oxyz$ with unit vectors $\{\mathbf{i}, \mathbf{j}, \mathbf{k}\}$, Lord Rayleigh performed the stability analysis of the thermal conduction solution (stationary

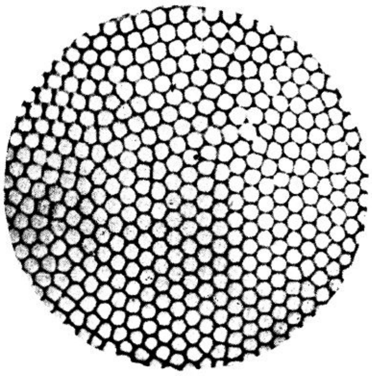

Figure 2.1: Bénard cells: a reproduction of one of Bénard's original photographs [10].

motionless solution) to the following problem

$$\begin{cases} \dfrac{\partial \mathbf{v}}{\partial t} + \mathbf{v} \cdot \nabla \mathbf{v} = -\frac{1}{\varrho_0} \nabla p - [1 - \alpha(T - T_0)] g\mathbf{k} + \nu \Delta \mathbf{v}, \\ \nabla \cdot \mathbf{v} = 0, \\ \dfrac{\partial T}{\partial t} + \mathbf{v} \cdot \nabla T = \kappa \Delta T, \end{cases} \tag{2.1}$$

under the following boundary conditions

$$\begin{aligned} \mathbf{v} \cdot \mathbf{n} = 0 &\quad \text{on } z = 0, d \\ T = T_L &\quad \text{on } z = 0 \\ T = T_U &\quad \text{on } z = d \end{aligned} \tag{2.2}$$

and

$$\begin{aligned} u = v = 0 &\quad \text{on } z = 0, d \quad \text{for rigid planes} \\ \frac{\partial u}{\partial z} = \frac{\partial v}{\partial z} = 0 &\quad \text{on } z = 0, d \quad \text{for stress-free planes} \end{aligned} \tag{2.3}$$

where $T_L > T_U$ (since the layer is uniformly heated from below) and $\mathbf{v} = (u, v, w), T, p$ are the kinematic, temperature and pressure fields, respectively, $\kappa = k/\varrho_0 c_p$ is the thermal conductivity coefficient, with ϱ_0 the fluid density at the reference temperature T_0, c_p specific heat and k the coefficient of heat conduction, $\nu = \mu/\varrho_0$ is the kinematic viscosity, with μ the fluid dynamic viscosity, α denotes the thermal expansion coefficient and $\mathbf{g} = -g\mathbf{k}$ is the gravity ($\mathbf{k}$ being the unit vector in the vertical direction). To write the governing equations (2.1), a *Oberbeck-Boussinesq approximation* has been employed, acceptable in reference to buoyancy driven flows: the density is assumed to

be constant except in the bouyancy force[1], where it has a linear dependence on the temperature field (and eventually on the concentration field, when a salt dissolved in the fluid is considered).
Lord Rayleigh established that *the instability threshold, above which the convective fluid motion sets in*, is related to a dimensionless control parameter, **the Rayleigh number**:

$$\mathrm{Ra} = \frac{g\alpha\beta d^4}{\kappa\nu}$$

where β is the adverse temperature gradient. He found that the thermal convection arises when Ra overcomes a certain threshold Ra_c. From a mathematical point of view, the critical value Ra_c is determined via the instability analysis of the thermal conduction solution.
Concerning the linear instability, requiring that all the eigenvalues of the linear operator have negative real part, one can find a threshold Ra_L such that the condition $\mathrm{Ra} > \mathrm{Ra}_L$ implies instability of the thermal conduction solution and, consequently, the onset of thermal convection. The nonlinear stability is topologically dependent. Introducing a suitable norm and choosing properly a Lyapunov functional, one needs to determine the conditions for which this functional is decreasing along the solutions of the nonlinear system, these conditions give rise to the nonlinear threshold $\mathrm{Ra}_N(\leq \mathrm{Ra}_L)$ such that the condition $\mathrm{Ra} < \mathrm{Ra}_N$ implies stability, i.e. if $\mathrm{Ra} < \mathrm{Ra}_N$ convection cannot occur. In order to have useful results for the applications, the challenge is to find a norm for which $\mathrm{Ra}_N = \mathrm{Ra}_L$.
Furthermore, in many applications, the thermal convection can arise via steady *or* oscillatory motions and convection is named steady or oscillatory convection, respectively. As described in [10], states of marginal stability — which separates the stable state and the unstable one — can be stationary or oscillatory. If the amplitude of a generic perturbation grow (or is damped) aperiodically, the transition from stability to instability takes place via a marginal state via a stationary pattern of motions. If the perturbations are characterized by oscillations of increasing (or decreasing) amplitude, the instability occurs through oscillatory motions with a definite characteristic frequency. If instability arises via stationary motions, the instability sets in as stationary cellular convection or secondary flow. If oscillatory motions prevail, then one has overstability. As regards oscillatory convection, there are many hand-made materials for which it is convenient that convection occurs through an oscillatory state, since it may be useful that instability sets in via a motion periodic in time.

[1]see Chapter 8 for further details and discussions.

Due to the many applications for real world phenomena of **porous materials**, the problem of the onset of thermal convection was later studied for a viscous incompressible fluid saturating a horizontal layer of porous medium, by Horton and Rogers in [13] in 1945 and by Lapwood in the paper [14] in 1948, the resulting problem of the onset of convection in fluids saturating porous media is indeed known in literature as the Horton-Rogers-Lapwood Problem or, equivalently, as the Darcy-Bénard Problem.
As defined in [1], porous media are materials consisting of a solid matrix with an interconnected void through which a fluid can flow, and the solid matrix is either rigid or it undergoes small deformation. The fundamental physical properties describing the behaviour of this kind of materials are:

- *porosity*, i.e. the ratio of the void space to the total volume of the medium;
- *permeability*, which is a property of the matrix independent of the fluid flowing through it and measures the flow conductivity in the porous medium. The permeability is constant if the porous body is isotropic, otherwise if the solid skeleton of the porous body presents a strong anisotropy, the permeability is a second order tensor.

Fluid flows in porous media are efficiently described by the Darcy's law, which is an experimental law of proportionality between the flow rate and the pressure gradient:

$$\frac{\mu}{K}\mathbf{v} = -\nabla p.$$

According to the Darcy's model, the boundary value problem describing the evolutionary behaviour of the thermal conduction solution in a horizontal layer of fluid-saturated porous medium, is [1]

$$\begin{cases} \dfrac{\mu}{K}\mathbf{v} = -\nabla p - \varrho_0[1-\alpha(T-T_0)]g\mathbf{k}, \\ \nabla\cdot\mathbf{v} = 0, \\ (\varrho c)_m \dfrac{\partial T}{\partial t} + (\varrho c)_F \mathbf{v}\cdot\nabla T = \kappa_m \Delta T, \end{cases} \tag{2.4}$$

$$\begin{aligned} \mathbf{v}\cdot\mathbf{n} = 0 &\quad \text{on } z = 0, d \\ T = T_L &\quad \text{on } z = 0 \\ T = T_U &\quad \text{on } z = d \end{aligned} \tag{2.5}$$

where

$$\mathbf{v} = \varphi\mathbf{V}$$

is the seepage velocity — defined via the Dupuit-Forchheimer relation, φ and $\mathbf{V}$ being the porosity of the medium and the intrinsic average velocity, respectively — while K denotes the permeability of the porous body. The subscripts m and F refer to the medium and the fluid, respectively. For the Horton-Rogers-Lapwood problem, the threshold phenomenon is related to the Darcy-Rayleigh number:

$$\mathrm{Ra} = \frac{\varrho_0 \alpha \beta d^2 K (\varrho c)_F}{\kappa_m \mu}. \tag{2.6}$$

It is well known that the critical Rayleigh number for clear fluids and the critical Darcy-Rayleigh number for fluid saturated porous media — above which cellular convective motion arises and below which all perturbations decay exponentially to zero — are

$$\mathrm{Ra}_{\text{Bénard}} = \frac{27}{4}\pi^4, \qquad \mathrm{Ra}_{\text{HRL}} = 4\pi^2,$$

respectively, so let us point out that the presence of the solid skeleton enhances the convective heat transfer.

2.2 Description of Bi-disperse Porous Media

As defined in [15], a bi-disperse porous medium, also indicated by BDPM, is a double porosity material characterized by a solid matrix with an interconnected void, but the solid skeleton has cracks or fissures in it. One of the possible causes of fractures formation in the solid skeleton of natural porous media is thermal stress, and this is one of the main reasons for which the study of thermal convection and other temperature effects in a BDPM is relevant. In particular, a BDPM is a compound of *clusters* of large particles that are themselves agglomerations of smaller particles. Therefore, this kind of materials are characterized by two different types of pores: macropores between the clusters and micropores within them, the macropores are referred to as f-phase (meaning "fractured phase"), while the remainder of the structure is referred to as p-phase (meaning "porous phase") [4].

A BDPM is characterized by two different permeabilities ($\mathbf{K}^f$ for the f-phase and $\mathbf{K}^p$ for the p-phase) and two different porosities. In particular, let φ be the porosity associated to the macropores, i.e. the ratio of the volume of the macropores to the total volume of the saturated porous material, let ϵ be the porosity associated to the micropores, i.e. the ratio of the volume of the micropores to the volume of porous body which remains once the macropores are removed, hence

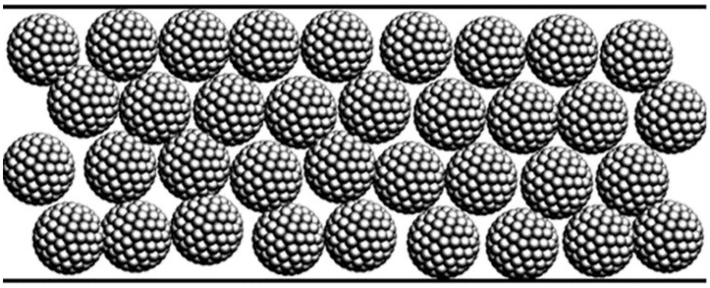

Figure 2.2: Sketch of a bi-disperse porous medium [4].

- $(1-\varphi)\epsilon$ is the fraction of volume occupied by the micropores,
- $\varphi + (1-\varphi)\epsilon$ is the fraction of volume occupied by the fluid,
- $(1-\epsilon)(1-\varphi)$ is the fraction of volume occupied by the solid skeleton.

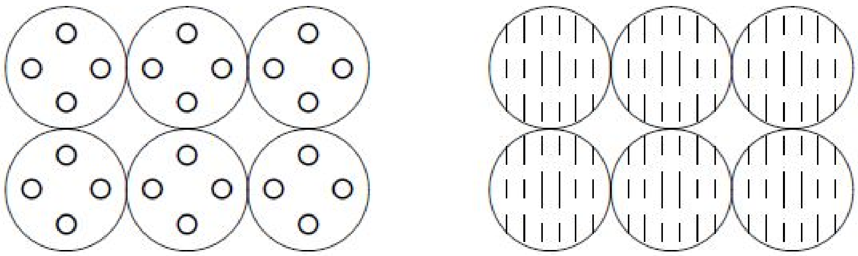

Figure 2.3: An example of a man made double porosity medium consisting of twelve spheres. The pattern can be continued by adding more spheres appropriately. The micro porosity is defined by the cylindrical holes in the spheres whereas the macro porosity is defined by the gaps between the larger spheres. The spheres to the right represent a view from the side of the material whereas the spheres to the left represent a view from the top [16].

A theoretical key development is attributable to Nield and Kuznetsov in [4, 17, 18]. They developed a refined model which employs different kinematic fields $\mathbf{v}^f$ and $\mathbf{v}^p$ in the macropores and in the micropores, different pressures p^f and p^p and different temperatures T^f and T^p (on the basis of the following observation: while the steady state of conductive heat transfer implies local thermal equilibrium, this LTE may not occur for a convection problem). In particular, let $\mathbf{V}^f$ and $\mathbf{V}^p$ be the pore averaged velocities in the macro- and micropores, respectively. Then, the analogous seepage velocities are given by the classical Dupuit-Forchheimer relation:

$$\mathbf{v}^f = \varphi \mathbf{V}^f, \quad \mathbf{v}^p = \epsilon(1-\varphi)\mathbf{V}^p.$$

Nield and Kuznetsov also supposed that the drag (per unit volume) is increased by an amount $\zeta(\mathbf{v}^f - \mathbf{v}^p)$ for the f-phase and decreased by the same amount for the p-phase, where ζ is an interaction coefficient between f-phase and p-phase.

Let $Oxyz$ be a reference frame with fundamental unit vectors $\mathbf{i}, \mathbf{j}, \mathbf{k}$ ($\mathbf{k}$ pointing vertically upward), the momentum equations developed by Nield and Kuznetsov for a saturated BDPM occupying an horizontal layer L of thickness d heated from below, according to the Darcy's model and to the Oberbeck-Boussinesq approximation, may be written as

$$\begin{aligned}
\nabla p^f &= -\frac{\mu}{K_f}\mathbf{v}^f - \zeta(\mathbf{v}^f - \mathbf{v}^p) + \\
+\varrho_F g\alpha\Big(&\frac{\varphi}{\varphi+\epsilon(1-\varphi)}T^f + \frac{\epsilon(1-\varphi)}{\varphi+\epsilon(1-\varphi)}T^p\Big)\mathbf{k} \\
\nabla p^p &= -\frac{\mu}{K_p}\mathbf{v}^p - \zeta(\mathbf{v}^p - \mathbf{v}^f) + \\
+\varrho_F g\alpha\Big(&\frac{\varphi}{\varphi+\epsilon(1-\varphi)}T^f + \frac{\epsilon(1-\varphi)}{\varphi+\epsilon(1-\varphi)}T^p\Big)\mathbf{k}.
\end{aligned} \tag{2.7}$$

Let us point out that, considering the Darcy's law, the pressure gradient is an intrinsic quantity, hence the pressure is the pressure in the fluid. The energy balance equations for the f-phase and the p-phase are

$$\begin{aligned}
\varphi(\varrho c)_f\Big(\frac{\partial T^f}{\partial t} + \mathbf{v}^f\cdot\nabla T^f\Big) &= \varphi k_f \Delta T^f + h(T^p - T^f), \\
(1-\varphi)(\varrho c)_p\Big(\frac{\partial T^p}{\partial t} + \mathbf{v}^p\cdot\nabla T^p\Big) &= (1-\varphi)k_p \Delta T^p + h(T^f - T^p),
\end{aligned} \tag{2.8}$$

where h is a thermal interaction coefficient. In addition, the fluid is regarded as incompressible in both the macro and micro parts of the BDPM, thus the velocities fields satisfy the continuity equations

$$\nabla\cdot\mathbf{v}^f = 0, \quad \nabla\cdot\mathbf{v}^p = 0. \tag{2.9}$$

To system (2.7)-(2.8)-(2.9) the following boundary conditions are appended

$$\begin{aligned}
\mathbf{v}^s\cdot\mathbf{n} &= 0, \qquad \text{on } z = 0, d, \quad s = \{f, p\} \\
T(x, y, 0, t) &= T_L, \\
T(x, y, d, t) &= T_U,
\end{aligned} \tag{2.10}$$

with $\mathbf{n}$ the unit outward normal to the impermeable horizontal planes delimiting the layer and $T_L > T_U$, since the layer is heated from below.
Through numerical simulations applied to a bi-disperse porous medium consisting of blocks of porous material which are themselves composed of smaller microblocks, Imani and Hooman in [19] show that when the macropores are relatively large compared to the micropores then one may assume the temperatures of the solid skeleton match those of the fluid in the macro and micropores, hence there is local thermal equilibrium. However, when large temperature differences are expected in the macro and micropores (for example when hot fluid is injected into a cold skeleton), the two temperatures theory should be used.
From a mathematical point of view, when the LTE theory is employed, it is possible to show that the *principle of exchange of stabilities* holds[2] and that the linear instability threshold and the global nonlinear one coincide. Thus, linear instability theory correctly captures the onset of thermal convection in a single temperature bi-disperse porous medium. As underlined in [20], such a result when two temperatures are present has not been proved. Employing a single temperature in the micropores and in the macropores, i.e. $T^f = T^p = T$, may suffices to represent many real situations (see for instance [21, 22, 23, 24]) and the resulting mathematical model is consistent with experiments related to heat transfer and thermal dispersion in bi-disperse porous media. Hence, Gentile and Straughan in [25] proposed as governing equations, describing the evolutionary behaviour of the thermal conduction solution in a *horizontal layer of single temperature BDPM*, the following:

$$\begin{cases} -\dfrac{\mu}{K_f}\mathbf{v}^f - \zeta(\mathbf{v}^f - \mathbf{v}^p) - \nabla p^f + \varrho_F \alpha g T \mathbf{k} = \mathbf{0}, \\ -\dfrac{\mu}{K_p}\mathbf{v}^p - \zeta(\mathbf{v}^p - \mathbf{v}^f) - \nabla p^p + \varrho_F \alpha g T \mathbf{k} = \mathbf{0}, \\ \nabla \cdot \mathbf{v}^f = 0, \\ \nabla \cdot \mathbf{v}^p = 0, \\ (\varrho c)_m \dfrac{\partial T}{\partial t} + (\varrho c)_f (\mathbf{v}^f + \mathbf{v}^p) \cdot \nabla T = k_m \Delta T. \end{cases} \tag{2.11}$$

The nomenclature used for the previous equations is the following: $\mathbf{x} = (x, y, z)$, $\mathbf{v}_s$ = seepage velocity, p_s = pressure, with $s = \{f, p\}$ (f and p referring to f-phase and p-phase, respectively), T = temperature, K_s = permeability for $s = \{f, p\}$, ϱ = density, ζ = interaction coefficient between the f-phase and the p-phase, $\mathbf{g} = -g\mathbf{k}$ = gravity, μ = fluid viscosity, ϱ_F = reference constant density, α = thermal expansion coefficient, c = specific heat,

[2] i.e. convection can arise only via steady motions, see Section 1.4.

c_p = specific heat at a constant pressure, $(\varrho c)_m = (1-\varphi)(1-\epsilon)(\varrho c)_{sol} + [\varphi + \epsilon(1-\varphi)](\varrho c)_F$, $k_m = (1-\varphi)(1-\epsilon)k_{sol} + \varphi k_f + \epsilon(1-\varphi)k_p$ = thermal conductivity (the subscript *sol* is referred to the solid skeleton).
Let us point out that in the case of single temperature BDPM, since the macropores and micropores are saturated by the same fluid, we expect that $(\varrho c)_f = (\varrho c)_p = (\varrho c)_F$ [26].

2.2.1 Brinkman Bi-Disperse Porous Media

The momentum equations (2.7) for macro and micropores are derived extending the Darcy's model to the dual porosity case. However, the original model developed by Nield and Kuznetsov relates to *Brinkman bi-disperse porous media*. In particular, they used Brinkman's law in both micropores and macropores in [18], accounting for the discussion on the dispersion in a BDPM made by Moutsopolous and Koch in [27]. In [27] the authors proved a good agreement between theoretical predictions end experimental measurements when one consider a dilute array of large spheres in a Brinkman medium and the flow around the large spheres is modeled using Brinkman's equation. Man-made materials for heat transfer industry such as metallic foams have high porosity (close to one), hence, since the Brinkman model is better suited for situations characterized by high fluid seepage velocities and high porosities, Nield and Kuznetsov extended the Brinkman model for porous media to the bi-disperse case and the coupled equations for the seepage velocities $\mathbf{v}^f$ e $\mathbf{v}^p$ are

$$\begin{aligned} \mathbf{G} &= \left(\frac{\mu}{K_f}\right)\mathbf{v}^f + \zeta(\mathbf{v}^f - \mathbf{v}^p) - \tilde{\mu}_f \Delta \mathbf{v}^f, \\ \mathbf{G} &= \left(\frac{\mu}{K_p}\right)\mathbf{v}^p + \zeta(\mathbf{v}^p - \mathbf{v}^f) - \tilde{\mu}_p \Delta \mathbf{v}^p, \end{aligned} \tag{2.12}$$

where $\mathbf{G}$ is the negative of the applied pressure gradient, μ is the fluid viscosity, K_f e K_p are the permeabilities of the two phases, ζ is the interaction coefficient between the macro and the micro phases and $\tilde{\mu}_p$ e $\tilde{\mu}_f$ are the effective (or Brinkman) viscosities in the two phases. Moreover, the effect of quadratic (Forchheimer) drag was neglected, and the hydrodynamic interaction between the two phases was modeled by the simplest possible expression.

It is possible to recover the Darcy'law from the Brinkman momentum equations (2.12) by *neglecting* the laplacian of the seepage velocities $\mathbf{v}^f$ and $\mathbf{v}^p$. Therefore, equalling the right-hand sides of $(2.12)_1$ and $(2.12)_2$, one gets

$$\mathbf{v}^f\left(\frac{\mu}{K_f} + 2\zeta\right) = \mathbf{v}^p\left(\frac{\mu}{K_p} + 2\zeta\right),$$

hence, the kinematic fields for the f-phase and the p-phase are:

$$\mathbf{v}^f = \frac{\left(\frac{\mu}{K_p} + 2\zeta\right)\mathbf{G}}{\frac{\mu^2}{K_f K_p} + \zeta\mu\left(\frac{1}{K_f} + \frac{1}{K_p}\right)},$$

$$\mathbf{v}^p = \frac{\left(\frac{\mu}{K_f} + 2\zeta\right)\mathbf{G}}{\frac{\mu^2}{K_f K_p} + \zeta\mu\left(\frac{1}{K_f} + \frac{1}{K_p}\right)}.$$

We finally recover the Darcy'law

$$\mathbf{G} = \frac{\mu}{K}\mathbf{v},$$

where the following positions were made:

$$\begin{aligned} \mathbf{v} =& \varphi \mathbf{v}_f + (1-\varphi)\mathbf{v}_p, \\ K =& \frac{\varphi K_f + (1-\varphi)K_p + 2(\zeta/\mu)K_f K_p}{1 + (\zeta/\mu)(K_f + K_p)}. \end{aligned}$$

We can conclude that the interaction coefficient ζ affects the permeability in the f-phase and in the p-phase through $\frac{\zeta}{\mu}$.

Let us point out that exchange of stabilities has not been proved in either the Brinkman–Brinkman or Darcy–Darcy case when there are two temperatures and so there is a possibility of oscillatory convection in addition to the already observed stationary convection. Also, in [28] it has been proven that the instability threshold for the onset thermal convection in the two temperature bidispersive theory with Brinkman effects in both the macro and micropores is less then the one obtained when Darcy effects in both phases are considered.
In [20], Straughan and Gentile developed a macro-Brinkman-micro-Darcy model, justified by envisaging a material with relatively large macropores, i.e. a relatively large macroporosity.

2.3 Rotating Porous Media

As underlined by Nield and Bejan in [1] and Vadasz in [29, 30, 31, 32], the applications of fluid flow through rotating packed beds can be drying process or extraction of soluble components, for instance. More generally, since rotation may affect the fluid flow through two mechanisms, the thermal buoyancy

caused by centrifugal forces and the Coriolis force (or a combination of both) [32], the study of fluid flow in rotating porous media is motivated by its theoretical significance and practical applications in geophysics and in engineering: geophysical problems such as flows in porous geological formations subject to earth rotation and the flow of magma in the earth mantle close to the earth crust, physiological processes in human body subject to rotating trajectories, cooling of electronic equipment in a rotating radar, cooling of rotors of electric machines, cooling of turbo-machinery blades, food and chemical processes, solidification and centrifugal casting of metals, rotating machineries, petroleum industry, biomechanics, the electrocatalysis of the oxygen reduction reaction in alkaline media on ultra-thin porous coating rotating electrodes (see [23, 32, 33, 34] and the references therein). Since bi-disperse porous media offer much more possibilities to design man-made materials then single porosity media [20, 35, 36], convection and heat transfer problems in rotating BDPM find many engineering or industrial applications as well. For instance, in [21] Capone *et al.* analyse the influence of vertical rotation on the onset of convection in a single temperature BDPM, according to Darcy's law, while [22] deals with the effect of horizontal isotropy on the onset of convection in a uniformly rotating bi-disperse porous medium. The experimental results and observations by Li *et al.* in [37] point out that the development of fractures and microfractures controls the physical properties and fluid productivity of reservoirs, and high-speed centrifugation enhances oil production from fractured porous media.
The analysis of flow and heat transfer in rotating single or double porosity materials can be applied to cooling devices, which are often constituted of an heat pipe subject to rotation, hence the comprehension of how Coriolis effects affect the heat transfer is relevant [32].

2.3.1 Hydrodynamics in a Rotating Layer

With the aim of analyse the onset of convection in a rotating horizontal layer of fluid-saturated porous material, a rotating frame of reference has to be considered and the Darcy's model has to be extended in order to include centrifugal and Coriolis effects.
The fluid motion is described with respect to two frames, a fixed inertial frame $O\xi\eta\zeta$ and a rotating frame of reference $Oxyz$, such that $z = \zeta$. In particular, the rotating reference frame $Oxyz$ has fundamental unit vectors $\mathbf{i}, \mathbf{j}, \mathbf{k}$ (with $\mathbf{k}$ pointing vertically upward) and rotates about the vertical axis z, with constant angular velocity $\boldsymbol{\Omega} = \Omega\mathbf{k}$.
The fluid motion is described as it appears to an *observer at rest* in the rotating frame. In this rotating frame of reference, velocities and accelerations

recognized by an observer at rest in it are obviously different with respect to velocities and accelerations recognized by an observer at rest in the fixed inertial frame. Therefore, the transformation related to these two reference frames is governed by the following equations (see [10]):

$$\begin{cases} x = \xi \cos \Omega t + \eta \sin \Omega t, \\ y = -\xi \sin \Omega t + \eta \cos \Omega t, \\ z = \zeta, \end{cases} \tag{2.13}$$

According to (2.13), the equations of a generic vector $\mathbf{q}$ are:

$$\begin{cases} q_x^{(0)} = q_\xi \cos \Omega t + q_\eta \sin \Omega t, \\ q_y^{(0)} = -q_\xi \sin \Omega t + q_\eta \cos \Omega t, \\ q_z^{(0)} = q_\zeta, \end{cases} \tag{2.14}$$

where q_ξ, q_η, q_ζ are the components of $\mathbf{q}$ in $O\xi\eta\zeta$, while the superscript (0) refers to the absolute components.
The first and second derivaties with respect to t of (2.13) are respectively given by:

$$\begin{cases} \dfrac{dx}{dt} = \left(\dfrac{d\xi}{dt} \cos \Omega t + \dfrac{d\eta}{dt} \sin \Omega t\right) - \Omega(\xi \sin \Omega t - \eta \cos \Omega t), \\ \dfrac{dy}{dt} = \left(-\dfrac{d\xi}{dt} \sin \Omega t + \dfrac{d\eta}{dt} \cos \Omega t\right) - \Omega(\xi \cos \Omega t + \eta \sin \Omega t), \\ \dfrac{dz}{dt} = \dfrac{d\zeta}{dt}, \end{cases} \tag{2.15}$$

$$\begin{cases} \dfrac{d^2x}{dt^2} = \left(\dfrac{d^2\xi}{dt^2} \cos \Omega t + \dfrac{d^2\eta}{dt^2} \sin \Omega t\right) + 2\Omega(-\dfrac{d\xi}{dt} \sin \Omega t + \dfrac{d\eta}{dt} \cos \Omega t) - \Omega^2 x, \\ \dfrac{d^2y}{dt^2} = \left(-\dfrac{d^2\xi}{dt^2} \sin \Omega t + \dfrac{d^2\eta}{dt^2} \cos \Omega t\right) + 2\Omega(-\dfrac{d\xi}{dt} \cos \Omega t - \dfrac{d\eta}{dt} \sin \Omega t) - \Omega^2 y, \\ \dfrac{d^2z}{dt^2} = \dfrac{d^2\zeta}{dt^2}, \end{cases} \tag{2.16}$$

Regarding the velocity $\mathbf{v}$ of a fluid element, by virtue of (2.15) we have

$$\begin{aligned} v_x &= v_x^{(0)} + \Omega y, \\ v_y &= v_y^{(0)} - \Omega x, \\ v_z &= v_z^{(0)}, \end{aligned} \tag{2.17}$$

i.e.

$$\mathbf{v} = \mathbf{v}^{(0)} - \boldsymbol{\Omega} \times \mathbf{x}, \tag{2.18}$$

with $\mathbf{x} = (x, y, z)$. Hence, equations (2.16) are equivalent to

$$\begin{cases} \dfrac{dv_x}{dt} = \left(\dfrac{dv_x^{(0)}}{dt}\right)^{(0)} + 2\Omega v_y^{(0)} - \Omega^2 x, \\ \dfrac{dv_y}{dt} = \left(\dfrac{dv_y^{(0)}}{dt}\right)^{(0)} - 2\Omega v_x^{(0)} - \Omega^2 y, \\ \dfrac{dv_z}{dt} = \left(\dfrac{dv_z^{(0)}}{dt}\right)^{(0)}, \end{cases} \tag{2.19}$$

that are, substituting $v_x^{(0)}$ and $v_y^{(0)}$,

$$\begin{cases} \left(\dfrac{dv_x^{(0)}}{dt}\right)^{(0)} = \dfrac{dv_x}{dt} - 2\Omega v_y - \Omega^2 x, \\ \left(\dfrac{dv_y^{(0)}}{dt}\right)^{(0)} = \dfrac{dv_y}{dt} + 2\Omega v_x - \Omega^2 y, \\ \left(\dfrac{dv_z^{(0)}}{dt}\right)^{(0)} = \dfrac{dv_z}{dt}. \end{cases} \tag{2.20}$$

Finally, we get

$$\left(\frac{d\mathbf{v}^{(0)}}{dt}\right)^{(0)} = \frac{d\mathbf{v}}{dt} + 2\mathbf{\Omega} \times \mathbf{x} - \frac{1}{2}\nabla(|\mathbf{\Omega} \times \mathbf{x}|^2), \tag{2.21}$$

where $2\mathbf{\Omega}\times\mathbf{x}$ is the Coriolis acceleration and $-\frac{1}{2}\nabla(|\mathbf{\Omega}\times\mathbf{x}|^2)$ is the centrifugal force.

2.3.2 Onset of Convection in Rotating Porous Layers

In the case of rotating clear fluids, it has been proved that oscillatory convection occurs only for a certain range of Prandtl number Pr values [10] (i.e. $Pr < 1$, Pr being defined as ν/α, with $\nu = \mu/\varrho_F$ the kinematic viscosity and $\alpha = k/(\varrho c)$ is the thermal diffusivity). Instead, when a porous domain is considered, in paper [30] (where rotation and inertia effects are simultaneously taken into account) Vadasz found that the onset of oscillatory convection is not limited to a particular domain of Prandtl number values, in contrast with the corresponding clear fluid case. Moreover, as underlined in [10] and [32], when rotation is taken into account in clear fluids or in porous media heated from below, the role of viscosity is inverted: the viscosity at high rotation rates has a destabilizing effect on the onset of stationary convection, hence the higher the viscosity the less stable is the fluid. On the other hand, it has been demonstrated that rotation has a stabilizing effect on the onset of convection, since the critical Rayleigh number Ra is an increasing function of the Taylor number $\mathcal{T}$ (non-dimensional representation of rotation rates, hence it describes Coriolis and centrifugal effects on the onset of convection). In the clear fluid case, one has

$$\mathrm{Ra}_{\text{Bénard}} = \min_{a^2} \frac{(\pi^2+a^2)^3}{a^2}, \qquad \mathrm{Ra}_c = \min_{a^2} \frac{(\pi^2+a^2)^3+\pi^2\mathcal{T}}{a^2} \tag{2.22}$$

where Ra_c is the critical Rayleigh number for the onset of stationary convection in a rotating layer of fluid. When a porous domain is considered, one gets

$$\mathrm{Ra}_{\text{HRL}} = \min_{a^2} \frac{(\pi^2+a^2)^2}{a^2}, \qquad \mathrm{Ra}_{p,c} = \min_{a^2} \frac{(\pi^2+a^2)(\pi^2+a^2+\pi^2\mathcal{T})}{a^2} \tag{2.23}$$

where $\mathrm{Ra}_{p,c}$ is the critical Darcy-Rayleigh number for the onset of stationary convection in a rotating fluid-saturated porous medium.

As regards rotating bi-disperse porous media, the instability threshold for the onset of convection in a rotating horizontal layer of fluid-saturated isotropic and single-temperature bi-disperse porous medium, according to Darcy's law, has been determined in [21] as follows:

$$\mathrm{Ra}_L = \min_{a^2\in\mathbb{R}^+} \frac{\Lambda\{\Gamma^2\Lambda^2+\gamma_1\mathcal{T}^2[\eta^2(1+\gamma_1)^2+(1+\gamma_2)^2+2\eta]\pi^2\Lambda+\gamma_1^4\mathcal{T}^4\pi^4\eta^2\}}{a^2\{\Gamma(4+\gamma_1+\gamma_2)\Lambda+\gamma_1^2\mathcal{T}^2\pi^2[\eta^2\gamma_1+\gamma_2+(\eta-1)^2]\}} \tag{2.24}$$

where $\Lambda = \pi^2 + a^2$ and

$$\gamma_1 = \frac{\mu}{\zeta K_f}, \quad \gamma_2 = \frac{\mu}{\zeta K_p}, \quad \eta = \frac{\varphi}{\epsilon}, \quad \Gamma = \gamma_1+\gamma_2+\gamma_1\gamma_2.$$

Let us point out that (2.24) is an increasing function of the Taylor number $\mathcal{T}$, hence, as expected, the rotation acts to delay the onset of convection. Moreover, as $K_p \to 0$, $\zeta \to 0$ and $\epsilon \to 0$ from (2.24) one recovers the critical Rayleigh number for the single porosity case

$$\mathrm{Ra}_{p,c} = \min_{a^2} \frac{(\pi^2+a^2)(\pi^2+a^2+\pi^2\mathcal{T})}{a^2}.$$

Part II

Chapter 3

Effect of anisotropy on the onset of convection in rotating bi-disperse Brinkman porous media

The goal of this Chapter is to study the onset of thermal convection in a horizontal isotropic bi-disperse porous medium uniformly rotating about a vertical axis. Moreover, accounting for the discussion done in 2.2.1, the validity of the Brinkman law is assumed for both micropores and macropores. Thermal convection and heat transfer problems in anisotropic single porosity media — for which permeability is a symmetric second-order tensor — have been widely studied due to the many examples of natural anisotropic porous materials (such as rock strata or wood, which behaves very differently along the grain to the way it does across the grain [2]) and the large number of engineering applications, since anisotropic permeability is a powerful tool to optimise heat transfer (see for instance [38, 39, 40] and references therein). However, anisotropy in bi-disperse porous materials (where there is the possibility of different permeabilities in the vertical and horizontal directions in both macropores and micropores) may have much more potentials due to many possibilities to design man-made materials for heat transfer or insulation problems, for oil recovery from underground reservoir, for nuclear waste recovery and so on (see [25, 28, 35, 36] and references therein).
The results presented in the following Chapter are based on the paper [41] with F. Capone and R. De Luca. The Chapter is organized as follows. In Section 3.1 we introduce the mathematical model and, in order to study the stability of the conduction solution, we introduce the dimensionless equations for the evolution (in time) of the perturbation fields. In Section 3.2

we perform the instability analysis of the conduction solution and we prove the validity of the strong form of the principle of exchange of stabilities, which means that if the convection sets in, it arises via a stationary state. Section 3.3 deals with the nonlinear stability analysis of the conduction solution and the coincidence between instability and (global) nonlinear stability thresholds in the L^2-norm is proved. Numerical simulations concerning the asymptotic behaviour of the instability threshold with respect to the meaningful parameters of the model are performed in Section 3.4.

3.1 Mathematical model

Let $Oxyz$ be a reference frame with fundamental unit vectors $\mathbf{i}, \mathbf{j}, \mathbf{k}$ ($\mathbf{k}$ pointing vertically upward). Let L be a bi-disperse porous layer of thickness d uniformly heated from below and rotating about the vertical axis z, with constant angular velocity $\mathbf{\Omega} = \Omega \mathbf{k}$. Let L be saturated by a homogeneous incompressible fluid at rest state and let us assume the validity of the local thermal equilibrium between the f-phase and the p-phase, i.e. $T^f = T^p = T$. The saturated bi-disperse porous medium is also supposed to be *horizontally isotropic*. Let the axes (x, y, z) be the *principal axes* of the permeability, so the macropermeability tensor and the micropermeability tensor may be written as

$$
\begin{gathered}
\mathbf{K}^f = \mathrm{diag}(K_x^f, K_y^f, K_z^f) = K_z^f \ \mathbf{K}^{f*}, \\
\mathbf{K}^p = \mathrm{diag}(K_x^p, K_y^p, K_z^p) = K_z^p \ \mathbf{K}^{p*}, \\
\mathbf{K}^{f*} = \mathrm{diag}(k, k, 1), \quad \mathbf{K}^{p*} = \mathrm{diag}(h, h, 1)
\end{gathered}
$$

where

$$
k = \frac{K_x^f}{K_z^f} = \frac{K_y^f}{K_z^f}, \quad h = \frac{K_x^p}{K_z^p} = \frac{K_y^p}{K_z^p}.
$$

A Boussinesq approximation is used, whereby the density is constant except in the buoyancy forces, which are linear in temperature. Taking into account the Coriolis terms due to the uniform rotation of the layer about the vertical axis z for the micropores and the macropores [21] and extending the Brinkman model for a simple porous medium to BDPM [18], the relevant equations are:

$$
\begin{cases}
\mathbf{v}^f = \mu^{-1}\mathbf{K}^f \cdot \left[-\zeta(\mathbf{v}^f - \mathbf{v}^p) - \nabla p^f + \varrho_F \alpha g T \mathbf{k} - \dfrac{2\varrho_F \Omega}{\varphi} \mathbf{k} \times \mathbf{v}^f + \tilde{\mu}_f \Delta \mathbf{v}^f \right], \\
\mathbf{v}^p = \mu^{-1}\mathbf{K}^p \cdot \left[-\zeta(\mathbf{v}^p - \mathbf{v}^f) - \nabla p^p + \varrho_F \alpha g T \mathbf{k} - \dfrac{2\varrho_F \Omega}{\epsilon} \mathbf{k} \times \mathbf{v}^p + \tilde{\mu}_p \Delta \mathbf{v}^p \right], \\
\nabla \cdot \mathbf{v}^f = 0, \\
\nabla \cdot \mathbf{v}^p = 0, \\
(\varrho c)_m T_{,t} + (\varrho c)_f (\mathbf{v}^f + \mathbf{v}^p) \cdot \nabla T = k_m \Delta T,
\end{cases}
\tag{3.1}
$$

where

$$
p^s = P^s - \frac{\varrho_F}{2} |\mathbf{\Omega} \times \mathbf{x}|^2, \quad s = \{f, p\}
$$

is the reduced pressure being $\mathbf{x} = (x, y, z)$, $\mathbf{v}^s$ = seepage velocity, P^s= pressure, ϱ= density, ζ = interaction coefficient between the f-phase and the p-phase, $\mathbf{g} = -g\mathbf{k}$ = gravity, μ = fluid viscosity, $\tilde{\mu}_s$ = effective viscosity, ϱ_F = reference constant density, α = thermal expansion coefficient, c = specific heat, c_p = specific heat at a constant pressure, $(\varrho c)_m = (1-\varphi)(1-\epsilon)(\varrho c)_{sol} + \varphi(\varrho c)_f + \epsilon(1-\varphi)(\varrho c)_p$, $k_m = (1-\varphi)(1-\epsilon)k_{sol} + \varphi k_f + \epsilon(1-\varphi)k_p$ = thermal conductivity (the subscript *sol* is referred to the solid skeleton).
To (3.1) the following boundary conditions are appended

$$
\begin{aligned}
&\mathbf{v}^s \cdot \mathbf{n} = 0\,, \quad s = \{f, p\} \qquad \text{on} \quad z = 0, d, \\
&T = T_L\,, \quad \text{on} \quad z = 0\,, \qquad T = T_U\,, \quad \text{on} \quad z = d
\end{aligned}
\tag{3.2}
$$

where $T_L > T_U$.
The problem (3.1)-(3.2) admits the stationary conduction solution:

$$
\overline{\mathbf{v}}^f = \mathbf{0}, \quad \overline{\mathbf{v}}^p = \mathbf{0}, \quad \overline{T} = -\beta z + T_L,
$$

where $\beta = \dfrac{T_L - T_U}{d}$ is the temperature gradient. Denoting by $\{\mathbf{u}^f, \mathbf{u}^p, \theta, \pi^f, \pi^p\}$ a perturbation to the steady solution, one recovers that the evolutionary system governing the perturbation fields is given by

$$
\begin{cases}
\mathbf{u}^f = \mu^{-1}\mathbf{K}^f \cdot \left[-\zeta(\mathbf{u}^f - \mathbf{u}^p) - \nabla \pi^f + \varrho_F \alpha g \theta \mathbf{k} - \dfrac{2\varrho_F \Omega}{\varphi} \mathbf{k} \times \mathbf{u}^f + \tilde{\mu}_f \Delta \mathbf{u}^f \right], \\
\mathbf{u}^p = \mu^{-1}\mathbf{K}^p \cdot \left[-\zeta(\mathbf{u}^p - \mathbf{u}^f) - \nabla \pi^p + \varrho_F \alpha g \theta \mathbf{k} - \dfrac{2\varrho_F \Omega}{\epsilon} \mathbf{k} \times \mathbf{u}^p + \tilde{\mu}_p \Delta \mathbf{u}^p \right], \\
\nabla \cdot \mathbf{u}^f = 0, \\
\nabla \cdot \mathbf{u}^p = 0, \\
(\varrho c)_m \theta_{,t} + (\varrho c)_f (\mathbf{u}^f + \mathbf{u}^p) \cdot \nabla \theta = (\varrho c)_f \beta (w^f + w^p) + k_m \Delta \theta,
\end{cases}
\tag{3.3}
$$

where $\mathbf{u}^f = (u^f, v^f, w^f)$, $\mathbf{u}^p = (u^p, v^p, w^p)$. Introducing the non-dimensional parameters

$$\mathbf{x}^* = \frac{\mathbf{x}}{d},\ t^* = \frac{t}{\tilde{t}},\ \theta^* = \frac{\theta}{\tilde{T}},\ \mathbf{u}^{s*} = \frac{\mathbf{u}^s}{\tilde{u}},\ \pi^{s*} = \frac{\pi^s}{\tilde{P}},\quad \text{for } s = \{f, p\},$$

$$\eta = \frac{\varphi}{\epsilon},\ \sigma = \frac{\tilde{\mu}_p}{\tilde{\mu}_f},\ \gamma_1 = \frac{\mu}{K_z^f \zeta},\ \gamma_2 = \frac{\mu}{K_z^p \zeta},$$

where the scales are given by

$$\tilde{u} = \frac{k_m}{(\varrho c)_f d},\ \tilde{t} = \frac{d^2 (\varrho c)_m}{k_m},\ \tilde{P} = \frac{\zeta k_m}{(\varrho c)_f},\ \tilde{T} = \sqrt{\frac{\beta k_m \zeta}{(\varrho c)_f \varrho_F \alpha g}},$$

and setting

$$\mathcal{T} = \frac{2\varrho_F \Omega K_z^f}{\varphi \mu}, \qquad Da_f = \frac{\tilde{\mu}_f K_z^f}{d^2 \mu}, \qquad R = \sqrt{\frac{\beta d^2 (\varrho c)_f \varrho_F \alpha g}{k_m \zeta}}$$

which are the Taylor number $\mathcal{T}$, the Darcy number Da_f and the thermal Rayleigh number R, respectively, the resulting non-dimensional perturbation equations, dropping all the asterisks, are

$$\begin{cases} \gamma_1 (\mathbf{K}^f)^{-1} \mathbf{u}^f + (\mathbf{u}^f - \mathbf{u}^p) = -\nabla \pi^f + R\theta \mathbf{k} - \gamma_1 \mathcal{T} \mathbf{k} \times \mathbf{u}^f + Da_f \gamma_1 \Delta \mathbf{u}^f, \\ \gamma_2 (\mathbf{K}^p)^{-1} \mathbf{u}^p - (\mathbf{u}^f - \mathbf{u}^p) = -\nabla \pi^p + R\theta \mathbf{k} - \eta \gamma_1 \mathcal{T} \mathbf{k} \times \mathbf{u}^p + Da_f \gamma_1 \sigma \Delta \mathbf{u}^p, \\ \nabla \cdot \mathbf{u}^f = 0, \\ \nabla \cdot \mathbf{u}^p = 0, \\ \theta_{,t} + (\mathbf{u}^f + \mathbf{u}^p) \cdot \nabla \theta = R(w^f + w^p) + \Delta \theta, \end{cases} \tag{3.4}$$

under the initial conditions

$$\mathbf{u}^s(\mathbf{x}, 0) = \mathbf{u}_0^s(\mathbf{x}), \qquad \pi^s(\mathbf{x}, 0) = \pi_0(\mathbf{x}), \qquad \theta(\mathbf{x}, 0) = \theta_0(\mathbf{x})$$

with $\nabla \cdot \mathbf{u}_0^s = 0$, $s = \{f, p\}$, and the stress-free boundary conditions [10]

$$u^f_{,z} = v^f_{,z} = u^p_{,z} = v^p_{,z} = w^f = w^p = \theta = 0 \quad \text{on } z = 0, 1. \tag{3.5}$$

Moreover, according to experimental results, let us assume that the perturbation fields are periodic functions in the x, y directions and denote by

$$V = \left[0, \frac{2\pi}{l}\right] \times \left[0, \frac{2\pi}{m}\right] \times [0, 1]$$

the periodicity cell.

3.2 Thermal instability of the conduction solution

To analyse the onset of convection, i.e. to find the linear instability threshold of the conduction solution, we consider the linear version of (3.4) and seek for solutions in which $\mathbf{u}^f, \mathbf{u}^p, \theta, \pi^f, \pi^p$ have time dependence like $e^{\overline{\sigma}t}$, i.e.

$$\begin{cases} \gamma_1(\mathbf{K}^f)^{-1}\mathbf{u}^f + (\mathbf{u}^f - \mathbf{u}^p) = -\nabla\pi^f + R\theta\mathbf{k} - \gamma_1\mathcal{T}\mathbf{k}\times\mathbf{u}^f + Da_f\gamma_1\Delta\mathbf{u}^f, \\ \gamma_2(\mathbf{K}^p)^{-1}\mathbf{u}^p - (\mathbf{u}^f - \mathbf{u}^p) = -\nabla\pi^p + R\theta\mathbf{k} - \eta\gamma_1\mathcal{T}\mathbf{k}\times\mathbf{u}^p + Da_f\gamma_1\sigma\Delta\mathbf{u}^p, \\ \overline{\sigma}\theta = R(w^f + w^p) + \Delta\theta \end{cases} \tag{3.6}$$

Denoting by

$$\Delta_1 f = f_{,xx} + f_{,yy}\,, \quad \Delta^m \equiv \underbrace{\Delta\Delta\cdots\Delta}_{m}\,, \quad \omega_3^s = (\nabla\times\mathbf{u}^s)\cdot\mathbf{k},\ s = \{f,p\}$$
$$\overline{a} = \frac{\gamma_1}{k} + 1\,, \quad \overline{b} = \frac{\gamma_2}{h} + 1$$

and defining the operators

$$A \equiv \overline{a} - Da_f\gamma_1\Delta\,, \qquad B \equiv \overline{b} - Da_f\sigma\gamma_1\Delta\,, \qquad \Psi \equiv (AB - 1) \tag{3.7}$$

the third components of curl and of double curl of $(3.4)_{1,2}$ are respectively given by

$$\begin{cases} A\omega_3^f - \omega_3^p = \gamma_1\mathcal{T}w^f_{,z}, \\ -\omega_3^f + B\omega_3^p = \eta\gamma_1\mathcal{T}w^p_{,z} \end{cases} \tag{3.8}$$

and

$$\begin{cases} -\dfrac{\gamma_1}{k}w^f_{,zz} - \gamma_1\Delta_1 w^f - \Delta w^f + \Delta w^p = -R\Delta_1\theta + \gamma_1\mathcal{T}\omega^f_{3,z} - Da_f\gamma_1\Delta^2 w^f, \\ \\ -\dfrac{\gamma_2}{h}w^p_{,zz} - \gamma_2\Delta_1 w^p + \Delta w^f - \Delta w^p = -R\Delta_1\theta + \eta\gamma_1\mathcal{T}\omega^p_{3,z} - Da_f\gamma_1\sigma\Delta^2 w^p. \end{cases} \tag{3.9}$$

Applying the operator B to $(3.8)_1$, by virtue of $(3.8)_2$, one has

$$\Psi\omega_3^f = \gamma_1\mathcal{T}Bw^f_{,z} + \eta\gamma_1\mathcal{T}w^p_{,z}.$$

This equation, together with that one obtained by applying the operator Ψ to $(3.8)_2$, leads to

$$\begin{cases} \Psi\omega_3^f = \gamma_1\mathcal{T}Bw^f_{,z} + \eta\gamma_1\mathcal{T}w^p_{,z}, \\ \\ \Psi B\omega_3^p = \gamma_1\mathcal{T}Bw^f_{,z} + \eta\gamma_1\mathcal{T}ABw^p_{,z}. \end{cases} \tag{3.10}$$

Applying the operator Ψ to $(3.9)_1$ and ΨB to $(3.9)_2$, one gets

$$\begin{cases} -\bar{a}\Psi w^f_{,zz} - \hat{\gamma}_1\Psi\Delta_1 w^f + \Psi\Delta_1 w^p + \Psi w^p_{,zz} = \\ \qquad -R\Psi\Delta_1\theta + \gamma_1\mathcal{T}\Psi\omega^f_{3,z} - Da_f\gamma_1\Psi\Delta^2 w^f, \\ \\ -\bar{b}\Psi B w^p_{,zz} - \hat{\gamma}_2\Psi B\Delta_1 w^p + \Psi B\Delta_1 w^f + \Psi B w^f_{,zz} = \\ \qquad -R\Psi B\Delta_1\theta + \eta\gamma_1\mathcal{T}\Psi B\omega^p_{3,z} - Da_f\sigma\gamma_1\Psi B\Delta^2 w^p, \end{cases} \tag{3.11}$$

with $\hat{\gamma}_r = \gamma_r + 1$, for $r = 1, 2$.
In view of (3.10), (3.11) can be written as

$$\begin{cases} [-\bar{a}\Psi - (\gamma_1\mathcal{T})^2 B]w^f_{,zz} - \hat{\gamma}_1\Psi\Delta_1 w^f + \Psi\Delta_1 w^p + \\ \quad [\Psi - \eta(\gamma_1\mathcal{T})^2]w^p_{,zz} + Da_f\gamma_1\Psi\Delta^2 w^f = -R\Psi\Delta_1\theta, \\ \\ [-\bar{b}\Psi B - (\eta\gamma_1\mathcal{T})^2 AB]w^p_{,zz} - \hat{\gamma}_2\Psi B\Delta_1 w^p + \Psi B\Delta_1 w^f + \\ \quad [\Psi B - \eta(\gamma_1\mathcal{T})^2 B]w^f_{,zz} + Da_f\sigma\gamma_1\Psi B\Delta^2 w^p = -R\Psi B\Delta_1\theta. \end{cases} \tag{3.12}$$

Therefore, to find the linear instability threshold, we consider $(3.6)_3$, $(3.12)_1$ and $(3.12)_2$, i.e.:

$$\begin{cases} [-\bar{a}\Psi - (\gamma_1\mathcal{T})^2 B]w^f_{,zz} - \hat{\gamma}_1\Psi\Delta_1 w^f + \Psi\Delta_1 w^p + \\ \quad [\Psi - \eta(\gamma_1\mathcal{T})^2]w^p_{,zz} + Da_f\gamma_1\Psi\Delta^2 w^f = -R\Psi\Delta_1\theta, \\ \\ [-\bar{b}\Psi B - (\eta\gamma_1\mathcal{T})^2 AB]w^p_{,zz} - \hat{\gamma}_2\Psi B\Delta_1 w^p + \Psi B\Delta_1 w^f + \\ \quad [\Psi B - \eta(\gamma_1\mathcal{T})^2 B]w^f_{,zz} + Da_f\sigma\gamma_1\Psi B\Delta^2 w^p = -R\Psi B\Delta_1\theta, \\ \\ \overline{\sigma}\theta = R(w^f + w^p) + \Delta\theta. \end{cases} \tag{3.13}$$

Employing normal modes in (3.13), i.e. assuming the following representation [10]

$$\begin{aligned} w^f &= W^f_0 \sin(n\pi z)e^{i(lx+my)}, \\ w^p &= W^p_0 \sin(n\pi z)e^{i(lx+my)}, \\ \theta &= \Theta_0 \sin(n\pi z)e^{i(lx+my)}, \end{aligned} \tag{3.14}$$

W_0^f, W_0^p, Θ_0 being real constants, setting $a^2 = l^2 + m^2$ and $\Lambda_n = a^2 + n^2\pi^2$, from (3.13) it turns out that

$$\begin{cases} \Big[\Lambda_n e(A_1 M + \sigma f n^2\pi^2) + \Lambda_n^2 e(Me\sigma + B_1) + f\bar{b}n^2\pi^2 + B_1 M + \\ \quad e^2\Lambda_n^3 A_1 + e^3\sigma\Lambda_n^4\Big] W_0^f + \Big[-B_1\Lambda_n - eA_1\Lambda_n^2 - e^2\sigma\Lambda_n^3 + \eta f n^2\pi^2\Big] W_0^p \\ \quad -Ra^2\Big[B_1 + e\Lambda_n A_1 + e^2\sigma\Lambda_n^2\Big]\Theta_0 = 0, \\ \\ \Big[\Lambda_n(e\sigma n^2\pi^2\eta f - \bar{b}B_1) + \eta f n^2\pi^2\bar{b} - \Lambda_n^2 eC \\ \quad -\Lambda_n^3 e^2\sigma(A_1 + \bar{b}) - \Lambda_n^4\sigma^2 e^3\Big] W_0^f + \\ \quad \Big\{\Lambda_n e(CN + \eta^2 f A_1 n^2\pi^2) + \Lambda_n^2 e\sigma[e(A_1 + \bar{b})N + \bar{b}B_1 + e\eta^2 f n^2\pi^2] + \\ \quad B_1\bar{b}N + e^2\Lambda_n^3\sigma(C + e\sigma N) + \Lambda_n^4 e^3\sigma^2(A_1 + \bar{b}) + \Lambda_n^5 e^4\sigma^3 + \\ \quad \eta^2 f n^2\pi^2\bar{a}\bar{b}\Big\} W_0^p - Ra^2\Big[\bar{b}B_1 + e\Lambda_n C + \Lambda_n^2 e^2\sigma(A_1 + \bar{b}) + e^3\sigma^2\Lambda_n^3\Big]\Theta_0 = 0, \\ \\ RW_0^f + RW_0^p - (\Lambda_n + \overline{\sigma})\Theta_0 = 0, \end{cases} \tag{3.15}$$

where

$$\begin{aligned} & A_1 = \sigma\bar{a} + \bar{b}, \;\; B_1 = \frac{\gamma_1}{k}\frac{\gamma_2}{h} + \frac{\gamma_1}{k} + \frac{\gamma_2}{h}, \;\; C = \sigma(2B_1 + 1) + \bar{b}^2, \\ & M = \frac{\gamma_1}{k}n^2\pi^2 + \gamma_1 a^2 + \Lambda_n, \;\; N = \frac{\gamma_2}{h}n^2\pi^2 + \gamma_2 a^2 + \Lambda_n, \\ & e = Da_f\gamma_1, \quad f = (\gamma_1\mathcal{T})^2. \end{aligned} \tag{3.16}$$

Setting

$$\begin{aligned} h_{11} =& \Lambda_n e(A_1 M + \sigma f n^2\pi^2) + \Lambda_n^2 e(Me\sigma + B_1) + f\bar{b}n^2\pi^2 + B_1 M + \\ & e^2\Lambda_n^3 A_1 + e^3\sigma\Lambda_n^4, \\ h_{12} =& - B_1\Lambda_n - eA_1\Lambda_n^2 - e^2\sigma\Lambda_n^3 + \eta f n^2\pi^2, \\ h_{13} =& B_1 + e\Lambda_n A_1 + e^2\sigma\Lambda_n^2, \\ h_{21} =& \Lambda_n(e\sigma n^2\pi^2\eta f - \bar{b}B_1) + \eta f n^2\pi^2\bar{b} - \Lambda_n^2 eC - \Lambda_n^3 e^2\sigma(A_1 + \bar{b}) - \Lambda_n^4\sigma^2 e^3, \\ h_{22} =& \Lambda_n e(CN + \eta^2 f A_1 n^2\pi^2) + \Lambda_n^2 e\sigma[e(A_1 + \bar{b})N + \bar{b}B_1 + e\eta^2 f n^2\pi^2] + \\ & B_1\bar{b}N + e^2\Lambda_n^3\sigma(C + e\sigma N) + \Lambda_n^4 e^3\sigma^2(A_1 + \bar{b}) + \Lambda_n^5 e^4\sigma^3 + \eta^2 f n^2\pi^2\bar{a}\bar{b}, \\ h_{23} =& \bar{b}B_1 + e\Lambda_n C + \Lambda_n^2 e^2\sigma(A_1 + \bar{b}) + e^3\sigma^2\Lambda_n^3, \end{aligned}$$

(3.15) can be written as

$$\begin{cases} h_{11}W_0^f + h_{12}W_0^p - Ra^2 h_{13}\Theta_0 = 0, \\ h_{21}W_0^f + h_{22}W_0^p - Ra^2 h_{23}\Theta_0 = 0, \\ RW_0^f + RW_0^p - (\Lambda_n + \overline{\sigma})\Theta_0 = 0. \end{cases} \tag{3.17}$$

Requiring zero determinant for system (3.17), one gets

$$R^2 = \frac{\Lambda_n + \overline{\sigma}}{a^2} \frac{h_{11}h_{22} - h_{12}h_{21}}{h_{13}h_{22} - h_{12}h_{23} + h_{11}h_{23} - h_{21}h_{13}}. \tag{3.18}$$

The growth rate of the system is $\overline{\sigma} = \sigma_R + i\sigma_I$, then (3.18) is

$$\begin{aligned} R^2 = & \frac{(\Lambda_n + \sigma_R)(h_{11}h_{22} - h_{12}h_{21})}{a^2(h_{12}h_{23} - h_{13}h_{22} - h_{11}h_{23} + h_{21}h_{13})} \\ & + i\frac{\sigma_I(h_{11}h_{22} - h_{12}h_{21})}{a^2(h_{12}h_{23} - h_{13}h_{22} - h_{11}h_{23} + h_{21}h_{13})} \end{aligned} \tag{3.19}$$

but the Rayleigh number R^2 is real, therefore one obtains

$$\sigma_I \frac{h_{11}h_{22} - h_{12}h_{21}}{a^2(h_{12}h_{23} - h_{13}h_{22} - h_{11}h_{23} + h_{21}h_{13})} = 0, \tag{3.20}$$

where both numerator $h_{11}h_{22} - h_{12}h_{21}$ and denominator $h_{12}h_{23} - h_{13}h_{22} - h_{11}h_{23} + h_{21}h_{13}$ are strictly positive. From (3.20) it follows necessarily $\sigma_I = 0$, i.e. $\overline{\sigma} \in \mathbb{R}$ and *the strong form of the principle of exchange of stability holds*: oscillatory convection cannot arise. The smallest value of R^2 which vanishes the determinant of (3.17) for $\overline{\sigma} = 0$ is the steady critical Rayleigh number for the onset of instability, i.e.

$$R_L^2 = \min_{(n,a^2)\in\mathbb{N}\times\mathbb{R}^+} f_L^2(n, a^2) \tag{3.21}$$

with

$$f_L^2(n, a^2) = \frac{\Lambda_n}{a^2} \frac{(h_{11}h_{22} - h_{12}h_{21})}{h_{13}h_{22} - h_{12}h_{23} + h_{11}h_{23} - h_{21}h_{13}}. \tag{3.22}$$

We have proved that: i) both numerator and denominator of (3.22) are strictly positive; ii) the minimum of f_L^2 with respect to n, by using numerical computations, is attained at $n = 1$. Hence

$$R_L^2 = \min_{a^2\in\mathbb{R}^+} f_L^2(1, a^2). \tag{3.23}$$

The minimum of $f_L^2(1, a^2)$ with respect to a^2 is analysed in Section 3.4.

Remark 3.2.1. *Let us observe that:*

i) if one assumes the validity of the Darcy's law ($Da_f = 0$), from (3.21) *one gets:*

$$R_L^2 = \min_{n,a^2} \frac{\Lambda_n}{a^2} \frac{B_1 MN - B_1\Lambda_n^2 + \eta^2 f^2 n^4\pi^4 + fn^2\pi^2(\bar{b}N + \eta^2\bar{a}M + 2\eta\Lambda_n)}{B_1(M + N + 2\Lambda_n) + fn^2\pi^2(\bar{a}\eta^2 - 2\eta + \bar{b})} \tag{3.24}$$

which coincides with the critical threshold found in [22];

ii) if $Da_f = 0$ and $h = k = 1$ (isotropic case), from (3.21) *one obtains the critical Rayleigh number found in [21], i.e.*

$$R_L^2 = \min_{n,a^2} \frac{\Lambda_n}{a^2} \frac{\Gamma^2\Lambda_n^2 + \gamma_1^2\mathcal{T}^2 n^2\pi^2\Lambda_n[\eta^2(\gamma_1+1)^2 + (\gamma_2+1)^2 + 2\eta] + \gamma_1^4\mathcal{T}^4 n^4\pi^4\eta^2}{\Gamma\Lambda_n(\gamma_1+\gamma_2+4) + \gamma_1^2\mathcal{T}^2 n^2\pi^2[\eta^2\gamma_1 + \gamma_2 + (\eta-1)^2]}$$

where $\Gamma = \gamma_1\gamma_2 + \gamma_1 + \gamma_2$;

iii) if $h = k = 1$, $\tilde{\mu}_p = 0$, in the limit as $\mathcal{T} \to 0$, i.e. assuming the validity of the Brinkman's law only in the momentum equation for the macropores and in the absence of rotation, from (3.21) *one obtains*

$$R^2 = \min_{n,a^2} \frac{\Lambda_n^2}{a^2} \frac{\gamma_1\gamma_2 + \gamma_1 + \gamma_2 + e(\gamma_2+1)\Lambda_n}{e\Lambda_n + \gamma_1 + \gamma_2 + 4} \tag{3.25}$$

and (3.25) *coincides with the critical threshold found in [20].*

3.3 Nonlinear stability of the conduction solution

In order to study the nonlinear stability of the conduction solution, by virtue of (3.7), since

$$\Psi \equiv \bar{a}\bar{b} - eA_1\Delta + e^2\sigma\Delta^2 - 1\,, \quad \Psi B \equiv \bar{b}B_1 - eC\Delta + e^2\sigma(A_1 + \bar{b})\Delta^2 - e^3\sigma^2\Delta^3$$

(3.12) and $(3.4)_5$ can be written as

$$\begin{cases} L_1 w^f + L_2 w^p + RL_3\theta = 0, \\ M_1 w^f + M_2 w^p + RM_3\theta = 0, \\ \theta_{,t} + (\mathbf{u}^f + \mathbf{u}^p)\cdot\nabla\theta = R(w^f + w^p) + \Delta\theta, \end{cases} \tag{3.26}$$

where the following differential operators have been defined

$$\begin{aligned}
L_1 \equiv & -\overline{a}B_1\partial_{zz} + e(\overline{a}A_1 + \sigma f)\partial_{zz}\Delta - f\overline{b}\partial_{zz} - \hat{\gamma}_1 B_1\Delta_1 - \overline{a}\sigma e^2\Delta^2\partial_{zz} \\
& + \hat{\gamma}_1 eA_1\Delta\Delta_1 - \hat{\gamma}_1 e^2\sigma\Delta^2\Delta_1 + eB_1\Delta^2 - e^2A_1\Delta^3 + e^3\sigma\Delta^4, \\
L_2 \equiv & B_1\Delta_1 + B_1\partial_{zz} - eA_1\Delta^2 + e^2\sigma\Delta^3 - \eta f\partial_{zz}, \\
L_3 \equiv & B_1\Delta_1 - eA_1\Delta\Delta_1 + e^2\sigma\Delta^2\Delta_1 \\
M_1 \equiv & \overline{b}B_1\Delta - eC\Delta^2 + e^2\sigma(A_1 + \overline{b})\Delta^3 - e^3\sigma^2\Delta^4 - \overline{b}\eta f\partial_{zz} + e\eta f\sigma\Delta\partial_{zz}, \\
M_2 \equiv & -\overline{b}(\overline{b}B_1 + \overline{a}\eta^2 f)\partial_{zz} + \sigma e\overline{b}B_1\Delta^2 - \hat{\gamma}_2\overline{b}B_1\Delta_1 \\
& + e(\overline{b}C + \eta^2 fA_1)\Delta\partial_{zz} - e^2\sigma[\overline{b}(A_1 + \overline{b}) + \eta^2 f]\Delta^2\partial_{zz} + e^3\overline{b}\sigma\Delta^3\partial_{zz} \\
& + \hat{\gamma}_2 eC\Delta\Delta_1 - \hat{\gamma}_2 e^2\sigma(A_1 + \overline{b})\Delta^2\Delta_1 \\
& + \hat{\gamma}_2 e^3\sigma^2\Delta^3\Delta_1 - \sigma e^2C\Delta^3 + \sigma^2e^3(A_1 + \overline{b})\Delta^4 - e^4\sigma^3\Delta^5, \\
M_3 \equiv & \overline{b}B_1\Delta_1 - eC\Delta\Delta_1 + e^2\sigma(A_1 + \overline{b})\Delta^2\Delta_1 - e^3\sigma^2\Delta^3\Delta_1.
\end{aligned}$$

To determine the nonlinear stability threshold, in order to evaluate the rotation effect, it is not possible to proceed via a standard energy analysis, since the Coriolis terms in the momentum equations are antisymmetric. For this reason, we employ the differential constraint approach (see [38, 42, 43]) and set

$$E(t) = \frac{1}{2}\|\theta\|^2, \tag{3.27}$$

$$I(t) = (w^f + w^p, \theta), \quad D(t) = \|\nabla\theta\|^2.$$

Retaining $(3.26)_{1,2}$ as constraints, multiplying $(3.26)_3$ by θ and integrating over the periodicity cell, one gets

$$\frac{dE}{dt} = RI - D \leq -D\left(1 - \frac{R}{R_E}\right), \tag{3.28}$$

where

$$\frac{1}{R_E} = \max_{\mathcal{H}^*} \frac{I}{D} \tag{3.29}$$

and

$$\begin{aligned}
\mathcal{H}^* = \{ & (w^f, w^p, \theta) \in (H^1)^3 | w^f = w^p = \theta = 0 \text{ on } z = 0,1; \text{periodic in } x, y \\
& \text{with periods } 2\pi/l, 2\pi/m; D < \infty; \text{verifying } (3.26)_{1,2} \}
\end{aligned}$$

is the space of kinematically admissible solutions.
The variational problem associated to the maximum problem (3.29) is equivalent to

$$\frac{1}{R_E} = \max_{\mathcal{H}} \frac{I + \int_V \lambda' g_1 \, dV + \int_V \lambda'' g_2 \, dV}{D}, \tag{3.30}$$

where $\lambda^{'}(\mathbf{x})$ and $\lambda^{''}(\mathbf{x})$ are *Lagrange multipliers* and

$$g_1 = L_1 w^f + L_2 w^p + RL_3\theta, \quad g_2 = M_1 w^f + M_2 w^p + RM_3\theta,$$

$$\mathcal{H} = \{(w^f, w^p, \theta) \in (H^1)^3 | w^f = w^p = \theta = 0 \text{ on } z = 0,1; \text{periodic in } x, y \text{ with periods } 2\pi/l, 2\pi/m, \text{ respectively}; D < \infty\}.$$

Applying the Poincaré inequality, one obtains that $D \geq \pi^2\|\theta\|^2$, hence from (3.28) it follows that the condition $R < R_E$ implies $E(t) \to 0$ at least exponentially.

Remark 3.3.1. *Multiplying* $(3.4)_1$ *by* $\mathbf{u}^f$, $(3.4)_2$ *by* $\mathbf{u}^p$, *integrating over the period cell* V *and adding the resulting equations one finds*

$$\begin{aligned}\gamma_1\int_V\Big\{k^{-1}[(u^f)^2+(v^f)^2]+(w^f)^2\Big\}dV+\gamma_2\int_V\Big\{h^{-1}[(u^p)^2+(v^p)^2]+(w^p)^2\Big\}dV\\ +\|\mathbf{u}^f-\mathbf{u}^p\|^2 = R(\theta, w^f+w^p) - Da_f\gamma_1\|\nabla\mathbf{u}^f\|^2 - \sigma Da_f\gamma_1\|\nabla\mathbf{u}^p\|^2.\end{aligned} \tag{3.31}$$

Setting $\hat{k} = \max(k,1)$ *and* $\hat{h} = \max(h,1)$, *by virtue of generalized Cauchy inequality and Poincaré-like inequality, from* (3.31) *one obtains*

$$\Big(\frac{\gamma_1}{\hat{k}}+2Da_f\gamma_1c_1\Big)\|\mathbf{u}^f\|^2+\Big(\frac{\gamma_2}{\hat{h}}+2Da_f\gamma_1\sigma c_2\Big)\|\mathbf{u}^p\|^2 \leq R^2\Big(\frac{\hat{k}}{\gamma_1}+\frac{\hat{h}}{\gamma_2}\Big)\|\theta\|^2 \tag{3.32}$$

where c_1, c_2 *are positive constants depending on the domain* V. *By virtue of* (3.32), *the condition* $R < R_E$ *also guarantees the exponential decay of* $\mathbf{u}^f$ *and* $\mathbf{u}^p$.

In order to determine the critical Rayleigh number R_E^2 by solving the variational problem (3.30), we need to solve the associated Euler-Lagrange equations given by

$$\begin{cases} R_E(w^f+w^p) + R_E L_3\lambda^{'} + R_E M_3\lambda^{''} + 2\Delta\theta = 0,\\ R_E\theta + L_1\lambda^{'} + M_1\lambda^{''} = 0,\\ R_E\theta + L_2\lambda^{'} + M_2\lambda^{''} = 0,\\ L_1 w^f + L_2 w^p + RL_3\theta = 0,\\ M_1 w^f + M_2 w^p + RM_3\theta = 0.\end{cases} \tag{3.33}$$

Eliminating the variable θ in (3.33) it turns out that

$$\begin{cases} -R_E^2 w^f - R_E^2 w^p + (2\Delta L_1 - R_E^2 L_3)\lambda^{'} + (2\Delta M_1 - R_E^2 M_3)\lambda^{''} = 0,\\ -R_E^2 w^f - R_E^2 w^p + (2\Delta L_2 - R_E^2 L_3)\lambda^{'} + (2\Delta M_2 - R_E^2 M_3)\lambda^{''} = 0,\\ (2\Delta L_1 - R_E^2 L_3)w^f + (2\Delta L_2 - R_E^2 L_3)w^p - R_E^2 L_3^2\lambda^{'} - R_E^2 L_3 M_3\lambda^{''} = 0,\\ (2\Delta M_1 - R_E^2 M_3)w^f + (2\Delta M_2 - R_E^2 M_3)w^p - R_E^2 L_3 M_3\lambda^{'} - R_E^2 M_3^2\lambda^{''} = 0.\end{cases} \tag{3.34}$$

By using $(3.14)_1$ and $(3.14)_2$ and choosing [42]

$$\begin{aligned} \lambda' &= \lambda_0' \sin(n\pi z) e^{i(lx+my)}, \\ \lambda'' &= \lambda_0'' \sin(n\pi z) e^{i(lx+my)}, \end{aligned} \tag{3.35}$$

from (3.34) one obtains

$$\begin{cases} -R_E^2 W_0^f - R_E^2 W_0^p + (-2\Lambda_n h_{11} + R_E^2 a^2 h_{13})\lambda_0' + \\ \quad (-2\Lambda_n h_{21} + R_E^2 a^2 h_{23})\lambda_0'' = 0, \\ -R_E^2 W_0^f - R_E^2 W_0^p + (-2\Lambda_n h_{12} + R_E^2 a^2 h_{13})\lambda_0' + \\ \quad (-2\Lambda_n h_{22} + R_E^2 a^2 h_{23})\lambda_0'' = 0, \\ (-2\Lambda_n h_{11} + R_E^2 a^2 h_{13}) W_0^f + (-2\Lambda_n h_{12} + R_E^2 a^2 h_{13}) W_0^p \\ \quad -R_E^2 a^4 h_{13}^2 \lambda_0' - R_E^2 a^4 h_{13} h_{23} \lambda_0'' = 0, \\ (-2\Lambda_n h_{21} + R_E^2 a^2 h_{23}) W_0^f + (-2\Lambda_n h_{22} + R_E^2 a^2 h_{23}) W_0^p \\ \quad -R_E^2 a^4 h_{13} h_{23} \lambda_0' - R_E^2 a^4 h_{23}^2 \lambda_0'' = 0. \end{cases} \tag{3.36}$$

Requiring a *zero determinant* for (3.36) we get

$$R_E^2 = R_L^2,$$

hence we have the coincidence between the instability threshold and the global nonlinear stability threshold with respect to the L^2-norm (subcritical instabilities do not exist).

3.4 Numerical results

In this section we numerically analyse the asymptotic behaviour of R_L^2 with respect to parameters h, k, $\mathcal{T}^2$, Da_f in order to study the influence of permeability, rotation and Brinkman law on the onset of convection. As pointed out in Section 3.2, in all the performed computations we set $n = 1$.

The tables 3.1 and 3.2 show that as h increases with k fixed, both critical Rayleigh and wave numbers decrease, so it is easier for convection to sets in and convection cells become wider; k increasing with h fixed leads to a similar trend, but in this case the Rayleigh number decreases *more slowly*, as we can see also from figure 3.1. These numerical simulations show that h and k have a destabilizing effect on the onset of convection (see also figure 3.4).

Table 3.3 and figure 3.2 show an expected behaviour: the Brinkman term

has a stabilizing effect on the onset of convection, i.e. as Da_f increases, the Rayleigh number increases and the system becomes more stable. Also, comparing the critical Rayleigh number R_L^2 in Table 3.4(a) for $Da_f = 0.001$ with that one in Table 3.4(b) for $Da_f = 1$, the stabilizing effect of Da_f arises.
The tables 3.4 − 3.5 and figures 3.3 display a similar trend, as the Taylor number $\mathcal{T}^2$ increases, the critical Rayleigh number increases, so the heat transfer due to convection is inhibited and rotation has a stabilizing effect on the onset of convection, as we expected. As $\mathcal{T}^2$ increases, the wavenumber a^2 also increases and this means that convection cells become narrower.

R_L^2	a_c^2	h
326.5116	7.6377	0.1
211.6567	6.1968	0.5
190.6873	5.7021	1
171.6278	5.1756	5
169.0585	5.0986	10

Table 3.1: Critical Rayleigh and wave numbers for $k = 1, \eta = 0.2, \sigma = 0.3, \gamma_1 = 0.9, \gamma_2 = 1.8, \mathcal{T}^2 = 10, Da_f = 1$ at different h.

R_L^2	a_c^2	k
208.1330	6.2007	0.1
192.9895	5.7772	0.5
190.6873	5.7021	1
188.7616	5.6372	5
188.5154	5.6287	10

Table 3.2: Critical Rayleigh and wave numbers for $h = 1, \eta = 0.2, \sigma = 0.3, \gamma_1 = 0.9, \gamma_2 = 1.8, \mathcal{T}^2 = 10, Da_f = 1$ at different k.

R_L^2	a_c^2	Da_f
56.3828	13.7917	0.001
100.9334	5.4036	0.5
169.0585	5.0986	1
716.2302	4.9566	5

Table 3.3: Critical Rayleigh and wave numbers for $h = 10, k = 1, \eta = 0.2, \sigma = 0.3, \gamma_1 = 0.9, \gamma_2 = 1.8, \mathcal{T}^2 = 10$ at different Darcy numbers. A typical *small* Darcy number is $Da_f = 0.001$, while a typical Darcy number is $Da_f = 1$ [4].

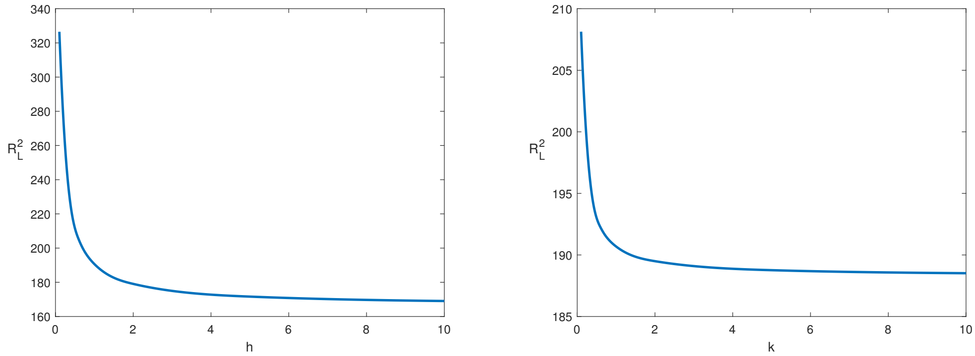

(a) (b)

Figure 3.1: (a): asymptotic behaviour of R_L^2 with respect to h for $k = 1, \eta = 0.2, \sigma = 0.3, \gamma_1 = 0.9, \gamma_2 = 1.8, \mathcal{T}^2 = 10, Da_f = 1$. (b): asymptotic behaviour of R_L^2 with respect to k for $h = 1, \eta = 0.2, \sigma = 0.3, \gamma_1 = 0.9, \gamma_2 = 1.8, \mathcal{T}^2 = 10, Da_f = 1$.

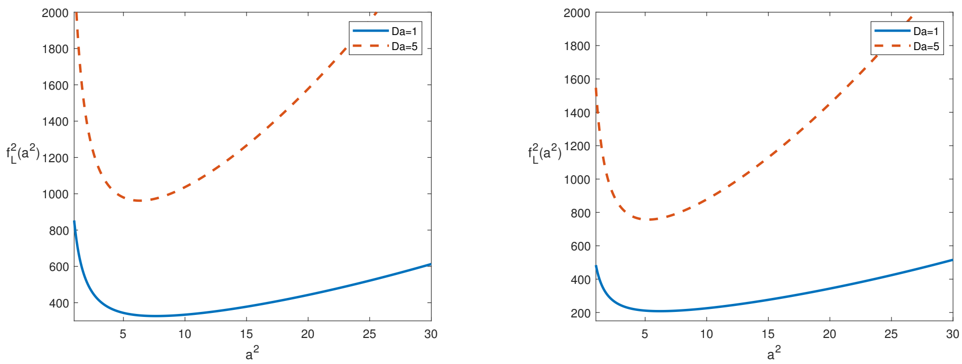

(a) $h = 0.1, k = 1$ (b) $h = 1, k = 0.1$

Figure 3.2: (a): steady instability thresholds at $Da_f = 1, 5$ and $h = 0.1, k = 1, \mathcal{T}^2 = 10, \eta = 0.2, \sigma = 0.3, \gamma_1 = 0.9, \gamma_2 = 1.8$. (b): steady instability thresholds at $h = 1, k = 0.1, \mathcal{T}^2 = 10, \eta = 0.2, \sigma = 0.3, \gamma_1 = 0.9, \gamma_2 = 1.8$.

Main results

The onset of thermal convection in an anisotropic BDPM, uniformly rotating about a vertical axis and uniformly heated from below, was analysed according to Brinkman law in both micropores and macropores. In particular, it was proved that:

(a) $Da_f = 0.001$

R_L^2	a_c^2	$\mathcal{T}^2$
52.2521	12.8790	0
52.7216	13.0444	0.1
54.5534	13.6882	0.5
56.7498	14.4563	1
71.7551	19.5421	5
86.7523	24.7523	10
211.5075	39.0022	100

(b) $Da_f = 1$

R_L^2	a_c^2	$\mathcal{T}^2$
323.9093	7.4974	0
323.9359	7.4988	0.1
324.0419	7.5046	0.5
324.1741	7.5118	1
325.2230	7.5685	5
326.5116	7.6377	10
346.4686	8.6407	100

Table 3.4: Critical Rayleigh and wave numbers for increasing Taylor numbers. *Table a*: $h = 0.1, k = 1, \eta = 0.2, \sigma = 0.3, \gamma_1 = 0.9, \gamma_2 = 1.8, Da_f = 0.001$. *Table b*: $h = 0.1, k = 1, \eta = 0.2, \sigma = 0.3, \gamma_1 = 0.9, \gamma_2 = 1.8, Da_f = 1$.

(a) $h = 1, k = 0.1$

R_L^2	a_c^2	$\mathcal{T}^2$
206.8022	6.1510	0
206.8155	6.1515	0.1
206.8690	6.1535	0.5
206.9358	6.1560	1
207.4692	6.1760	5
208.1330	6.2007	10

(b) $h = 0.1, k = 1$

R_L^2	a_c^2	$\mathcal{T}^2$
323.9093	7.4974	0
323.9359	7.4988	0.1
324.0419	7.5046	0.5
324.1741	7.5118	1
325.2230	7.5685	5
326.5116	7.6377	10

Table 3.5: Critical Rayleigh and wave numbers for increasing Taylor numbers. *Table a*: $h = 1, k = 0.1, \eta = 0.2, \sigma = 0.3, \gamma_1 = 0.9, \gamma_2 = 1.8, Da_f = 1$. *Table b*: $h = 0.1, k = 1, \eta = 0.2, \sigma = 0.3, \gamma_1 = 0.9, \gamma_2 = 1.8, Da_f = 1$.

- the strong form of the principle of exchange of stabilities holds and hence, when convection occurs, it sets in through a stationary motion;
- the linear instability threshold and the global nonlinear stability threshold in the L^2-norm coincide: this is an optimal result since the stability threshold furnishes a necessary and sufficient condition to guarantee the global (i.e. for all initial data) nonlinear stability;
- the critical Rayleigh number for the onset of convection increases with the Taylor number, i.e. rotation has a stabilizing effect on the onset of convection;
- the critical Rayleigh number for the onset of convection increases with the Darcy number, i.e. the Brinkman law has a stabilizing effect.

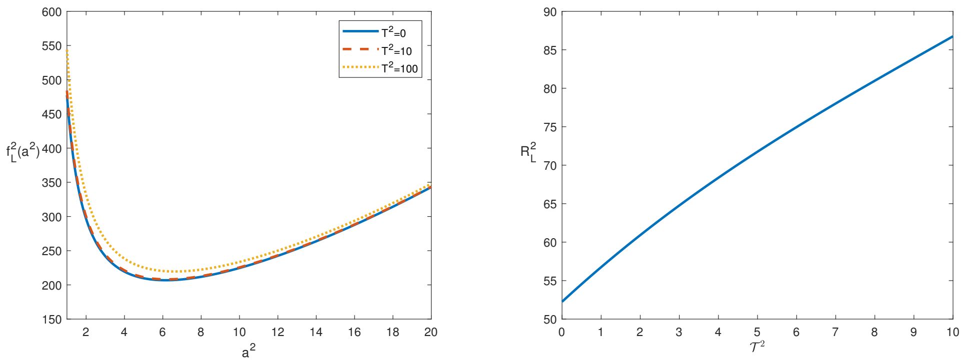

(a) (b)

Figure 3.3: (a): steady instability thresholds at $\mathcal{T}^2 = 0, 10, 100$ and for $h = 0.1, k = 10, Da_f = 1, \eta = 0.2, \sigma = 0.3, \gamma_1 = 0.9, \gamma_2 = 1.8$. (b): asymptotic behavior of R_L^2 with respect to $\mathcal{T}^2$ for $h = 0.1, k = 1, \eta = 0.2, \sigma = 0.3, \gamma_1 = 0.9, \gamma_2 = 1.8, Da_f = 0.001$

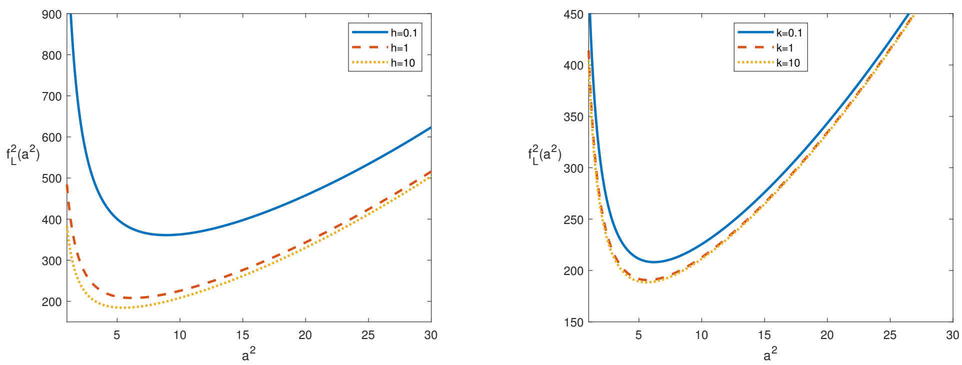

(a) (b)

Figure 3.4: (a): steady instability thresholds at $h = 0.1, 1, 10$ and $k = 1, \mathcal{T}^2 = 10, \eta = 0.2, \sigma = 0.3, \gamma_1 = 0.9, \gamma_2 = 1.8, Da_f = 1$. (b): steady instability thresholds at $k = 0.1, 1, 10$ and $h = 1, \mathcal{T}^2 = 10, \eta = 0.2, \sigma = 0.3, \gamma_1 = 0.9, \gamma_2 = 1.8, Da_f = 1$.

Chapter 4

The effects of Vadasz term, anisotropy and rotation on bi-disperse convection

The goal of the present Chapter is to analyse the combined effects of anisotropic permeabilities, uniform rotation about a vertical axis and inertia on the onset of thermal convection in an incompressible fluid saturating a single temperature bi-disperse porous medium.
The *Vadasz term* effect has been largely analysed by many authors in single porosity media (see for instance [39, 44, 45, 46]) since the Vadasz term has a remarkable effect on the onset of convection in a rotating porous layer. In this regard, a very interesting work is [30] by Vadasz, where the onset of convection in a fluid-saturated porous medium that rotates about an axis orthogonal to the layer in the direction of gravity, is investigated. Through linear instability and weakly nonlinear techniques, the author finds out that if the inertia term is taken into account in the momentum equation, convection may set in via oscillatory motions.
On the other hand, the effect of Vadasz term on the onset of bi-disperse convection has been investigated by Straughan in [47] — where he considered a fluid mixture saturating a BDPM — and by Capone and De Luca in [23], which deals with an isotropic and rotating BDPM.
From a mathematical point of view, to analyse how inertia affects the onset of convection, the Darcy's model has to be extended with a time derivative of the seepage velocity, that is an additional term that accounts for time dynamics of the evolving values of the seepage velocity.

The present Chapter is based on the joint paper [48] with F. Capone and is organized as follows. In Section 4.1 the mathematical model and the associated perturbation equations are introduced. In Section 4.2 we perform linear instability analysis of the thermal conduction solution, in particular, we find out that the Vadasz term allows the onset of thermal convection via an oscillatory state (named as oscillatory convection), but it does not directly affect the onset of thermal convection via a steady state (named as stationary convection). In Sections 4.2.1 and 4.2.2 we determine the critical Rayleigh numbers for the onset of steady and oscillatory convection, respectively. In Section 4.3 we perform numerical simulations in order to analyse the behaviour of the instability thresholds with respect to fundamental parameters.

4.1 Statement of the Problem

Let $Oxyz$ be a reference frame with fundamental unit vectors $\mathbf{i}, \mathbf{j}, \mathbf{k}$ and let us assume that the plane layer L, of thickness d, of saturated bi-disperse porous medium is uniformly heated from below and rotates about the vertical axis z, let $\boldsymbol{\Omega} = \Omega\mathbf{k}$ be the constant angular velocity of the layer. Furthermore, we consider a single temperature bi-disperse porous medium, i.e. $T^f = T^p = T$. We restrict our attention to the case in which the permeabilities of the saturated bi-disperse porous medium are *horizontally isotropic*.
Let the axes (x, y, z) be the *principal axes* of the permeabilities, so the macropermeability tensor and the micropermeability tensor may be written as

$$\mathbf{K}^f = \mathrm{diag}(K_x^f, K_y^f, K_z^f) = K_z^f \; \mathbf{K}^{f*},$$
$$\mathbf{K}^p = \mathrm{diag}(K_x^p, K_y^p, K_z^p) = K_z^p \; \mathbf{K}^{p*},$$
$$\mathbf{K}^{f*} = \mathrm{diag}(k, k, 1),$$
$$\mathbf{K}^{p*} = \mathrm{diag}(h, h, 1),$$

where

$$k = \frac{K_x^f}{K_z^f} = \frac{K_y^f}{K_z^f},$$
$$h = \frac{K_x^p}{K_z^p} = \frac{K_y^p}{K_z^p}.$$

Darcy's model, with the Oberbeck-Boussinesq approximation, is employed, in particular it is extended in both micropores and macropores in order to include the Coriolis terms and is extended only in the macropores to include the time derivative term of the macro seepage velocity (see [23, 47]). The equations describing the evolutionary behaviour of thermal convection in a rotating horizontally isotropic bi-disperse porous medium are, cf. [23, 21],

$$\begin{cases} \varrho_F c_a \dfrac{\partial \mathbf{v}^f}{\partial t} = -\mu(\mathbf{K}^f)^{-1}\mathbf{v}^f - \zeta(\mathbf{v}^f - \mathbf{v}^p) - \nabla p^f + \varrho_F \alpha g T \mathbf{k} - \dfrac{2\varrho_F \Omega}{\varphi}\mathbf{k}\times\mathbf{v}^f, \\ -\mu(\mathbf{K}^p)^{-1}\mathbf{v}^p - \zeta(\mathbf{v}^p - \mathbf{v}^f) - \nabla p^p + \varrho_F \alpha g T \mathbf{k} - \dfrac{2\varrho_F \Omega}{\epsilon}\mathbf{k}\times\mathbf{v}^p = \mathbf{0}, \\ \nabla\cdot\mathbf{v}^f = 0, \\ \nabla\cdot\mathbf{v}^p = 0, \\ (\varrho c)_m \dfrac{\partial T}{\partial t} + (\varrho c)_f(\mathbf{v}^f + \mathbf{v}^p)\cdot\nabla T = k_m \Delta T, \end{cases} \tag{4.1}$$

where

$$p^s = P^s - \frac{\varrho_F}{2}|\mathbf{\Omega}\times\mathbf{x}|^2, \quad s = \{f, p\}$$

are the reduced pressures, $\mathbf{x} = (x, y, z)$, $\mathbf{v}^s$ = seepage velocity for $s = \{f, p\}$, ζ = interaction coefficient between the f-phase and the p-phase, $\mathbf{g} = -g\mathbf{k}$ = gravity, μ = fluid viscosity, ϱ_F = reference constant density, α = thermal expansion coefficient, c = specific heat, c_p = specific heat at a constant pressure, c_a= acceleration coefficient, $(\varrho c)_m = (1-\varphi)(1-\epsilon)(\varrho c)_{sol} + \varphi(\varrho c)_f + \epsilon(1-\varphi)(\varrho c)_p$, $k_m = (1-\varphi)(1-\epsilon)k_{sol} + \varphi k_f + \epsilon(1-\varphi)k_p$ = thermal conductivity (the subscript *sol* is referred to the solid skeleton).

To 4.1 the following boundary conditions are appended

$$\begin{array}{l} \mathbf{v}^s\cdot\mathbf{n} = 0 \text{ on } z = 0, d, \text{ for } s = \{f, p\} \\ T = T_L \text{ on } z = 0, \quad T = T_U \text{ on } z = d, \end{array} \tag{4.2}$$

where $T_L > T_U$.

System (4.1)-(4.2) admits the stationary conduction solution:

$$\overline{\mathbf{v}}^f = 0, \ \overline{\mathbf{v}}^p = 0, \ \overline{T} = -\beta z + T_L,$$

where $\beta = \dfrac{T_L - T_U}{d}$ is the temperature gradient. Denoting by $\{\mathbf{u}^f, \mathbf{u}^p, \theta, \pi^f, \pi^p\}$ a generic perturbation to the steady solution, the resulting perturbation equations are

$$\begin{cases} \varrho_F c_a \dfrac{\partial \mathbf{u}^f}{\partial t} = -\mu(\mathbf{K}^f)^{-1}\mathbf{u}^f - \zeta(\mathbf{u}^f - \mathbf{u}^p) - \nabla \pi^f + \varrho_F \alpha g \theta \mathbf{k} - \dfrac{2\varrho_F \Omega}{\varphi}\mathbf{k}\times\mathbf{u}^f, \\ -\mu(\mathbf{K}^p)^{-1}\mathbf{u}^p - \zeta(\mathbf{u}^p - \mathbf{u}^f) - \nabla \pi^p + \varrho_F \alpha g \theta \mathbf{k} - \dfrac{2\varrho_F \Omega}{\epsilon}\mathbf{k}\times\mathbf{u}^p = \mathbf{0}, \\ \nabla\cdot\mathbf{u}^f = 0, \\ \nabla\cdot\mathbf{u}^p = 0, \\ (\varrho c)_m \dfrac{\partial \theta}{\partial t} + (\varrho c)_f(\mathbf{u}^f + \mathbf{u}^p)\cdot\nabla\theta = (\varrho c)_f\beta(w^f + w^p) + k_m\Delta\theta. \end{cases} \tag{4.3}$$

where $\mathbf{u}^f = (u^f, v^f, w^f)$ and $\mathbf{u}^p = (u^p, v^p, w^p)$. The above system (4.3) may be non-dimensionalized with the following non-dimensional parameters

$$\begin{aligned}
&\mathbf{x}^* = \frac{\mathbf{x}}{d},\ t^* = \frac{t}{\tilde{t}},\ \theta^* = \frac{\theta}{\tilde{T}},\\
&\mathbf{u}^{s*} = \frac{\mathbf{u}^s}{\tilde{u}},\ \pi^{s*} = \frac{\pi^s}{\tilde{P}},\ \text{for } s = \{f, p\}\\
&\eta = \frac{\varphi}{\epsilon},\ \gamma = \frac{K_z^f \zeta}{\mu},\ K_r = \frac{K_z^f}{K_z^p},
\end{aligned}$$

where the scales are given by

$$\tilde{u} = \frac{k_m}{(\varrho c)_f d},\ \tilde{t} = \frac{d^2(\varrho c)_m}{k_m},\ \tilde{P} = \frac{\mu k_m}{(\varrho c)_f K_z^f},\ \tilde{T} = \sqrt{\frac{\beta k_m \mu}{(\varrho c)_f \varrho_F \alpha g K_z^f}}.$$

The resulting non-dimensional perturbation equations, dropping all the asterisks, are

$$\begin{cases}
-J\dfrac{\partial \mathbf{u}^f}{\partial t} - (\mathbf{K}^f)^{-1}\mathbf{u}^f - \gamma(\mathbf{u}^f - \mathbf{u}^p) - \nabla \pi^f + R\theta\mathbf{k} - \mathcal{T}\mathbf{k}\times\mathbf{u}^f = \mathbf{0},\\
-K_r(\mathbf{K}^p)^{-1}\mathbf{u}^p - \gamma(\mathbf{u}^p - \mathbf{u}^f) - \nabla\pi^p + R\theta\mathbf{k} - \eta\mathcal{T}\mathbf{k}\times\mathbf{u}^p = \mathbf{0},\\
\nabla\cdot\mathbf{u}^f = 0,\\
\nabla\cdot\mathbf{u}^p = 0,\\
\dfrac{\partial\theta}{\partial t} + (\mathbf{u}^f + \mathbf{u}^p)\cdot\nabla\theta = w^f + w^p + \Delta\theta,
\end{cases} \tag{4.4}$$

where the Taylor number $\mathcal{T}$, the Vadasz number J and the Rayleigh number R are

$$\mathcal{T} = \frac{2\varrho_F \Omega K_z^f}{\varphi\mu}, \quad J = \frac{K_z^f \varrho_F c_a k_m}{\mu d^2 (\varrho c)_m}, \quad R = \sqrt{\frac{\beta d^2 (\varrho c)_f \varrho_F \alpha g K_z^f}{k_m \mu}}.$$

To system (4.4) the following initial and boundary conditions are appended:

$$\mathbf{u}^s(\mathbf{x}, 0) = \mathbf{u}_0^s(\mathbf{x}), \quad \pi^s(\mathbf{x}, 0) = \pi_0^s(\mathbf{x}), \quad \theta(\mathbf{x}, 0) = \theta_0(\mathbf{x}),$$

with $\nabla\cdot\mathbf{u}_0^s = 0$, for $s = \{f, p\}$, and

$$w^f = w^p = \theta = 0 \quad \text{on } z = 0, 1. \tag{4.5}$$

According to experimental results, the solutions are required to be periodic in the horizontal directions x and y and in the sequel we will denote by

$$V = \left[0, \frac{2\pi}{l}\right] \times \left[0, \frac{2\pi}{m}\right] \times [0, 1]$$

the periodicity cell.

4.2 Onset of convective flows

In order to determine the linear instability threshold of the thermal conduction solution, let us linearise system (4.4), i.e.

$$\begin{cases} -J\dfrac{\partial \mathbf{u}^f}{\partial t} - (\mathbf{K}^f)^{-1}\mathbf{u}^f - \gamma(\mathbf{u}^f - \mathbf{u}^p) - \nabla\pi^f + R\theta\mathbf{k} - \mathcal{T}\mathbf{k}\times\mathbf{u}^f = \mathbf{0}, \\ -K_r(\mathbf{K}^p)^{-1}\mathbf{u}^p - \gamma(\mathbf{u}^p - \mathbf{u}^f) - \nabla\pi^p + R\theta\mathbf{k} - \eta\mathcal{T}\mathbf{k}\times\mathbf{u}^p = \mathbf{0}, \\ \nabla\cdot\mathbf{u}^f = 0, \\ \nabla\cdot\mathbf{u}^p = 0, \\ \dfrac{\partial\theta}{\partial t} = w^f + w^p + \Delta\theta. \end{cases} \tag{4.6}$$

Being system (4.6) autonomous, we seek solutions with time-dependence like $e^{\sigma t}$, i.e.

$$\begin{aligned} \mathbf{u}^s(t,\mathbf{x}) &= e^{\sigma t}\mathbf{u}^s(\mathbf{x}), \\ \theta(t,\mathbf{x}) &= e^{\sigma t}\theta(\mathbf{x}), \\ \pi^s(t,\mathbf{x}) &= e^{\sigma t}\pi^s(\mathbf{x}), \end{aligned} \tag{4.7}$$

with $\sigma \in \mathbb{C}$ and $s = \{f, p\}$. By virtue of (4.7), (4.6) becomes

$$\begin{cases} -J\sigma\mathbf{u}^f - (\mathbf{K}^f)^{-1}\mathbf{u}^f - \gamma(\mathbf{u}^f - \mathbf{u}^p) - \nabla\pi^f + R\theta\mathbf{k} - \mathcal{T}\mathbf{k}\times\mathbf{u}^f = \mathbf{0}, \\ -K_r(\mathbf{K}^p)^{-1}\mathbf{u}^p - \gamma(\mathbf{u}^p - \mathbf{u}^f) - \nabla\pi^p + R\theta\mathbf{k} - \eta\mathcal{T}\mathbf{k}\times\mathbf{u}^p = \mathbf{0}, \\ \nabla\cdot\mathbf{u}^f = 0, \\ \nabla\cdot\mathbf{u}^p = 0, \\ \sigma\theta = w^f + w^p + \Delta\theta. \end{cases} \tag{4.8}$$

Setting

$$\omega_3^s = (\nabla\times\mathbf{u}^s)\cdot\mathbf{k}, \ \ s = \{f, p\},$$

let us consider the third components of curl and of double curl of $(4.8)_{1,2}$, i.e.

$$\begin{cases} (J\sigma + \dfrac{1}{k} + \gamma)\omega_3^f - \gamma\omega_3^p - \mathcal{T}\dfrac{\partial w^f}{\partial z} = 0, \\ (K_r\dfrac{1}{h} + \gamma)\omega_3^p - \gamma\omega_3^f - \eta\mathcal{T}\dfrac{\partial w^p}{\partial z} = 0, \end{cases} \tag{4.9}$$

and

$$\begin{cases} (J\sigma+\dfrac{1}{k}+\gamma)\dfrac{\partial^2 w^f}{\partial z^2}+(J\sigma+1+\gamma)\Delta_1 w^f \\ \quad -\gamma\Big(\Delta_1 w^p+\dfrac{\partial^2 w^p}{\partial z^2}\Big)-R\Delta_1\theta+\mathcal{T}\dfrac{\partial\omega_3^f}{\partial z}=0, \\ \\ (K_r\dfrac{1}{h}+\gamma)\dfrac{\partial^2 w^p}{\partial z^2}+(K_r+\gamma)\Delta_1 w^p \\ \quad -\gamma\Big(\Delta_1 w^f+\dfrac{\partial^2 w^f}{\partial z^2}\Big)-R\Delta_1\theta+\eta\mathcal{T}\dfrac{\partial\omega_3^p}{\partial z}=0, \end{cases} \tag{4.10}$$

where $\Delta_1 \equiv \partial^2/\partial x^2 + \partial^2/\partial y^2$ is the horizontal laplacian. Solving (4.9) with respect to ω_3^f and ω_3^p, one obtains

$$\begin{cases} \omega_3^f = \dfrac{B_1}{H}\mathcal{T}\dfrac{\partial w^f}{\partial z} + \dfrac{\gamma}{H}\eta\mathcal{T}\dfrac{\partial w^p}{\partial z}, \\ \omega_3^p = \dfrac{\gamma}{H}\mathcal{T}\dfrac{\partial w^f}{\partial z} + \dfrac{A_1}{H}\eta\mathcal{T}\dfrac{\partial w^p}{\partial z}, \end{cases} \tag{4.11}$$

where we set

$$A_1 = J\sigma + \frac{1}{k} + \gamma,$$

$$B_1 = K_r\frac{1}{h} + \gamma,$$

$$H = \Big(J\sigma + \frac{1}{k}\Big)\Big(K_r\frac{1}{h} + \gamma\Big) + K_r\frac{1}{h}\gamma.$$

Substituting the derivative with respect to z of (4.11) into (4.10), one gets

$$\begin{cases} \Big(A_1 + \dfrac{B_1}{H}\mathcal{T}^2\Big)\dfrac{\partial^2 w^f}{\partial z^2} + A_2\Delta_1 w^f - \gamma\Delta_1 w^p \\ \quad +\Big(\dfrac{\gamma}{H}\eta\mathcal{T}^2 - \gamma\Big)\dfrac{\partial^2 w^p}{\partial z^2} - R\Delta_1\theta = 0, \\ \\ \Big(\dfrac{\gamma}{H}\eta\mathcal{T}^2 - \gamma\Big)\dfrac{\partial^2 w^f}{\partial z^2} - \gamma\Delta_1 w^f + B_2\Delta_1 w^p \\ \quad +\Big(B_1 + \dfrac{A_1}{H}\eta^2\mathcal{T}^2\Big)\dfrac{\partial^2 w^p}{\partial z^2} - R\Delta_1\theta = 0, \end{cases} \tag{4.12}$$

with $A_2 = J\sigma + 1 + \gamma,\ B_2 = K_r + \gamma$. Hence, considering $(4.12)_{1,2}$ and $(4.8)_5$ we get the following problem in w^f, w^p, θ

$$\begin{cases} \Big(A_1 + \dfrac{B_1}{H}\mathcal{T}^2\Big)\dfrac{\partial^2 w^f}{\partial z^2} + A_2\Delta_1 w^f - \gamma\Delta_1 w^p \\ \quad +\Big(\dfrac{\gamma}{H}\eta\mathcal{T}^2 - \gamma\Big)\dfrac{\partial^2 w^p}{\partial z^2} - R\Delta_1\theta = 0, \\ \Big(\dfrac{\gamma}{H}\eta\mathcal{T}^2 - \gamma\Big)\dfrac{\partial^2 w^f}{\partial z^2} - \gamma\Delta_1 w^f + B_2\Delta_1 w^p \\ \quad +\Big(B_1 + \dfrac{A_1}{H}\eta^2\mathcal{T}^2\Big)\dfrac{\partial^2 w^p}{\partial z^2} - R\Delta_1\theta = 0, \\ \sigma\theta = w^f + w^p + \Delta\theta. \end{cases} \tag{4.13}$$

According to the boundary conditions (4.5) and to the periodicity of the perturbations fields, being $\{\sin(n\pi z)\}_{n\in\mathbb{N}}$ a complete orthogonal system for $L^2([0,1])$, we seek for normal modes solutions

$$\begin{aligned} w^f &= W_0^f \sin(n\pi z)e^{i(lx+my)}, \\ w^p &= W_0^p \sin(n\pi z)e^{i(lx+my)}, \\ \theta &= \Theta_0 \sin(n\pi z)e^{i(lx+my)}, \end{aligned} \tag{4.14}$$

with W_0^f, W_0^p, Θ_0 real constants. Hence, employing normal modes solutions, system (4.13) becomes

$$\begin{cases} -\Big[\Big(A_1 + \dfrac{B_1}{H}\mathcal{T}^2\Big)n^2\pi^2 + A_2 a^2\Big]W_0^f \\ \quad +\Big[\gamma\Lambda_n - \dfrac{\gamma}{H}\eta\mathcal{T}^2 n^2\pi^2\Big]W_0^p + Ra^2\Theta_0 = 0, \\ \Big[\gamma\Lambda_n - \dfrac{\gamma}{H}\eta\mathcal{T}^2 n^2\pi^2\Big]W_0^f \\ \quad -\Big[\Big(B_1 + \dfrac{A_1}{H}\eta^2\mathcal{T}^2\Big)n^2\pi^2 + B_2 a^2\Big]W_0^p + Ra^2\Theta_0 = 0, \\ W_0^f + W_0^p - \Theta_0(\Lambda_n + \sigma) = 0, \end{cases} \tag{4.15}$$

i.e.

$$\begin{cases} -\Big[(J\sigma+\gamma)\Lambda_n+\Lambda_n^k+\dfrac{B_1}{H}\mathcal{T}^2n^2\pi^2\Big]W_0^f \\ \quad +\Big[\gamma\Lambda_n-\dfrac{\gamma}{H}\eta\mathcal{T}^2n^2\pi^2\Big]W_0^p+Ra^2\Theta_0=0 \\ \Big[\gamma\Lambda_n-\dfrac{\gamma}{H}\eta\mathcal{T}^2n^2\pi^2\Big]W_0^f-\Big[\gamma\Lambda_n+K_r\Lambda_n^h \\ \quad +\dfrac{A_1}{H}\eta^2\mathcal{T}^2n^2\pi^2\Big]W_0^p+Ra^2\Theta_0=0, \\ W_0^f+W_0^p-\Theta_0(\Lambda_n+\sigma)=0, \end{cases} \tag{4.16}$$

where $a^2 = l^2 + m^2$ is the wavenumber and

$$\Lambda_n = n^2\pi^2 + a^2, \quad \Lambda_n^k = \frac{1}{k}n^2\pi^2 + a^2, \quad \Lambda_n^h = \frac{1}{h}n^2\pi^2 + a^2.$$

Requiring zero determinant for (4.16), one obtains

$$\begin{aligned} R =& \frac{\Lambda_n+\sigma}{a^2}\frac{1}{H(J\sigma+4\gamma)\Lambda_n+H\Psi+E\mathcal{T}^2n^2\pi^2}\Big\{HJ\gamma\sigma\Lambda_n^2 \\ &+\Big[\gamma\Lambda_n^k+(J\sigma+\gamma)K_r\Lambda_n^h\Big]H\Lambda_n+K_rH\Lambda_n^k\Lambda_n^h \\ &+M\Lambda_n\mathcal{T}^2n^2\pi^2+\eta^2\mathcal{T}^4n^4\pi^4+N\mathcal{T}^2n^2\pi^2\Big\} \end{aligned} \tag{4.17}$$

where the following positions were made

$$\begin{aligned} \Psi &= \Lambda_n^k + K_r\Lambda_n^h, \\ M &= \gamma^2(\eta+1)^2+\eta^2\Big(J\sigma+2\gamma+\frac{1}{k}\Big)J\sigma+\gamma\Big(\frac{1}{k}\eta^2+K_r\frac{1}{h}\Big), \\ N &= \eta^2\Big(J\sigma+\frac{1}{k}+\gamma\Big)\Lambda_n^k+K_r\Big(K_r\frac{1}{h}+\gamma\Big)\Lambda_n^h, \\ E &= \gamma(\eta-1)^2+K_r\frac{1}{h}+\eta^2\Big(J\sigma+\frac{1}{k}\Big). \end{aligned}$$

4.2.1 Stationary convective motions

In order to determine the instability threshold for the onset of steady convection, let us set $\sigma = 0$ into (4.17). Then the critical Rayleigh number for the onset of stationary convection is given by

$$\begin{aligned} R_S =& \min_{(n,a^2)\in\mathbb{N}\times\mathbb{R}^+}\frac{\Lambda_n}{a^2}\frac{1}{Q4\gamma\Lambda_n+Q\Psi+E_S\mathcal{T}^2n^2\pi^2}\Big\{\gamma\Psi Q\Lambda_n+K_rQ\Lambda_n^k\Lambda_n^h \\ &+M_S\Lambda_n\mathcal{T}^2n^2\pi^2+\eta^2\mathcal{T}^4n^4\pi^4+N_S\mathcal{T}^2n^2\pi^2\Big\}, \end{aligned} \tag{4.18}$$

where

$$\begin{aligned}
Q &= \gamma\Big(K_r\frac{1}{h} + \frac{1}{k}\Big) + K_r\frac{1}{hk}, \\
M_S &= \gamma^2(\eta+1)^2 + \gamma\Big(\frac{1}{k}\eta^2 + K_r\frac{1}{h}\Big), \\
N_S &= \eta^2\Big(\frac{1}{k} + \gamma\Big)\Lambda_n^k + K_r\Big(K_r\frac{1}{h} + \gamma\Big)\Lambda_n^h, \\
E_S &= \gamma(\eta-1)^2 + K_r\frac{1}{h} + \eta^2\frac{1}{k},
\end{aligned}$$

the solution of (4.18) will be analysed through numerical simulations in Section 4.3. Let us observe that

i) R_S does not depend on J, and hence the Vadasz number does not directly affect the onset of steady convection;

ii) Since $\dfrac{\partial R_S}{\partial \mathcal{T}^2} > 0$, as expected, rotation delays the onset of stationary convection.

4.2.2 Oscillatory convective motions

In order to determine the oscillatory convection threshold, let us set $\sigma = i\sigma_1$, with $\sigma_1 \in \mathbb{R} - \{0\}$, and $\Gamma = K_r\dfrac{1}{h} + \gamma$, so (4.17) becomes

$$R = \frac{\Lambda_n + i\sigma_1}{a^2}\frac{f}{g}, \tag{4.19}$$

with

$$\begin{aligned}
f =& \Lambda_n\Big(-\Lambda_n^h J^2\sigma_1^2\Gamma K_r + \gamma\Psi Q\Big) - \Gamma J^2\sigma_1^2\gamma\Lambda_n^2 + K_r\Lambda_n^h\Lambda_n^k Q \\
&+ \eta^2\mathcal{T}^4 n^4\pi^4 + \Lambda_n\mathcal{T}^2 n^2\pi^2\Big[\gamma^2(\eta+1)^2 + \gamma\Big(\frac{1}{k}\eta^2 + K_r\frac{1}{h}\Big) \\
&- \eta^2 J^2\sigma_1^2\Big] + \Big[\eta^2\Big(\frac{1}{k} + \gamma\Big)\Lambda_n^k + K_r\Gamma\Lambda_n^h\Big]\mathcal{T}^2 n^2\pi^2 \\
&+ Ji\sigma_1\Big\{\Lambda_n^2 Q\gamma + \Lambda_n\Big[QK_r\Lambda_n^h + \gamma\Psi\Gamma \\
&+ \mathcal{T}^2 n^2\pi^2\eta^2\Big(2\gamma + \frac{1}{k}\Big)\Big] + K_r\Lambda_n^h\Lambda_n^k\Gamma + \eta^2\Lambda_n^k\mathcal{T}^2 n^2\pi^2\Big\},
\end{aligned}$$

$$\begin{aligned}
g =& \Lambda_n(-J^2\sigma_1^2\Gamma + 4\gamma Q) + Q\Psi \\
&+ \mathcal{T}^2 n^2\pi^2\Big[\gamma(\eta-1)^2 + K_r\frac{1}{h} + \eta^2\frac{1}{k}\Big] \\
&+ Ji\sigma_1[\Lambda_n(Q + 4\gamma\Gamma) + \Psi\Gamma + \eta^2\mathcal{T}^2 n^2\pi^2].
\end{aligned}$$

Hence, setting

$$
\begin{aligned}
a_1 =&\Lambda_n\gamma\Psi Q + K_r\Lambda_n^h\Lambda_n^k Q + \eta^2\mathcal{T}^4 n^4\pi^4\\
&+\Lambda_n\mathcal{T}^2n^2\pi^2\Big[\gamma^2(\eta+1)^2+\gamma\Big(\frac{1}{k}\eta^2+K_r\frac{1}{h}\Big)\Big]\\
&+\Big[\eta^2\Big(\frac{1}{k}+\gamma\Big)\Lambda_n^k + K_r\Gamma\Lambda_n^h\Big]\mathcal{T}^2n^2\pi^2,\\
a_2 =&\Gamma\gamma\Lambda_n^2+\Lambda_n\Lambda_n^h\Gamma K_r+\Lambda_n\mathcal{T}^2n^2\pi^2\eta^2,\\
a_3 =&\Lambda_n^2Q\gamma+\Lambda_n\Big[QK_r\Lambda_n^h+\gamma\Psi\Gamma+\mathcal{T}^2n^2\pi^2\eta^2\Big(2\gamma+\frac{1}{k}\Big)\Big]\\
&+K_r\Lambda_n^h\Lambda_n^k\Gamma+\eta^2\Lambda_n^k\mathcal{T}^2n^2\pi^2,\\
b_1 =&4\gamma Q\Lambda_n+Q\Psi+\mathcal{T}^2n^2\pi^2\Big[\gamma(\eta-1)^2+K_r\frac{1}{h}+\eta^2\frac{1}{k}\Big],\\
b_2 =&\Lambda_n\Gamma,\\
b_3 =&\Lambda_n(Q+4\gamma\Gamma)+\Psi\Gamma+\eta^2\mathcal{T}^2n^2\pi^2,
\end{aligned}
\tag{4.20}
$$

from (4.19) one gets

$$
R=\frac{\Lambda_n+i\sigma_1}{a^2}\frac{a_1-J^2\sigma_1^2a_2+i\sigma_1Ja_3}{b_1-J^2\sigma_1^2b_2+i\sigma_1Jb_3},
\tag{4.21}
$$

and consequently

$$
R=\frac{\Lambda_n(\bar{a}+J^2\sigma_1^2a_3b_3)-\sigma_1^2J\bar{b}+i\sigma_1(\bar{a}+J^2\sigma_1^2a_3b_3+\Lambda_nJ\bar{b})}{a^2[(b_1-J^2\sigma_1^2b_2)^2+\sigma_1^2J^2b_3^2]},
\tag{4.22}
$$

where

$$
\begin{aligned}
\bar{a}&=(a_1-J^2\sigma_1^2a_2)(b_1-J^2\sigma_1^2b_2),\\
\bar{b}&=a_3(b_1-J^2\sigma_1^2b_2)-b_3(a_1-J^2\sigma_1^2a_2).
\end{aligned}
$$

Imposing the vanishing of the imaginary part of (4.22), i.e.

$$
\bar{a}+J^2\sigma_1^2a_3b_3+\Lambda_nJ\bar{b}=0,
\tag{4.23}
$$

that is

$$
\begin{aligned}
&J^4a_2b_2\sigma_1^4-J^2\sigma_1^2[a_2b_1+a_1b_2-a_3b_3+\Lambda_nJ(a_3b_2-a_2b_3)]\\
&\quad+a_1b_1+\Lambda_nJ(a_3b_1-b_3a_1)=0,
\end{aligned}
\tag{4.24}
$$

the critical Rayleigh number for the onset of the oscillatory convection is given by:

$$
R_O=\min_{(n,a^2)\in\mathbb{N}\times\mathbb{R}^+}\frac{\Lambda_n[\bar{a}+J^2\sigma_1^2a_3b_3]-\sigma_1^2J\bar{b}}{a^2[(b_1-J^2\sigma_1^2b_2)^2+\sigma_1^2J^2b_3^2]},
\tag{4.25}
$$

where σ_1^2 is the positive root of (4.24). Let us point out that if

$$[a_2b_1+a_1b_2-a_3b_3+\Lambda_n J(a_3b_2-a_2b_3)]^2-4a_2b_2[a_1b_1+\Lambda_n J(a_3b_1-b_3a_1)]<0, \quad (4.26)$$

or if

$$\begin{aligned} &a_2b_1 + a_1b_2 - a_3b_3 + \Lambda_n J(a_3b_2 - a_2b_3) < 0, \\ &a_1b_1 + \Lambda_n J(a_3b_1 - b_3a_1) > 0, \end{aligned} \quad (4.27)$$

oscillatory convection cannot occur. Due to its complicated algebraic form, the minimization (4.25) will be numerically investigated in section 4.3.

Neglecting the Vadasz number, i.e. considering $J = 0$, from (4.17) it follows that σ is a real number and hence convection can arise only through a stationary motion, according to the results found in [22].

4.3 Numerical simulations for the instability thresholds

The aim of this section is to solve (4.18) and (4.25) and numerically describe the asymptotic behaviour of the steady and oscillatory critical Rayleigh numbers with respect to $\mathcal{T}^2$, J, k, h, in order to describe the influence of rotation, Vadasz number, anisotropic macropermeability and anisotropic micropermeability on the onset of convection. Through numerical simulations, we showed that the minimum of both (4.18) and (4.25) with respect to n is attained at $n = 1$, hence let us define

$$f_S(a^2) = \frac{\Lambda_1}{a^2}\frac{a_1}{b_1} \ , \quad (4.28)$$

and

$$f_O(a^2) = \frac{\Lambda_1(\overline{a} + J^2\sigma_1^2 a_3 b_3) - \sigma_1^2 J\overline{b}}{a^2[(b_1 - J^2\sigma_1^2 b_2)^2 + \sigma_1^2 J^2 b_3^2]} \ , \quad (4.29)$$

where a_i and b_i, for $i = 1, 2, 3$, are now given by (4.20) for $n = 1$. As reported in [49], there is a need for measurements of the double porosity parameters K_r and γ. In our numerical simulations we chose $K_r > 1$ and $\eta < 1$ envisaging an engineered bi-disperse porous medium with vertical macropermeability and porosity of the p-phase greater then vertical micropermeability and porosity of the f-phase, respectively. In particular, in all numerical simulations we set $\{K_r = 1.5, \gamma = 0.8, \eta = 0.2\}$, in order to compare our numerical results with those ones found in [23] and hence evaluate the effect of the anisotropic permeability parameters. Varying $k, h, \mathcal{T}^2, J$ in turn we found some critical values of these parameters for which oscillatory convection cannot occur. In particular

- from table 4.1(a), for large values of the Vadasz number ($J = 10$), we find out that exists $k^* \in (0.53, 0.54)$ such that if $k < k^*$ convection can arise only through stationary motion; for $k \in (0.57, 0.58)$ there is a switch from steady to oscillatory convection;

- table 4.1(b) shows that for large values of J and for increasing h, if convection occurs, it can set in only via an oscillatory state;

- table 4.2(a) displays that there is a similar behaviour between the small Vadasz number case ($J = 0.5$) and the large J case, but for smaller J the threshold k^{**} for which oscillatory convection cannot occur is higher, in particular there exists $k^{**} \in (0.82, 0.83)$ such that if $k < k^{**}$ convection can arise only via stationary motion, while for $k \in (0.83, 0.84)$ there is a transition from steady to oscillatory convection;

- for small Vadasz number J, from table 4.2(b) we find a threshold $h^* \in (0.45, 0.46)$ such that if $h < h^*$ oscillatory convection cannot occur; for $h \in (0.49, 0.5)$ there is a reversal from steady to oscillatory convection;

- from tables 4.1 and 4.2 it arises that R_O decreases for both increasing k and h, hence, when convection occurs via oscillatory motion, the system become more unstable at increasing permeability parameters;

- in tables 4.3(a) and 4.3(b) we have numerically confirmed that for $J = 0$ convection can arise only via a stationary motion, since R_O doesn't exist. Moreover, in table 4.3(a), fixing $\{h = 0.1, k = 10, \mathcal{T}^2 = 10\}$, since $R_S = 111.7045$ and comparing R_O with R_S, it arises that for $J \geq 0.11$ convection can set in only via oscillatory motion. In table 4.3(b) we have considered the case $h >> k$, fixing $\{h = 10, k = 0.1, \mathcal{T}^2 = 10\}$, and we have numerically obtained that oscillatory convection cannot arise;

- from table 4.3(a) we may remark that for $h << k$ R_O is a decreasing function of J, as already observed in [23] for $h = k = 1$;

- from table 4.4(a) we notice that if $h << k$ there exists a threshold $\mathcal{T}^{2*} \in (2.09, 2.1)$ such that for $\mathcal{T}^2 < \mathcal{T}^{2*}$ oscillatory convection cannot arise and stationary convection sets in for $\mathcal{T}^2$ up to 2.3, while for $\mathcal{T}^2 \in (2.3, 2.4)$ there is a switch from stationary to oscillatory convection; from table 4.4(b) we recover the same behaviour shown in table 4.3(b);

- tables 4.4(a) and 4.4(b) numerically show off the stabilizing effect of rotation on the onset of convection, since both R_S and R_O are increasing functions with respect to $\mathcal{T}^2$, as one is expected; in particular R_O, if it exists, has a *slower* increase with respect to $\mathcal{T}^2$ than R_S.

In figures 4.1 and 4.2 the instability thresholds at quoted values of the permeability parameters h and k are shown, for small and large Vadasz number J, respectively. From figure 4.3 we may visualize the stabilizing effect of the Taylor number $\mathcal{T}^2$ on the onset of convection, in particular from figure 4.3(a) two very different growth rates of the steady and of the oscillatory instability thresholds arise. Figure 4.4 shows the destabilizing effect on the onset of oscillatory convection of the Vadasz number J. The numerical results of table 4.2 are graphically shown in figure 4.5, where steady and oscillatory instability thresholds are represented as functions of the anisotropic permeability parameters k and h.

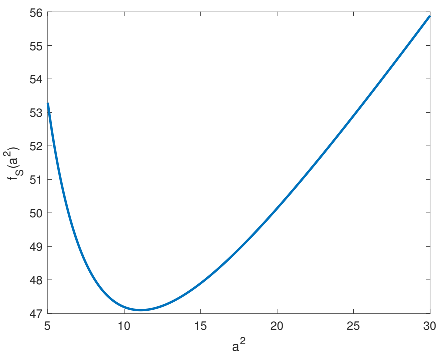

(a) $h >> k$

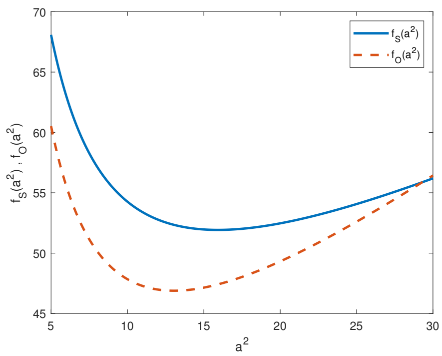

(b) $h = k$

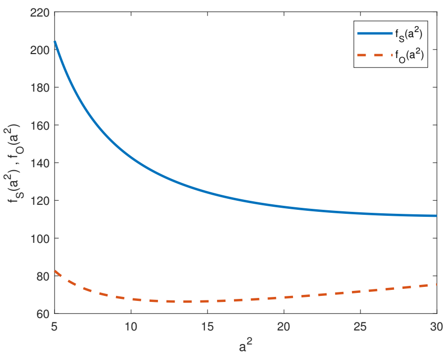

(c) $h << k$

Figure 4.1: Instability thresholds for quoted values of k and h and for $\mathcal{T}^2 = 10, \mathbf{J = 0.5}, K_r = 1.5, \eta = 0.2, \gamma = 0.8$. (a): $h = 10, k = 0.1$, (b): $h = k = 1$, (c): $h = 0.1, k = 10$.

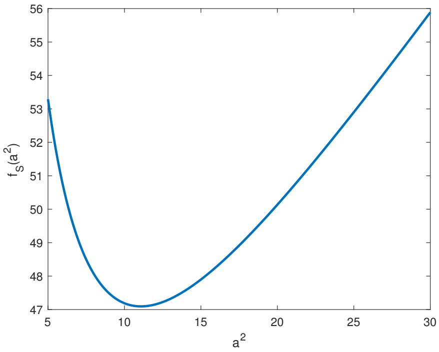

(a) $h >> k$

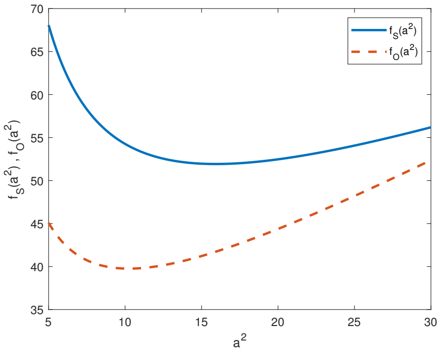

(b) $h = k$

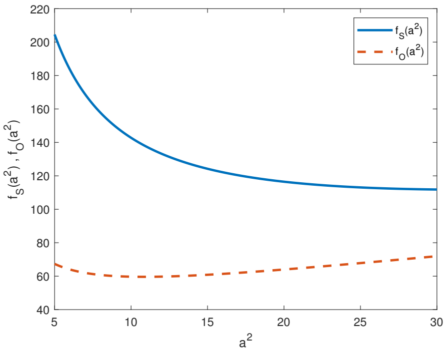

(c) $h << k$

Figure 4.2: Instability thresholds for quoted values of k and h and for $\mathcal{T}^2 = 10, \mathbf{J} = \mathbf{10}, K_r = 1.5, \eta = 0.2, \gamma = 0.8$. (a): $h = 10, k = 0.1$, (b): $h = k = 1$, (c): $h = 0.1, k = 10$.

Main results

The onset of convection in a rotating and anisotropic bi-disperse porous medium, taking into account the Vadasz term, was studied via linear instability analysis. Let us remark that the Vadasz term allows the onset of oscillatory convection, which is not present when the inertia is neglected (see [22]). Moreover, if $h = k = 1$, i.e. confining ourselves to the isotropic case, from (4.18) and (4.25) we recover the stationary and oscillatory thresholds found in [23], respectively. Lastly, it was numerically investigated the relationship between the critical steady and oscillatory Rayleigh numbers and the fundamental parameters $h, k, \mathcal{T}^2, J$ and we found out that:

- R_S and R_O are increasing functions of $\mathcal{T}^2$;

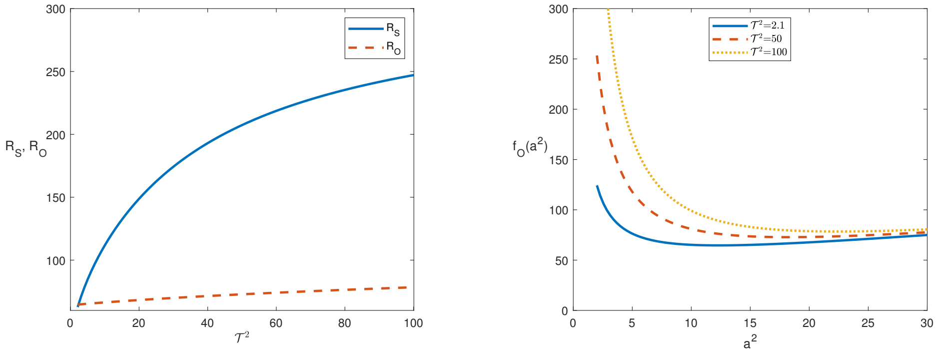

(a) (b)

Figure 4.3: (a): Stationary and Oscillatory instability thresholds as functions of the Taylor number $\mathcal{T}^2$ for $k = 10, h = 0.1, J = 0.5, K_r = 1.5, \eta = 0.2, \gamma = 0.8$. (b): Oscillatory thresholds at quoted values of the Taylor number $\mathcal{T}^2$ and for $k = 10, h = 0.1, J = 0.5, K_r = 1.5, \eta = 0.2, \gamma = 0.8$.

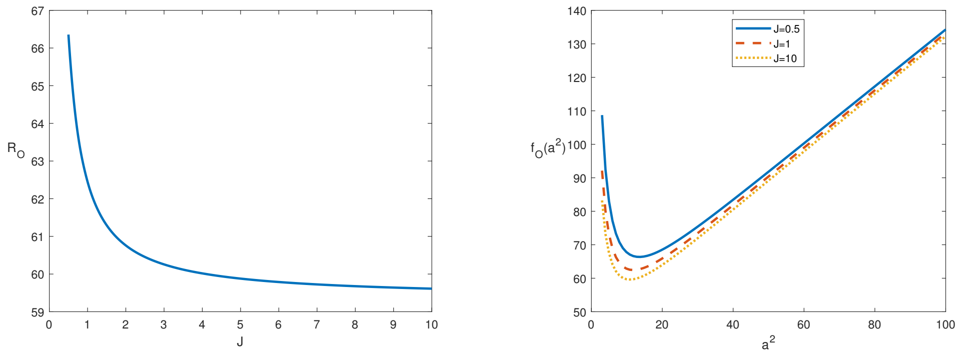

(a) (b)

Figure 4.4: (a): Oscillatory instability threshold as function of the Vadasz number J for $k = 10, h = 0.1, \mathcal{T}^2 = 10, K_r = 1.5, \eta = 0.2, \gamma = 0.8$. (b): Oscillatory thresholds at quoted values of the Vadasz number J and for $k = 10, h = 0.1, \mathcal{T}^2 = 10, K_r = 1.5, \eta = 0.2, \gamma = 0.8$.

- R_O, if it exists, is a decreasing function of J;
- comparing our results with those ones found in [23], anisotropic macropermeability and anisotropic micropermeability lead to higher steady and oscillatory thresholds.

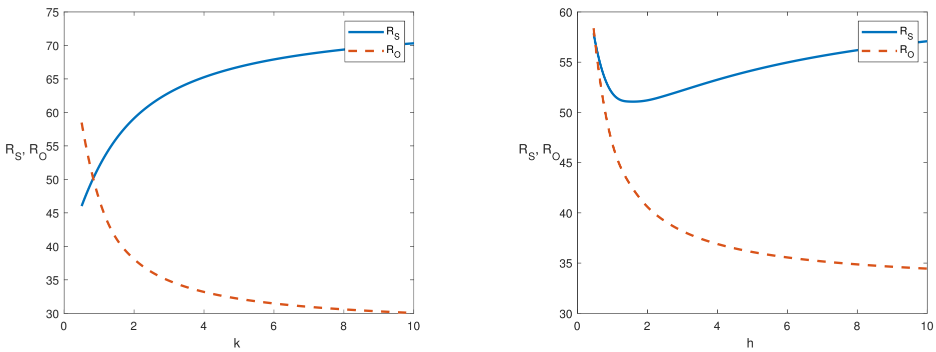

(a) (b)

Figure 4.5: Asymptotic behaviour of the steady and oscillatory instability thresholds as functions of the anisotropic permeability parameters k and h. (a): $h = 1, \mathcal{T}^2 = 10, J = 0.5, K_r = 1.5, \eta = 0.2, \gamma = 0.8$. (b): $k = 1, \mathcal{T}^2 = 10, J = 0.5, K_r = 1.5, \eta = 0.2, \gamma = 0.8$.

(a)

R_S	R_O	a_S^2	a_O^2	k
55.5802	$\nexists$	15.0097	$\nexists$	0.1
46.4633	$\nexists$	15.4106	$\nexists$	0.5
46.7672	$\nexists$	15.4530	$\nexists$	0.53
46.8724	48.0833	15.4670	10.8010	0.54
46.9790	47.7998	15.4809	10.7872	0.55
47.0871	47.5233	15.4947	10.7733	0.56
47.1964	47.2537	15.5084	10.7596	0.57
47.3067	46.9906	15.5220	10.7459	0.58
47.5300	46.4833	15.5487	10.7186	0.6
51.9256	39.7591	15.9190	10.2433	1
66.8036	28.7339	15.6424	8.7834	5
70.3183	27.0015	15.3278	8.4389	10

(b)

R_S	R_O	a_S^2	a_O^2	h
146.5652	133.6558	22.0926	10.6720	0.01
88.7111	86.2352	26.9067	14.1899	0.1
56.9286	48.5663	18.8637	11.9393	0.5
51.9256	39.7591	15.9190	10.2433	1
54.1833	31.1656	13.6497	8.3863	5
57.0855	30.0809	13.6502	8.2253	10
61.7553	29.1760	13.8544	8.1706	100

Table 4.1: Critical steady and oscillatory Rayleigh numbers and wavenumbers for quoted values of k (a) and for quoted values of h (b). *Table a*: $h = 1, \mathcal{T}^2 = 10, J = 10, K_r = 1.5, \eta = 0.2, \gamma = 0.8$. *Table b*: $k = 1, \mathcal{T}^2 = 10, J = 10, K_r = 1.5, \eta = 0.2, \gamma = 0.8$.

(a)

R_S	R_O	a_S^2	a_O^2	k
55.5802	$\nexists$	15.0097	$\nexists$	0.1
46.4633	$\nexists$	15.4106	$\nexists$	0.5
49.8064	$\nexists$	15.7735	$\nexists$	0.8
50.0286	$\nexists$	15.7914	$\nexists$	0.82
50.1389	50.2184	15.8001	13.4683	0.83
50.2488	49.9896	15.8085	13.4404	0.84
50.3581	49.7655	15.8168	13.4130	0.85
50.8960	48.7116	15.8553	13.2826	0.9
51.9256	46.8876	15.9190	13.0503	1
66.8036	32.1661	15.6424	10.6842	5
70.3183	30.0517	15.3278	10.2302	10

(b)

R_S	R_O	a_S^2	a_O^2	h
88.7111	$\nexists$	26.9067	$\nexists$	0.1
59.6059	$\nexists$	20.0551	$\nexists$	0.4
58.1248	$\nexists$	19.4148	$\nexists$	0.45
57.8653	58.3814	19.2980	15.3814	0.46
57.6164	57.9856	19.1847	15.3599	0.47
57.3777	57.6028	19.0746	15.2905	0.48
57.1486	57.2324	18.9676	15.2227	0.49
56.9286	56.8737	18.8637	15.1563	0.5
51.9256	46.8876	15.9190	13.0503	1
54.1833	36.1050	13.6497	10.4542	5
57.0855	34.4490	13.6502	10.1144	10

Table 4.2: Critical steady and oscillatory Rayleigh numbers and wavenumbers for quoted values of k (a) and for quoted values of h (b). *Table a*: $h = 1, \mathcal{T}^2 = 10, J = 0.5, K_r = 1.5, \eta = 0.2, \gamma = 0.8$. *Table b*: $k = 1, \mathcal{T}^2 = 10, J = 0.5, K_r = 1.5, \eta = 0.2, \gamma = 0.8$.

(a) $h << k$

R_O	a_O^2	J
$\nexists$	$\nexists$	0
$\nexists$	$\nexists$	0.1
94.6887	27.8062	0.11
85.6326	23.1078	0.15
66.3568	13.5068	0.5
62.4493	11.8203	1
59.8788	10.9098	5
59.6123	10.8360	10
59.4095	10.7843	50
59.3849	10.7784	100

(b) $h >> k$

R_O	a_O^2	J
$\nexists$	$\nexists$	0
$\nexists$	$\nexists$	0.5
$\nexists$	$\nexists$	1
$\nexists$	$\nexists$	5
$\nexists$	$\nexists$	10
$\nexists$	$\nexists$	50
$\nexists$	$\nexists$	100

Table 4.3: Critical oscillatory Rayleigh numbers and wavenumbers for quoted values of J for $h << k$ (a) and for $h >> k$ (b). *Table a*: fixing $h = 0.1, k = 10, \mathcal{T}^2 = 10, K_r = 1.5, \eta = 0.2, \gamma = 0.8$, the critical Rayleigh number and wavenumber for the steady convection are $R_S = 111.7045, a_S^2 = 32.4936$, respectively. *Table b*: for $h = 10, k = 0.1, \mathcal{T}^2 = 10, K_r = 1.5, \eta = 0.2, \gamma = 0.8$.

(a) $h << k$

R_S	R_O	a_S^2	a_O^2	$\mathcal{T}^2$
37.9913	$\nexists$	8.8113	$\nexists$	0
61.7538	$\nexists$	17.9673	$\nexists$	2
62.5794	$\nexists$	18.2713	$\nexists$	2.09
62.6704	64.6393	18.3047	12.2819	2.1
63.5719	64.6626	18.6347	12.2984	2.2
64.4590	64.6858	18.9577	12.3149	2.3
65.3325	64.7090	19.2739	12.3313	2.4
66.1929	64.7321	19.5835	12.3477	2.5
84.6085	65.2968	25.6964	12.7489	5
111.7045	66.3568	32.4936	13.5068	10

(b) $h >> k$

R_S	R_O	a_S^2	a_O^2	$\mathcal{T}^2$
39.6844	$\nexists$	8.8024	$\nexists$	0
43.4949	$\nexists$	10.0015	$\nexists$	5
47.0944	$\nexists$	11.0770	$\nexists$	10
100.1927	$\nexists$	22.9601	$\nexists$	100

Table 4.4: Critical steady and oscillatory Rayleigh numbers and wavenumbers for quoted values of $\mathcal{T}^2$ for $h << k$ (a) and for $h >> k$ (b). *Table a*: for $h = 0.1, k = 10, J = 0.5, K_r = 1.5, \eta = 0.2, \gamma = 0.8$. *Table b*: for $h = 10, k = 0.1, J = 0.5, K_r = 1.5, \eta = 0.2, \gamma = 0.8$.

Chapter 5

The onset of thermal convection in anisotropic and rotating bidisperse porous media

As reported in [35], bi-disperse porous media are increasingly important in the chemical engineering field. Regarding *anisotropic* materials, while anisotropic single porosity media have been widely studied by several authors (see for example [38, 39, 40]), anisotropic bi-disperse porous materials may have much more potentials, since they offer many possibilities to design man-made materials for heat transfer or insulation problems, for oil recovery from underground reservoir, for nuclear waste recovery and so on (see [22, 20, 36] and references therein). Therefore, in the following Chapter we allow *fully anisotropic permeabilities in both f-phase and p-phase.*
Envisaging a rotating machinery constituted by an engineered fully anisotropic bi-disperse porous material, the aim of this Chapter is to analyse the onset of thermal convection in an anisotropic bi-disperse porous medium uniformly rotating about a vertical axis, through linear and nonlinear stability theory. The present Chapter is based on the paper [50] with F. Capone and M. Gentile and is organized as follows. The mathematical model and the associated perturbation equations are introduced in Section 5.1. In Section 5.2 the strong version of the principle of exchange of stabilities is proved and the linear instability analysis of the thermal conduction solution is performed, to determine the steady instability threshold. In Section 5.3 the nonlinear stability analysis of the thermal conduction solution is performed, proving the coincidence between the linear and the nonlinear stability thresholds with respect to the L^2-norm. In Section 5.4, in order to analyse the influence of ro-

tation and of anisotropic permeability on the onset of convection, numerical simulations are presented.

5.1 Governing equations

Let $Oxyz$ be a reference frame with fundamental unit vectors $\mathbf{i}, \mathbf{j}, \mathbf{k}$ ($\mathbf{k}$ pointing vertically upward) and let L be a layer of an *anisotropic* bi-disperse porous medium, saturated by an homogeneous incompressible fluid heated from below. Let us assume that the layer L – of thickness d – rotates about the vertical axis z, with constant angular velocity $\mathbf{\Omega} = \Omega\mathbf{k}$ and that the temperature in the macropores (T_f) and the temperature in the micropores (T_p) are the same, i.e. $T^f = T^p = T$.
Let us assume that the axes (x, y, z) are the *principal axes* of the permeability tensors in the macropores and in the micropores, hence:

$$\begin{aligned}\mathbf{K}^f &= \mathrm{diag}(K_x^f, K_y^f, K_z^f) = K_z^f \ \mathbf{K}^{f*},\\ \mathbf{K}^p &= \mathrm{diag}(K_x^p, K_y^p, K_z^p) = K_z^p \ \mathbf{K}^{p*},\end{aligned}$$

$$\mathbf{K}^{f*} = \mathrm{diag}(k_1, k_2, 1), \quad \mathbf{K}^{p*} = \mathrm{diag}(h_1, h_2, 1),$$

where

$$k_1 = \frac{K_x^f}{K_z^f}, \quad k_2 = \frac{K_y^f}{K_z^f},$$

$$h_1 = \frac{K_x^p}{K_z^p}, \quad h_2 = \frac{K_y^p}{K_z^p}.$$

In the Oberbeque-Boussinesq approximation and extending the Darcy's Law in order to include the Coriolis term in the momentum equations for the micropores and the macropores, the governing equations for thermal convection are [21, 35]:

$$\begin{cases}\mathbf{v}^f = \dfrac{1}{\mu}\mathbf{K}^f \cdot \left[-\zeta(\mathbf{v}^f - \mathbf{v}^p) - \nabla p^f + \varrho_F \alpha g T\mathbf{k} - \dfrac{2\varrho_F\Omega}{\varphi}\mathbf{k}\times\mathbf{v}^f\right],\\ \mathbf{v}^p = \dfrac{1}{\mu}\mathbf{K}^p \cdot \left[-\zeta(\mathbf{v}^p - \mathbf{v}^f) - \nabla p^p + \varrho_F \alpha g T\mathbf{k} - \dfrac{2\varrho_F\Omega}{\epsilon}\mathbf{k}\times\mathbf{v}^p\right],\\ \nabla\cdot\mathbf{v}^f = 0,\\ \nabla\cdot\mathbf{v}^p = 0,\\ (\varrho c)_m\dfrac{\partial T}{\partial t} + (\varrho c)_f(\mathbf{v}^f + \mathbf{v}^p)\cdot\nabla T = k_m\Delta T.\end{cases} \tag{5.1}$$

where

$$p^s = P^s - \frac{\varrho_F}{2}|\mathbf{\Omega}\times\mathbf{x}|^2, \quad s = \{f, p\}$$

are the reduced pressures, $\mathbf{x} = (x, y, z)$, $\mathbf{v}^s$ = seepage velocity for $s = \{f, p\}$, ζ = interaction coefficient between the f-phase and the p-phase, $\mathbf{g} = -g\mathbf{k}$ = gravity, μ = fluid viscosity, ϱ_F = reference constant density, α = thermal expansion coefficient, c = specific heat, c_p = specific heat at a constant pressure, $(\varrho c)_m = (1-\varphi)(1-\epsilon)(\varrho c)_{sol} + \varphi(\varrho c)_f + \epsilon(1-\varphi)(\varrho c)_p$, $k_m = (1-\varphi)(1-\epsilon)k_{sol} + \varphi k_f + \epsilon(1-\varphi)k_p$ = thermal conductivity (the subscript *sol* is referred to the solid skeleton).

To (5.1), the following boundary conditions are appended

$$\begin{aligned} \mathbf{v}^s \cdot \mathbf{n} = 0 \text{ on } z = 0, d,\ s = \{f, p\} \\ T = T_L \text{ on } z = 0, \\ T = T_U \text{ on } z = d, \end{aligned} \tag{5.2}$$

whit $T_L > T_U$.

The problem (5.1) – (5.2) admits the steady state (conduction solution):

$$\overline{\mathbf{v}}^f = \mathbf{0},\ \overline{\mathbf{v}}^p = \mathbf{0},\ \overline{T} = -\beta z + T_L,\ \beta = \frac{T_L - T_U}{d}.$$

Defining $\{\mathbf{u}^f, \mathbf{u}^p, \theta, \pi^f, \pi^p\}$ a perturbation to the steady solution, the evolution equations for the perturbation fields are

$$\begin{cases} \mathbf{u}^f = \dfrac{1}{\mu}\mathbf{K}^f \cdot \left[-\zeta(\mathbf{u}^f - \mathbf{u}^p) - \nabla\pi_f + \varrho_F\alpha g\theta\mathbf{k} - \dfrac{2\varrho_F\Omega}{\varphi}\mathbf{k}\times\mathbf{u}^f\right], \\ \mathbf{u}^p = \dfrac{1}{\mu}\mathbf{K}^p \cdot \left[-\zeta(\mathbf{u}^p - \mathbf{u}^f) - \nabla\pi_f + \varrho_F\alpha g\theta\mathbf{k} - \dfrac{2\varrho_F\Omega}{\epsilon}\mathbf{k}\times\mathbf{u}^p\right], \\ \nabla\cdot\mathbf{u}^f = 0, \\ \nabla\cdot\mathbf{u}^p = 0, \\ (\varrho c)_m\dfrac{\partial\theta}{\partial t} + (\varrho c)_f(\mathbf{u}^f + \mathbf{u}^p)\cdot\nabla\theta = (\varrho c)_f\beta(w^f + w^p) + k_m\Delta\theta. \end{cases} \tag{5.3}$$

where $\mathbf{u}^f = (u^f, v^f, w^f)$, $\mathbf{u}^p = (u^p, v^p, w^p)$. Using the following non-dimensional parameters

$$\begin{aligned} &\mathbf{x}^* = \frac{\mathbf{x}}{d},\ t^* = \frac{t}{\tilde{t}},\ \theta^* = \frac{\theta}{\tilde{T}}, \\ &\mathbf{u}^{s*} = \frac{\mathbf{u}^s}{\tilde{u}},\ \pi^{s*} = \frac{\pi^s}{\tilde{P}},\ \text{for } s = \{f, p\}, \\ &\eta = \frac{\varphi}{\epsilon},\ \gamma_1 = \frac{\mu}{K_z^f\zeta},\ \gamma_2 = \frac{\mu}{K_z^p\zeta}, \end{aligned}$$

where the scales are given by

$$\tilde{u} = \frac{k_m}{(\varrho c)_f d},\ \tilde{t} = \frac{d^2(\varrho c)_m}{k_m},\ \tilde{P} = \frac{\zeta k_m}{(\varrho c)_f},\ \tilde{T} = \sqrt{\frac{\beta k_m\zeta}{(\varrho c)_f\varrho_F\alpha g}}$$

and introducing the Taylor number $\mathcal{T}$ and the thermal Rayleigh number R, respectively given by

$$\mathcal{T} = \frac{2\varrho_F \Omega K_z^f}{\varphi \mu}, \qquad R = \sqrt{\frac{\beta d^2 (\varrho c)_f \varrho_F \alpha g}{k_m \zeta}},$$

the resulting non-dimensional perturbation equations, omitting all the asterisks, are

$$\begin{cases} \gamma_1 (\mathbf{K}^f)^{-1} \mathbf{u}^f + (\mathbf{u}^f - \mathbf{u}^p) = -\nabla \pi^f + R\theta \mathbf{k} - \gamma_1 \mathcal{T} \mathbf{k} \times \mathbf{u}^f, \\ \gamma_2 (\mathbf{K}^p)^{-1} \mathbf{u}^p - (\mathbf{u}^f - \mathbf{u}^p) = -\nabla \pi^p + R\theta \mathbf{k} - \eta \gamma_1 \mathcal{T} \mathbf{k} \times \mathbf{u}^p, \\ \nabla \cdot \mathbf{u}^f = 0, \\ \nabla \cdot \mathbf{u}^p = 0, \\ \dfrac{\partial \theta}{\partial t} + (\mathbf{u}^f + \mathbf{u}^p) \cdot \nabla \theta = R(w^f + w^p) + \Delta \theta, \end{cases} \tag{5.4}$$

under the initial conditions

$$\mathbf{u}^s(\mathbf{x}, 0) = \mathbf{u}_0^s(\mathbf{x}), \quad \pi^s(\mathbf{x}, 0) = \pi_0^s(\mathbf{x}), \quad \theta(\mathbf{x}, 0) = \theta_0(\mathbf{x}),$$

with $\nabla \cdot \mathbf{u}_0^s = 0$, for $s = \{f, p\}$, and the boundary conditions

$$w^f = w^p = \theta = 0 \quad \text{on } z = 0, 1. \tag{5.5}$$

The above equations are defined in $\{(x, y, z, t) \in \mathbb{R}^4 | z \in (0, 1), t > 0\}$.
In the sequel, we'll suppose that the perturbation fields are periodic in the x and y directions of period $\dfrac{2\pi}{l}$ and $\dfrac{2\pi}{m}$, respectively, and we'll denote by

$$V = \left[0, \frac{2\pi}{l}\right] \times \left[0, \frac{2\pi}{m}\right] \times [0, 1]$$

the periodicity cell.

5.2 Hydrodynamic instability

In this section we will perform linear instability analysis of the basic solution, to this aim let us first *linearise* the perturbation equations (5.4), i.e.

$$\begin{cases} \gamma_1 (\mathbf{K}^f)^{-1} \mathbf{u}^f + (\mathbf{u}^f - \mathbf{u}^p) = -\nabla \pi^f + R\theta \mathbf{k} - \gamma_1 \mathcal{T} \mathbf{k} \times \mathbf{u}^f, \\ \gamma_2 (\mathbf{K}^p)^{-1} \mathbf{u}^p - (\mathbf{u}^f - \mathbf{u}^p) = -\nabla \pi^p + R\theta \mathbf{k} - \eta \gamma_1 \mathcal{T} \mathbf{k} \times \mathbf{u}^p, \\ \nabla \cdot \mathbf{u}^f = 0, \\ \nabla \cdot \mathbf{u}^p = 0, \\ \dfrac{\partial \theta}{\partial t} = R(w^f + w^p) + \Delta \theta, \end{cases} \tag{5.6}$$

Since system (5.6) is autonomous, we seek solutions which have time-dependence like $e^{\sigma t}$, i.e. solutions of form

$$\begin{aligned}\mathbf{u}^s(t,\mathbf{x}) &= e^{\sigma t}\mathbf{u}^s(\mathbf{x}),\\ \theta(t,\mathbf{x}) &= e^{\sigma t}\theta(\mathbf{x}),\\ \pi^s(t,\mathbf{x}) &= e^{\sigma t}\pi^s(\mathbf{x}),\end{aligned} \tag{5.7}$$

with $\sigma \in \mathbb{C}$ and $s = \{f, p\}$. By virtue of (5.7), (5.6) becomes

$$\begin{cases}\gamma_1(\mathbf{K}^f)^{-1}\mathbf{u}^f + (\mathbf{u}^f - \mathbf{u}^p) = -\nabla\pi^f + R\theta\mathbf{k} - \gamma_1\mathcal{T}\mathbf{k}\times\mathbf{u}^f,\\ \gamma_2(\mathbf{K}^p)^{-1}\mathbf{u}^p - (\mathbf{u}^f - \mathbf{u}^p) = -\nabla\pi^p + R\theta\mathbf{k} - \eta\gamma_1\mathcal{T}\mathbf{k}\times\mathbf{u}^p,\\ \sigma\theta = R(w^f + w^p) + \Delta\theta.\end{cases} \tag{5.8}$$

i.e.:

$$\begin{cases}\dfrac{\gamma_1}{k_1}u^f + u^f - u^p = -\pi^f_x + \gamma_1\mathcal{T}v^f,\\ \dfrac{\gamma_1}{k_2}v^f + v^f - v^p = -\pi^f_y - \gamma_1\mathcal{T}u^f,\\ \gamma_1 w^f + w^f - w^p = -\pi^f_z + R\theta,\\ \dfrac{\gamma_2}{h_1}u^p + u^p - u^f = -\pi^p_x + \eta\gamma_1\mathcal{T}v^p,\\ \dfrac{\gamma_2}{h_2}v^p + v^p - v^f = -\pi^p_y - \eta\gamma_1\mathcal{T}u^p,\\ \gamma_2 w^p + w^p - w^f = -\pi^p_z + R\theta,\\ u^f_x + v^f_y + w^f_z = 0,\\ u^p_x + v^p_y + w^p_z = 0,\\ \sigma\theta = Rw^f + Rw^p + \Delta\theta.\end{cases} \tag{5.9}$$

From system (5.9), one obtains

$$\begin{cases}u^f = \dfrac{1}{D}\Big\{H\pi^p_x + \gamma_1\mathcal{T}(L+\eta)\pi^f_y + [L(b+1)-(c+1)]\pi^f_x + \gamma_1\mathcal{T}N\pi^p_y\Big\},\\ u^p = \dfrac{1}{D}\Big\{H\pi^f_x + \gamma_1\mathcal{T}(\eta K+1)\pi^p_y + [K(d+1)-(a+1)]\pi^p_x + \gamma_1\mathcal{T}M\pi^f_y\Big\},\\ v^f = \dfrac{1}{D}\Big\{G\pi^p_y - \gamma_1\mathcal{T}(L+\eta)\pi^f_x + [L(a+1)-(d+1)]\pi^f_y - \gamma_1\mathcal{T}M\pi^p_x\Big\},\\ v^p = \dfrac{1}{D}\Big\{G\pi^f_y - \gamma_1\mathcal{T}(\eta K+1)\pi^p_x + [K(c+1)-(b+1)]\pi^p_y - \gamma_1\mathcal{T}N\pi^f_x\Big\},\end{cases} \tag{5.10}$$

where A is the coefficients matrix of system $(5.9)_{1,2}$–$(5.9)_{4,5}$ and

$$
\begin{aligned}
&a = \frac{\gamma_1}{k_1},\ b = \frac{\gamma_1}{k_2},\ c = \frac{\gamma_2}{h_1},\ d = \frac{\gamma_2}{h_2},\\
&H = (b+1)(d+1) - 1 - \eta(\gamma_1 \mathcal{T})^2,\\
&G = (a+1)(c+1) - 1 - \eta(\gamma_1 \mathcal{T})^2,\\
&K = (a+1)(b+1) + (\gamma_1 \mathcal{T})^2,\\
&L = (d+1)(c+1) + \eta^2(\gamma_1 \mathcal{T})^2,\\
&M = (d+1) + \eta(a+1),\\
&N = (c+1) + \eta(b+1),\\
&D = \det(A)\,.
\end{aligned}
$$

Hence, differentiating equations (5.10) with respect to z and equations $(5.9)_3$–$(5.9)_6$ with respect to x and y, by virtue of the incompressibility conditions $(5.9)_7$–$(5.9)_8$, differentiating with respect to z, i.e.

$$
\begin{aligned}
u^f_{xz} + v^f_{yz} &= -w^f_{zz},\\
u^p_{xz} + v^p_{yz} &= -w^p_{zz},
\end{aligned}
\tag{5.11}
$$

one obtains the following system

$$
\begin{cases}
a_1 w^f_{xx} + a_2 w^f_{yy} + D w^f_{zz} + a_3 w^p_{xx} + a_4 w^p_{yy} + c_1 w^f_{xy}\\
\quad -c_1 \hat{\gamma}_2 w^p_{xy} + R a_5 \theta_{xx} + R a_6 \theta_{yy} + R c_1 \theta_{xy} = 0,\\[2mm]
b_1 w^f_{xx} + b_2 w^f_{yy} + b_3 w^p_{xx} + b_4 w^p_{yy} + D w^p_{zz} + c_1 \hat{\gamma}_1 w^f_{xy}\\
\quad -c_1 w^p_{xy} + R b_5 \theta_{xx} + R b_6 \theta_{yy} - R c_1 \theta_{xy} = 0,\\[2mm]
\sigma\theta = R w^f + R w^p + \Delta\theta.
\end{cases}
\tag{5.12}
$$

where $\hat{\gamma}_s = \gamma_s + 1$, for $s = 1, 2$ and

$$\begin{aligned}
a_1 &= H - \hat{\gamma}_1[L(b+1) - (c+1)],\\
a_2 &= G - \hat{\gamma}_1[L(a+1) - (d+1)],\\
a_3 &= -\hat{\gamma}_2 H + L(b+1) - (c+1),\\
a_4 &= -\hat{\gamma}_2 G + L(a+1) - (d+1),\\
a_5 &= H + L(b+1) - (c+1),\\
a_6 &= G + L(a+1) - (d+1),\\
b_1 &= -\hat{\gamma}_1 H + K(d+1) - (a+1),\\
b_2 &= -\hat{\gamma}_1 G + K(c+1) - (b+1),\\
b_3 &= H - \hat{\gamma}_2[K(d+1) - (a+1)],\\
b_4 &= G - \hat{\gamma}_2[K(c+1) - (b+1)],\\
b_5 &= H + K(d+1) - (a+1),\\
b_6 &= G + K(c+1) - (b+1),\\
c_1 &= \gamma_1 \mathcal{T}(N - M).
\end{aligned}$$

By virtue of periodicity of perturbation fields in the horizontal directions x and y, taking into account the boundary conditions (5.5), $\{\sin(n\pi z)\}_{n\in\mathbb{N}}$ is a complete orthogonal system for $L^2([0,1])$, so let us employ *normal modes* solutions [10]:

$$\begin{aligned}
w^f &= W_0^f \sin(n\pi z) e^{i(lx+my)},\\
w^p &= W_0^p \sin(n\pi z) e^{i(lx+my)},\\
\theta &= \Theta_0 \sin(n\pi z) e^{i(lx+my)},
\end{aligned} \tag{5.13}$$

from (5.12) one obtains

$$\begin{cases}
h_{11} W_0^f + h_{12} W_0^p + R h_{13} \Theta_0 = 0,\\
h_{21} W_0^f + h_{22} W_0^p + R h_{23} \Theta_0 = 0,\\
R W_0^f + R W_0^p - (\Lambda_n + \sigma)\Theta_0 = 0.
\end{cases} \tag{5.14}$$

where $\Lambda_n = n^2\pi^2 + l^2 + m^2$ and

$$\begin{aligned}
h_{11} &= a_1 l^2 + a_2 m^2 + D n^2 \pi^2 + c_1 lm,\\
h_{12} &= a_3 l^2 + a_4 m^2 - c_1 \hat{\gamma}_2 lm,\\
h_{13} &= a_5 l^2 + a_6 m^2 + c_1 lm,\\
h_{21} &= b_1 l^2 + b_2 m^2 + c_1 \hat{\gamma}_1 lm,\\
h_{22} &= b_3 l^2 + b_4 m^2 + D n^2 \pi^2 - c_1 lm,\\
h_{23} &= b_5 l^2 + b_6 m^2 - c_1 lm.
\end{aligned}$$

Finally, requiring a *zero determinant* for (5.14), one gets:

$$R^2 = \frac{(\Lambda_n + \sigma)(h_{11}h_{22} - h_{12}h_{21})}{h_{12}h_{23} - h_{13}h_{22} - h_{11}h_{23} + h_{21}h_{13}} \tag{5.15}$$

Setting $\sigma = \sigma_R + i\sigma_I$, (5.15) is

$$R^2 = \frac{(\Lambda_n + \sigma_R)(h_{11}h_{22} - h_{12}h_{21})}{h_{12}h_{23} - h_{13}h_{22} - h_{11}h_{23} + h_{21}h_{13}} + i\frac{\sigma_I(h_{11}h_{22} - h_{12}h_{21})}{h_{12}h_{23} - h_{13}h_{22} - h_{11}h_{23} + h_{21}h_{13}} \tag{5.16}$$

Since the Rayleigh number R^2 is real, one finally obtains

$$\sigma_I \frac{h_{11}h_{22} - h_{12}h_{21}}{h_{12}h_{23} - h_{13}h_{22} - h_{11}h_{23} + h_{21}h_{13}} = 0 \tag{5.17}$$

where both numerator $h_{11}h_{22} - h_{12}h_{21}$ and denominator $h_{12}h_{23} - h_{13}h_{22} - h_{11}h_{23} + h_{21}h_{13}$ are strictly positive. From (5.17) it follows

$$\sigma_I = 0 \;\Rightarrow\; \sigma \in \mathbb{R}$$

and hence the strong version of the principle of exchange of stabilities holds: if the convection sets in, it arises necessarily via a stationary motion (steady convection). Therefore, the linear instability threshold for the onset of stationary convection is found imposing $\sigma = 0$ in (5.15):

$$R_L^2 = \min_{n,l,m} \frac{\Lambda_n(h_{11}h_{22} - h_{12}h_{21})}{h_{12}h_{23} - h_{13}h_{22} - h_{11}h_{23} + h_{21}h_{13}} \tag{5.18}$$

The minimization (5.18) is numerically analysed in section 5.4.

Let us point out that

(i) assuming $h_1 = h_2 = h$, $k_1 = k_2 = k$ (horizontally isotropic case) and for $\mathcal{T} \to 0$, i.e. in absence of rotation, we get

$$R_L^2 = \min_{n,a^2} \frac{\hat{\Gamma}\Lambda_n}{a^2} \frac{a^4\Gamma\hat{\Gamma}^{-1} + n^4\pi^4 + a^2n^2\pi^2\hat{K}\hat{\Gamma}^{-1}}{a^2(4 + \gamma_1 + \gamma_2) + n^2\pi^2(\frac{\gamma_1}{k} + \frac{\gamma_2}{h} + 4)}$$

where $a^2 = l^2 + m^2$ and

$$\hat{K} = \left[\gamma_1 + \gamma_2 + \frac{\gamma_1}{k} + \frac{\gamma_2}{h} + \gamma_1\gamma_2\left(\frac{1}{k} + \frac{1}{h}\right)\right],$$
$$\Gamma = \gamma_1\gamma_2 + \gamma_1 + \gamma_2,$$
$$\hat{\Gamma} = \frac{\gamma_1}{k} + \frac{\gamma_2}{h} + \frac{\gamma_1}{k}\frac{\gamma_2}{h},$$

that coincides with the instability threshold found in [36];

(ii) the case of a non-rotating layer of isotropic bi-disperse porous medium (assuming $h_s = k_s = 1$ for $s = 1, 2$ and as $\mathcal{T} \to 0$) leads to

$$R_L^2 = \min_{n,a^2} \frac{\Lambda^2}{a^2} \frac{\gamma_1\gamma_2 + \gamma_1 + \gamma_2}{\gamma_1 + \gamma_2 + 4}$$

that is the same threshold found in [25].

5.3 Optimal result: coincidence between linear and nonlinear thresholds

In order to study the influence of rotation on the nonlinear stability of the conduction solution, since the Coriolis terms in momentum equations are antisymmetric, instead of applying the standard energy method, let us apply the differential constraint approach (see [38, 42, 43]).
To this end, let us set

$$\begin{aligned} E(t) &= \frac{1}{2}\|\theta\|^2, \\ I(t) &= (w^f + w^p, \theta), \\ D(t) &= \|\nabla\theta\|^2, \end{aligned} \tag{5.19}$$

and by virtue of $(5.4)_5$, one obtains

$$\frac{dE}{dt} = \left(R\frac{I}{D} - 1\right)D\,. \tag{5.20}$$

Setting

$$\frac{1}{R_E} = \max_{\mathcal{H}^*} \frac{I}{D} \tag{5.21}$$

with

$$\begin{aligned} \mathcal{H}^* = \{(w^f, w^p, \theta) \in (H^1)^3 | w^f = w^p = \theta = 0 \text{ on } z = 0, 1; \\ \text{periodic in } x, y \text{ with periods } 2\pi/l, 2\pi/m; D < \infty; \\ \text{verifying } (5.12)_{1,2}\} \end{aligned}$$

the space of kinematically admissible solutions. The variational problem (5.21) is equivalent to the following variational problem:

$$\frac{1}{R_E} = \max_{\mathcal{H}} \frac{I + \int_V \lambda g_1 \, dV + \int_V \psi g_2 \, dV}{D}, \tag{5.22}$$

where $\lambda(\mathbf{x})$ and $\psi(\mathbf{x})$ are *Lagrange multipliers* and

$$\begin{aligned} g_1 \equiv & R^{-1}(a_1 w^f_{xx} + a_2 w^f_{yy} + D w^f_{zz} + a_3 w^p_{xx} + a_4 w^p_{yy} + c_1 w^f_{xy} - c_1\hat{\gamma}_2 w^p_{xy}) \\ & + a_5\theta_{xx} + a_6\theta_{yy} + c_1\theta_{xy}, \\ g_2 \equiv & R^{-1}(b_1 w^f_{xx} + b_2 w^f_{yy} + b_3 w^p_{xx} + b_4 w^p_{yy} + D w^p_{zz} + c_1\hat{\gamma}_1 w^f_{xy} - c_1 w^p_{xy}) \\ & + b_5\theta_{xx} + b_6\theta_{yy} - c_1\theta_{xy}, \end{aligned} \tag{5.23}$$

$$\begin{aligned} \mathcal{H} = \{ & (w^f, w^p, \theta) \in (H^1)^3 | w^f = w^p = \theta = 0 \text{ on } z = 0, 1; \\ & \text{periodic in } x, y \text{ with periods } 2\pi/l, 2\pi/m; D < \infty \}. \end{aligned}$$

By virtue of Poincaré inequality, since

$$D \geq \pi^2 \|\theta\|^2,$$

from (5.20) one obtains that condition $R < R_E$ guarantees the global nonlinear stability of the conduction solution with respect to the L^2-norm, according to the following remark and the following inequality

$$E(t) \leq E(0) \exp\Big[\frac{R - R_E}{R_E}\, t\Big].$$

Remark 5.3.1. *Multiplying* $(5.4)_1$ *by* $\mathbf{u}^f$*,* $(5.4)_2$ *by* $\mathbf{u}^p$*, integrating over the period cell* V *and adding the resulting equations, one finds*

$$\begin{aligned} & \gamma_1 \int_V \Big[\frac{1}{k_1}(u^f)^2 + \frac{1}{k_2}(v^f)^2 + (w^f)^2\Big] dV + \gamma_2 \int_V \Big[\frac{1}{h_1}(u^p)^2 + \frac{1}{h_2}(v^p)^2 + (w^p)^2\Big] dV \\ & \quad + \|\mathbf{u}^f - \mathbf{u}^p\|^2 = R(\theta, w^f + w^p). \end{aligned} \tag{5.24}$$

Setting $\hat{k} = \max(k_1, k_2, 1)$ *and* $\hat{h} = \max(h_1, h_2, 1)$ *and using the generalized Cauchy inequality on the right hand side of* (5.24)*, one obtains*

$$\frac{\gamma_1}{\hat{k}}\|\mathbf{u}^f\|^2 + \frac{\gamma_2}{\hat{h}}\|\mathbf{u}^p\|^2 \leq R^2\Big(\frac{\hat{k}}{\gamma_1} + \frac{\hat{h}}{\gamma_2}\Big)\|\theta\|^2 \tag{5.25}$$

and hence condition $R < R_E$ *guarantees that* $\|\mathbf{u}^f\|^2 \to 0$ *and* $\|\mathbf{u}^p\|^2 \to 0$ *as* $t \to \infty$*, too.*

In order to solve the variational problem (5.22), let us consider the associated

Euler-Lagrange equations:

$$\begin{cases} R_E(a_5\lambda_{xx} + a_6\lambda_{yy} + c_1\lambda_{xy} + b_5\psi_{xx} + b_6\psi_{yy} - c_1\psi_{xy}) + 2\Delta\theta \\ \qquad + R_E(w^f + w^p) = 0, \\ R_E\theta + a_1\lambda_{xx} + a_2\lambda_{yy} + D\lambda_{zz} + c_1\lambda_{xy} + b_1\psi_{xx} + b_2\psi_{yy} + c_1\hat{\gamma}_1\psi_{xy} = 0, \\ R_E\theta + a_3\lambda_{xx} + a_4\lambda_{yy} - c_1\hat{\gamma}_2\lambda_{xy} + b_3\psi_{xx} + b_4\psi_{yy} + D\psi_{zz} - c_1\psi_{xy} = 0, \\ a_1 w^f_{xx} + a_2 w^f_{yy} + D w^f_{zz} + a_3 w^p_{xx} + a_4 w^p_{yy} + c_1 w^f_{xy} - c_1\hat{\gamma}_2 w^p_{xy} \\ \qquad + R_E(a_5\theta_{xx} + a_6\theta_{yy} + c_1\theta_{xy}) = 0, \\ b_1 w^f_{xx} + b_2 w^f_{yy} + b_3 w^p_{xx} + b_4 w^p_{yy} + D w^p_{zz} + c_1\hat{\gamma}_1 w^f_{xy} - c_1 w^p_{xy} \\ \qquad + R_E(b_5\theta_{xx} + b_6\theta_{yy} - c_1\theta_{xy}) = 0. \end{cases} \tag{5.26}$$

Defining the operators

$$\begin{aligned} \Delta_f &\equiv a_1\partial_{xx} + a_2\partial_{yy} + D\partial_{zz}, \\ \Delta^*_p &\equiv a_3\partial_{xx} + a_4\partial_{yy}, \\ \Delta^*_f &\equiv b_1\partial_{xx} + b_2\partial_{yy}, \\ \Delta_p &\equiv b_3\partial_{xx} + b_4\partial_{yy} + D\partial_{zz}, \\ \mathcal{L}_1 &\equiv a_5\partial_{xx} + a_6\partial_{yy}, \\ \mathcal{L}_2 &\equiv b_5\partial_{xx} + b_6\partial_{yy}. \end{aligned}$$

and taking 2Δ of $(5.26)_{2,3,4,5}$, the Euler-Lagrange equations become

$$\begin{cases} R_E(w^f + w^p) + R_E(\mathcal{L}_1\lambda + c_1\lambda_{xy} + \mathcal{L}_2\psi - c_1\psi_{xy}) = -2\Delta\theta, \\ 2\Delta\Delta_f\lambda + 2c_1\Delta\lambda_{xy} + 2\Delta\Delta^*_f\psi + 2c_1\hat{\gamma}_1\Delta\psi_{xy} = -2R_E\Delta\theta, \\ 2\Delta\Delta^*_p\lambda - 2c_1\hat{\gamma}_2\Delta\lambda_{xy} + 2\Delta\Delta_p\psi - 2c_1\Delta\psi_{xy} = -2R_E\Delta\theta, \\ 2\Delta\Delta_f w^f + 2c_1\Delta w^f_{xy} + 2\Delta\Delta^*_p w^p - 2c_1\hat{\gamma}_2\Delta w^p_{xy} \\ \quad + 2R_E\mathcal{L}_1\Delta\theta + 2R_E c_1\Delta\theta_{xy} = 0, \\ 2\Delta\Delta^*_f w^f + 2c_1\hat{\gamma}_1\Delta w^f_{xy} + 2\Delta\Delta_p w^p - 2c_1\Delta w^p_{xy} \\ \quad + 2R_E\mathcal{L}_2\Delta\theta - 2R_E c_1\Delta\theta_{xy} = 0 \end{cases} \tag{5.27}$$

Eliminating variable θ and setting

$$\begin{aligned}
\mathcal{M}_1 &\equiv 2\Delta\Delta_f + 2c_1\Delta\partial_{xy} - R_E^2\mathcal{L}_1 - R_E^2 c_1\partial_{xy},\\
\mathcal{M}_2 &\equiv 2\Delta\Delta_f^* + 2c_1\hat{\gamma}_1\Delta\partial_{xy} - R_E^2\mathcal{L}_2 + R_E^2 c_1\partial_{xy},\\
\mathcal{M}_3 &\equiv 2\Delta\Delta_p^* - 2c_1\hat{\gamma}_2\Delta\partial_{xy} - R_E^2\mathcal{L}_1 - R_E^2 c_1\partial_{xy},\\
\mathcal{M}_4 &\equiv 2\Delta\Delta_p - 2c_1\Delta\partial_{xy} - R_E^2\mathcal{L}_2 + R_E^2 c_1\partial_{xy},\\
\mathcal{N}_1 &\equiv -R_E(\mathcal{L}_1 + c_1\partial_{xy})^2,\\
\mathcal{N}_2 &\equiv -R_E^2(\mathcal{L}_1 + c_1\partial_{xy})(\mathcal{L}_2 - c_1\partial_{xy}),\\
\mathcal{N}_3 &\equiv -R_E^2(\mathcal{L}_2 - c_1\partial_{xy})^2,
\end{aligned}$$

one obtains

$$\begin{cases}
-R_E^2 w^f - R_E^2 w^p + \mathcal{M}_1\lambda + \mathcal{M}_2\psi = 0,\\
-R_E^2 w^f - R_E^2 w^p + \mathcal{M}_3\lambda + \mathcal{M}_4\psi = 0,\\
\mathcal{M}_1 w^f + \mathcal{M}_3 w^p + \mathcal{N}_1\lambda + \mathcal{N}_2\psi = 0,\\
\mathcal{M}_2 w^f + \mathcal{M}_4 w^p + \mathcal{N}_2\lambda + \mathcal{N}_3\psi = 0.
\end{cases} \tag{5.28}$$

By employing *normal modes* solutions

$$\begin{aligned}
w^f &= W_0^f \sin(n\pi z)e^{i(lx+my)},\\
w^p &= W_0^p \sin(n\pi z)e^{i(lx+my)},
\end{aligned} \tag{5.29}$$

and choosing [51, 42]

$$\begin{aligned}
\lambda &= \lambda_0 \sin(n\pi z)e^{i(lx+my)},\\
\psi &= \psi_0 \sin(n\pi z)e^{i(lx+my)},
\end{aligned} \tag{5.30}$$

from (5.28) one obtains

$$\begin{cases}
-R_E^2 W_0^f - R_E^2 W_0^p + (2\Lambda_n h_{11} + R_E^2 h_{13})\lambda_0 + (2\Lambda_n h_{21} + R_E^2 h_{23})\psi_0 = 0,\\
-R_E^2 W_0^f - R_E^2 W_0^p + (2\Lambda_n h_{12} + R_E^2 h_{13})\lambda_0 + (2\Lambda_n h_{22} + R_E^2 h_{23})\psi_0 = 0,\\
(2\Lambda_n h_{11} + R_E^2 h_{13})W_0^f + (2\Lambda_n h_{12} + R_E^2 h_{13})W_0^p - R_E^2 h_{13}^2\lambda_0 - R_E^2 h_{13}h_{23}\psi_0 = 0,\\
(2\Lambda_n h_{21} + R_E^2 h_{23})W_0^f + (2\Lambda_n h_{22} + R_E^2 h_{23})W_0^p - R_E^2 h_{13}h_{23}\lambda_0 - R_E^2 h_{23}^2\psi_0 = 0.
\end{cases} \tag{5.31}$$

Requiring a *zero determinant* for (5.31) we find

$$R_E^2 = R_L^2,$$

and hence the global non linear stability threshold and the linear instability threshold coincide and subcritical instabilities do not exist.

5.4 Asymptotic behaviour of the instability threshold and cell patterns

We now present numerical results to solve (5.18), in order to analyse the asymptotic behaviour of R_L^2 with respect to $\mathcal{T}$, h_i, k_i, for $i = 1, 2$, i.e. to study the influence of rotation and anisotropic permeability on the onset of convection. As regards the physical parameters, in all numerical simulations we chose a set of values analogous to those ones fixed in [35], in order to compare our results with those ones obtained in [35], to stress the influence of rotation and anisotropy on the onset of convection.
In all the computations we performed, the minimum of R_L^2 with respect to n is attained at $n = 1$. Each of the following tables and figures show the *stabilizing effect of rotation* on the onset of convection.

R_L^2	l	m	$\mathcal{T}$
342.0314	0.8681	2.9868	0
342.1650	0.8683	2.9874	0.1
355.1930	0.8845	3.0385	1
606.4105	1.2509	3.5844	5
1096.6	2.1500	2.5456	10
4476.3	4.4554	0	50
12228	6.2551	0	100

Table 5.1: Critical R_L^2, l, m for increasing $\mathcal{T}$ and $h_1 = 10, h_2 = 1, k_1 = 0.1, k_2 = 1, \eta = 0.2, \gamma_1 = 10, \gamma_2 = 50$

R_L^2	l	m	$\mathcal{T}$
216.7792	2.0756	0	0
219.6234	2.0991	0	0.1
416.4060	3.2100	0	1
594.6478	3.7883	0.9462	1.5
795.6823	4.2006	1.5401	2
1653	3.8717	2.8998	4
1808.9	2.4736	3.1779	4.5
1860.3	0	3.2761	5
1988.1	0	3.1874	10
3408.4	0	3.9766	100

Table 5.2: Critical R_L^2, l, m for increasing $\mathcal{T}$ and $h_1 = 0.1, h_2 = 1, k_1 = 10, k_2 = 1, \eta = 0.2, \gamma_1 = 10, \gamma_2 = 50$

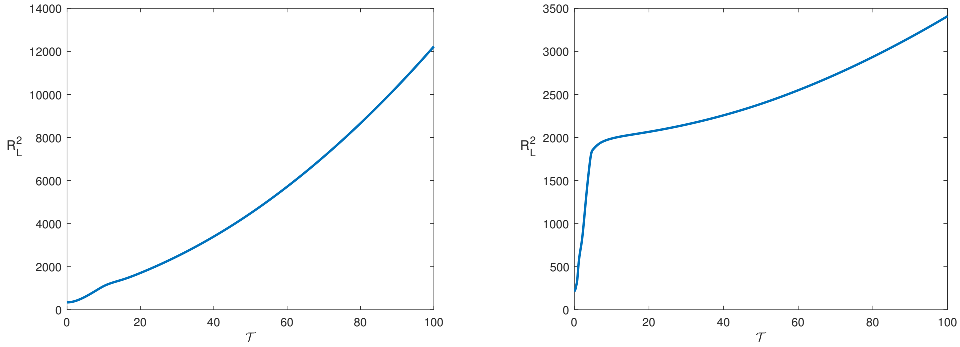

(a) $h_1 >> k_1$ (b) $h_1 << k_1$

Figure 5.1: (a): critical Rayleigh number R_L^2 as function of the Taylor number $\mathcal{T}$ for $h_1 = 10, h_2 = 1, k_1 = 0.1, k_2 = 1, \eta = 0.2, \gamma_1 = 10, \gamma_2 = 50$. (b): critical Rayleigh number R_L^2 as function of the Taylor number $\mathcal{T}$ for $h_1 = 0.1, h_2 = 1, k_1 = 10, k_2 = 1, \eta = 0.2, \gamma_1 = 10, \gamma_2 = 50$.

The table 5.1 shows that for large values of the Taylor number $\mathcal{T}$ and when $h_1 >> k_1$, m becomes zero, this means that, as rotation increases, the convection cells become rolls with the axis in the y-direction. The table 5.2 shows a *transition* from convection patterns as rolls along y-axis ($m = 0$ for very small $\mathcal{T}$) to convection patterns as rolls along x-axis ($l = 0$), as the rotation increases and for $h_1 << k_1$. For these physical values, the asymptotic behaviour of R_L^2 with respect to $\mathcal{T}$ is shown in the figure 5.1. We can also observe that, as $\mathcal{T}$ increases, R_L^2 increases more slowly when $h_1 << k_1$ then $h_1 >> k_1$.
Let us point out that bi-dimensional convection cells (rolls along x-axis for $l = 0$ and rolls along y-axis for $m = 0$) were already found in [35] as an effect of anisotropic macropermeability and micropermeability in absence of rotation.

From table 5.3, we numerically find out that for parameters $\{h_1 = 1, h_2 = 0.1, k_1 = 1, k_2 = 10, \eta = 0.2, \gamma_1 = 2, \gamma_2 = 0.2\}$ the critical value of m is mainly zero, except for very small values of the Taylor number $\mathcal{T} \in [0, 3)$, for which l and m are both non-zero, i.e. for very little rotation of the layer, three-dimensional convection cells are expected.
As a matter of fact, the wavelengths in the x and y directions are $\hat{x} = \frac{2\pi}{l}$ and $\hat{y} = \frac{2\pi}{m}$. The condition $\hat{y}/\hat{x} = 0$ implies $l = 0$, this means that the convective fluid motion occurs in the y and z directions (the solution is a function of y and z), i.e. the convection cells are rolls in the x-direction. Instead, the condition $\hat{y}/\hat{x} \to \infty$ implies $m = 0$ and the convective fluid motion occurs in

(a)

R_L^2	l	m	$\mathcal{T}$
16.5555	3.1416	0.0334	0
16.5570	3.1415	0.0413	0.01
16.7028	3.1399	0.3139	0.1
19.7124	3.1420	1.3606	0.5
26.4272	3.2505	2.1111	1
42.8398	3.6375	2.1076	2
50.3892	3.8240	0.1504	2.5
54.2050	3.8079	0.0011	2.8
56.6389	3.8030	0	3
79.6444	3.9576	0	5
152.0288	4.8151	0	10
1815	10.0471	0	50
6581.4	14.1637	0	100

(b)

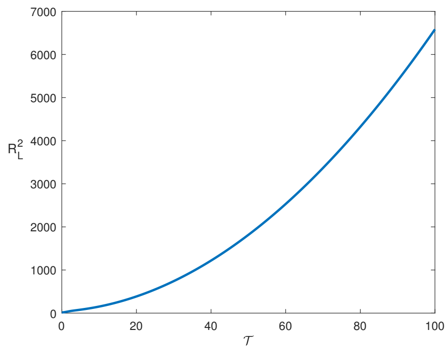

Table 5.3: (a): critical R_L^2, l, m for increasing $\mathcal{T}$. (b): critical Rayleigh number R_L^2 as function of the Taylor number $\mathcal{T}$. For $h_1 = 1, h_2 = 0.1, k_1 = 1, k_2 = 10, \eta = 0.2, \gamma_1 = 2, \gamma_2 = 0.2$.

the x and z directions, so the cells are rolls in the y-direction [35].

Tables 5.4 – 5.5 exhibit the influence of anisotropy parameters for both macropores and micropores on the onset of convection, and the values of h_1, h_2, k_1, k_2 are fixed such that the permeability ratios in the macropores and micropores are different, in particular we set $\{h_1 = 3.3, h_2 = 0.9, k_1 = 0.2, k_2 = 1.1\}$ (see [35]) and we vary h_s, k_s for $s = 1, 2$ in turn to see how each parameter affects the Rayleigh number. As in [35], we numerically find out a very complex relationship between the macro and micro permeability parameters and the critical Rayleigh and wave numbers. For increasing h_1, h_2, k_1, k_2 we can see a similar trend, i.e. R_L^2 increases up to a maximum before decreasing. From 5.3(a) and from 5.4(a) we can see a first transition from rolls along x-axis to three-dimensional cells and then another transition to rolls along y-axis, while 5.3(b) and 5.4(b) displays a mirror behaviour with respect to 5.3(a) and 5.4(a), respectively.
In figure 5.2 the critical Rayleigh number R_L^2 is represented as function of the Taylor number $\mathcal{T}$ for $h_1 = 0.1, 1, 5, 10$ and the others parameters are fixed as $h_2 = 0.9, k_1 = 0.2, k_2 = 1.1, \eta = 0.2, \gamma_1 = 0.9, \gamma_2 = 1.8$, with the aim to graphically analyse the values shown in table 5.3(a).

Let us underline that the behaviour (increasing or decreasing) of the

(a)

R_L^2	l	m	h_1
72.0664	0	3.9779	0.1
80.3593	0	4.2133	0.5
87.5331	0	4.4002	1
99.4378	0.0023	4.6828	2.5
101.3657	1.8730	4.0969	3
101.9684	2.2477	3.7690	3.3
102.5416	3.0110	2.3960	5
101.6569	3.2416	1.0423	7
101.4029	3.2703	0.5478	7.5
101.1561	3.2772	0.0030	8
100.4043	3.2598	0	10
97.6476	3.1953	0	100

(b)

R_L^2	l	m	h_2
77.2756	3.0012	0	0.1
93.7839	3.2485	0	0.5
97.2253	3.2919	0.0025	0.6
99.9532	3.0972	2.1071	0.7
101.9684	2.2477	3.7690	0.9
101.6923	1.4139	4.3715	1
98.0214	0	4.5583	1.5
92.1505	0	4.3049	5
90.7919	0	4.2441	10
89.5334	0	4.1871	100

Table 5.4: Critical R_L^2, l, m for quoted values of h_1 (a) and for quoted values of h_2 (b). *Table a*: $h_2 = 0.9, k_1 = 0.2, k_2 = 1.1, \eta = 0.2, \gamma_1 = 0.9, \gamma_2 = 1.8, \mathcal{T} = 10$. *Table b*: $h_1 = 3.3, k_1 = 0.2, k_2 = 1.1, \eta = 0.2, \gamma_1 = 0.9, \gamma_2 = 1.8, \mathcal{T} = 10$.

(a)

R_L^2	l	m	k_1
58.9329	0	4.4430	0.05
77.3354	0	4.7150	0.1
91.5765	0.0028	4.7810	0.15
101.9684	2.2477	3.7690	0.2
106.2647	3.3934	0.3203	0.25
106.2066	3.4023	0	0.3
106.0864	3.4078	0	0.5
105.9929	3.4121	0	1
105.9159	3.4157	0	5
105.9061	3.4162	0	10

(b)

R_L^2	l	m	k_2
66.4721	3.8969	0	0.1
87.3683	3.6711	0	0.3
96.2862	3.5414	0.0011	0.5
101.1517	2.7734	3.0504	0.8
101.9684	2.2477	3.7690	1.1
102.1598	1.5167	4.3633	2
101.8944	0.7318	4.6887	5
101.7847	0.3533	4.7594	8
101.7447	0.0135	4.7805	10
101.5976	0.0017	4.7825	100
101.5829	0.0016	4.7827	10^3

Table 5.5: Critical R_L^2, l, m for quoted values of k_1 (a) and for quoted values of k_2 (b). *Table a*: $h_1 = 3.3, h_2 = 0.9, k_2 = 1.1, \eta = 0.2, \gamma_1 = 0.9, \gamma_2 = 1.8, \mathcal{T} = 10$. *Table b*: $h_1 = 3.3, h_2 = 0.9, k_1 = 0.2, \eta = 0.2, \gamma_1 = 0.9, \gamma_2 = 1.8, \mathcal{T} = 10$.

critical Rayleigh number with respect to anisotropic parameters and the type of arising cells (rolls in x or in y directions) strictly depend on the relationship between the ratios $\frac{k_1}{h_1}$ and $\frac{k_2}{h_2}$.

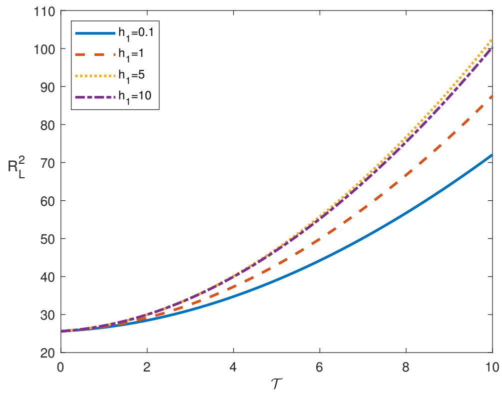

Figure 5.2: Critical Rayleigh number R_L^2 as function of the Taylor number $\mathcal{T}$ for $h_1 = 0.1, 1, 5, 10$ and $h_2 = 0.9, k_1 = 0.2, k_2 = 1.1, \eta = 0.2, \gamma_1 = 0.9, \gamma_2 = 1.8$.

In particular, when

$$\frac{k_1}{h_1} > \frac{k_2}{h_2} \quad \Rightarrow \quad m = 0, \tag{5.32}$$

i.e. rolls in the x-direction are expected, while if

$$\frac{k_1}{h_1} < \frac{k_2}{h_2} \quad \Rightarrow \quad l = 0, \tag{5.33}$$

so rolls in the y-direction will arise. To study this behaviour, in the fixed set of parameters: $\{\mathcal{T} = 10, \eta = 0.2, \gamma_1 = 0.8, \gamma_2 = 1.9\}$, we obtained Figures 5.3: in Figure 5.3(a) we fixed $\frac{k_2}{h_2} = 10$ and assumed $\frac{k_1}{h_1} \in \left[0, \frac{k_1}{h_1}\right]$, therefore we chose $k_2 = 10, h_1 = 0.1, h_2 = 1$ and $k_1 \in [0, 1]$, meanwhile in Figure 5.3(b) we fixed $\frac{k_1}{h_1} = 10$ and assumed $\frac{k_2}{h_2} \in \left[0, \frac{k_1}{h_1}\right]$, choosing $k_1 = 10, h_1 = 1, h_2 = 0.1$ and $k_2 \in [0, 1]$.
For a different set of values for the anisotropic parameters - i.e. $h_1 = 3.3, k_1 = 0.2, k_2 = 1.1$ and $h_2 \in [0.2]$ - in Figures 5.4 we plotted the critical Rayleigh number R_L^2 and the critical wave numbers l and m as functions of h_2, and we found that (i) R_L^2 increases up to a maximum before decreasing (ii) for increasing h_2, there is a transition from convection patterns as rolls along y-axis ($m = 0$) to three-dimensional convection cells (l and m are both non-zero) and then a transition from three-dimensional convection cells to convection patterns as rolls along x-axis ($l = 0$).

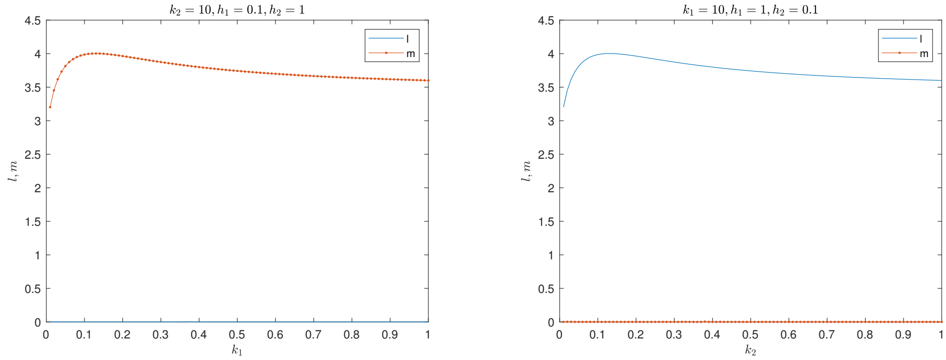

(a) (b)

Figure 5.3: (a): Critical wave numbers l and m as function of k_1. (b): Critical wave numbers l and m as function of k_2.

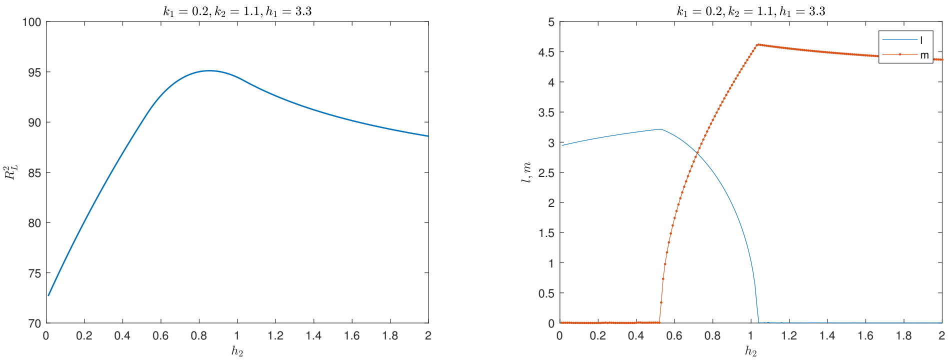

(a) (b)

Figure 5.4: (a): Critical Rayleigh number R_L^2 as function of h_2. (b): Critical wave numbers l and m as function of h_2.

Main results

The onset of thermal convection in a horizontal layer of anisotropic BDPM, uniformly rotating about a vertical axis and uniformly heated from below, was analysed, according to Darcy's law in both micropores and macropores. In particular, it was proved that:

- the strong version of the principle of exchange of stabilities holds and hence, when the convection arises, it sets in through a stationary motion;
- the linear instability threshold and the global nonlinear stability thresh-

old in the L^2-norm coincide: this is an optimal result since the stability threshold furnishes a necessary and sufficient condition to guarantee the global (i.e. for all initial data) nonlinear stability.

Moreover, the influence of the rotation and the influence of the anisotropy on the onset of convection were numerically analysed.

Chapter 6

The onset of double diffusive convection in a rotating bi-disperse porous medium

As regards applicative implications of convection problems, to obtain even more useful results in applications involving, for instance, food and chemical processes, solidification and centrifugal casting of metals, rotating machineries, petroleum industry, biomechanics and geophysical problems, the presence of one or more chemicals (salts) dissolved in the fluid has been largely analysed either in rotating clear fluids [34] or in rotating single porosity media [52, 53]. The analysis of double-diffusive convection requires to suppose that there is a salt dissolved in the fluid, so one considers simultaneous temperature and salt gradients, i.e. simultaneous mass diffusion and thermal diffusion in a liquid mixture.
From a mathematical point of view, when a fluid mixture in a rotating layer heated from below is considered, the competing effects of heating from below (that has a destabilizing effect on the conduction solution) and of rotation and salting from below (that both have a stabilizing effect) are challenging to analyse, since rotation and salt concentration give rise to a skewsymmetric part in the linear operator of the governing equations. Double diffusive bi-dispersive convection was studied by Straughan in [49, 47], by Challoob et al. in [54] under generalized boundary conditions, while Badday and Harfash in [3, 55] deal with bi-dispersive double diffusive convection, taking into account chemical reaction effects. However, in the present Chapter we focus our attention to double diffusive convection in a uniformly rotating single temperature bi-disperse porous material.

Unlike the diffusion of heat, the diffusion of salt can take place only through

the fluid phase, so there are two physical effects to consider: the Soret effect, i.e. the mass flux created by a temperature gradient, and the Dufour effect, i.e. the energy flux induced by a concentration gradient, but, according to experimental results, the Dufour effect plays a minor role in comparison with the Soret effect when a binary liquid mixture saturating a porous medium is considered (see [56] and the references therein).
As defined in [57], the *Soret effect*, also known as *thermodiffusion*, is the mass diffusion in a liquid mixture when a temperature gradient exists and is constantly maintained across the multicomponent mixture, causing all species to move. In response to a gradual and continuous migration of all particles from the hot side to the cold side, following the direction of the heat flow, a concentration gradient starts to develop within the mixture, which slows down the migration of the species to the cold side and causes some of the particles to move on the opposite direction. The contrast between thermal and concentration forces causes the rearrangement of the species until the final steady state. Some applications of the Soret effect are optimum oil recovery from hydrocarbon reservoirs, fabrication of semiconductor devices in molten metal and semiconductor mixtures, separation of species such as polymers, manipulation of macromolecules such as DNA [57].
The present Chapter is based on the paper [58] with F. Capone and R. De Luca and is organized as follows. In Section 6.1 the mathematical model and the associated perturbation equations are introduced. In Section 6.2 we perform linear instability analysis of the thermal conduction solution and prove that if $\epsilon_1 Le \leq 1$ the strong principle of exchange of stabilities holds. Hence, in Sections 6.2.1 and 6.2.2 we determine the critical Rayleigh numbers for the onset of steady and oscillatory convection, respectively. In Section 6.2.3 some mathematical aspects shared by the stationary and the oscillatory instability thresholds are discussed. In Section 6.3 the differential constraint approach is utilized to derive the global nonlinear instability threshold and we found that there are regions of subcritical instabilities. In Section 6.4 we perform some numerical simulations in order to analyse the behaviour of the instability thresholds with respect to fundamental physical parameters.

6.1 Problem formulation

Let us consider a reference frame $Oxyz$ with fundamental unit vectors $\mathbf{i}, \mathbf{j}, \mathbf{k}$ ($\mathbf{k}$ pointing vertically upward) and a plane layer $L = \mathbb{R}^2 \times [0, d]$ of saturated bi-disperse porous medium that is uniformly and simultaneously *heated* and *salted* from below, and that is filled by an incompressible Newtonian fluid. Furthermore, we confine ourselves to the case of a single temperature bi-disperse porous material, so there is thermal equilibrium between the f-phase and the p-phase, i.e. $T^f = T^p = T$. The layer L rotates about the vertical axis with constant angular velocity $\Omega\mathbf{k}$, hence Darcy's model is extended in order to include Coriolis forces in the momentum equations in the macropores and in the micropores. Moreover, a Boussinesq approximation is applied and the density in the buoyancy force has a linear dependence on temperature and concentration:

$$\varrho = \varrho_F[1 - \alpha(T - T_0) + \alpha_C(C - C_0)],$$

α and α_C being thermal and chemical expansion coefficients, respectively. The governing equations for the onset of thermal convection in a uniformly rotating bi-disperse porous medium heated and salted from below, taking into account the Soret effect, are (cf. [21, 49])

$$\begin{cases} -\dfrac{\mu}{K_f}\mathbf{v}^f - \zeta(\mathbf{v}^f - \mathbf{v}^p) - \nabla p^f + \varrho_F\alpha g T\mathbf{k} - \varrho_F\alpha_C g C\mathbf{k} - \dfrac{2\varrho_F\Omega}{\varphi}\mathbf{k}\times\mathbf{v}^f = \mathbf{0}, \\ -\dfrac{\mu}{K_p}\mathbf{v}^p - \zeta(\mathbf{v}^p - \mathbf{v}^f) - \nabla p^p + \varrho_F\alpha g T\mathbf{k} - \varrho_F\alpha_C g C\mathbf{k} - \dfrac{2\varrho_F\Omega}{\epsilon}\mathbf{k}\times\mathbf{v}^p = \mathbf{0}, \\ \nabla\cdot\mathbf{v}^f = 0, \\ \nabla\cdot\mathbf{v}^p = 0, \\ (\varrho c)_m\dfrac{\partial T}{\partial t} + (\varrho c)_F(\mathbf{v}^f + \mathbf{v}^p)\cdot\nabla T = k_m\Delta T, \\ \epsilon_1\dfrac{\partial C}{\partial t} + (\mathbf{v}^f + \mathbf{v}^p)\cdot\nabla C = \epsilon_2\Delta C + S\Delta T, \end{cases} \tag{6.1}$$

where p^f and p^p are the reduced pressures, i.e.

$$p^s = P^s - \frac{\varrho_F}{2}|\mathbf{\Omega}\times\mathbf{x}|^2, \quad s = f, p$$

$\mathbf{x} = (x, y, z)$, $\mathbf{v}^s$ = seepage velocity for $s = \{f, p\}$, T = temperature field, C = concentration field, ζ = interaction coefficient between the f-phase and the p-phase, $\mathbf{g} = -g\mathbf{k}$ = gravity, μ = fluid viscosity, ϱ_F = reference constant density, K_s = permeability for $s = \{f, p\}$, c = specific heat, k_m = thermal conductivity, k_s = thermal conductivity for $s = \{f, p\}$, k_C^s = salt diffusivity for $s = \{f, p\}$, $S = \varphi S_T^f + \epsilon(1-\varphi)S_T^p$, S_T^s = Soret coefficient for $s = \{f, p\}$,

$$\begin{aligned} &(\varrho c)_m = (1-\varphi)(1-\epsilon)(\varrho c)_{sol} + \varphi(\varrho c)_f + \epsilon(1-\varphi)(\varrho c)_p, \\ &k_m = (1-\varphi)(1-\epsilon)k_{sol} + \varphi k_f + \epsilon(1-\varphi)k_p, \\ &\epsilon_1 = \varphi + \epsilon(1-\varphi), \;\; \epsilon_2 = \varphi k_C^f + \epsilon(1-\varphi)k_C^p, \end{aligned}$$

where the subscript *sol* is referred to the solid skeleton. Let us remark that in the case of single temperature BDPM, since macropores and micropores are saturated by the same fluid, we expect that $(\varrho c)_f = (\varrho c)_p = (\varrho c)_F$, hence $(\varrho c)_m = (1-\varphi)(1-\epsilon)(\varrho c)_{sol} + [\varphi + \epsilon(1-\varphi)](\varrho c)_F$ [26] .

The boundary conditions associated to (6.1) are

$$\begin{array}{l}
\mathbf{v}^s \cdot \mathbf{n} = 0 \text{ on } z = 0, d, \text{ for } s = \{f, p\} \\
T = T_L \text{ on } z = 0, \quad T = T_U \text{ on } z = d, \\
C = C_L \text{ on } z = 0, \quad C = C_U \text{ on } z = d
\end{array} \tag{6.2}$$

where $\mathbf{n}$ is the unit outward normal to the impermeable horizontal planes delimiting the layer. Moreover, since the layer of BDPM is heated and salted from below, we assume $T_L > T_U$ and $C_L > C_U$.

System (6.1)-(6.2) admits the the stationary *thermosolutal* conduction solution

$$\begin{array}{l}
\overline{\mathbf{v}}^f = 0, \ \overline{\mathbf{v}}^p = 0, \ \overline{T} = -\beta z + T_L, \ \overline{C} = -\beta_C z + C_L, \\
\dfrac{1}{\varrho_F}\overline{p}^s(z) = g(-\alpha\beta + \alpha_C\beta_C)\dfrac{z^2}{2} + g(\alpha T_L - \alpha_C C_L)z + \overline{p}^s(0), \text{ with } s = \{f, p\}
\end{array}$$

where $\beta = \dfrac{T_L - T_U}{d}$ is the temperature gradient, $\beta_C = \dfrac{C_L - C_U}{d}$ is the concentration gradient and $\overline{p}^s(0)$ are assigned constants, for $s = \{f, p\}$. Introducing a perturbation $\{\mathbf{u}^f, \mathbf{u}^p, \theta, \gamma, \pi^f, \pi^p\}$ to the steady solution, with $\mathbf{u}^f = (u^f, v^f, w^f)$ and $\mathbf{u}^p = (u^p, v^p, w^p)$, the arising perturbation equations are

$$\begin{cases}
-\dfrac{\mu}{K_f}\mathbf{u}^f - \zeta(\mathbf{u}^f - \mathbf{u}^p) - \nabla\pi^f + \varrho_F\alpha g\theta\mathbf{k} - \varrho_F\alpha_C g\gamma\mathbf{k} - \dfrac{2\varrho_F\Omega}{\varphi}\mathbf{k} \times \mathbf{u}^f = \mathbf{0}, \\
-\dfrac{\mu}{K_p}\mathbf{u}^p - \zeta(\mathbf{u}^p - \mathbf{u}^f) - \nabla\pi^p + \varrho_F\alpha g\theta\mathbf{k} - \varrho_F\alpha_C g\gamma\mathbf{k} - \dfrac{2\varrho_F\Omega}{\epsilon}\mathbf{k} \times \mathbf{u}^p = \mathbf{0}, \\
\nabla \cdot \mathbf{u}^f = 0, \\
\nabla \cdot \mathbf{u}^p = 0, \\
(\varrho c)_m\dfrac{\partial\theta}{\partial t} + (\varrho c)_F(\mathbf{u}^f + \mathbf{u}^p) \cdot \nabla\theta = (\varrho c)_f(w^f + w^p)\beta + k_m\Delta\theta, \\
\epsilon_1\dfrac{\partial\gamma}{\partial t} + (\mathbf{u}^f + \mathbf{u}^p) \cdot \nabla\gamma = (w^f + w^p)\beta_C + \epsilon_2\Delta\gamma + S\Delta\theta.
\end{cases} \tag{6.3}$$

Let us introduce the following non-dimensional parameters:

$$\mathbf{x}^* = \frac{\mathbf{x}}{d},\ t^* = \frac{t}{t^\#},\ \theta^* = \frac{\theta}{T^\#},\ \gamma^* = \frac{\gamma}{C^\#}$$

$$\mathbf{u}^{s*} = \frac{\mathbf{u}^s}{U},\ \pi^{s*} = \frac{\pi^s}{P^\#},\ \text{for } s = \{f, p\}$$

$$\eta = \frac{\varphi}{\epsilon},\ \xi = \frac{K_f \zeta}{\mu},\ K_r = \frac{K_f}{K_p},\ A = \frac{(\varrho c)_m}{(\varrho c)_F}$$

where the scales are given by

$$U = \frac{k_m}{(\varrho c)_F d},\ t^\# = \frac{d^2 (\varrho c)_m}{k_m},\ P^\# = \frac{k_m \mu}{(\varrho c)_F K_f},\ T^\# = \frac{\beta d^2 U (\varrho c)_F}{k_m},\ C^\# = \frac{\beta_C U d^2}{\epsilon_2},$$

and let us define the Lewis number Le, the non-dimensional Soret number $\mathcal{S}$, the Taylor number $\mathcal{T}$, the Rayleigh number Ra and the Rayleigh number for the salt field $\mathcal{C}$, respectively given by

$$Le = \frac{k_m}{\epsilon_2 (\varrho c)_m}, \quad \mathcal{S} = \frac{S T^\#}{\epsilon_2 C^\#}, \quad \mathcal{T} = \frac{2 \varrho_F \Omega K_f}{\varphi \mu},$$

$$\mathrm{Ra} = \frac{\beta d^2 (\varrho c)_F \varrho_F \alpha g K_f}{\mu k_m}, \quad \mathcal{C} = \frac{K_f \varrho_F \alpha_C g \beta_C d^2}{\mu \epsilon_2}.$$

The dimensionless equations describing the evolutionary behaviour of the perturbation fields, dropping all the asterisks, are

$$\begin{cases} -\mathbf{u}^f - \xi(\mathbf{u}^f - \mathbf{u}^p) - \nabla \pi^f + \mathrm{Ra}\theta\mathbf{k} - \mathcal{C}\gamma\mathbf{k} - \mathcal{T}\mathbf{k} \times \mathbf{u}^f = \mathbf{0}, \\ -K_r \mathbf{u}^p - \xi(\mathbf{u}^p - \mathbf{u}^f) - \nabla \pi^p + \mathrm{Ra}\theta\mathbf{k} - \mathcal{C}\gamma\mathbf{k} - \eta\mathcal{T}\mathbf{k} \times \mathbf{u}^p = \mathbf{0}, \\ \nabla \cdot \mathbf{u}^f = 0, \\ \nabla \cdot \mathbf{u}^p = 0, \\ \dfrac{\partial \theta}{\partial t} + (\mathbf{u}^f + \mathbf{u}^p) \cdot \nabla \theta = w^f + w^p + \Delta\theta, \\ \epsilon_1 Le \dfrac{\partial \gamma}{\partial t} + A\, Le (\mathbf{u}^f + \mathbf{u}^p) \cdot \nabla \gamma = w^f + w^p + \Delta\gamma + \mathcal{S}\Delta\theta. \end{cases} \tag{6.4}$$

The initial conditions and the boundary conditions appended to system (6.4) are

$$\mathbf{u}^s(\mathbf{x}, 0) = \mathbf{u}_0^s(\mathbf{x}), \quad \pi^s(\mathbf{x}, 0) = \pi_0^s(\mathbf{x}), \quad \theta(\mathbf{x}, 0) = \theta_0(\mathbf{x}), \quad \gamma(\mathbf{x}, 0) = \gamma_0(\mathbf{x})$$

with $\nabla \cdot \mathbf{u}_0^s = 0$, for $s = \{f, p\}$, and

$$w^f = w^p = \theta = \gamma = 0 \quad \text{on } z = 0, 1, \tag{6.5}$$

respectively.

Remark 6.1.1. *With the aim to perform the stability analysis of the conduction solution to system* (6.1)-(6.2)*, so of the null solution to* (6.4)-(6.5)*, let us denote by*

$$V = \left[0, \frac{2\pi}{l}\right] \times \left[0, \frac{2\pi}{m}\right] \times [0,1]$$

the periodicity cell, let us assume that $\forall f \in \{\nabla\pi^s, u^s, v^s, w^s, \theta, \gamma\}$ *for* $s = \{f,p\}$, $f \in W^{2,2}(V)$ $\forall t \in \mathbb{R}^+$, *and that* f *is a periodic function in the* x *and* y *directions of period* $2\pi/l$ *and* $2\pi/m$*, respectively.*

6.2 Double-diffusive convection: linear instability analysis

In order to study the linear instability of the thermal conduction solution, let us consider the linear version of system (6.4) and seek for a solution $\mathbf{u}^f, \mathbf{u}^p, \pi^f, \pi^p, \theta, \gamma$ with time dependence like $e^{\sigma t}$, with $\sigma \in \mathbb{C}$, so we get

$$\begin{cases} -\mathbf{u}^f - \xi(\mathbf{u}^f - \mathbf{u}^p) - \nabla\pi^f + \mathrm{Ra}\theta\mathbf{k} - \mathcal{C}\gamma\mathbf{k} - \mathcal{T}\mathbf{k}\times\mathbf{u}^f = \mathbf{0}, \\ -K_r\mathbf{u}^p - \xi(\mathbf{u}^p - \mathbf{u}^f) - \nabla\pi^p + \mathrm{Ra}\theta\mathbf{k} - \mathcal{C}\gamma\mathbf{k} - \eta\mathcal{T}\mathbf{k}\times\mathbf{u}^p = \mathbf{0}, \\ \nabla\cdot\mathbf{u}^f = 0, \\ \nabla\cdot\mathbf{u}^p = 0, \\ \sigma\theta = w^f + w^p + \Delta\theta, \\ \epsilon_1 Le\,\sigma\,\gamma = w^f + w^p + \Delta\gamma + \mathcal{S}\Delta\theta. \end{cases} \tag{6.6}$$

Setting

$$\omega_3^s = (\nabla\times\mathbf{u}^s)\cdot\mathbf{k},\ \ s = \{f,p\},$$

and taking the third component of curl of $(6.6)_1$ and $(6.6)_2$, we get

$$\begin{cases} (\xi+1)\omega_3^f - \xi\omega_3^p = \mathcal{T}\dfrac{\partial w^f}{\partial z}, \\ (\xi+K_r)\omega_3^p - \xi\omega_3^f = \eta\mathcal{T}\dfrac{\partial w^p}{\partial z}, \end{cases} \tag{6.7}$$

i.e.

$$\begin{cases} \omega_3^f = \Gamma^{-1}\mathcal{T}\Big[(\xi+K_r)\dfrac{\partial w^f}{\partial z} + \eta\xi\dfrac{\partial w^p}{\partial z}\Big], \\ \omega_3^p = \Gamma^{-1}\mathcal{T}\Big[\xi\dfrac{\partial w^f}{\partial z} + \eta(\xi+1)\dfrac{\partial w^p}{\partial z}\Big], \end{cases} \tag{6.8}$$

where $\Gamma = \xi + \xi K_r + K_r$. Now, substituting the derivative with respect to z of (6.8) in the third component of double curl of $(6.6)_1$ and $(6.6)_2$, that is

$$\begin{cases} (1+\xi)\Delta w^f - \xi\Delta w^p - \mathrm{Ra}\Delta_1\theta + \mathcal{C}\Delta_1\gamma + \mathcal{T}\dfrac{\partial\omega_3^f}{\partial z} = 0, \\ (K_r+\xi)\Delta w^p - \xi\Delta w^f - \mathrm{Ra}\Delta_1\theta + \mathcal{C}\Delta_1\gamma + \eta\mathcal{T}\dfrac{\partial\omega_3^p}{\partial z} = 0, \end{cases} \tag{6.9}$$

where $\Delta_1 = \partial^2/\partial x^2 + \partial^2/\partial y^2$ is the horizontal Laplacian, we finally get the following boundary value problem in w^f, w^p, θ, γ

$$\begin{cases} (1+\xi)\Delta w^f - \xi\Delta w^p - \mathrm{Ra}\Delta_1\theta + \mathcal{C}\Delta_1\gamma + \Gamma^{-1}\mathcal{T}^2\Big[(\xi+K_r)\dfrac{\partial^2 w^f}{\partial z^2} + \eta\xi\dfrac{\partial^2 w^p}{\partial z^2}\Big] = 0, \\ (K_r+\xi)\Delta w^p - \xi\Delta w^f - \mathrm{Ra}\Delta_1\theta + \mathcal{C}\Delta_1\gamma + \Gamma^{-1}\eta\mathcal{T}^2\Big[\xi\dfrac{\partial^2 w^f}{\partial z^2} + \eta(\xi+1)\dfrac{\partial^2 w^p}{\partial z^2}\Big] = 0 \\ \sigma\theta = w^f + w^p + \Delta\theta, \\ \epsilon_1 Le\,\sigma\,\gamma = w^f + w^p + \Delta\gamma + \mathcal{S}\Delta\theta. \end{cases} \tag{6.10}$$

According to boundary conditions (6.5) and to the periodicity of the perturbations fields, being $\{\sin(n\pi z)\}_{n\in\mathbb{N}}$ a complete orthogonal system for $L^2([0,1])$, we employ normal modes solutions in (6.10):

$$\begin{aligned} w^f &= \sum_{n=1}^{\infty} W_{0n}^f \sin(n\pi z) e^{i(lx+my)}, \\ w^p &= \sum_{n=1}^{\infty} W_{0n}^p \sin(n\pi z) e^{i(lx+my)}, \\ \theta &= \sum_{n=1}^{\infty} \Theta_{0n} \sin(n\pi z) e^{i(lx+my)}, \\ \gamma &= \sum_{n=1}^{\infty} \Gamma_{0n} \sin(n\pi z) e^{i(lx+my)}, \end{aligned} \tag{6.11}$$

where $W_{0n}^f, W_{0n}^p, \Theta_{0n}, \Gamma_{0n}$ are real constants. Consequently we get

$$\begin{cases} \Big[(1+\xi)\Lambda_n + \Gamma^{-1}\mathcal{T}^2 n^2\pi^2(\xi+K_r)\Big]W_{0n}^f + \Big[-\xi\Lambda_n + \Gamma^{-1}\mathcal{T}^2 n^2\pi^2\eta\xi\Big]W_{0n}^p \\ \qquad - \mathrm{Ra}a^2\Theta_{0n} + \mathcal{C}a^2\Gamma_{0n} = 0, \\ \Big[-\xi\Lambda_n + \Gamma^{-1}\mathcal{T}^2 n^2\pi^2\eta\xi\Big]W_{0n}^f + \Big[(K_r+\xi)\Lambda_n + \Gamma^{-1}\mathcal{T}^2 n^2\pi^2\eta^2(\xi+1)\Big]W_{0n}^p \\ \qquad - \mathrm{Ra}a^2\Theta_{0n} + \mathcal{C}a^2\Gamma_{0n} = 0, \\ W_{0n}^f + W_{0n}^p - (\Lambda_n+\sigma)\Theta_{0n} = 0, \\ W_{0n}^f + W_{0n}^p - (\Lambda_n + \epsilon_1 Le\sigma)\Gamma_{0n} - \mathcal{S}\Lambda_n\Theta_{0n} = 0. \end{cases} \tag{6.12}$$

$a^2 = l^2 + m^2$ being the wavenumber and $\Lambda_n = n^2\pi^2 + a^2$. Setting

$$\begin{aligned} H_1 &= (1+\xi)\Lambda_n + \Gamma^{-1}\mathcal{T}^2 n^2\pi^2(\xi + K_r), \\ H_2 &= -\xi\Lambda_n + \Gamma^{-1}\mathcal{T}^2 n^2\pi^2\eta\xi \\ H_3 &= (K_r+\xi)\Lambda_n + \Gamma^{-1}\mathcal{T}^2 n^2\pi^2\eta^2(\xi+1) \end{aligned}$$

and requiring the determinant of (6.12) to be zero, we obtain

$$\begin{aligned} &\sigma^2\epsilon_1 Le(H_1H_3 - H_2^2) + \sigma[\Lambda_n(H_1H_3 - H_2^2)(1+\epsilon_1 Le) \\ &\quad + (H_1 - 2H_2 + H_3)a^2(\mathcal{C} - \mathrm{Ra}\epsilon_1 Le)] \\ &\quad + \Lambda_n^2(H_1H_3 - H_2^2) - a^2\Lambda_n(H_1 - 2H_2 + H_3)[\mathrm{Ra} - \mathcal{C}(1-\mathcal{S})] = 0, \end{aligned} \tag{6.13}$$

hence

$$\mathrm{Ra} = \frac{(\Lambda_n+\sigma)(\Lambda_n+\epsilon_1 Le\sigma)(H_1H_3-H_2^2) + a^2[\Lambda_n\mathcal{C}(1-\mathcal{S}) + \sigma\mathcal{C}](H_1-2H_2+H_3)}{a^2(H_1 - 2H_2 + H_3)(\Lambda_n + \epsilon_1 Le\sigma)} \tag{6.14}$$

Theorem 6.2.1. *Condition $\epsilon_1 Le \le 1$ implies the validity of the strong form of the Principle of exchange of stabilities and, in this case, convection can arise only via stationary motions.*

Proof. Both roots of (6.13) are real if

$$\begin{aligned} &[\Lambda_n(H_1H_3-H_2^2)(1+\epsilon_1 Le)+(H_1-2H_2+H_3)a^2(\mathcal{C}-\mathrm{Ra}\epsilon_1 Le)]^2 - \\ &4\epsilon_1 Le(H_1H_3-H_2^2)\{\Lambda_n^2(H_1H_3-H_2^2)-a^2\Lambda_n(H_1-2H_2+H_3)[\mathrm{Ra}-\mathcal{C}(1-\mathcal{S})]\} \ge 0 \end{aligned} \tag{6.15}$$

i.e.

$$\begin{aligned} &\Lambda_n^2(H_1H_3 - H_2^2)^2(1-\epsilon_1 Le)^2 + (\mathcal{C} - \epsilon_1 Le\mathrm{Ra})^2(H_1 - 2H_2 + H_3)^2 a^4 + \\ &2(H_1-2H_2+H_3)(H_1H_3-H_2^2)a^2\Lambda_n[(1-\epsilon_1 Le)(\epsilon_1 Le\mathrm{Ra}+\mathcal{C})+2\mathcal{S}\mathcal{C}\epsilon_1 Le] \ge 0 \end{aligned} \tag{6.16}$$

that is surely satisfied if $\epsilon_1 Le \le 1$, since

$$\begin{aligned} H_1 - 2H_2 + H_3 =& \Lambda_n(1 + K_r + 4\xi) + \Gamma^{-1}\mathcal{T}^2 n^2\pi^2[K_r + \eta^2 + \xi(\eta-1)^2] \\ H_1H_3 - H_2^2 =& \Gamma\Lambda_n^2 + \Gamma^{-1}\mathcal{T}^2 n^2\pi^2\Lambda_n[\eta^2(\xi+1)^2 + 2\eta\xi^2 + (\xi + K_r)^2] \\ &+ \Gamma^{-1}\mathcal{T}^4 n^4\pi^4\eta^2 \end{aligned} \tag{6.17}$$

are positive. Therefore

$$\epsilon_1 Le \le 1 \;\Rightarrow\; \sigma \in \mathbb{R}. \tag{6.18}$$

□

6.2.1 Steady convection threshold

When convective instability occurs via steady motions, the marginal state is characterized by $\sigma = 0$, so from (6.14) we derive the critical Rayleigh number for the onset of stationary convection:

$$\mathrm{Ra}_S = \min_{(n,a^2)} \frac{\Lambda_n}{a^2} \frac{\Gamma\Lambda_n^2 + \Gamma^{-1}\mathcal{T}^2 n^2\pi^2\Lambda_n\mathcal{A} + \Gamma^{-1}\mathcal{T}^4 n^4\pi^4\eta^2}{\Lambda_n(1+K_r+4\xi)+\Gamma^{-1}\mathcal{T}^2 n^2\pi^2[K_r+\eta^2+\xi(\eta-1)^2]} + \mathcal{C}(1-\mathcal{S}) \tag{6.19}$$

where $\mathcal{A} = \eta^2(\xi+1)^2 + 2\eta\xi^2 + (\xi+K_r)^2$. The minimum with respect to $n \in \mathbb{N}$ is attained at $n = 1$, so the steady critical Rayleigh number is given by

$$\mathrm{Ra}_S = f(a_c^2) + \mathcal{C}(1-\mathcal{S}), \tag{6.20}$$

where

$$f(a_c^2) = \min_{a^2\in\mathbb{R}^+} \frac{\Lambda_1}{a^2} \frac{\Gamma\Lambda_1^2 + \Gamma^{-1}\mathcal{T}^2\pi^2\Lambda_1\mathcal{A} + \Gamma^{-1}\mathcal{T}^4\pi^4\eta^2}{\Lambda_1(1+K_r+4\xi)+\Gamma^{-1}\mathcal{T}^2\pi^2[K_r+\eta^2+\xi(\eta-1)^2]} \tag{6.21}$$

Moreover, the minimum (6.21) is attained at the positive solution of the fourth-order algebraic equations $s(x) = 0$, with $x = a^2$ and

$$s(x) = h_1x^4 + h_2x^3 + h_3x^2 + h_4x + h_5,$$

where

$$\begin{aligned} h_1 &= \Gamma(1+K_r+4\xi), \\ h_5 &= -\pi^8 c_1 \cdot c_2. \end{aligned}$$

and

$$\begin{aligned} c_1 &= 1+K_r+4\xi+\Gamma^{-1}K_r\mathcal{T}^2+\Gamma^{-1}\mathcal{T}^2[\eta^2+\xi(\eta-1)^2], \\ c_2 &= \Gamma+\Gamma^{-1}\mathcal{T}^2[2\xi^2\eta+\eta^2(1+\xi)^2+(K_r+\xi)^2+\mathcal{T}^2\eta^2]. \end{aligned}$$

As matter of fact, the equation $s(x) = 0$ admits at least one positive root since

$$s(0) = h_5 < 0 \quad \text{and} \quad \lim_{x\to\infty} s(x) = +\infty.$$

Let us finally point out that in absence of rotation (i.e. for $\mathcal{T} \to 0$) from (6.19) we recover the stationary threshold found in [49], while confining ourselves to the case of a single component fluid (i.e. for $\mathcal{C} \to 0$), (6.19) coincides with the instability threshold found in [21]. When the Soret effect is neglected (i.e. for $\mathcal{S} \to 0$), one obtains that $\mathrm{Ra}_S = f(a_c^2) + \mathcal{C}$.

6.2.2 Oscillatory convection threshold

In order to determine the instability threshold for the onset of oscillatory convection, the growth rate of the system σ needs to be purely imaginary, hence let us consider $\sigma = i\sigma_1$, with $\sigma_1 \in \mathbb{R} - \{0\}$, so (6.14) becomes

$$\mathrm{Ra} = Re(\mathrm{Ra}) + i\ Im(\mathrm{Ra})\,. \tag{6.22}$$

whit

$$\begin{aligned} Re(\mathrm{Ra}) =& \frac{\Lambda_n(H_1H_3 - H_2^2)}{a^2(H_1 - 2H_2 + H_3)} + \frac{\mathcal{C}(1-\mathcal{S})\Lambda_n^2 + \epsilon_1 Le\sigma_1^2\mathcal{C}}{\Lambda_n^2 + (\epsilon_1 Le\sigma_1)^2} \\ Im(\mathrm{Ra}) =& \sigma_1\left[\frac{H_1H_3 - H_2^2}{a^2(H_1 - 2H_2 + H_3)} + \frac{\Lambda_n\mathcal{C} - \Lambda_n\epsilon_1 Le\mathcal{C}(1-\mathcal{S})}{\Lambda_n^2 + (\epsilon_1 Le\sigma_1)^2}\right] \end{aligned} \tag{6.23}$$

Imposing the imaginary part $Im(\mathrm{Ra})$ of (6.22) to vanish, we get

$$(H_1H_3 - H_2^2)[\Lambda_n^2 + (\epsilon_1 Le\sigma_1)^2] + a^2(H_1 - 2H_2 + H_3)\Lambda_n\mathcal{C}(1 - \epsilon_1 Le + \epsilon_1 Le\mathcal{S}) = 0. \tag{6.24}$$

Hence, *necessary conditions* for the onset of oscillatory convection are

$$\begin{aligned} &\epsilon_1 Le > 1, \\ &\Lambda_n^2(H_1H_3 - H_2^2) + a^2(H_1 - 2H_2 + H_3)\Lambda_n\mathcal{C}(1 - \epsilon_1 Le + \epsilon_1 Le\mathcal{S}) < 0. \end{aligned} \tag{6.25}$$

Consequently, the critical Rayleigh number for the onset of oscillatory convection is

$$\mathrm{Ra}_O = \min_{(n,a^2)} \frac{\Lambda_n}{a^2} \frac{\Gamma\Lambda_n^2 + \Gamma^{-1}\mathcal{T}^2n^2\pi^2\Lambda_n\mathcal{A} + \Gamma^{-1}\mathcal{T}^4n^4\pi^4\eta^2}{\Lambda_n(1 + K_r + 4\xi) + \Gamma^{-1}\mathcal{T}^2n^2\pi^2[K_r + \eta^2 + \xi(\eta - 1)^2]}\mathcal{B} + \frac{\mathcal{C}}{\epsilon_1 Le} \tag{6.26}$$

where $\mathcal{B} = \left(1 + \dfrac{1}{\epsilon_1 Le}\right)$, while the frequency of the oscillations is given by

$$\sigma_1^2 = \frac{a^2(H_1 - 2H_2 + H_3)\Lambda_n\mathcal{C}(\epsilon_1 Le - 1 - \epsilon_1 Le\mathcal{S}) - \Lambda_n^2(H_1H_3 - H_2^2)}{(\epsilon_1 Le)^2(H_1H_3 - H_2^2)} \tag{6.27}$$

Since the minimum of (6.26) with respect to $n \in \mathbb{N}$ is attained at $n = 1$, the oscillatory critical Rayleigh number is given by

$$\mathrm{Ra}_O = f(a_c^2)\left(1 + \frac{1}{\epsilon_1 Le}\right) + \frac{\mathcal{C}}{\epsilon_1 Le}\,, \tag{6.28}$$

or, equivalently,

$$\mathrm{Ra}_O = \mathrm{Ra}_S\left(1 + \frac{1}{\epsilon_1 Le}\right) + \mathcal{C}\left[\mathcal{S}\left(1 + \frac{1}{\epsilon_1 Le}\right) - 1\right], \tag{6.29}$$

hence, while the oscillatory Rayleigh number given by (6.28) does not depend on the Soret number $\mathcal{S}$, i.e. the Soret effect does not *directly* affect the oscillatory instability threshold, from (6.29) one gets

$$\mathcal{S} > \frac{\epsilon_1 Le}{\epsilon_1 Le + 1} \quad \Rightarrow \quad \mathrm{Ra}_O > \mathrm{Ra}_S \tag{6.30}$$

and convection arises through stationary motions. As shown for the stationary threshold, in absence of rotation from (6.26) we recover the same oscillatory instability threshold found in [49]. Let us remark that when a binary mixture and the Soret effect are considered, convection can arise via steady *or* oscillatory motions, while the principle of exchange of stabilities was proved for the single component case, so, in that case, oscillatory convection cannot occur (see [21]).

6.2.3 Remarks

Since

$$\frac{\partial \mathrm{Ra}_S}{\partial \mathcal{C}} > 0 \quad \text{and} \quad \frac{\partial \mathrm{Ra}_O}{\partial \mathcal{C}} > 0,$$

the chemical component dissolved at the bottom of the layer has a stabilizing effect on the onset of convection, i.e. it delays the onset of convection through both stationary and oscillatory motions. Moreover,

$$\frac{\partial \mathrm{Ra}_S}{\partial \mathcal{T}^2} > 0 \quad \text{and} \quad \frac{\partial \mathrm{Ra}_O}{\partial \mathcal{T}^2} > 0,$$

this means that rotation has a stabilizing effect on the onset of both steady and oscillatory convection. As one is expected, both the rotation and the dissolved solute act to stop heat transfer and fluid motion through convection.

From (6.20) and (6.28) one obtains

$$\mathrm{Ra}_O > \mathrm{Ra}_S \quad \Leftrightarrow \quad f(a_c^2) > \mathcal{C}[\epsilon_1 Le(1-\mathcal{S}) - 1], \tag{6.31}$$

that is a *necessary and sufficient condition* for the onset of stationary convection. Moreover, the steady and oscillatory instability thresholds (6.20) and (6.28) are straight lines in the $(\mathcal{C}, \mathrm{Ra})$ plane, so for increasing $\mathcal{C}$ there is a transition from steady to oscillatory convection in correspondence of the intersection point

$$\mathcal{C}^* = \frac{f(a_c^2)}{\epsilon_1 Le(1-\mathcal{S}) - 1} \tag{6.32}$$

6.3 Differential constraint approach for nonlinear stability analysis

Let us consider the nonlinear system $(6.10)_{1,2}$ and $(6.4)_{5,6}$

$$\begin{cases} (1+\xi)\Delta w^f - \xi\Delta w^p - \mathrm{Ra}\Delta_1\theta + \mathcal{C}\Delta_1\gamma + \Gamma^{-1}\mathcal{T}^2\left[(\xi+K_r)\dfrac{\partial^2 w^f}{\partial z^2} + \eta\xi\dfrac{\partial^2 w^p}{\partial z^2}\right] = 0, \\ (K_r+\xi)\Delta w^p - \xi\Delta w^f - \mathrm{Ra}\Delta_1\theta + \mathcal{C}\Delta_1\gamma + \Gamma^{-1}\eta\mathcal{T}^2\left[\xi\dfrac{\partial^2 w^f}{\partial z^2} + \eta(\xi+1)\dfrac{\partial^2 w^p}{\partial z^2}\right] = 0, \\ \dfrac{\partial\theta}{\partial t} + (\mathbf{u}^f + \mathbf{u}^p)\cdot\nabla\theta = w^f + w^p + \Delta\theta, \\ \epsilon_1 Le\dfrac{\partial\gamma}{\partial t} + A\,Le(\mathbf{u}^f + \mathbf{u}^p)\cdot\nabla\gamma = w^f + w^p + \Delta\gamma + \mathcal{S}\Delta\theta. \end{cases} \tag{6.33}$$

The threshold for the nonlinear stability of the conduction solution will be determined employing the differential constraint approach [42]. Therefore, denoting by $(\cdot,\cdot)$ and $\|\cdot\|$ inner product and norm on the Hilbert space $L^2(V)$, respectively, let us set

$$E(t) = \frac{1}{2}\|\theta\|^2 + \epsilon_1 Le\frac{\mu}{2}\|\gamma\|^2, \tag{6.34}$$

$$I(t) = (w^f + w^p, \theta) + \mu(w^f + w^p, \gamma) + \mu\mathcal{S}(\Delta\theta, \gamma), \quad D(t) = \|\nabla\theta\|^2 + \mu\|\nabla\gamma\|^2,$$

where μ is a positive coupling parameter to be chosen. Retaining $(6.33)_{1,2}$ as constraints, integrating over the periodicity cell equation $(6.33)_3$ multiplied by θ and equation $(6.33)_4$ multiplied by γ, adding the resulting equations one gets

$$\frac{dE}{dt} = I - D \le D\,(m-1)\,, \tag{6.35}$$

where

$$m = \max_{\mathcal{H}^*}\frac{I}{D} \tag{6.36}$$

and

$$\mathcal{H}^* = \{(w^f, w^p, \theta, \gamma) \in (H^1)^4 \mid w^f = w^p = \theta = \gamma = 0 \text{ on } z = 0,1; \text{periodic in } x, y \\ \text{with periods } 2\pi/l, 2\pi/m; D < \infty; \text{verifying } (6.33)_{1,2}\}$$

is the space of kinematically admissible solutions.
Let us introduce the *Lagrange multipliers* $\lambda^{'}(\mathbf{x})$ and $\lambda^{''}(\mathbf{x})$, hence, the maximum problem (6.36) is equivalent to

$$m = \max_{\mathcal{H}}\frac{I + \int_V \lambda^{'} f_1\, dV + \int_V \lambda^{''} f_2\, dV}{D}, \tag{6.37}$$

where

$$f_1 = M_1 w^f + M_2 w^p - \mathrm{Ra}\Delta_1\theta + \mathcal{C}\Delta_1\gamma, \quad f_2 = M_2 w^f + M_3 w^p - \mathrm{Ra}\Delta_1\theta + \mathcal{C}\Delta_1\gamma,$$

$$\begin{aligned}\mathcal{H} = \{&(w^f, w^p, \theta, \gamma) \in (H^1)^4 \mid w^f = w^p = \theta = \gamma = 0 \text{ on } z = 0,1; \text{periodic in } x, y \\ &\text{with periods } 2\pi/l, 2\pi/m, \text{ respectively}; D < \infty\},\end{aligned}$$

and the following operators were defined:

$$\begin{aligned}
M_1 &\equiv (1+\xi)\Delta + \Gamma^{-1}\mathcal{T}^2(\xi + K_r)\partial_{zz}, \\
M_2 &\equiv -\xi\Delta + \Gamma^{-1}\mathcal{T}^2\eta\xi\partial_{zz}, \\
M_3 &\equiv (K_r + \xi)\Delta + \Gamma^{-1}\mathcal{T}^2\eta^2(\xi + 1)\partial_{zz}.
\end{aligned}$$

Theorem 6.3.1. *Condition $m < 1$ guarantees the global, nonlinear stability of the stationary conduction solution with respect to the $E-$norm.*

Proof. By virtue of Poincaré inequality, one obtains that $D \geq \pi^2\|\theta\|^2 + \mu\pi^2\|\gamma\|^2$, hence, if $m < 1$ from (6.35) it follows

$$\dot{E}(t) \leq D\,(m-1) \leq \pi^2\hat{\alpha}(m-1)E(t), \implies E(t) \leq E(0)\exp(\pi^2\hat{\alpha}(m-1)t), \tag{6.38}$$

with $\hat{\alpha} = \min(1, 1/\epsilon_1 Le)$, i.e. condition $m < 1$ implies $E(t) \to 0$ at least exponentially. Moreover, multiplying $(6.4)_1$ by $\mathbf{u}^f$ and $(6.4)_2$ by $\mathbf{u}^p$, one gets

$$\begin{aligned}
(1+\xi)\|\mathbf{u}^f\|^2 - \xi(\mathbf{u}^f, \mathbf{u}^p) &= \mathrm{Ra}(\theta, w^f) - \mathcal{C}(\gamma, w^f), \\
(K_r + \xi)\|\mathbf{u}^p\|^2 - \xi(\mathbf{u}^f, \mathbf{u}^p) &= \mathrm{Ra}(\theta, w^p) - \mathcal{C}(\gamma, w^p),
\end{aligned} \tag{6.39}$$

hence, by virtue of Cauchy-Schwarz inequality,

$$\begin{aligned}
(1+\xi)\|\mathbf{u}^f\| - \xi\|\mathbf{u}^p\| &\leq \|\mathrm{Ra}\theta - \mathcal{C}\gamma\|, \\
(K_r + \xi)\|\mathbf{u}^p\| - \xi\|\mathbf{u}^f\| &\leq \|\mathrm{Ra}\theta - \mathcal{C}\gamma\|.
\end{aligned} \tag{6.40}$$

Adding $(6.40)_1$ and $(6.40)_2$ one finally obtains

$$\|\mathbf{u}^f\| + K_r\|\mathbf{u}^p\| \leq 2\|\mathrm{Ra}\theta - \mathcal{C}\gamma\|, \tag{6.41}$$

i.e. if $m < 1$ the seepage velocities $\mathbf{u}^f$ and $\mathbf{u}^p$ exponentially go to zero, hence, the global, nonlinear stability of the conduction solution with respect to the $E-$norm is guaranteed. □

Remark 6.3.1. *If* Ra_E *is the critical value of the Rayleigh number such that $m = 1$, condition $m < 1$ is equivalent to condition* $\mathrm{Ra} < \mathrm{Ra}_E$.

The Euler-Lagrange equations associated to (6.37) are

$$\begin{cases} M_1 w^f + M_2 w^p - \mathrm{Ra}\Delta_1\theta + \mathcal{C}\Delta_1\gamma = 0, \\ M_2 w^f + M_3 w^p - \mathrm{Ra}\Delta_1\theta + \mathcal{C}\Delta_1\gamma = 0, \\ \theta + \mu\gamma + M_1\lambda^{'} + M_2\lambda^{''} = 0, \\ \theta + \mu\gamma + M_2\lambda^{'} + M_3\lambda^{''} = 0, \\ w^f + w^p + \mu\mathcal{S}\Delta\gamma - \mathrm{Ra}(\Delta_1\lambda^{'} + \Delta_1\lambda^{''}) + 2\Delta\theta = 0, \\ \mu(w^f + w^p) + \mu\mathcal{S}\Delta\theta + \mathcal{C}(\Delta_1\lambda^{'} + \Delta_1\lambda^{''}) + 2\mu\Delta\gamma = 0, \end{cases} \tag{6.42}$$

Employing normal modes representation in (6.42):

$$\begin{aligned} w_n^f &= W_{0n}^f \sin(n\pi z) e^{i(lx+my)}, \\ w_n^p &= W_{0n}^p \sin(n\pi z) e^{i(lx+my)}, \\ \theta_n &= \Theta_{0n} \sin(n\pi z) e^{i(lx+my)}, \\ \gamma_n &= \Gamma_{0n} \sin(n\pi z) e^{i(lx+my)}, \\ \lambda_n^{'} &= \lambda_{0n}^{'} \sin(n\pi z) e^{i(lx+my)}, \\ \lambda_n^{''} &= \lambda_{0n}^{''} \sin(n\pi z) e^{i(lx+my)}, \end{aligned} \tag{6.43}$$

the global nonlinear stability threshold with respect to the $E-$norm is found requiring *zero determinant* for the system

$$\begin{cases} H_1 W_{0n}^f + H_2 W_{0n}^p - \mathrm{Ra}a^2\Theta_{0n} + \mathcal{C}a^2\Gamma_{0n} = 0, \\ H_2 W_{0n}^f + H_3 W_{0n}^p - \mathrm{Ra}a^2\Theta_{0n} + \mathcal{C}a^2\Gamma_{0n} = 0, \\ \Theta_{0n} + \mu\Gamma_{0n} - H_1\lambda_{0n}^{'} - H_2\lambda_{0n}^{''} = 0, \\ \Theta_{0n} + \mu\Gamma_{0n} - H_2\lambda_{0n}^{'} - H_3\lambda_{0n}^{''} = 0, \\ W_{0n}^f + W_{0n}^p - \mu\mathcal{S}\Lambda_n\Gamma_{0n} + \mathrm{Ra}a^2(\lambda_{0n}^{'} + \lambda_{0n}^{''}) - 2\Lambda_n\Theta_{0n} = 0, \\ \mu(W_{0n}^f + W_{0n}^p) - \mu\mathcal{S}\Lambda_n\Theta_{0n} - \mathcal{C}a^2(\lambda_{0n}^{'} + \lambda_{0n}^{''}) - 2\mu\Lambda_n\Gamma_{0n} = 0, \end{cases} \tag{6.44}$$

$a^2 = l^2 + m^2$ being the wavenumber, while $\Lambda_n = a^2 + n^2\pi^2$. Hence, one obtains the stability condition

$$\mathrm{Ra} < \mathrm{Ra}_E \tag{6.45}$$

where the critical nonlinear Rayleigh number is found to be

$$\mathrm{Ra}_E = \max_{\mu} \min_{n,a^2} \frac{2\sqrt{(H_1H_3 - H_2^2)\Lambda_n X}\sqrt{1+\mu(1-\mathcal{S})} + \mu\mathcal{S}\Lambda_n(H_1H_3 - H_2^2) - Y}{\mu a^2(H_1 - 2H_2 + H_3)} \tag{6.46}$$

where $X = \mathcal{C}a^2(H_1 - 2H_2 + H_3) + \Lambda_n(H_1H_3 - H_2^2)$ and $Y = \mathcal{C}a^2(H_1 - 2H_2 + H_3) + 2\Lambda_n(H_1H_3 - H_2^2)$. The maximum of (6.46) with respect to μ is attained at

$$\mu_c = \frac{\mathcal{C}a^2(H_1 - 2H_2 + H_3)}{\Lambda_n(H_1H_3 - H_2^2)(1 - \mathcal{S})}$$

consequently

$$\mathrm{Ra}_E = \min_{n,a^2} \frac{\Lambda_n}{a^2} \frac{\Gamma\Lambda_n^2 + \Gamma^{-1}\mathcal{T}^2n^2\pi^2\Lambda_n\mathcal{A} + \Gamma^{-1}\mathcal{T}^4n^4\pi^4\eta^2}{\Lambda_n(1 + K_r + 4\xi) + \Gamma^{-1}\mathcal{T}^2n^2\pi^2[K_r + \eta^2 + \xi(\eta - 1)^2]} \tag{6.47}$$

In conclusion, we obtained that $\mathrm{Ra}_E = f(a_c^2)$ and

$$\mathrm{Ra}_E < \min(\mathrm{Ra}_S, \mathrm{Ra}_O),$$

therefore, there are regions of subcritical instabilities. However, for $\mathcal{S} \to 1$ the coincidence between the stationary threshold Ra_S and the global nonlinear threshold Ra_E is achieved, even though the dependence of the instability thresholds on the concentration field is lost.
Let us observe that the nonlinear stability threshold Ra_E coincides with the stability threshold obtained when the Soret effect is not taken into account, therefore, if $\mathrm{Ra} < \mathrm{Ra}_E$, the thermal conduction solution is unconditionally stable, regardless of what value $\mathcal{C}$ has and no matter of whether the Soret effect is taken into account or not, hence, the global nonlinear stability threshold obtained by the energy (6.34) is affected only by rotation and the stabilizing effect of the concentration gradient on the onset of convection is not achieved. Let us remark that condition (6.31) becomes

$$\mathrm{Ra}_O > \mathrm{Ra}_S \quad \Longleftrightarrow \quad \mathrm{Ra}_E > \mathcal{C}[\epsilon_1 Le(1 - \mathcal{S}) - 1] \tag{6.48}$$

6.4 Numerical analysis of the stability results

The purpose of this Section is to numerically investigate the asymptotic behaviour of steady and oscillatory thresholds (6.20) and (6.28) with respect to the meaningful parameters of the model. Since our thresholds are consistent with those ones found in [49], let us fix $\{\xi = 0.1, K_r = 1.5, \eta = 1.5, \epsilon_1 Le = 55.924\}$ in the following simulations.

For high concentrations of the dissolved chemical component, convection sets in through oscillatory motions, indeed in Figure 6.1(a) the linear dependence of the Rayleigh number on the chemical Rayleigh number is depicted, and, for the chosen set of parameters, the critical value of the concentration Rayleigh

number for which there is a switch from stationary to oscillatory convection is $\mathcal{C}^* = 4.0839$.
In Tables 6.1(a) and 6.1(b) the stabilizing effect of rotation on the onset of convection is displayed, for low salt concentration - cfr. 6.1(a) - and for high salt concentration - cfr. 6.1(b).
Table 6.3 and Figure 6.1(b) show the stabilizing effect of salt concentration on the onset of convection and, in particular, as $\mathcal{C}$ increases, the increasing of Ra_O is slower than the increasing of Ra_S and, as already observed, for $\mathcal{C}^* = 4.0839$ there is the switch from steady to oscillatory convection.
While the Soret effect does not directly affect the oscillatory instability threshold, as already pointed out, its increasing leads to a decreasing of the thermal critical stationary Rayleigh number, so the Soret effect has a inhibiting effect on the onset of stationary convection (see Tables 6.2 and Figure 6.2(b)).
On the other hand, $\epsilon_1 Le$ does not directly affect the steady instability threshold but has a destabilizing effect on the onset of oscillatory convection (see Figure 6.2(a)).
The condition (6.31) gives us a prediction of the type of motions through which convection will arise and it is tested in Table 6.4, in particular Table 6.4(a) shows that for $\epsilon_1 Le \leq 1$ the necessary conditions for the onset of oscillatory convection are not satisfied, so convection can arise only via stationary motions.
In Figures (6.3)(a) and (6.3)(b) the steady and oscillatory thresholds and the global nonlinear threshold are depicted for quoted values of the Soret number, in particular for $\mathcal{S} = 1$ the coincidence between Ra_E and Ra_S is depicted in (6.3)(b).

Main results

In the present Chapter the onset of convection in a bi-disperse porous layer, filled by an incompressible fluid mixture, that uniformly rotates about a vertical axis and that is simultaneously heated and salted from below, was studied. Taking into account the Soret effect, via linear instability analysis it was determined that convection can set in via stationary or oscillatory motions, and that the critical thermal Rayleigh numbers for the onset of convection and the concentration Rayleigh number have a linear dependence on each other. Moreover, both rotation and salt concentration have a stabilizing effect on the onset of steady and oscillatory convection. Through differential constraint approach, the global nonlinear stability threshold was determined and it was found that regions of possible subcritical instabilities are present. Numerical simulations were performed in order to test the theoretical proven

(a) $\mathcal{C} = 1$

Ra_S	Ra_O	a_c^2	$\mathcal{T}^2$
24.3232	24.2671	9.8696	0
29.9262	29.9703	12.0674	0.5
35.1123	35.2491	13.9204	1
70.9153	71.6923	24.0472	5
110.6114	112.0982	32.5315	10
719.9107	732.2926	98.4287	100

(b) $\mathcal{C} = 5$

Ra_S	Ra_O	a_c^2	$\mathcal{T}^2$
26.3232	24.3386	9.8696	0
31.9262	30.0418	12.0674	0.5
37.1123	35.3206	13.9204	1
72.9153	71.7638	24.0472	5
112.6114	112.1697	32.5315	10
721.9107	732.3641	98.4287	100

Table 6.1: Critical steady and oscillatory Rayleigh numbers and critical wavenumber at low concentration ($\mathcal{C} = 1$) (a) and at high concentration ($\mathcal{C} = 5$) (b) for quoted values of the Taylor number $\mathcal{T}^2$. *Table a*: $\xi = 0.1, K_r = 1.5, \eta = 1.5, \epsilon_1 Le = 55.924, \mathcal{S} = 0.5, \mathcal{C} = 1$. *Table b*: $\xi = 0.1, K_r = 1.5, \eta = 1.5, \epsilon_1 Le = 55.924, \mathcal{S} = 0.5, \mathcal{C} = 5$.

results.

(a) $\mathcal{C} = 1$

Ra_S	$\mathcal{S}$
111.0114	0.1
110.6114	0.5
110.1114	1

(b) $\mathcal{C} = 5$

Ra_S	$\mathcal{S}$
114.6114	0.1
112.6114	0.5
110.1114	1

Table 6.2: Steady instability thresholds at low concentration ($\mathcal{C} = 1$) (a) and at high concentration ($\mathcal{C} = 5$) (b) and for quoted values of the Soret number $\mathcal{S}$ (b). *Table a*: $\xi = 0.1, K_r = 1.5, \eta = 1.5, \epsilon_1 Le = 55.924, \mathcal{T}^2 = 10, \mathcal{C} = 1$. *Table b*: $\xi = 0.1, K_r = 1.5, \eta = 1.5, \epsilon_1 Le = 55.924, \mathcal{T}^2 = 10, \mathcal{C} = 5$.
In the first case, $\mathrm{Ra}_O = 112.0982$, in the second one, $\mathrm{Ra}_O = 112.1697$, while $a_c^2 = 32.5315$.

Ra_S	Ra_O	$\mathcal{C}$
110.1114	112.0803	0
110.3614	112.0893	0.5
110.6114	112.0982	1
112.1114	112.1519	4
112.1533	112.1533	4.0839
112.1614	112.1537	4.1
112.3614	112.1608	4.5
112.6114	112.1697	5

Table 6.3: Critical steady and oscillatory Rayleigh numbers as functions of the concentration Rayleigh number. $\xi = 0.1, K_r = 1.5, \eta = 1.5, \epsilon_1 Le = 55.924, \mathcal{T}^2 = 10, \mathcal{S} = 0.5$.
$a_c^2 = 32.5315$.

(a)

Ra_O	$\mathcal{C}(\epsilon_1 Le(1-\mathcal{S})-1)$	$\epsilon_1 Le$
$\nexists$	-3.8000	0.1
$\nexists$	-3	0.5
$\nexists$	-2	1
129.1300	8	6
121.5225	16	10
115.8170	36	20
112.3936	96	50
112.1519	107.8480	55.924
112.0133	116	60
111.7416	136	70
111.2525	196	100

(b)

Ra_S	Ra_O	$\mathcal{C}(\epsilon_1 Le(1-\mathcal{S})-1)$	$\mathcal{C}$
110.3614	112.0893	13.4810	0.5
110.6114	112.0982	26.9620	1
111.1114	112.1161	53.9240	2
111.8614	112.1429	94.3670	3.5
112.1114	112.1519	107.8480	4
112.3614	112.1608	121.3290	4.5
112.6114	112.1697	134.8100	5

Table 6.4: (a) Oscillatory thresholds at quoted values of $\epsilon_1 Le$, while $\mathcal{C} = 4, \mathcal{S} = 0.5$. For these values, the critical steady Rayleigh number is $\mathrm{Ra}_S = 112.1114$. (b) Steady and oscillatory thresholds at quoted values of the chemical Rayleigh number $\mathcal{C}$, while $\epsilon_1 Le = 55.924, \mathcal{S} = 0.5$.
The other physical parameters are fixed as $\xi = 0.1, K_r = 1.5, \eta = 1.5, \mathcal{T}^2 = 10$, and, for this set of parameters, the critical wavenumber is $a_c^2 = 32.5315$, while $f(a_c^2) = 110.1114$.

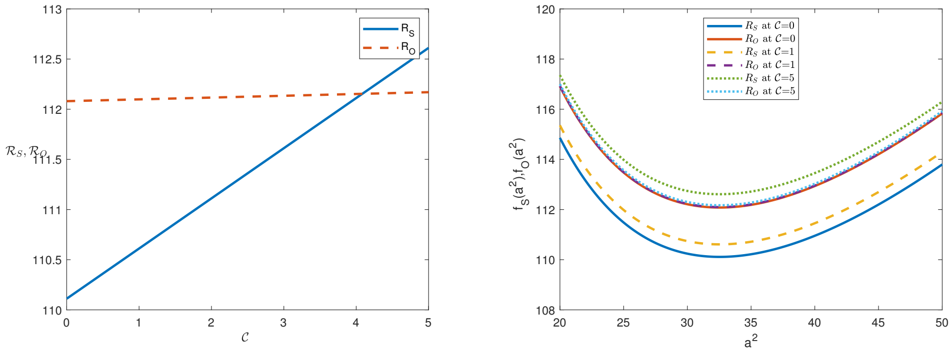

(a) (b)

Figure 6.1: (a) Critical steady and oscillatory Rayleigh numbers plotted as functions of the concentration Rayleigh number. (b): Steady and oscillatory thresholds for quoted values of the concentration Rayleigh number. The other parameters are fixed as $\xi = 0.1, K_r = 1.5, \eta = 1.5, \epsilon_1 Le = 55.924, \mathcal{T}^2 = 10, \mathcal{S} = 0.5$.

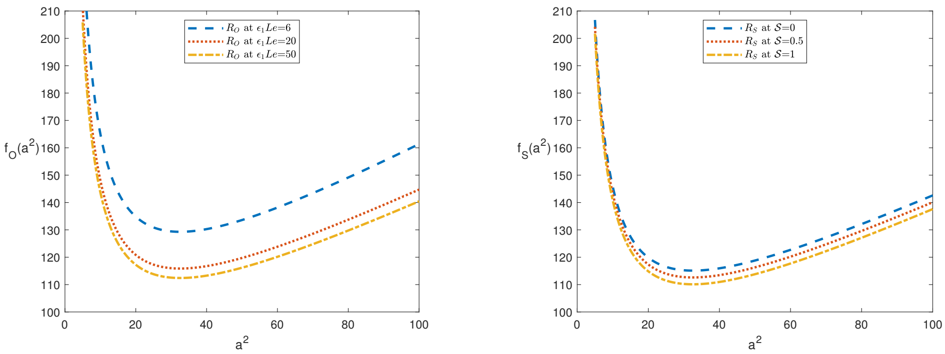

(a) (b)

Figure 6.2: (a): Oscillatory thresholds for quoted values of $\epsilon_1 Le$ for $\xi = 0.1, K_r = 1.5, \eta = 1.5, \mathcal{C} = 5, \mathcal{T}^2 = 10, \mathcal{S} = 0.5$. (b): Stationary thresholds for quoted values of the Soret number $\mathcal{S}$ for $\xi = 0.1, K_r = 1.5, \eta = 1.5, \epsilon_1 Le = 55.924, \mathcal{T}^2 = 10, \mathcal{C} = 5$.

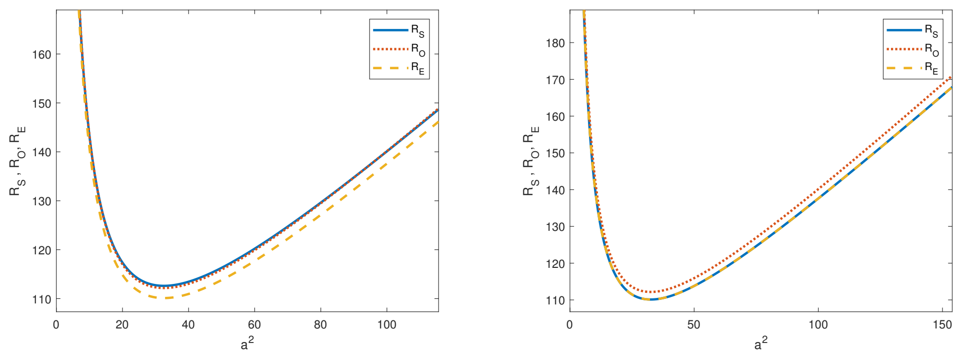

(a) $\mathcal{S} = 0.5$ (b) $\mathcal{S} = 1$

Figure 6.3: The steady and oscillatory thresholds and the global nonlinear threshold are plotted for quoted values of the Soret number. The other parameters are fixed as $\xi = 0.1, K_r = 1.5, \eta = 1.5, \epsilon_1 Le = 55.924, \mathcal{T}^2 = 10, \mathcal{C} = 5$.

Chapter 7

The combined effects of rotation and anisotropy on double diffusive bi-disperse convection

In the previous Chapter, we described how a salt dissolved at the bottom of the bi-disperse porous layer affects the onset of convective motions: we found that double-diffusive convection requires higher critical values of the Rayleigh number to set in with respect to those ones required by the onset of convection for a single component fluid, and we also found that there is a possibility for convection to arise via oscillatory motions.
As already explained, dual porosity materials represent an effective tool to design man-made materials for heat transfer problems and this is the reason why the analysis of anisotropic bi-disperse porous media is relevant, since a proper use of anisotropy leads to an optimization of the heat transfer. With this in mind, the aim of the present Chapter is to *improve* the results found in Chapter 3 — envisaging a rotating machinery constituted by an engineered anisotropic bi-disperse porous material [36, 59] — and further analyse the onset of bi-disperse double-diffusive convection: we assume that the rotating horizontal layer heated from below is occupied by an anisotropic BDPM filled by an incompressible fluid binary mixture. The present Chapter, based on the the joint work [60] with F. Capone and R. De Luca, is organized as follows. In Section 7.1 the mathematical model is presented and the equations governing the evolutionary behaviour of the perturbation to the thermosolutal conduction solution are derived. In Section 7.2 linear instability analysis is performed to find the instability thresholds for the onset of steady and oscillatory double-diffusive convection. In Section 7.3 the instability thresholds

are numerically analysed in order to display the influence of the fundamental physical parameters on the onset of convection.

7.1 Mathematical set-up

Let us consider a reference frame $Oxyz$ with fundamental unit vectors $\mathbf{i}, \mathbf{j}, \mathbf{k}$ ($\mathbf{k}$ pointing vertically upward) and a horizontal layer $L = \mathbb{R}^2 \times [0, d]$ occupied by a bi-disperse porous medium saturated by an incompressible fluid binary mixture at rest state and uniformly heated from below. Moreover, the layer L rotates about the vertical axis z, with constant angular velocity $\mathbf{\Omega} = \Omega\mathbf{k}$. Let us assume the local thermal equilibrium hypothesis - between the f-phase and the p-phase - i.e. $T^f = T^p = T$ [25]. Furthermore, the fluid-saturated bi-disperse porous medium is *horizontally isotropic*. Hence, as in Chapter 3, if the axes (x, y, z) are the *principal axes* of the permeability, the macropermeability tensor and the micropermeability tensor are

$$\mathbf{K}^f = \text{diag}(K_x^f, K_y^f, K_z^f) = K_z^f \ \mathbf{K}^{f*},$$
$$\mathbf{K}^p = \text{diag}(K_x^p, K_y^p, K_z^p) = K_z^p \ \mathbf{K}^{p*},$$
$$\mathbf{K}^{f*} = \text{diag}(k, k, 1), \quad \mathbf{K}^{p*} = \text{diag}(h, h, 1)$$

where

$$k = \frac{K_x^f}{K_z^f} = \frac{K_y^f}{K_z^f}, \quad h = \frac{K_x^p}{K_z^p} = \frac{K_y^p}{K_z^p}.$$

To derive the governing system, a Boussinesq approximation is employed: the density is constant except in the buoyancy forces due to the gravity $\mathbf{g} = -g\mathbf{k}$, where it has a linear dependence on temperature and concentration fields, i.e.

$$\varrho = \varrho_F[1 - \alpha(T - T_0) + \alpha_C(C - C_0)],$$

α and α_C being the thermal and the salt expansion coefficient, respectively, while ϱ_F is the fluid density at the reference constant temperature T_0 and concentration C_0.

In order to take into account the Coriolis terms due to the uniform rotation of the layer about z for the micropores and the macropores, we extend the

Brinkman model, obtaining the following governing system:

$$\begin{cases} \mathbf{v}^f = \frac{1}{\mu}\mathbf{K}^f \cdot \left[-\zeta(\mathbf{v}^f - \mathbf{v}^p) - \nabla p^f + \varrho_F \alpha g T \mathbf{k} - \varrho_F \alpha_C g C \mathbf{k} - \dfrac{2\varrho_F \Omega}{\varphi} \mathbf{k} \times \mathbf{v}^f + \tilde{\mu}_f \Delta \mathbf{v}^f \right], \\ \mathbf{v}^p = \frac{1}{\mu}\mathbf{K}^p \cdot \left[-\zeta(\mathbf{v}^p - \mathbf{v}^f) - \nabla p^p + \varrho_F \alpha g T \mathbf{k} - \varrho_F \alpha_C g C \mathbf{k} - \dfrac{2\varrho_F \Omega}{\epsilon} \mathbf{k} \times \mathbf{v}^p + \tilde{\mu}_p \Delta \mathbf{v}^p \right], \\ \nabla \cdot \mathbf{v}^f = 0, \\ \nabla \cdot \mathbf{v}^p = 0, \\ (\varrho c)_m T_{,t} + (\varrho c)_F (\mathbf{v}^f + \mathbf{v}^p) \cdot \nabla T = k_m \Delta T, \\ \epsilon_1 \dfrac{\partial C}{\partial t} + (\mathbf{v}^f + \mathbf{v}^p) \cdot \nabla C = \epsilon_2 \Delta C \end{cases} \tag{7.1}$$

where

$$p^s = P^s - \frac{\varrho_F}{2} |\mathbf{\Omega} \times \mathbf{x}|^2, \quad s = f, p$$

are the reduced pressures, with $\mathbf{x} = (x, y, z)$, $\mathbf{v}^s$ is the seepage velocity for $s = \{f, p\}$, T and C are the temperature and concentration fields, ζ is an interaction coefficient between the f-phase and the p-phase, μ is the fluid viscosity, $\tilde{\mu}_s$ is the effective fluid viscosity, c is the specific heat, k_s is the thermal conductivity for $s = \{f, p\}$, k_C^s = salt diffusivity for $s = \{f, p\}$,

$$\begin{aligned} &(\varrho c)_m = (1-\varphi)(1-\epsilon)(\varrho c)_{sol} + \varphi(\varrho c)_f + \epsilon(1-\varphi)(\varrho c)_p, \\ &k_m = (1-\varphi)(1-\epsilon)k_{sol} + \varphi k_f + \epsilon(1-\varphi)k_p, \\ &\epsilon_1 = \varphi + \epsilon(1-\varphi), \ \ \epsilon_2 = \varphi k_C^f + \epsilon(1-\varphi)k_C^p. \end{aligned}$$

To (7.1) the following boundary conditions are appended

$$\begin{aligned} &\mathbf{v}^s \cdot \mathbf{n} = 0\,, \quad s = \{f, p\} \qquad \text{on} \quad z = 0, d, \\ &T = T_L\,, \quad \text{on} \quad z = 0\,, \qquad T = T_U\,, \quad \text{on} \quad z = d \\ &C = C_L\,, \quad \text{on} \quad z = 0\,, \qquad C = C_U\,, \quad \text{on} \quad z = d \end{aligned} \tag{7.2}$$

where $\mathbf{n}$ is the unit outward normal to the impermeable horizontal planes delimiting the layer and $T_L > T_U$, $C_L > C_U$, since the layer is uniformly and simultaneously heated and salted from below.

The problem (7.1)-(7.2) admits the stationary motionless solution (thermosolutal conduction solution):

$$\overline{\mathbf{v}}^f = \mathbf{0}, \quad \overline{\mathbf{v}}^p = \mathbf{0}, \quad \overline{T} = -\beta z + T_L, \quad \overline{C} = -\beta_C z + C_L,$$

where $\beta = \dfrac{T_L - T_U}{d}$ is the temperature gradient, while $\beta_C = \dfrac{C_L - C_U}{d}$ is the concentration gradient. To perform the stability analysis of the basic solution, let us introduce a generic perturbation $\{\mathbf{u}^f, \mathbf{u}^p, \theta, \gamma, \pi^f, \pi^p\}$ to the steady conduction solution, so the evolutionary equations governing the perturbation fields are:

$$\begin{cases} \mathbf{u}^f = \frac{1}{\mu}\mathbf{K}^f \cdot \left[-\zeta(\mathbf{u}^f - \mathbf{u}^p) - \nabla\pi^f + \varrho_F \alpha g \theta \mathbf{k} - \varrho_F \alpha_C g \gamma \mathbf{k} - \dfrac{2\varrho_F \Omega}{\varphi}\mathbf{k} \times \mathbf{u}^f + \tilde{\mu}_f \Delta \mathbf{u}^f \right], \\ \mathbf{u}^p = \frac{1}{\mu}\mathbf{K}^p \cdot \left[-\zeta(\mathbf{u}^p - \mathbf{u}^f) - \nabla\pi^p + \varrho_F \alpha g \theta \mathbf{k} - \varrho_F \alpha_C g \gamma \mathbf{k} - \dfrac{2\varrho_F \Omega}{\epsilon}\mathbf{k} \times \mathbf{u}^p + \tilde{\mu}_p \Delta \mathbf{u}^p \right], \\ \nabla \cdot \mathbf{u}^f = 0, \\ \nabla \cdot \mathbf{u}^p = 0, \\ (\varrho c)_m \theta_{,t} + (\varrho c)_F (\mathbf{u}^f + \mathbf{u}^p) \cdot \nabla\theta = (\varrho c)_F \beta (w^f + w^p) + k_m \Delta\theta, \\ \epsilon_1 \dfrac{\partial \gamma}{\partial t} + (\mathbf{u}^f + \mathbf{u}^p) \cdot \nabla\gamma = \beta_C (w^f + w^p) + \epsilon_2 \Delta\gamma \end{cases} \tag{7.3}$$

where $\mathbf{u}^f = (u^f, v^f, w^f)$, $\mathbf{u}^p = (u^p, v^p, w^p)$. To derive the dimensionless perturbed system, let us introduce the non-dimensional parameters

$$\mathbf{x}^* = \frac{\mathbf{x}}{d},\ t^* = \frac{t}{\tilde{t}},\ \theta^* = \frac{\theta}{\tilde{T}},\ \gamma^* = \frac{\gamma}{\tilde{C}},\ \mathbf{u}^{s*} = \frac{\mathbf{u}^s}{\tilde{u}},\ \pi^{s*} = \frac{\pi^s}{\tilde{P}}, \quad \text{for } s = \{f, p\},$$

$$\eta = \frac{\varphi}{\epsilon},\ \sigma = \frac{\tilde{\mu}_p}{\tilde{\mu}_f},\ \gamma_1 = \frac{\mu}{K_z^f \zeta},\ \gamma_2 = \frac{\mu}{K_z^p \zeta},\ A = \frac{(\varrho c)_m}{(\varrho c)_F},$$

where the scales are given by

$$\tilde{u} = \frac{k_m}{(\varrho c)_f d},\ \tilde{t} = \frac{d^2 (\varrho c)_m}{k_m},\ \tilde{P} = \frac{\zeta k_m}{(\varrho c)_f},\ \tilde{T} = \sqrt{\frac{\beta k_m \zeta}{(\varrho c)_f \varrho_F \alpha g}},\ \tilde{C} = \frac{k_m}{(\varrho c)_F}\sqrt{\frac{\beta_C \zeta}{\epsilon_2 \varrho_F \alpha_C g}},$$

and let us define the Lewis number Le, the Taylor number $\mathcal{T}$, the Darcy number Da_f, the thermal Rayleigh number Ra, the chemical Rayleigh number $\mathcal{C}$,

$$Le = \frac{k_m}{\epsilon_2 (\varrho c)_m}, \quad \mathcal{T} = \frac{2\varrho_F \Omega K_z^f}{\varphi \mu}, \quad Da_f = \frac{\tilde{\mu}_f K_z^f}{d^2 \mu},$$

$$\mathrm{Ra} = \sqrt{\frac{\beta d^2 (\varrho c)_f \varrho_F \alpha g}{k_m \zeta}}, \quad \mathcal{C} = \sqrt{\frac{\beta_C d^2 \varrho_f \alpha_C g}{\epsilon_2 \zeta}},$$

respectively. The resulting non-dimensional perturbation equations, dropping all the asterisks for notational convenience, are

$$\begin{cases} \gamma_1 (\mathbf{K}^f)^{-1} \mathbf{u}^f + (\mathbf{u}^f - \mathbf{u}^p) = -\nabla\pi^f + \mathrm{Ra}\theta\mathbf{k} - \mathcal{C}\gamma\mathbf{k} - \gamma_1 \mathcal{T}\mathbf{k} \times \mathbf{u}^f + Da_f \gamma_1 \Delta\mathbf{u}^f, \\ \gamma_2 (\mathbf{K}^p)^{-1} \mathbf{u}^p - (\mathbf{u}^f - \mathbf{u}^p) = -\nabla\pi^p + \mathrm{Ra}\theta\mathbf{k} - \mathcal{C}\gamma\mathbf{k} - \eta\gamma_1 \mathcal{T}\mathbf{k} \times \mathbf{u}^p + Da_f \gamma_1 \sigma \Delta\mathbf{u}^p, \\ \nabla \cdot \mathbf{u}^f = 0, \\ \nabla \cdot \mathbf{u}^p = 0, \\ \theta_{,t} + (\mathbf{u}^f + \mathbf{u}^p) \cdot \nabla\theta = \mathrm{Ra}(w^f + w^p) + \Delta\theta, \\ \epsilon_1 Le \dfrac{\partial \gamma}{\partial t} + A\ Le(\mathbf{u}^f + \mathbf{u}^p) \cdot \nabla\gamma = \mathcal{C}(w^f + w^p) + \Delta\gamma \end{cases} \tag{7.4}$$

under the initial conditions

$$\mathbf{u}^s(\mathbf{x},0) = \mathbf{u}_0^s(\mathbf{x})\,, \quad \pi^s(\mathbf{x},0) = \pi_0^s(\mathbf{x})\,, \quad \theta(\mathbf{x},0) = \theta_0(\mathbf{x})\,, \quad \gamma(\mathbf{x},0) = \gamma_0(\mathbf{x})$$

with $\nabla \cdot \mathbf{u}_0^s = 0$, $s = \{f,p\}$, and the stress-free boundary conditions [10]

$$u^f_{,z} = v^f_{,z} = u^p_{,z} = v^p_{,z} = w^f = w^p = \theta = \gamma = 0 \quad \text{on } z = 0,1. \tag{7.5}$$

Remark 7.1.1. *According to experimental results, let us assume the perturbation fields being periodic functions in the horizontal directions x, y of period $2\pi/l$ and $2\pi/m$, respectively, and let us denote by*

$$V = \left[0, \frac{2\pi}{l}\right] \times \left[0, \frac{2\pi}{m}\right] \times [0,1]$$

the periodicity cell. Moreover, let us assume that $\forall f \in \{\nabla\pi^s, u^s, v^s, w^s, \theta, \gamma\}$ for $s = \{f,p\}$, $f \in W^{2,2}(V)$ $\forall t \in \mathbb{R}^+$.

7.2 Onset of instability

To determine the linear instability threshold for the onset of double diffusive convection, we linearise system (7.4) and seek for solutions $\mathbf{u}^f, \mathbf{u}^p, \theta, \gamma, \pi^f, \pi^p$ with time dependence like $e^{\overline{\sigma}t}$:

$$\begin{cases} \gamma_1(\mathbf{K}^f)^{-1}\mathbf{u}^f + (\mathbf{u}^f - \mathbf{u}^p) = -\nabla\pi^f + \mathrm{Ra}\theta\mathbf{k} - \mathcal{C}\gamma\mathbf{k} - \gamma_1\mathcal{T}\mathbf{k}\times\mathbf{u}^f + Da_f\gamma_1\Delta\mathbf{u}^f, \\ \gamma_2(\mathbf{K}^p)^{-1}\mathbf{u}^p - (\mathbf{u}^f - \mathbf{u}^p) = -\nabla\pi^p + \mathrm{Ra}\theta\mathbf{k} - \mathcal{C}\gamma\mathbf{k} - \eta\gamma_1\mathcal{T}\mathbf{k}\times\mathbf{u}^p + Da_f\gamma_1\sigma\Delta\mathbf{u}^p, \\ \overline{\sigma}\theta = \mathrm{Ra}(w^f + w^p) + \Delta\theta \\ \epsilon_1 Le\overline{\sigma} = \mathcal{C}(w^f + w^p) + \Delta\gamma \end{cases} \tag{7.6}$$

Let us denote by

$$\Delta_1 f = f_{,xx} + f_{,yy}\,, \quad \Delta^m \equiv \underbrace{\Delta\Delta\cdots\Delta}_{m}, \qquad \omega_3^s = (\nabla\times\mathbf{u}^s)\cdot\mathbf{k}, \ s = \{f,p\}$$
$$\overline{a} = \frac{\gamma_1}{k} + 1\,, \quad \overline{b} = \frac{\gamma_2}{h} + 1$$

and define the following operators

$$A \equiv \overline{a} - Da_f\gamma_1\Delta\,, \qquad B \equiv \overline{b} - Da_f\sigma\gamma_1\Delta\,, \qquad \Psi \equiv (AB - 1). \tag{7.7}$$

We compute the third components of curl and of double curl of $(7.4)_{1,2}$, that are given by

$$\begin{cases} A\omega_3^f - \omega_3^p = \gamma_1\mathcal{T}w^f_{,z}, \\ -\omega_3^f + B\omega_3^p = \eta\gamma_1\mathcal{T}w^p_{,z} \end{cases} \tag{7.8}$$

and

$$\begin{cases} -\dfrac{\gamma_1}{k} w^f_{,zz} - \gamma_1 \Delta_1 w^f - \Delta w^f + \Delta w^p = -\mathrm{Ra}\Delta_1\theta + \mathcal{C}\Delta_1\gamma, + \gamma_1 \mathcal{T}\omega^f_{3,z} - Da_f\gamma_1\Delta^2 w^f, \\ -\dfrac{\gamma_2}{h} w^p_{,zz} - \gamma_2\Delta_1 w^p + \Delta w^f - \Delta w^p = -\mathrm{Ra}\Delta_1\theta + \mathcal{C}\Delta_1\gamma, + \eta\gamma_1\mathcal{T}\omega^p_{3,z} - Da_f\gamma_1\sigma\Delta^2 w^p, \end{cases} \tag{7.9}$$

respectively. Applying the operator B to $(7.8)_1$, by virtue of $(7.8)_2$, we get

$$\Psi\omega_3^f = \gamma_1\mathcal{T}Bw^f_{,z} + \eta\gamma_1\mathcal{T}w^p_{,z}.$$

Then, applying the operator Ψ to $(7.8)_2$, one obtains

$$\begin{cases} \Psi\omega_3^f = \gamma_1\mathcal{T}Bw^f_{,z} + \eta\gamma_1\mathcal{T}w^p_{,z}, \\ \Psi B\omega_3^p = \gamma_1\mathcal{T}Bw^f_{,z} + \eta\gamma_1\mathcal{T}ABw^p_{,z}. \end{cases} \tag{7.10}$$

Applying the operator Ψ to $(7.9)_1$ and ΨB to $(7.9)_2$, we obtain

$$\begin{cases} -\overline{a}\Psi w^f_{,zz} - \hat{\gamma}_1\Psi\Delta_1 w^f + \Psi\Delta_1 w^p + \Psi w^p_{,zz} = \\ \qquad -\mathrm{Ra}\Psi\Delta_1\theta + \mathcal{C}\Psi\Delta_1\gamma + \gamma_1\mathcal{T}\Psi\omega^f_{3,z} - Da_f\gamma_1\Psi\Delta^2 w^f, \\ -\bar{b}\Psi Bw^p_{,zz} - \hat{\gamma}_2\Psi B\Delta_1 w^p + \Psi B\Delta_1 w^f + \Psi Bw^f_{,zz} = \\ \qquad -\mathrm{Ra}\Psi B\Delta_1\theta + \mathcal{C}\Psi B\Delta_1\gamma + \eta\gamma_1\mathcal{T}\Psi B\omega^p_{3,z} - Da_f\sigma\gamma_1\Psi B\Delta^2 w^p, \end{cases} \tag{7.11}$$

with $\hat{\gamma}_r = \gamma_r + 1$, for $r = 1, 2$. In view of (7.10), (7.11) can be written as

$$\begin{cases} [-\overline{a}\Psi - (\gamma_1\mathcal{T})^2 B]w^f_{,zz} - \hat{\gamma}_1\Psi\Delta_1 w^f + \Psi\Delta_1 w^p + \\ \quad [\Psi - \eta(\gamma_1\mathcal{T})^2]w^p_{,zz} + Da_f\gamma_1\Psi\Delta^2 w^f = -\mathrm{Ra}\Psi\Delta_1\theta + \mathcal{C}\Psi\Delta_1\gamma, \\ [-\bar{b}\Psi B - (\eta\gamma_1\mathcal{T})^2 AB]w^p_{,zz} - \hat{\gamma}_2\Psi B\Delta_1 w^p + \Psi B\Delta_1 w^f + \\ \quad [\Psi B - \eta(\gamma_1\mathcal{T})^2 B]w^f_{,zz} + Da_f\sigma\gamma_1\Psi B\Delta^2 w^p = -\mathrm{Ra}\Psi B\Delta_1\theta + \mathcal{C}\Psi B\Delta_1\gamma. \end{cases} \tag{7.12}$$

Consequently, we consider $(7.6)_{3,4}$, $(7.12)_1$ and $(7.12)_2$, i.e.:

$$\begin{cases} [-\overline{a}\Psi - (\gamma_1\mathcal{T})^2 B]w^f_{,zz} - \hat{\gamma}_1\Psi\Delta_1 w^f + \Psi\Delta_1 w^p + \\ \quad [\Psi - \eta(\gamma_1\mathcal{T})^2]w^p_{,zz} + Da_f\gamma_1\Psi\Delta^2 w^f = -\mathrm{Ra}\Psi\Delta_1\theta + \mathcal{C}\Psi\Delta_1\gamma, \\ [-\bar{b}\Psi B - (\eta\gamma_1\mathcal{T})^2 AB]w^p_{,zz} - \hat{\gamma}_2\Psi B\Delta_1 w^p + \Psi B\Delta_1 w^f + \\ \quad [\Psi B - \eta(\gamma_1\mathcal{T})^2 B]w^f_{,zz} + Da_f\sigma\gamma_1\Psi B\Delta^2 w^p = -\mathrm{Ra}\Psi B\Delta_1\theta + \mathcal{C}\Psi B\Delta_1\gamma, \\ \overline{\sigma}\theta = \mathrm{Ra}(w^f + w^p) + \Delta\theta, \\ \epsilon_1 Le\overline{\sigma} = \mathcal{C}(w^f + w^p) + \Delta\gamma. \end{cases} \tag{7.13}$$

Let us employ normal modes solutions in (7.13) [10]:

$$\begin{aligned} w^s &= W_0^s \sin(n\pi z) e^{i(lx+my)}, \quad s = \{f, p\} \\ \theta &= \Theta_0 \sin(n\pi z) e^{i(lx+my)}, \\ \gamma &= \Gamma_0 \sin(n\pi z) e^{i(lx+my)}, \end{aligned} \tag{7.14}$$

$W_0^f, W_0^p, \Theta_0, \Gamma_0$ being real constants, so from (7.13) it turns out that

$$\begin{cases} \Big[\Lambda_n e(A_1 M + \sigma f n^2\pi^2) + \Lambda_n^2 e(Me\sigma + B_1) + f\bar{b}n^2\pi^2 + B_1 M + \\ \quad e^2\Lambda_n^3 A_1 + e^3\sigma\Lambda_n^4\Big] W_0^f + \Big[-B_1\Lambda_n - eA_1\Lambda_n^2 - e^2\sigma\Lambda_n^3 + \eta f n^2\pi^2\Big] W_0^p \\ \quad -\mathrm{Ra}a^2\Big[B_1 + e\Lambda_n A_1 + e^2\sigma\Lambda_n^2\Big]\Theta_0 + \mathcal{C}a^2\Big[B_1 + e\Lambda_n A_1 + e^2\sigma\Lambda_n^2\Big]\Gamma_0 = 0, \\ \\ \Big[\Lambda_n(e\sigma n^2\pi^2\eta f - \bar{b}B_1) + \eta f n^2\pi^2\bar{b} - \Lambda_n^2 eC \\ \quad -\Lambda_n^3 e^2\sigma(A_1 + \bar{b}) - \Lambda_n^4\sigma^2 e^3\Big] W_0^f + \\ \quad \Big\{\Lambda_n e(CN + \eta^2 f A_1 n^2\pi^2) + \Lambda_n^2 e\sigma[e(A_1 + \bar{b})N + \bar{b}B_1 + e\eta^2 f n^2\pi^2] + \\ \quad B_1\bar{b}N + e^2\Lambda_n^3\sigma(C + e\sigma N) + \Lambda_n^4 e^3\sigma^2(A_1 + \bar{b}) + \Lambda_n^5 e^4\sigma^3 + \\ \quad \eta^2 f n^2\pi^2\bar{a}\bar{b}\Big\} W_0^p - \mathrm{Ra}a^2\Big[\bar{b}B_1 + e\Lambda_n C + \Lambda_n^2 e^2\sigma(A_1 + \bar{b}) + e^3\sigma^2\Lambda_n^3\Big]\Theta_0 \\ \quad +\mathcal{C}a^2\Big[\bar{b}B_1 + e\Lambda_n C + \Lambda_n^2 e^2\sigma(A_1 + \bar{b}) + e^3\sigma^2\Lambda_n^3\Big]\Gamma_0 = 0, \\ \\ \mathrm{Ra}W_0^f + \mathrm{Ra}W_0^p - (\Lambda_n + \bar{\sigma})\Theta_0 = 0, \\ \\ \mathcal{C}W_0^f + \mathcal{C}W_0^p - (\Lambda_n + \epsilon_1 Le\bar{\sigma})\Gamma_0 = 0, \end{cases} \tag{7.15}$$

where $a^2 = l^2 + m^2$ and $\Lambda_n = a^2 + n^2\pi^2$, while $e = Da_f\gamma_1$, $\quad f = (\gamma_1\mathcal{T})^2$ and

$$\begin{aligned} &A_1 = \sigma\bar{a} + \bar{b}, \;\; B_1 = \frac{\gamma_1}{k}\frac{\gamma_2}{h} + \frac{\gamma_1}{k} + \frac{\gamma_2}{h}, \;\; C = \sigma(2B_1 + 1) + \bar{b}^2, \\ &M = \frac{\gamma_1}{k}n^2\pi^2 + \gamma_1 a^2 + \Lambda_n, \;\; N = \frac{\gamma_2}{h}n^2\pi^2 + \gamma_2 a^2 + \Lambda_n. \end{aligned} \tag{7.16}$$

Setting

$$
\begin{aligned}
h_{11} =&\Lambda_n e(A_1 M + \sigma f n^2\pi^2) + \Lambda_n^2 e(Me\sigma + B_1) + f\overline{b}n^2\pi^2 + B_1 M + \\
&e^2\Lambda_n^3 A_1 + e^3\sigma\Lambda_n^4, \\
h_{12} =& - B_1\Lambda_n - eA_1\Lambda_n^2 - e^2\sigma\Lambda_n^3 + \eta f n^2\pi^2, \\
h_{13} =&B_1 + e\Lambda_n A_1 + e^2\sigma\Lambda_n^2, \\
h_{21} =&\Lambda_n(e\sigma n^2\pi^2\eta f - \overline{b}B_1) + \eta f n^2\pi^2\overline{b} - \Lambda_n^2 eC - \Lambda_n^3 e^2\sigma(A_1 + \overline{b}) - \Lambda_n^4\sigma^2 e^3, \\
h_{22} =&\Lambda_n e(CN + \eta^2 f A_1 n^2\pi^2) + \Lambda_n^2 e\sigma[e(A_1 + \overline{b})N + \overline{b}B_1 + e\eta^2 f n^2\pi^2] + \\
&B_1\overline{b}N + e^2\Lambda_n^3\sigma(C + e\sigma N) + \Lambda_n^4 e^3\sigma^2(A_1 + \overline{b}) + \Lambda_n^5 e^4\sigma^3 + \eta^2 f n^2\pi^2\overline{a}\overline{b}, \\
h_{23} =&\overline{b}B_1 + e\Lambda_n C + \Lambda_n^2 e^2\sigma(A_1 + \overline{b}) + e^3\sigma^2\Lambda_n^3,
\end{aligned}
$$

(7.15) can be written as

$$
\begin{cases}
h_{11}W_0^f + h_{12}W_0^p - \mathrm{Ra}a^2 h_{13}\Theta_0 + \mathcal{C}a^2 h_{13}\Gamma_0 = 0, \\
h_{21}W_0^f + h_{22}W_0^p - \mathrm{Ra}a^2 h_{23}\Theta_0 + \mathcal{C}a^2 h_{23}\Gamma_0 = 0, \\
\mathrm{Ra}W_0^f + \mathrm{Ra}W_0^p - (\Lambda_n + \overline{\sigma})\Theta_0 = 0, \\
\mathcal{C}W_0^f + \mathcal{C}W_0^p - (\Lambda_n + \epsilon_1 Le\overline{\sigma})\Gamma_0 = 0.
\end{cases} \tag{7.17}
$$

To get a non-trivial solution, we require zero determinant for system (7.17), finding:

$$
\mathrm{Ra}^2 = \frac{\Lambda_n + \overline{\sigma}}{a^2}\frac{h_{11}h_{22} - h_{12}h_{21}}{h_{13}h_{22} - h_{12}h_{23} + h_{11}h_{23} - h_{21}h_{13}} + \mathcal{C}^2\frac{\Lambda_n + \overline{\sigma}}{\Lambda_n + \epsilon_1 Le\overline{\sigma}} \tag{7.18}
$$

The growth rate is $\overline{\sigma} = \sigma_R + i\sigma_I$, so (7.18) is

$$
\mathrm{Ra}^2 = Re(\mathrm{Ra}^2) + i\ Im(\mathrm{Ra}^2), \tag{7.19}
$$

where the real part and the imaginary part are respectively given by

$$
\begin{aligned}
Re(\mathrm{Ra}^2) =& \frac{(\Lambda_n + \sigma_R)(h_{11}h_{22} - h_{12}h_{21})}{a^2(h_{12}h_{23} - h_{13}h_{22} - h_{11}h_{23} + h_{21}h_{13})} \\
&+ \mathcal{C}^2\frac{(\Lambda_n + \sigma_R)(\Lambda_n + \epsilon_1 Le\sigma_R) + \epsilon_1 Le\sigma_I^2}{(\Lambda_n + \epsilon_1 Le\sigma_R)^2 + (\epsilon_1 Le\sigma_I)^2}, \\
Im(\mathrm{Ra}^2) =& \sigma_I\Big[\frac{h_{11}h_{22} - h_{12}h_{21}}{a^2(h_{12}h_{23} - h_{13}h_{22} - h_{11}h_{23} + h_{21}h_{13})} \\
&+ \mathcal{C}^2\frac{\Lambda_n(1 - \epsilon_1 Le)}{(\Lambda_n + \epsilon_1 Le\sigma_R)^2 + (\epsilon_1 Le\sigma_I)^2}\Big].
\end{aligned} \tag{7.20}
$$

Theorem 7.2.1. *If $\epsilon_1 Le \leq 1$, the strong form of the principle of exchange of stabilities holds, i.e. oscillatory convection cannot arise.*

Proof. Let us underline that, after several algebraic computations, it can checked that $h_{11}h_{22}-h_{12}h_{21}$ and $h_{12}h_{23}-h_{13}h_{22}-h_{11}h_{23}+h_{21}h_{13}$ are strictly positive. Since Ra^2 is a real number, the imaginary part of (7.19) has to vanish:

$$\begin{aligned}\sigma_I\Big\{&(h_{11}h_{22}-h_{12}h_{21})[(\Lambda_n+\epsilon_1 Le\sigma_R)^2+(\epsilon_1 Le\sigma_I)^2]\\ &+\mathcal{C}^2a^2(h_{12}h_{23}-h_{13}h_{22}-h_{11}h_{23}+h_{21}h_{13})\Lambda_n(1-\epsilon_1 Le)\Big\}=0.\end{aligned} \tag{7.21}$$

Under the assumption $\epsilon_1 Le \leq 1$, from (7.21) it necessarily follows $\sigma_I = 0$, i.e. $\overline{\sigma} \in \mathbb{R}$. □

Remark 7.2.1. *If we confine ourselves to the case of a single component fluid (i.e. for $\mathcal{C}^2 \to 0$), we actually recover the model describing the evolutionary behaviour of a fluid-saturated anisotropic Brinkman bi-disperse porous medium, rotating about the vertical axis, already analysed in Chapter 3. In particular,* (7.19) *becomes*

$$\begin{aligned}\mathrm{Ra}^2 =&\frac{(\Lambda_n+\sigma_R)(h_{11}h_{22}-h_{12}h_{21})}{a^2(h_{12}h_{23}-h_{13}h_{22}-h_{11}h_{23}+h_{21}h_{13})}\\ &+i\frac{\sigma_I(h_{11}h_{22}-h_{12}h_{21})}{a^2(h_{12}h_{23}-h_{13}h_{22}-h_{11}h_{23}+h_{21}h_{13})}\end{aligned} \tag{7.22}$$

therefore

$$\sigma_I\frac{h_{11}h_{22}-h_{12}h_{21}}{a^2(h_{12}h_{23}-h_{13}h_{22}-h_{11}h_{23}+h_{21}h_{13})}=0, \tag{7.23}$$

From (7.23) *it follows $\sigma_I = 0$, i.e. $\overline{\sigma} \in \mathbb{R}$ and the strong form of the principle of exchange of stabilities holds, under no additional hypotheses. Therefore, when there is no concentration gradient, convection can set in only through stationary motions.*

7.2.1 Stationary secondary flow

The marginal state for stationary convective instabilities is reached for $\overline{\sigma} = 0$ ($\sigma_R = 0, \sigma_I = 0$), so from (7.18) we derive the critical Rayleigh number for the onset of stationary convection:

$$\mathrm{Ra}_S^2 = \min_{(n,a^2)\in\mathbb{N}\times\mathbb{R}^+}\frac{\Lambda_n}{a^2}\frac{h_{11}h_{22}-h_{12}h_{21}}{h_{12}h_{23}-h_{13}h_{22}-h_{11}h_{23}+h_{21}h_{13}}+\mathcal{C}^2 \tag{7.24}$$

As already pointed out, if we consider a single component fluid (i.e. for $\mathcal{C}^2 \to 0$), (7.24) coincides with the instability threshold (3.21).

7.2.2 Overstability threshold

The marginal state for oscillatory convection is characterized by $\overline{\sigma} = i\sigma_I$, $(\sigma_I \in \mathbb{R} - \{0\}, \sigma_R = 0)$, so from (7.18) and (7.21) it follows

$$\mathrm{Ra}_O^2 = \min_{(n,a^2)\in\mathbb{N}\times\mathbb{R}^+} \frac{\Lambda_n}{a^2} \frac{h_{11}h_{22}-h_{12}h_{21}}{h_{12}h_{23}-h_{13}h_{22}-h_{11}h_{23}+h_{21}h_{13}} + \mathcal{C}^2 \frac{\Lambda_n^2+\epsilon_1 Le\sigma_I^2}{\Lambda_n^2+(\epsilon_1 Le\sigma_I)^2} \quad (7.25)$$

where the frequency of the oscillations σ_I is given by

$$\sigma_I^2 = \frac{a^2(h_{12}h_{23}-h_{13}h_{22}-h_{11}h_{23}+h_{21}h_{13})\Lambda_n\mathcal{C}^2(\epsilon_1 Le-1)-\Lambda_n^2(h_{11}h_{22}-h_{12}h_{21})}{(\epsilon_1 Le)^2(h_{11}h_{22}-h_{12}h_{21})} \quad (7.26)$$

Therefore, the linear instability threshold for the onset of oscillatory convection is

$$\mathrm{Ra}_O^2 = \min_{(n,a^2)\in\mathbb{N}\times\mathbb{R}^+} \frac{\Lambda_n}{a^2} \frac{h_{11}h_{22}-h_{12}h_{21}}{h_{12}h_{23}-h_{13}h_{22}-h_{11}h_{23}+h_{21}h_{13}} \left(1+\frac{1}{\epsilon_1 Le}\right) + \frac{\mathcal{C}^2}{\epsilon_1 Le} \quad (7.27)$$

Let us underline that the relation between the steady and the oscillatory thresholds is given by

$$\mathrm{Ra}_O^2 = \mathrm{Ra}_S^2\left(1+\frac{1}{\epsilon_1 Le}\right) - \mathcal{C}^2, \quad (7.28)$$

so for increasing $\mathcal{C}^2$, i.e. for high salt concentrations, convection will arise via oscillatory motions.

7.3 Influence of the fundamental physical parameters on the onset of instability

Due to the complicated algebraic form of the instability thresholds (7.24) and (7.27), we perform numerical simulations via Matlab software in order to outline *how* rotation, Brinkman model, anisotropy and concentration gradient affect the onset of convection, i.e. to outline the influence of the fundamental parameters $\mathcal{T}^2, Da_f, h, k, \mathcal{C}^2$ on the steady and oscillatory instability thresholds (7.24) and (7.27), respectively. In the following simulations, we employ the following set of parameters: $\{\eta = 0.2, \sigma = 0.3, \gamma_1 = 0.9, \gamma_2 = 1.8, \epsilon_1 Le = 55.924\}$ (see [49, 59, 36, 23]).
We numerically obtained that the minimum (7.24) and (7.27) with respect to n is attained at $n = 1$ and in Figure 7.1 the neutral curves are shown, where we set

$$\begin{aligned} f_S^2(a^2) &= \frac{\Lambda_1}{a^2} \frac{h_{11}h_{22}-h_{12}h_{21}}{h_{12}h_{23}-h_{13}h_{22}-h_{11}h_{23}+h_{21}h_{13}} + \mathcal{C}^2, \\ f_O^2(a^2) &= \frac{\Lambda_1}{a^2} \frac{h_{11}h_{22}-h_{12}h_{21}}{h_{12}h_{23}-h_{13}h_{22}-h_{11}h_{23}+h_{21}h_{13}} \left(1+\frac{1}{\epsilon_1 Le}\right) + \frac{\mathcal{C}^2}{\epsilon_1 Le}. \end{aligned} \quad (7.29)$$

In Figures 7.2(a) and 7.2(b) the steady and oscillatory Rayleigh numbers Ra_S^2 and Ra_O^2 are depicted as functions of the Taylor number $\mathcal{T}^2$, we can conclude that the instability thresholds are increasing functions with respect to $\mathcal{T}^2$, so the rotation of the layer has a stabilizing effect on the onset of double-diffusive convection. In particular, the instability thresholds are represented for a low concentration Rayleigh number $\mathcal{C}^2$ in Figure 7.2(a) and for a high concentration Rayleigh number in Figure 7.2(b): when the concentration gradient in the layer is low, convection sets in via stationary motions, but when the concentration gradient is high, oscillatory convection arises.
The asymptotic behaviour of the instability thresholds with respect to the Rayleigh number for the salt field is clearly depicted in Figure 7.3: both Ra_S^2 and Ra_O^2 are linear and increasing function of $\mathcal{C}^2$, so (i) when a salt dissolved at the bottom of the layer is considered, the convection is delayed, (ii) for increasing concentration Rayleigh numbers, double-diffusive convection occurs via oscillatory motions.
In Tables 7.1(a) and 7.1(b) the combined effects of anisotropy and the Brinkman model on the onset of double-diffusive convection are depicted. In particular, the critical steady and oscillatory Rayleigh numbers Ra_S^2 and Ra_O^2 are shown for increasing quoted values of the Darcy number Da_f when the micropermeability parameter h is lower - Table 7.1(a) - and higher - 7.1(b) - than the macropermeability parameter k. Both critical steady and oscillatory Rayleigh numbers increase as the Darcy number increases, i.e. Da_f has a stabilizing effect on the onset of convection. Moreover, for very law Da_f, oscillatory convection occurs, while as Da_f increases, there is a switch from oscillatory to steady convection. Let us finally observe that when $h << k$, the instability thresholds are larger then the ones for the case $h >> k$, so when the micropermeability parameter is larger then the macropermeability parameter, the onset of convection is facilitated. This behaviour is depicted also in Figures 7.4(a) and 7.4(b).

(a) $h << k$

R_S^2	R_O^2	Da_f
106.1926	103.0914	0.001
408.1480	410.4462	1
1615.8	1639.7	5

(b) $h >> k$

R_S^2	R_O^2	Da_f
54.0168	49.9827	0.001
369.6938	371.3044	1
1560	1582.9	5

Table 7.1: (a): Critical steady and oscillatory Rayleigh numbers for increasing Darcy number Da_f for $h = 0.1, k = 10$. (b): Critical steady and oscillatory Rayleigh numbers for increasing Darcy number Da_f for $h = 10, k = 0.1$. The other parameters are $\mathcal{T}^2 = 10, \mathcal{C}^2 = 5$.

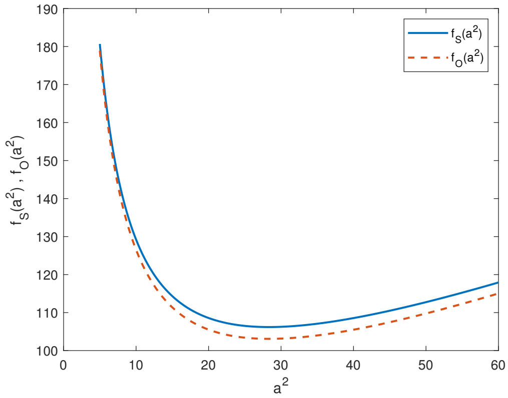

Figure 7.1: Neutral curves for $h = 0.1, k = 10, \mathcal{T}^2 = 10, Da = 0.001, \mathcal{C}^2 = 5$.

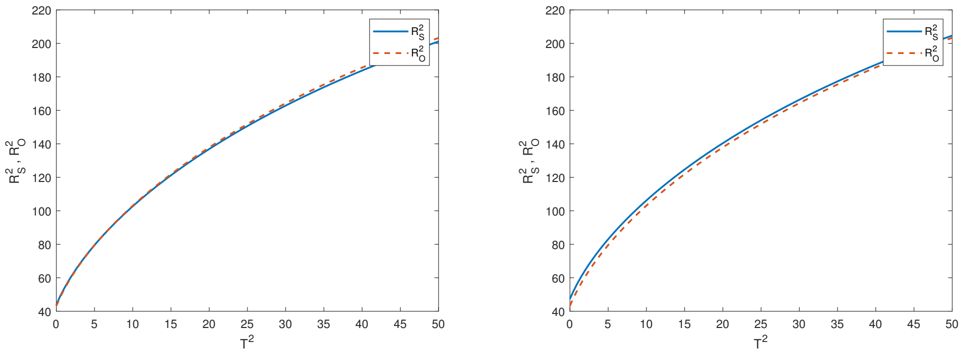

(a) $\mathcal{C}^2 = 1.5$

(b) $\mathcal{C}^2 = 5$

Figure 7.2: (a): Asymptotic behaviour of Ra_S^2 and Ra_O^2 with respect to $\mathcal{T}^2$ for $h = 0.1, k = 10, \mathcal{C} = 1.5, Da = 0.001$. (b): asymptotic behaviour of Ra_S^2 and Ra_O^2 with respect to $\mathcal{T}^2$ for $h = 0.1, k = 10, \mathcal{C} = 5, Da = 0.001$.

Main results

In this Chapter, the onset of convection in a rotating horizontal layer of anisotropic bi-disperse porous material simultaneously heated and salted from below was analysed. We determined the instability thresholds for the onset of double-diffusive convection via steady and oscillatory motions. Moreover, we proved the validity of the principle of exchange of stabilities under the assumption $\epsilon_1 Le \leq 1$, so in this case only stationary convection can occur. Numerical simulations were performed in order to analyse the behaviour of the instability thresholds with respect to the fundamental parameters, in particular we found that rotation and concentration gradient act to delay the

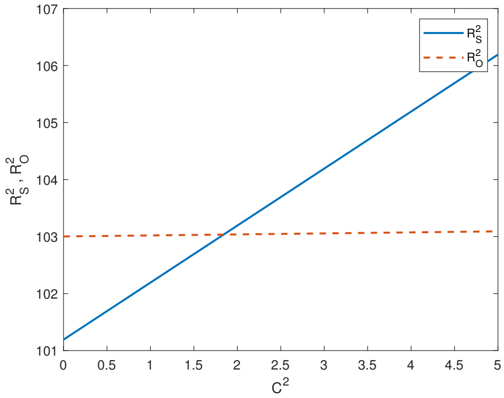

Figure 7.3: Asymptotic behaviour of Ra_S^2 and Ra_O^2 with respect to $\mathcal{C}^2$ for $h = 0.1, k = 10, \mathcal{T}^2 = 10, Da = 0.001$.

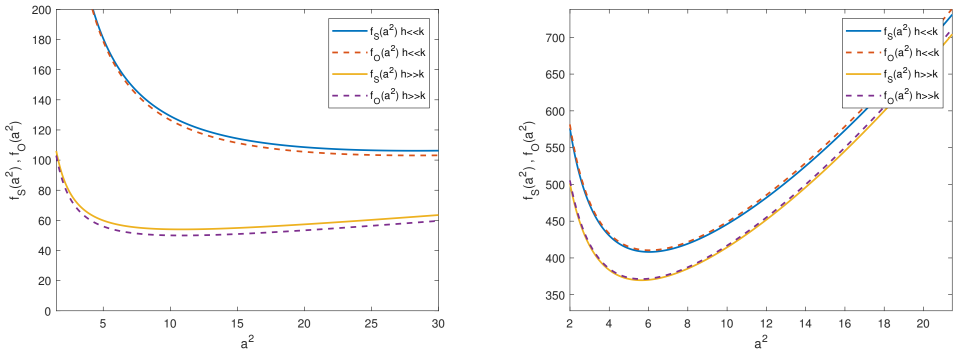

(a) $Da_f = 0.001$ (b) $Da_f = 1$

Figure 7.4: (a): Neutral curves at $Da_f = 0.001$. (b): Neutral curves at $Da_f = 1$.
The other parameters are $\mathcal{T}^2 = 10, \mathcal{C}^2 = 5$. The case $h << k$ is $h = 0.1, k = 10$, while the case $h >> k$ is $h = 10, k = 0.1$

onset of convection.

Part III

Chapter 8

Oberbeck-Boussinesq Approximation and Compressibility effect

When dealing with thermal convection problems, a Newtonian and homogeneous incompressible fluid (eventually saturating a horizontal layer of porous material) is usually considered. However, this is an approximation of the real phenomenon, since perfectly incompressible fluids do not exist in nature and, moreover, when the process is not isothermal, the notion of incompressibility is not well defined, see [61]. From a mathematical point of view, the pressure for a compressible fluid is a constitutive function, while the pressure for an incompressible fluid is a Lagrange multiplier that comes from the constraint of incompressibility. To study and compare the mathematical results and solutions of both compressible and incompressible media, we will consider the pressure p and the temperature T as thermodynamic variables, therefore $V = V(p, T)$ and $\varepsilon = \varepsilon(p, T)$ are the constitutive equations for the specific volume $V = \frac{1}{\varrho}$ (ϱ being the fluid density) and the internal energy of the system ε [62].
According to Müller, see [63], an incompressible fluid can be defined as a medium whose constitutive equations depend only on temperature T and not on pressure p, in particular:

$$\varrho = \varrho(T), \quad \varepsilon = \varepsilon(T). \tag{8.1}$$

Nevertheless, as pointed out by Gouin *et al.* in [64], Müller proved that the definition (8.1) is compatible with the entropy principle only if the density is a constant function $\varrho(T) = \varrho_0$. On assuming constant fluid density, no buoyancy-driven convective instabilities are allowed. However, according to experimental observations, fluids expand when heated and a theoretical assumption such as the very widely employed Oberbeck-Boussinesq approximation (see [65, 66]) — which consists in setting constant the density of the fluid in all terms of the governing equations except in the body force term due to gravity — is actually reasonable. Therefore, in order to account for the experimental validity of the problem and its thermodynamic consistency, Gouin *et. al* in [64] defined a new class of fluids, the "quasi-thermal-incompressible fluids", modifying the constitutive equations (8.1): *a quasi-thermal-incompressible fluid is a medium for which the only equation independent of the pressure p among all the constitutive equations is the fluid density.* For such class of fluids, the constitutive equations (8.1) become:

$$\varrho = \varrho(T), \quad \varepsilon = \varepsilon(p, T). \tag{8.2}$$

Using the above definition, the authors proved that a quasi-thermal-incompressible fluid tends to be perfectly incompressible, in the sense of Müller, when the following estimate for the pressure holds:

$$p \ll \frac{c_p}{|V'|} = \frac{\varrho^2 c_p}{|\varrho'|} \tag{8.3}$$

where c_p is the specific heat capacity at constant pressure. In convection problems, there are no sharp temperature variations and, since the temperature variation usually does not exceed $10K$, the density variation is of 1%, see [10], therefore the Oberbeck-Boussinesq approximation is coherently employed. When one does not expect large differences in temperature, one may assume the fluid density in the body force term has a linear dependence on temperature:

$$\varrho(T) = \varrho_0[1 - \alpha(T - T_0)], \tag{8.4}$$

where ϱ_0 is the fluid density at the reference temperature T_0, while α is the thermal expansion coefficient, defined as:

$$\alpha = \frac{V_T}{V}$$

V being the specific volume and V_T the partial derivative of V with respect to temperature T. When (8.4) is assumed, the estimate (8.3) becomes:

$$p \ll p_{cr} = \frac{c_p \varrho_0}{\alpha}, \tag{8.5}$$

The critical pressure value p_{cr} gives a limit of validity for the Oberbeck-Boussinesq approximation and due to estimate (8.5), Gouin *et. al* concluded that a quasi-thermal-incompressible fluid is experimentally similar to a perfectly incompressible fluid.

Later on, with the aim of proposing a more realistic model for fluid dynamics problems, Gouin and Ruggeri in [61] introduced the definition of *extended-quasi-thermal-incompressible* fluid by which they modified the Oberbeck-Boussinesq approximation as follows:

$$\varrho(p,T) = \varrho_0[1 - \alpha(T - T_0) + \beta(p - p_0)], \tag{8.6}$$

where p_0 is the reference pressure, while β is the compressibility factor defined as

$$\beta = -\frac{V_p}{V},$$

with V_p the partial derivative of the volume with respect to the pressure. Moreover, the Authors carried out a detailed analysis of the thermodynamic stability, proving that the compressibility factor has a lower bound, namely:

$$\beta > \beta_{cr} = \frac{\alpha^2 TV}{c_p}(> 0). \tag{8.7}$$

It is possible to evaluate the order of magnitude of both critical pressure p_{cr} and compressibility factor β_{cr}, (8.5) and (8.7) in the case of liquid **water** (see [67]), since:

$$T_0 = 293\ K,\ p_0 = 10^5\ Pa,\ V_0 = 10^{-3}\ m^3/kg,\ \varrho_0 = 10^3\ kg/m^3,$$

$$c_p = 4.2 \cdot 10^3\ J/kg\ K,\ \alpha = 207 \cdot 10^{-6}/K,$$

they assume the following values:

$$p_{cr} = 2 \cdot 10^{10}\ Pa = 2 \cdot 10^5\ atm \quad \text{and} \quad \beta_{cr} = 3 \cdot 10^{-12}/Pa.$$

Remark 8.0.1. *Since bi-disperse porous media find a large number of applications in industrial sectors, let us evaluate the critical pressure p_{cr} for some relevant fluids related to those fields, see [68]:*

- ***Gasoline**: $T_0 = 15°C,\ \varrho_0 = 715-780\ kg/m^3,\ c_p = 2.22 \cdot 10^3\ J/kg\ K,\ \alpha = 950 \cdot 10^{-6}/K$, hence $p_{cr} = 1.67 \cdot 10^9\ Pa$.*

- ***Kerosene**: $T_0 = 15°C,\ \varrho_0 = 775-840\ kg/m^3,\ c_p = 2.01 \cdot 10^3\ J/kg\ K,\ \alpha = 990 \cdot 10^{-6}/K$, hence $p_{cr} = 1.57 \cdot 10^9\ Pa$.*

Those values of the critical pressures are actually very large with respect to usual pressure conditions. We can conclude that for very large pressures no body can be approximated as perfectly incompressible, for usual pressures the incompressibility model is both experimentally and theoretically valid and it is compatible with the principles of thermodynamics.

In [69] the extended approximation was employed for the linear instability analysis of the conduction solution for the classical Bénard problem, and the Authors proved via linear instability analysis the destabilizing effect of a dimensionless parameter $\widehat{\beta}$, proportional to the positive compressibility factor β, on the onset of convection.
To the best of our knowledge, there is a lack of investigations on the onset of convective motions in porous media assuming the definition of extended-quasi-thermal-incompressible fluid. This lack motivated the following Sections, whose results are based on [70], joint work with G. Arnone, F. Capone and R. De Luca. In Section 8.1 we derive the mathematical model describing the onset of convection for the Darcy-Bénard problem employing an extended-quasi-thermal-incompressible fluid, while in Section 8.2 we perform a linear instability analysis of the thermal conduction solution. In Section 8.3 we analyse the asymptotic behaviour of the critical Rayleigh-Darcy number Ra with respect to the dimensionless compressibility factor $\widehat{\beta}$, proving the destabilizing effect of $\widehat{\beta}$ on the onset of convective instabilities.

8.1 Compressibility effect on Darcy porous convection

Let us consider a reference frame $Oxyz$ with fundamental unit vectors $\{\mathbf{i}, \mathbf{j}, \mathbf{k}\}$ ($\mathbf{k}$ pointing vertically upwards) and a horizontal layer $L = \mathbb{R}^2 \times [0, d]$ of fluid-saturated porous medium. To derive the governing equations for the seepage velocity $\mathbf{v}$, the temperature field T and the pressure field p, let us employ the modified Oberbeck-Boussinesq approximation, see [69]:

- the fluid density ϱ is constant in all terms of the governing equations (i.e. $\varrho = \varrho_0$), except in the buoyancy term;
- in the body force term, the constitutive law for the fluid density is given by
$$\varrho(T) = \varrho_0[1 - \alpha(T - T_0) + \beta(p - p_0)], \tag{8.8}$$
with α and β the thermal expansion coefficient and the compressibility factor, respectively, defined as
$$\alpha = \frac{V_T}{V}, \quad \beta = -\frac{V_p}{V},$$
- $\nabla \cdot \mathbf{v} = 0$ and $\mathbf{D} : \mathbf{D} \approx 0$.

Therefore, the mathematical model, according to Darcy's law, is the following

$$\begin{cases} \dfrac{\mu}{K}\mathbf{v} = -\nabla p - \varrho_0[1-\alpha(T-T_0)+\beta(p-p_0)]g\mathbf{k}, \\ \nabla\cdot\mathbf{v} = 0, \\ \varrho c_V\left(\dfrac{\partial T}{\partial t} + \mathbf{v}\cdot\nabla T\right) = \chi\Delta T, \end{cases} \tag{8.9}$$

where μ, K, χ, c_V are fluid viscosity, permeability of the porous body, thermal conductivity and specific heat at constant volume, respectively.
To system (8.9) the boundary conditions are appended, i.e.:

$$\begin{aligned} \mathbf{v}\cdot\mathbf{k} = 0 \quad & \text{on } z = 0, d \\ T = T_L \quad & \text{on } z = 0 \\ T = T_U \quad & \text{on } z = d \\ \nabla p\cdot\mathbf{k} + \varrho_0 d\beta g\, p = 0 \quad & \text{on } z = 0, d \end{aligned} \tag{8.10}$$

with $T_L > T_U$, since the layer is heated from below. Assuming the reference temperature $T_0 = T_L$, system (8.9)-(8.10) admits the following stationary conduction solution

$$\begin{aligned} & \mathbf{v}_b = \mathbf{0},\ T_b(z) = T_L - \frac{T_L - T_U}{d}z, \\ & p_b(z) = \frac{1}{\beta d} + \left[\frac{1}{\beta} - \frac{\alpha(T_L - T_U)}{\beta^2\varrho_0 g d}\right](e^{-\varrho_0 g\beta z} - 1) - \frac{\alpha(T_L - T_U)}{\beta d}z. \end{aligned} \tag{8.11}$$

Let $(\mathbf{u}, \theta, \pi)$ be a perturbation to the basic solution, so the equations governing the perturbation fields are

$$\begin{cases} \dfrac{\mu}{K}\mathbf{u} = -\nabla\pi + \varrho_0\alpha g\theta\mathbf{k} - \varrho_0\beta g\pi\mathbf{k}, \\ \nabla\cdot\mathbf{u} = 0, \\ \dfrac{\partial\theta}{\partial t} + \mathbf{u}\cdot\nabla\theta = \dfrac{T_L - T_U}{d}\mathbf{u}\cdot\mathbf{k} + k\Delta\theta, \end{cases} \tag{8.12}$$

where $k = \frac{\chi}{\varrho c_V}$ is the thermal diffusivity. Let us introduce the following scales

$$\pi = P\pi^*, \quad \mathbf{u} = U\mathbf{u}^*, \quad \theta = T^\#\theta^*, \quad t = \tau t^*, \quad x = dx^*,$$

where:

$$P = \frac{\mu k}{K}, \quad U = \frac{k}{d}, \quad T^\# = T_L - T_U, \quad \tau = \frac{d^2}{k}.$$

Therefore, the corresponding dimensionless system of equations, omitting all the stars, is the following:

$$\begin{cases} \mathbf{u} = -\nabla\pi + \mathrm{Ra}\theta\mathbf{k} - \widehat{\beta}\pi\mathbf{k}, \\ \nabla\cdot\mathbf{u} = 0, \\ \dfrac{\partial\theta}{\partial t} + \mathbf{u}\cdot\nabla\theta = w + \Delta\theta, \end{cases} \tag{8.13}$$

where $u = \mathbf{u}\cdot\mathbf{i}$ and $w = \mathbf{u}\cdot\mathbf{k}$ and

$$\mathrm{Ra} = \frac{\varrho_0\alpha g d(T_L - T_U)K}{\mu k}, \quad \widehat{\beta} = \varrho_0 d g\beta$$

are the Rayleigh-Darcy number and the dimensionless compressibility factor, respectively.

To system (8.13) we add the following boundary conditions

$$w = \theta = \nabla\pi\cdot\mathbf{k} + \widehat{\beta}\pi = 0 \qquad \text{on } z = 0, 1 \tag{8.14}$$

and initial conditions

$$\mathbf{u}(\mathbf{x}, 0) = \mathbf{u}_0(\mathbf{x}), \quad \pi(\mathbf{x}, 0) = \pi_0(\mathbf{x}), \quad \theta(\mathbf{x}, 0) = \theta_0(\mathbf{x}). \tag{8.15}$$

Accounting for $(8.13)_2$, taking the divergence of $(8.13)_1$, system (8.13) becomes:

$$\begin{cases} \Delta\pi + \widehat{\beta}\dfrac{\partial\pi}{\partial z} = \mathrm{Ra}\dfrac{\partial\theta}{\partial z}, \\ \mathbf{u} = -\nabla\pi + \mathrm{Ra}\theta\mathbf{k} - \widehat{\beta}\pi\mathbf{k}, \\ \dfrac{\partial\theta}{\partial t} + \mathbf{u}\cdot\nabla\theta = w + \Delta\theta. \end{cases} \tag{8.16}$$

Remark 8.1.1. *In the sequel, we will focus on bi-dimensional perturbations in the plane (x, z) and assume the perturbations fields $\pi, \boldsymbol{u}, \theta$ to be periodic functions in the horizontal direction x with period $\frac{2\pi}{a_x}$, a_x being the wavenumber. Without loss of generality, in the sequel we will assume that the wavelength is 1, so $\frac{2\pi}{a_x} = 1$ (see [69, 71]) and we will consider the periodicity cell V given by:*

$$V = [0, 1] \times [0, 1].$$

Moreover, with $\|\cdot\|$ and $\langle\cdot,\cdot\rangle$ we will denote norm and scalar product on $L^2(V)$, respectively.

8.2 Fourier method for linear instability analysis

To perform the linear instability analysis of the basic solution, let us consider the linear version of (8.16):

$$\begin{cases} \Delta\pi + \widehat{\beta}\dfrac{\partial \pi}{\partial z} = \mathrm{Ra}\dfrac{\partial \theta}{\partial z}, \\ \mathbf{u} = -\nabla\pi + \mathrm{Ra}\theta\mathbf{k} - \widehat{\beta}\pi\mathbf{k}, \\ \dfrac{\partial \theta}{\partial t} = w + \Delta\theta, \end{cases} \tag{8.17}$$

together with boundary conditions:

$$w = \theta = 0 \quad \text{and} \quad \frac{\partial \pi}{\partial z} = -\widehat{\beta}\pi \qquad \text{on } z = 0, 1 \tag{8.18}$$

By virtue of the Robin boundary condition (8.18) on the pressure, it is possible to choose:

$$\pi = e^{-\widehat{\beta}z}\Pi(x, z, t). \tag{8.19}$$

Therefore equation $(8.17)_1$ becomes:

$$\Delta\Pi - \widehat{\beta}\frac{\partial \Pi}{\partial z} = \mathrm{Ra}e^{\widehat{\beta}z}\frac{\partial \theta}{\partial z}, \tag{8.20}$$

and the Robin boundary conditions $\dfrac{\partial \pi}{\partial z} = -\widehat{\beta}\pi$ becomes the Neumann condition given by:

$$\frac{\partial \Pi}{\partial z} = 0 \qquad z = 0, 1 \tag{8.21}$$

Introducing the stream function Φ such that

$$u = -\frac{\partial \Phi}{\partial z}, \quad w = \frac{\partial \Phi}{\partial x} \tag{8.22}$$

and considering the curl of $(8.17)_2$ projected on the y-axis, one obtains:

$$\Delta\Phi = \mathrm{Ra}\frac{\partial \theta}{\partial x} - \widehat{\beta}e^{-\widehat{\beta}z}\frac{\partial \Pi}{\partial x}. \tag{8.23}$$

Hence, to perform the linear instability analysis of the conduction solution, we consider the following system:

$$\begin{cases} \Delta\Pi - \widehat{\beta}\dfrac{\partial\Pi}{\partial z} = \mathrm{Ra}e^{\widehat{\beta}z}\dfrac{\partial\theta}{\partial z}, \\ \Delta\Phi = \mathrm{Ra}\dfrac{\partial\theta}{\partial x} - \widehat{\beta}e^{-\widehat{\beta}z}\dfrac{\partial\Pi}{\partial x}, \\ \dfrac{\partial\theta}{\partial t} = \dfrac{\partial\Phi}{\partial x} + \Delta\theta, \end{cases} \tag{8.24}$$

to which we add the boundary conditions:

$$\theta = \frac{\partial\Pi}{\partial z} = \Delta\Phi = 0 \qquad \text{on } z = 0, 1. \tag{8.25}$$

By virtue of (8.25), since system (8.24) is linear, we assume normal mode solutions:

$$\begin{aligned} \theta(x,z,t) &= \sum_{m,n=0}^{\infty} [A^1_{mn}(t)\cos(2\pi mx)\sin(\pi nz) + A^2_{mn}(t)\sin(2\pi mx)\sin(\pi nz)], \\ \Pi(x,z,t) &= \sum_{m,n=0}^{\infty} [B^1_{mn}(t)\cos(2\pi mx)\cos(\pi nz) + B^2_{mn}(t)\sin(2\pi mx)\cos(\pi nz)], \\ \Delta\Phi(x,z,t) &= \sum_{m,n=0}^{\infty} [C^1_{mn}(t)\cos(2\pi mx)\sin(\pi nz) + C^2_{mn}(t)\sin(2\pi mx)\sin(\pi nz)]. \end{aligned} \tag{8.26}$$

In order to get zero mean value on V, we assume $(m,n) \in \mathbb{N}\times\mathbb{N}_0$. Applying the laplacian operator to $(8.24)_3$ and by virtue of (8.26), one obtains:

$$\begin{cases} \displaystyle\sum_{m,n}[B^1_{mn}\cos(2\pi mx) + B^2_{mn}\sin(2\pi mx)][-\alpha_{mn}\cos(n\pi z) + \widehat{\beta}n\pi\sin(n\pi z)] \\ \qquad \displaystyle = \mathrm{Ra}\sum_{m,n} n\pi[A^1_{mn}\cos(2\pi mx) + A^2_{mn}\sin(2\pi mx)]e^{\widehat{\beta}z}\cos(n\pi z), \\ \displaystyle\sum_{m,n}[C^1_{mn}\cos(2\pi mx) + C^2_{mn}\sin(2\pi mx)]\sin(n\pi z) \\ \qquad \displaystyle = \sum_{m,n=0} 2\pi m\Big\{\mathrm{Ra}[-A^1_{mn}\sin(2\pi mx) + A^2_{mn}\cos(2\pi mx)]\sin(\pi nz) \\ \qquad\quad -\widehat{\beta}e^{-\widehat{\beta}z}[-B^1_{mn}\sin(2\pi mx) + B^2_{mn}\cos(2\pi mx)]\cos(n\pi z)\Big\}, \\ \displaystyle\sum_{m,n} -\alpha_{mn}[(\dot{A}^1_{mn} + \alpha_{mn}A^1_{mn})\cos(2\pi mx) + (\dot{A}^2_{mn} + \alpha_{mn}A^2_{mn})\sin(2\pi mx)]\sin(n\pi z) \\ \qquad \displaystyle = \sum_{m,n} 2\pi m[-C^1_{mn}\sin(2\pi mx) + C^2_{mn}\cos(2\pi mx)]\sin(n\pi z), \end{cases} \tag{8.27}$$

where $\alpha_{mn} = (2\pi m)^2 + (\pi n)^2$ and $\dot{A}^i_{mn} = \dfrac{dA^i_{mn}}{dt}$. From $(8.27)_3$, it immediately follows that

$$\begin{aligned} C^1_{mn} &= \frac{\alpha_{mn}}{2\pi m}(\dot{A}^2_{mn} + \alpha_{mn} A^2_{mn}), \\ C^2_{mn} &= -\frac{\alpha_{mn}}{2\pi m}(\dot{A}^1_{mn} + \alpha_{mn} A^1_{mn}). \end{aligned} \tag{8.28}$$

Let us multiply $(8.27)_1$ by $\cos(k\pi z)$ and integrate with respect to $z \in (0,1)$, therefore we get:

$$\begin{aligned} &\sum_{m,n}[B^1_{mn}\cos(2\pi mx) + B^2_{mn}\sin(2\pi mx)] \\ &\left[-\alpha_{mn}\int_0^1 \cos(n\pi z)\cos(k\pi z)dz + \widehat{\beta} n\pi \int_0^1 \sin(n\pi z)\cos(k\pi z)dz\right] = \\ &\sum_{m,n} \mathrm{Ra}\; n\pi[A^1_{mn}\cos(2\pi mx) + A^2_{mn}\sin(2\pi mx)]\int_0^1 e^{\widehat{\beta}z}\cos(n\pi z)\cos(k\pi z)dz \end{aligned} \tag{8.29}$$

namely:

$$\begin{aligned} &\sum_{m,n}[B^1_{mn}\cos(2\pi mx) + B^2_{mn}\sin(2\pi mx)]\left[-\frac{1}{2}\alpha_{mk}\delta_{nk} + \widehat{\beta}F_{nk}\right] = \\ &\qquad \mathrm{Ra}\sum_{m,n}[A^1_{mn}\cos(2\pi mx) + A^2_{mn}\sin(2\pi mx)]\frac{\widehat{\beta}}{2}\mathcal{L}_{nk}(\widehat{\beta}) \end{aligned} \tag{8.30}$$

with:

$$\begin{aligned} F_{nk} &= \begin{cases} 0 & \text{if } n = k \\ \dfrac{n^2((-1)^{n+k}-1)}{(k-n)(k+n)} & \text{if } n \neq k \end{cases} \\ \mathcal{L}_{nk}(\widehat{\beta}) &= n\pi(e^{\widehat{\beta}}(-1)^{k+n} - 1)\left(\frac{1}{\pi^2(k+n)^2 + \widehat{\beta}^2} + \frac{1}{\pi^2(k-n)^2 + \widehat{\beta}^2}\right). \end{aligned} \tag{8.31}$$

Setting

$$\mathcal{D}^m_{nk}(\widehat{\beta}) = \delta_{nk} + \widehat{\beta}\begin{cases} \dfrac{-2n}{\alpha_{mk}}\left(\dfrac{1}{n-k} + \dfrac{1}{n+k}\right) & \text{if} \quad n+k \ \text{ odd} \\ 0 & \text{if} \quad n+k \ \text{ even} \end{cases} \tag{8.32}$$

by virtue of linearity, from (8.30) one obtains

$$\sum_{n=0}^{\infty} B^i_{mn}\mathcal{D}^m_{nk}(\widehat{\beta}) = -\frac{\mathrm{Ra}\widehat{\beta}}{\alpha_{mk}}\sum_{n=0}^{\infty} A^i_{mn}\mathcal{L}_{nk}(\widehat{\beta}), \qquad i = 1, 2. \tag{8.33}$$

Let us remark that the $N \times N$ matrix $\mathcal{D}^m$ is invertible since it is strictly diagonally dominant for small $\widehat{\beta}$ (see [72]). Moreover, through a fixed point argument, an estimate on the compressibility factor $\widehat{\beta}$ guaranteeing the invertibility of the matrix $\mathcal{D}^m$ for all $N \in \mathbb{N}$ is obtained. The following theorem holds.

Theorem 8.2.1. *If*

$$\widehat{\beta} < \frac{\pi^2}{2c} \tag{8.34}$$

with $c = \frac{1}{8}[2\pi\coth(2\pi) + 1]$, *then the matrix* $\mathcal{D}^m$ *is invertible for all* $N \in \mathbb{N}$.

Proof. Let us consider the basis functions:

$$\varphi^i_{mn}(x,z) = \begin{cases}\cos(2\pi m x)\cos(n\pi z) & \text{if } i = 1\\ \sin(2\pi m x)\cos(n\pi z) & \text{if } i = 2\end{cases} \tag{8.35}$$

which are the eigenfunctions of the Laplace operator:

$$\Delta\varphi^i_{mn} = -\alpha_{mn}\varphi^i_{mn}, \tag{8.36}$$

$\alpha_{mn} = 4\pi^2 m^2 + \pi^2 n^2$ being the eigenvalues. Since:

$$b_{mn} := \|\varphi^i_{mn}\|^2 = \begin{cases}\frac{1}{2} & n = 0\\ \frac{1}{4} & \text{otherwise}\end{cases} \tag{8.37}$$

defining $\gamma_{mn} = \sqrt{\alpha_{mn} b_{mn}}$, the following normalization can be introduced:

$$\psi^i_{mn} = \frac{\varphi^i_{mn}}{\gamma_{mn}}. \tag{8.38}$$

Equation $(8.24)_1$ can be written in terms of (8.38) as:

$$-\sum_{\substack{i=1,2\\ m,n}} B^i_{mn}(-\Delta\psi^i_{mn}) - \widehat{\beta}\sum_{\substack{i=1,2\\ m,n}} B^i_{mn}\frac{\partial\psi^i_{mn}}{\partial z} = \sum_{\substack{i=1,2\\ m,n}} e^{\widehat{\beta}z}\mathrm{Ra}A^i_{mn}\frac{\partial\psi^i_{mn}}{\partial z}. \tag{8.39}$$

If we multiply (8.39) by ψ_{lr}^j and integrate on V we obtain:

$$-\sum_{\substack{i=1,2\\m,n}} B_{mn}^i \left\langle \nabla\psi_{mn}^i, \nabla\psi_{lr}^j \right\rangle - \widehat{\beta} \sum_{\substack{i=1,2\\m,n}} B_{mn}^i \left\langle \frac{\partial \psi_{mn}^i}{\partial z}, \psi_{lr}^j \right\rangle = \sum_{\substack{i=1,2\\m,n}} F_{mnlr}^{i,j} \tag{8.40}$$

where:

$$F_{mnlr}^{i,j} = e^{\widehat{\beta} z} \mathrm{Ra} A_{mn}^i \left\langle \frac{\partial \psi_{mn}^i}{\partial z}, \psi_{lr}^j \right\rangle. \tag{8.41}$$

From (8.35) and (8.38), it follows that:

$$\begin{aligned} \left\langle \frac{\partial \psi_{mn}^i}{\partial z}, \psi_{lr}^j \right\rangle &= \frac{1}{\gamma_{mn}\gamma_{lr}} \left\langle \frac{\partial \varphi_{mn}^i}{\partial z}, \varphi_{lr}^j \right\rangle \\ &= -\frac{\delta_{ij}\delta_{ml}}{\gamma_{mn}\,\gamma_{lr}} \frac{n}{2} \begin{cases} \frac{1}{n+r} + \frac{1}{n-r} & \text{se } n+r \geq 1 \text{ odd} \\ 0 & \text{otherwise} \end{cases} \end{aligned} \tag{8.42}$$

and equation (8.40) becomes:

$$-B_{lr}^j + \widehat{\beta} \sum_{\substack{i\,|\,m,n\\ n+r\geq 1 \text{ odd}}} B_{mn}^i \frac{n}{2} \frac{\delta_{ij}\delta_{ml}}{\gamma_{mn}\gamma_{lr}} \left(\frac{1}{n+r} + \frac{1}{n-r} \right) - \sum_{i|m,n} F_{mnlr}^{i,j} = 0. \tag{8.43}$$

Now, let us introduce the following continuous functions:

$$\begin{aligned} \mathcal{P} : B \in \mathbb{R}^N &\longmapsto -B_{lr}^j + \widehat{\beta} \sum_{\substack{i|m,n\\ n+r\geq 1 \text{ odd}}} B_{mn}^i \frac{n}{2} \frac{\delta_{ij}\delta_{ml}}{\gamma_{mn}\gamma_{lr}} \left(\frac{1}{n+r} + \frac{1}{n-r} \right) - \sum_{i|m,n} F_{mnlr}^{i,j} \in \mathbb{R}^N \\ \mathcal{G} : B \in \mathbb{R}^N &\longmapsto \widehat{\beta} \sum_{\substack{i|m,n\\ n+r\geq 1 \text{ odd}}} B_{mn}^i \frac{n}{2} \frac{\delta_{ij}\delta_{ml}}{\gamma_{mn}\gamma_{lr}} \left(\frac{1}{n+r} + \frac{1}{n-r} \right) - \sum_{i|m,n} F_{mnlr}^{i,j} \in \mathbb{R}^N \end{aligned} \tag{8.44}$$

so the algebraic system (8.43) - equivalent to system (8.33) - can be written as $\mathcal{P}(B) = 0$. Let us observe that the invertibility of $\mathcal{D}^m$ is equivalent to prove that system (8.43) admits a nontrivial solution, moreover, B is a solution of (8.43) if and only if B is a fixed point of $\mathcal{G}$:

$$\mathcal{P}(B) = 0 \quad \Longleftrightarrow \quad \mathcal{G}(B) = B. \tag{8.45}$$

The existence of a fixed point for $\mathcal{G}$ is guaranteed by the Leray–Schauder theorem, provided that:

$$\{B \in \mathbb{R}^N \mid B = \lambda\mathcal{G}(B),\ 0 \le \lambda \le 1\} \subset B_R(0), \tag{8.46}$$

$B_R(0)$ being a ball of radius $R > 0$ centered in 0, hence:

$$\{B\in\mathbb{R}^N|B=\lambda\mathcal{G}(B), 0 \le \lambda \le 1\}^{\complement} \supset \mathscr{B} := \{B\in\mathbb{R}^N|B = \lambda\mathcal{G}(B), \lambda>1\}. \tag{8.47}$$

If $B \in \mathscr{B}$, then $\lambda B + (1-\lambda)B = \lambda\mathcal{G}(B)$, i.e. $(1-\lambda)B = \lambda\mathcal{P}(B)$, therefore:

$$\frac{1-\lambda}{\lambda}|B|^2 = \mathcal{P}(B)\cdot B, \tag{8.48}$$

$|\cdot|$ being the standard euclidean norm. Therefore, from (8.46) and (8.48) we can state that the proof of the existence of a fixed pointy for $\mathcal{G}$ is equivalent to prove that:

$$\begin{aligned}\mathcal{P}(B)\cdot B = &-\sum_{l,r}(B^j_{lr})^2 + \frac{\widehat{\beta}}{2}\sum_{\substack{i|m,n,r\\ n+r\ge 1 \text{ odd}}} B^i_{mn}B^i_{mr}\frac{1}{\gamma_{mn}\gamma_{mr}}\left(\frac{n}{n+r}+\frac{n}{n-r}\right)\\ &-\sum_{i|m,n,l,r} F^{i,j}_{mnlr}B^i_{lr}\end{aligned} \tag{8.49}$$

is negative for $|B| > R$. For notational convenience let us set:

$$\widetilde{B}^i_{mnr} = \frac{B^i_{mn}}{\gamma_{mr}} \qquad \text{and} \qquad \widetilde{B}^i_{mrn} = \frac{B^i_{mr}}{\gamma_{mn}} \tag{8.50}$$

and, hence, from (8.49) we have:

$$\frac{1}{2}\sum_{\substack{i|m,n,r\\ n+r\ge 1 \text{ odd}}} \widetilde{B}^i_{mnr}\widetilde{B}^i_{mrn}\left(\frac{n}{n+r} + \frac{n}{n-r}\right) =: I + J. \tag{8.51}$$

Therefore:

$$\begin{aligned}I = &\sum_{\substack{i|m,n,r\\ n+r\ge 1 \text{ odd}}} \widetilde{B}^i_{mnr}\widetilde{B}^i_{mrn}\frac{n}{n+r} = \sum_{\substack{i|m\\ n \text{ even},\, r \text{ odd}}} \widetilde{B}^i_{mnr}\widetilde{B}^i_{mrn}\frac{n}{n+r} + \sum_{\substack{i|m\\ n \text{ odd},\, r \text{ even}}} \widetilde{B}^i_{mnr}\widetilde{B}^i_{mrn}\frac{n}{n+r}\\ = &\sum_{\substack{i|m\\ n \text{ even},\, r \text{ odd}}} \widetilde{B}^i_{mnr}\widetilde{B}^i_{mrn}\frac{n}{n+r} + \sum_{\substack{i|m\\ n \text{ even},\, r \text{ odd}}} \widetilde{B}^i_{mnr}\widetilde{B}^i_{mrn}\frac{r}{n+r} = \sum_{\substack{i|m\\ n \text{ even},\, r \text{ odd}}} \widetilde{B}^i_{mnr}\widetilde{B}^i_{mrn},\end{aligned} \tag{8.52}$$

and similarly with J

$$\begin{aligned} J = & \sum_{\substack{i|m,n,r \\ n+r\geq 1 \ \text{odd}}} \widetilde{B}^i_{mnr}\widetilde{B}^i_{mrn}\frac{n}{n-r} = \sum_{\substack{i|m \\ n \text{ even}, \, r \text{ odd}}} \widetilde{B}^i_{mnr}\widetilde{B}^i_{mrn}\frac{n}{n-r} + \sum_{\substack{i|m \\ n \text{ odd}, \, r \text{ even}}} \widetilde{B}^i_{mnr}\widetilde{B}^i_{mrn}\frac{n}{n-r} \\ = & \sum_{\substack{i|m \\ n \text{ even}, \, r \text{ odd}}} \widetilde{B}^i_{mnr}\widetilde{B}^i_{mrn}\frac{n}{n-r} + \sum_{\substack{i|m \\ n \text{ even}, \, r \text{ odd}}} \widetilde{B}^i_{mnr}\widetilde{B}^i_{mrn}\frac{r}{n-r} = \sum_{\substack{i|m \\ n \text{ even}, \, r \text{ odd}}} \widetilde{B}^i_{mnr}\widetilde{B}^i_{mrn}. \end{aligned} \tag{8.53}$$

By virtue of (8.52) and (8.53), Cauchy-Schwarz and Young inequalities and since $\gamma^2_{mn} \geq \dfrac{4\pi^2+n^2\pi^2}{4}$, from (8.51) it follows:

$$\begin{aligned} \sum_{\substack{i|m \\ n \text{ even}, \, r \text{ odd}}} \widetilde{B}^i_{mnr}\widetilde{B}^i_{mrn} = & \sum_{\substack{i \\ n \text{ even}, \, r \text{ odd}}} \widetilde{B}^i_{\cdot,nr}\cdot\widetilde{B}^i_{\cdot,rn} \leq \sum_{\substack{i \\ n \text{ even}, \, r \text{ odd}}} |\widetilde{B}^i_{\cdot,nr}|\,|\widetilde{B}^i_{\cdot,rn}| \\ & \leq \frac{1}{2}\left[\sum_{\substack{i \\ n \text{ even}, \, r \text{ odd}}} |\widetilde{B}^i_{\cdot,nr}|^2 + \sum_{\substack{i \\ n \text{ even}, \, r \text{ odd}}} |\widetilde{B}^i_{\cdot,rn}|^2\right] \\ & = \frac{1}{2}\left[\sum_{\substack{i\,|\,m \\ n \text{ even}, \, r \text{ odd}}} \frac{|B^i_{mn}|^2}{\gamma^2_{mr}} + \sum_{\substack{i\,|\,m \\ n \text{ even}, \, r \text{ odd}}} \frac{|B^i_{mr}|^2}{\gamma^2_{mn}}\right] \\ & \leq 2\Big[\sum_{\substack{i\,|\,m \\ n \text{ even}}} |B^i_{mn}|^2 \sum_{r \text{ odd}} \frac{1}{4\pi^2+r^2\pi^2} \\ & \qquad + \sum_{\substack{i\,|\,m \\ r \text{ odd}}} |B^i_{mr}|^2 \sum_{n \text{ even}} \frac{1}{4\pi^2+n^2\pi^2}\Big] \\ & \leq \frac{2}{\pi^2}\left[\sum_{\substack{i\,|\,m \\ n \text{ even}}} |B^i_{mn}|^2 + \sum_{\substack{i\,|\,m \\ r \text{ odd}}} |B^i_{mr}|^2\right]\sum_n \frac{1}{4+n^2} \\ & = \frac{2}{\pi^2}|B|^2\sum_n\frac{1}{4+n^2} = \frac{2}{\pi^2}|B|^2 c, \end{aligned} \tag{8.54}$$

where $c = \frac{1}{8}[2\pi\coth(2\pi)+1]$. Finally, from (8.49) and (8.54) one gets:

$$\mathcal{P}(B)\cdot B \leq -|B|^2 + \widehat{\beta}c\frac{2}{\pi^2}|B|^2 + K|B|, \tag{8.55}$$

with $K = |F|$. Therefore, for $|B| > R := K/(1-\widehat{\beta}c2\pi^{-2})$ and if

$$\widehat{\beta} < \frac{\pi^2}{2c} \tag{8.56}$$

it follows $\mathcal{P}(B) \cdot B < 0$. $\square$

Solving system (8.33), we get component-wise the same relation for the coefficients B^1_{mj} and B^2_{mj}, i.e. for $i = 1, 2$:

$$B^i_{mj} = -\frac{\mathrm{Ra}\widehat{\beta}}{\alpha_{mk}} \sum_{n,k=0}^{\infty} A^i_{mn} \mathcal{L}_{nk}(\widehat{\beta})[\mathcal{D}^m(\widehat{\beta})]^{-1}_{kj}. \tag{8.57}$$

Now, let us substitute (8.28) and (8.57) in $(8.27)_2$, obtaining:

$$\begin{aligned}
&\sum_{m,j=0}^{\infty} [\frac{\alpha_{mj}}{2\pi m}(\dot{A}^2_{mj} + \alpha_{mj} A^2_{mj}) \cos(2\pi m x) - \frac{\alpha_{mj}}{2\pi m}(\dot{A}^1_{mj} + \alpha_{mj} A^1_{mj}) \sin(2\pi m x)] \sin(j\pi z) \\
&\quad = \sum_{m,j=0}^{\infty} 2\pi m \Big\{ \mathrm{Ra}[-A^1_{mj} \sin(2\pi m x) + A^2_{mj} \cos(2\pi m x)] \sin(\pi j z) \\
&\qquad - \widehat{\beta} e^{-\widehat{\beta} z} \Big[\frac{\mathrm{Ra}\widehat{\beta}}{\alpha_{mj}} \sum_{n,k=0}^{\infty} A^1_{mn} \mathcal{L}_{nk}(\widehat{\beta})[\mathcal{D}^m(\widehat{\beta})]^{-1}_{kj} \sin(2\pi m x) \\
&\qquad\qquad - \frac{\mathrm{Ra}\widehat{\beta}}{\alpha_{mj}} \sum_{n,k=0}^{\infty} A^2_{mn} \mathcal{L}_{nk}(\widehat{\beta})[\mathcal{D}^m(\widehat{\beta})]^{-1}_{kj} \cos(2\pi m x) \Big] \cos(j\pi z) \Big\}
\end{aligned} \tag{8.58}$$

Let us multiply (8.58) by $\sin(h\pi z)$ and integrate with respect to $z \in (0, 1)$, therefore we get:

$$\begin{aligned}
&\sum_{m,j=0}^{\infty} \Big[\frac{\alpha_{mj}}{2\pi m}(\dot{A}^2_{mj} + \alpha_{mj} A^2_{mj}) \cos(2\pi m x) - \frac{\alpha_{mj}}{2\pi m}(\dot{A}^1_{mj} + \alpha_{mj} A^1_{mj}) \sin(2\pi m x) \Big] \int_0^1 \sin(j\pi z) \sin(h\pi z) dz \\
&= \sum_{m,j=0}^{\infty} 2\pi m \Big\{ \mathrm{Ra}[-A^1_{mj} \sin(2\pi m x) + A^2_{mj} \cos(2\pi m x)] \int_0^1 \sin(\pi j z) \sin(h\pi z) dz \\
&- \widehat{\beta} \Big[\frac{\mathrm{Ra}\widehat{\beta}}{\alpha_{mj}} \sum_{n,k=0}^{\infty} A^1_{mn} \mathcal{L}_{nk}(\widehat{\beta})[\mathcal{D}^m(\widehat{\beta})]^{-1}_{kj} \sin(2\pi m x) \\
&- \frac{\mathrm{Ra}\widehat{\beta}}{\alpha_{mj}} \sum_{n,k=0}^{\infty} A^2_{mn} \mathcal{L}_{nk}(\widehat{\beta})[\mathcal{D}^m(\widehat{\beta})]^{-1}_{kj} \cos(2\pi m x) \Big] \int_0^1 e^{-\widehat{\beta} z} \cos(j\pi z) \sin(h\pi z) dz \Big\}
\end{aligned} \tag{8.59}$$

Hence:

$$
\begin{aligned}
\sum_{m=0}^{\infty}\Big[\frac{\alpha_{mh}}{2\pi m}(\dot{A}^2_{mh}+\alpha_{mh}A^2_{mh})\cos(2\pi mx)-\frac{\alpha_{mh}}{2\pi m}(\dot{A}^1_{mh}+\alpha_{mh}A^1_{mh})\sin(2\pi mx)\Big]& \\
=\sum_{m=0}^{\infty}2\pi m\mathrm{Ra}[-A^1_{mh}\sin(2\pi mx)+A^2_{mh}\cos(2\pi mx)]& \\
-\sum_{m=0}^{\infty}\widehat{\beta}^2\mathrm{Ra}2\pi m\sum_{j,n,k=0}^{\infty}\frac{1}{\alpha_{mj}}A^1_{mn}\mathcal{L}_{nk}(\widehat{\beta})[\mathcal{D}^m(\widehat{\beta})]^{-1}_{kj}\mathcal{N}_{jh}(\widehat{\beta})\sin(2\pi mx)& \\
+\sum_{m=0}^{\infty}\widehat{\beta}^2\mathrm{Ra}2\pi m\sum_{j,n,k=0}^{\infty}\frac{1}{\alpha_{mj}}A^2_{mn}\mathcal{L}_{nk}(\widehat{\beta})[\mathcal{D}^m(\widehat{\beta})]^{-1}_{kj}\mathcal{N}_{jh}(\widehat{\beta})\cos(2\pi mx)&
\end{aligned}
\tag{8.60}
$$

with

$$
\mathcal{N}_{jh}(\widehat{\beta})=\pi(1-e^{-\widehat{\beta}}(-1)^{h+j})\left(\frac{h+j}{\pi^2(h+j)^2+\widehat{\beta}^2}+\frac{h-j}{\pi^2(h-j)^2+\widehat{\beta}^2}\right). \tag{8.61}
$$

By the linear independence of the sinus and cosinus functions with respect to the variable x, we get, for $i=1,2$:

$$
\begin{aligned}
\frac{\alpha_{mh}}{2\pi m}(\dot{A}^i_{mh}+\alpha_{mh}A^i_{mh}) =&2\pi m\mathrm{Ra}A^i_{mh}+ \\
&\widehat{\beta}^2\mathrm{Ra}2\pi m\sum_{j,n,k=0}^{\infty}\frac{1}{\alpha_{mj}}A^i_{mn}\mathcal{L}_{nk}(\widehat{\beta})[\mathcal{D}^m(\widehat{\beta})]^{-1}_{kj}\mathcal{N}_{jh}(\widehat{\beta}).
\end{aligned}
\tag{8.62}
$$

Equations (8.62) are first order ODEs with respect to time t. To get a unique solution, system (8.62) decouples and let A^i_{mh} be the only non-vanishing coefficient, which satisfies the following first-order ordinary differential equation:

$$
\begin{aligned}
\dot{A}^i_{mh}+\alpha_{mh}A^i_{mh} =&\frac{4\pi^2m^2}{\alpha_{mh}}\mathrm{Ra}\ A^i_{mh}+ \\
&\widehat{\beta}^2\mathrm{Ra}\frac{4\pi^2m^2}{\alpha_{mh}}A^i_{mh}\sum_{j,k=0}^{\infty}\frac{1}{\alpha_{mj}}\mathcal{L}_{hk}(\widehat{\beta})[\mathcal{D}^m(\widehat{\beta})]^{-1}_{kj}\mathcal{N}_{jh}(\widehat{\beta})
\end{aligned}
\tag{8.63}
$$

together with the initial conditions on A^i_{mh} that can be derived from $(8.15)_3$ and $(9.48)_1$. Setting

$$
\mathcal{G}_{mh}(\widehat{\beta})=\frac{4\pi^2m^2}{\alpha_{mh}}\sum_{j,k=0}^{\infty}\frac{1}{\alpha_{mj}}\mathcal{L}_{hk}(\widehat{\beta})[\mathcal{D}^m(\widehat{\beta})]^{-1}_{kj}\mathcal{N}_{jh}(\widehat{\beta}), \tag{8.64}
$$

(8.63) is equivalent to

$$\dot{A}^i_{mh} + A^i_{mh}\Big[\alpha_{mh} - \mathrm{Ra}\frac{4\pi^2 m^2}{\alpha_{mh}} - \widehat{\beta}^2 \mathrm{Ra}\ \mathcal{G}_{mh}(\widehat{\beta})\Big] = 0, \tag{8.65}$$

whose solution can be easily computed to be:

$$A^i_{mh}(t) = \gamma e^{\Big(-\alpha_{mh} + \mathrm{Ra}\frac{4\pi^2 m^2}{\alpha_{mh}} + \widehat{\beta}^2 \mathrm{Ra}\ \mathcal{G}_{mh}(\widehat{\beta})\Big)t}, \tag{8.66}$$

γ being a constant depending on the initial conditions. We obtain that the perturbation fields (9.48) have an exponential dependence on time t, so let us define the generalized eigenvalue σ_{mh}:

$$\sigma_{mh} = -\alpha_{mh} + \mathrm{Ra}\frac{4\pi^2 m^2}{\alpha_{mh}} + \widehat{\beta}^2 \mathrm{Ra}\ \mathcal{G}_{mh}(\widehat{\beta}). \tag{8.67}$$

8.3 Results and discussion

Remark 8.3.1. *Let us first underline that the eigenvalues* (8.67) *are real* $\forall\ m, h$. *Therefore, the strong principle of exchange of stabilities holds and convection can arise only via stationary motions.*

Remark 8.3.2. *In the limit case* $\widehat{\beta} \to 0$ *(i.e. according to the classical Oberbeck-Boussinesq approximation),* (8.67) *becomes*

$$\sigma_{mh} = -\alpha_{mh} + \mathrm{Ra}\frac{4\pi^2 m^2}{\alpha_{mh}}, \tag{8.68}$$

so, requiring the eigenvalue σ_{mh} *to be positive, we get*

$$-\alpha_{mh} + \mathrm{Ra}\frac{4\pi^2 m^2}{\alpha_{mh}} > 0. \tag{8.69}$$

Therefore, convection arises if the Rayleigh-Darcy number is greater than the critical value

$$\mathrm{Ra}_c = \min_{m,h} \frac{[(2\pi m)^2 + (h\pi)^2]^2}{4\pi^2 m^2}. \tag{8.70}$$

The minimum (8.70) *is obtained for* $h = 1$ *and* $m^* = \frac{1}{2}$, *so the classical result is recovered, i.e. the critical wavenumber is* $(2\pi m^*)^2 = \pi^2$, *while the critical Rayleigh-Darcy number is:*

$$\mathrm{Ra}_c = 4\pi^2. \tag{8.71}$$

According to (8.67), the marginal instability threshold is given setting $\sigma_{mn} = 0$, i.e.

$$\mathrm{Ra}\Big(\frac{4\pi^2 m^2}{\alpha_{mh}} + \widehat{\beta}^2 \mathcal{G}_{mh}(\widehat{\beta})\Big) - \alpha_{mh} = 0, \tag{8.72}$$

so, when the horizontal layer of porous medium is saturated by an extended-quasi-thermal-incompressible fluid, the critical Rayleigh-Darcy number for the onset of convection is given by:

$$\mathrm{Ra}_L = \inf_{m,h} \frac{\alpha_{mh}^2}{4\pi^2 m^2 + \widehat{\beta}^2 \alpha_{mh} \mathcal{G}_{mh}(\widehat{\beta})}. \tag{8.73}$$

In order to analyse the influence of the dimensionless compressibility factor $\widehat{\beta}$ on the onset of convection, we numerically solved (8.73) for quoted values of $\widehat{\beta}$, under the restriction (8.34) found in Theorem 8.2.1.
We found that the function $\mathcal{G}_{mh}$ is always positive and the dimensionless compressibility factor $\widehat{\beta}$ has a *destabilizing* effect on the onset of convective flows: the behaviour of the critical Rayleigh-Darcy number with respect to $\hat{\beta}$ is decreasing (see Figures 8.1 – 8.2) and

$$\mathrm{Ra}_L < \mathrm{Ra}_c \qquad \forall\ \widehat{\beta} > 0. \tag{8.74}$$

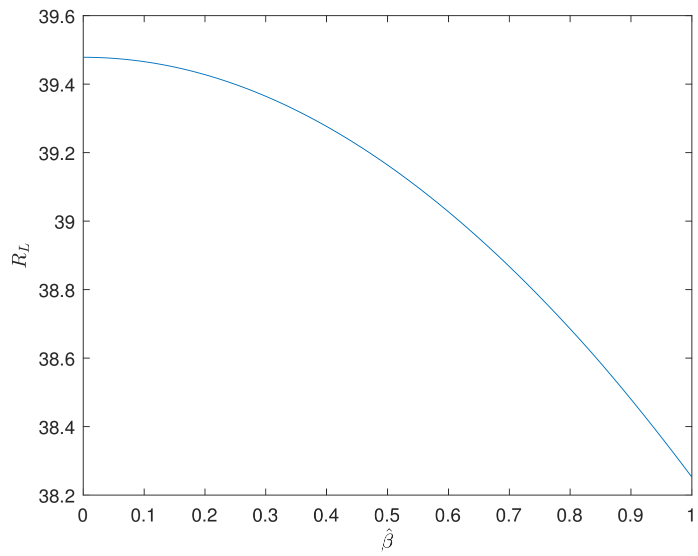

Figure 8.1: Critical Rayleigh-Darcy number Ra_L as function of the compressibility factor $\hat{\beta}$.

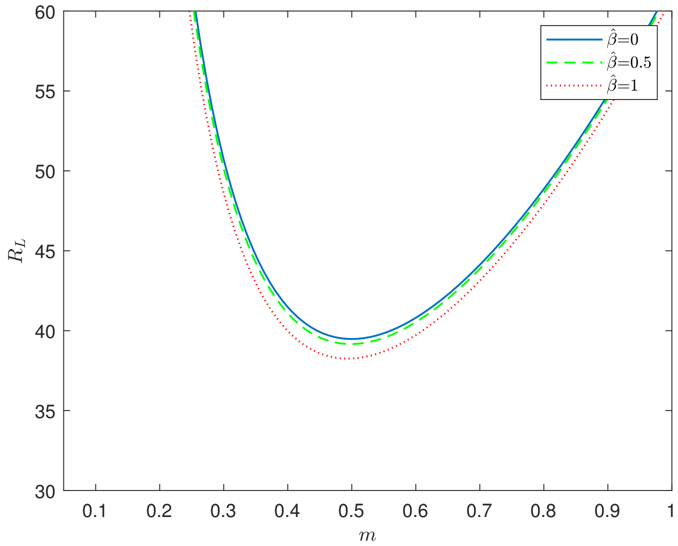

Figure 8.2: Neutral curves for quoted values of the compressibility factor $\hat{\beta}$.

Concluding remarks

To the best of our knowledge, in this Chapter the Darcy-Bénard problem for an extended-quasi-thermal-incompressible fluid has been studied for the first time. We determined the instability threshold for the onset of convection via linear instability analysis of the conduction solution: through a closed algebraic form, we showed that the critical Rayleigh-Darcy number depends on the dimensionless compressibility factor $\widehat{\beta}$ and we rigorously proved that $\widehat{\beta}$ has a destabilizing effect. Moreover, in the limit case $\widehat{\beta} \to 0$ (i.e. according to the classical Oberbeck-Boussinesq approximation), the critical threshold for the Darcy-Bénard problem $4\pi^2$ is recovered.

Chapter 9

A weakly nonlinear analysis of vertical throughflow on Darcy-Bénard convection

In Chapter 2, convection problems in clear fluids and porous media saturated by incompressible fluids have been described. These problems attracted the attention of many researchers, in the past as nowadays, due to the many applications in geophysics and engineering fields [1, 10]. However, there is a lack of comprehensive analyses describing the onset of convection in a horizontal layer of porous media heated from below when a downward net mass flow is considered across the layer.

In many applications — such as geothermal energy extraction, oil recovery process in petroleum industry, insulation of reactor vessels, in situ coal gasification and packed bed reactors — control of convective instability plays an important role [73], and one way to control the onset of convective motions in the layer is considering a *throughflow* [74].

In general, the effect of throughflow is rather complex. In [1] the authors described a throughflow as a net mass flow and explained that, when the strength of the throughflow is large, the effect is to confine significant thermal gradients to a thermal boundary layer at the boundary toward which the throughflow is directed. Not only the temperature profile is altered, but also the perturbation equations, where contributions arise from the interaction between temperature and velocity [74]. In this Chapter, we are going to study the onset of instability in a horizontal fluid-saturated porous layer heated from below subject to the action of a suction. Planes delimiting the layer are permeable and *injection* of fluid on the top and *removal* at the bottom take place. Thus, the basic velocity will have a constant downward vertical profile. We are going to refer to this problem as Sutton Problem, since she was the first researcher to analyse the problem of Darcy-Bénard convection under the action of net throughflow. In particular, in [75] Sutton studied the onset of convection in a porous channel in order to determine how the critical Rayleigh number is affected by the strength of the thourghflow for different values of the aspect ratio. The Sutton problem, in its dimensionless form, is affected by the Péclet number, which is directly proportional to the strength of the throughflow. As the Péclet number goes to zero, the problem reduces to the Darcy-Bénard problem. On the other hand, for very large Péclet number, the problem reduces to the Wooding problem [76] (named as such in [77]). The latter shares some features with the Darcy-Bénard problem with the main difference of a background vertical fluid motion. Such a motion causes a thermal boundary layer to form naturally. A huge amount of heat is confined in that boundary layer close to the bottom of the horizontal porous layer. Consequently, the fluid convective motion will take place far from the upper plane delimiting the layer and boundary conditions on this plane will not affect the motion. Hence, with a good approximation, the layer appears to be of infinite height.

In the Darcy-Bénard problem the onset of instability is well-known to be supercritical, while in the Wooding problem it turns out to be subcritical. It seems reasonable to imagine a transition from one problem to another for increasing Péclet number. Hence, what motivated the derivation of the results presented in the present Chapter is the wish of understanding how the transition happens and determining the Péclet number beyond which the onset of instability is no longer supercritical. To study the transition, a weakly nonlinear stability analysis of the basic steady solution is performed. According to this analysis we investigate the behaviour of the basic solution close to onset of convection. A weakly nonlinear analysis for the Darcy-Bénard problem was easily performed analytically, but when dealing with more complicated systems, the analysis of the dynamic of the system is performed employing numerical methods [78, 79].

The present Chapter is based on a joint future publication with F. Capone, J.A. Gianfrani and D.S.A. Rees and is organised as follows. In Section 9.1 the mathematical model is described and the dimensionless form of the system is determined along with the basic stationary solution, determined and discussed in Section 9.2. In Section 9.3 the principle of exchange of stabilities is proved and the instability of the basic flow is analysed by the linear instability analysis. We provide and discuss the tenth order system of ODEs to determine the critical Rayleigh number for the onset of instability. In Section 9.4 the weakly nonlinear analysis is performed in order to determine the Landau equation, which is then numerically solved. In the last Section of the Chapter, the obtained results are collected and the future perspective

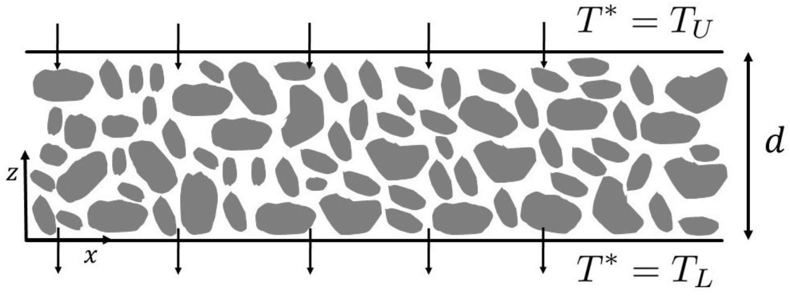

Figure 9.1: Depicting a horizontal porous layer

are presented.

9.1 The Sutton Problem

Let us consider a fluid-saturated horizontal planar porous layer $L = \mathbb{R} \times [0, d]$ uniformly heated from below and let Ox^*z^* be the reference frame. Let T_L be the fixed temperature at $z^* = 0$ and let T_U be the fixed temperature at $z^* = d$, where $T_L > T_U$. The temperature T_U is also regarded as being the reference temperature. The two bounding surfaces are permeable and admit a constant downward vertical throughflow of magnitude Q across the layer. Let $\mathbf{v}^*, T^*, p^*$ be the velocity, temperature and pressure fields, respectively. The governing system is derived by employing the Boussinesq approximation - the fluid density ϱ is constant in all terms of the governing equations, except for in the buoyancy term - and we shall assume that ϱ is linearly dependent on temperature T^*:

$$\varrho(T^*) = \varrho_0[1 - \alpha(T^* - T_U)], \tag{9.1}$$

where α is the thermal expansion coefficient and ϱ_0 is the fluid density at the reference temperature T_U. Therefore, the governing equations, according to the Darcy's model, are well known to be, cf. [1],

$$\begin{cases} \dfrac{\mu}{K}\mathbf{v}^* = -\nabla^* p^* + \varrho_0 \alpha g T^* \mathbf{k}, \\ \nabla^* \cdot \mathbf{v}^* = 0, \\ (\varrho c)_m T^*_{,t^*} + (\varrho c)_f \mathbf{v}^* \cdot \nabla^* T^* = k \nabla^{*2} T^*, \end{cases} \tag{9.2}$$

where k is the overall thermal conductivity, K the permeability, μ the viscosity of the fluid, $\mathbf{g} = -g\mathbf{k}$ the gravitational acceleration, and c the specific heat. The subscripts m and f refer to the porous medium and the fluid, respectively. The system (9.2) is completed by the following boundary conditions:

$$\begin{aligned} \mathbf{v}^* &= -Q\mathbf{k} \quad \text{on} \quad z^* = 0, d, \\ T^* &= T_L \quad \text{on} \quad z^* = 0, \\ T^* &= T_U \quad \text{on} \quad z^* = d. \end{aligned} \tag{9.3}$$

In order to write the non-dimensional versions of (9.2) and (9.3), we introduce the following non-dimensional parameters:

$$\mathbf{x}^* = d\mathbf{x},\ \mathbf{v}^* = U\mathbf{u},\ p^* + \varrho_0 \alpha g T_U z^* = Pp,\ T^* = \theta(T_L - T_U) + T_U,\ t^* = \hat{\tau} t, \tag{9.4}$$

where typical velocity, pressure and time scales are given by,

$$U = \frac{k}{d(\varrho c)_f}, \quad P = \frac{k\mu}{K(\varrho c)_f}, \quad \hat{\tau} = \frac{(\varrho c)_m d^2}{k}. \tag{9.5}$$

In the above, the values $\mathbf{u} = (u, w)$, θ and p are the dimensionless velocity, temperature and pressure fields, respectively.
The governing non-dimensional system is,

$$\begin{cases} \mathbf{u} = -\nabla p + \mathrm{Ra}\theta\, \mathbf{k}, \\ \nabla \cdot \mathbf{u} = 0, \\ \theta_{,t} + \mathbf{u} \cdot \nabla \theta = \nabla^2 \theta, \end{cases} \tag{9.6}$$

with the boundary conditions

$$\begin{aligned} w &= -\mathrm{Pe} \quad \text{on} \quad z = 0, 1, \\ \theta &= 1 \quad \text{on} \quad z = 0, \\ \theta &= 0 \quad \text{on} \quad z = 1, \end{aligned} \tag{9.7}$$

where

$$\mathrm{Ra} = \frac{d\varrho_0 \alpha g (T_L - T_U) K (\varrho c)_F}{\mu k} \tag{9.8}$$

is the Darcy-Rayleigh number (hereinafter called the Rayleigh number), and

$$\mathrm{Pe} = \frac{Q(\varrho c)_F d}{k} \tag{9.9}$$

is the Péclet number.

9.2 The basic state

The basic dimensionless solution of (9.6)-(9.7) is

$$\mathbf{u}_b = -\mathrm{Pe}\,\mathbf{k}, \qquad \theta_b = g(z), \qquad p_b = \overline{p}(z). \tag{9.10}$$

where

$$g(z)=\frac{e^{-\mathrm{Pe}z}-e^{-\mathrm{Pe}}}{1-e^{-\mathrm{Pe}}} \text{ and } \overline{p}(z)=-\frac{\mathrm{Ra}}{1-e^{-\mathrm{Pe}}}\left(\frac{e^{-\mathrm{Pe}z}}{\mathrm{Pe}}+e^{-\mathrm{Pe}}z-\frac{1}{\mathrm{Pe}}\right)+p_b(0) \tag{9.11}$$

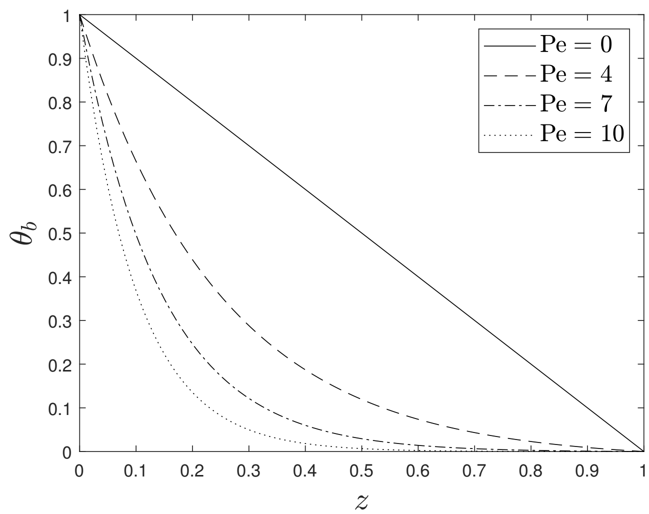

Figure 9.2: Basic temperature profiles for the quoted values of the Péclet number, Pe.

We may begin our discussion of the basic state with the following remarks.

Remark 9.2.1. *When the limit as* Pe $\to 0$ *is taken of the basic temperature profile,* θ_b*, the well-known Darcy linear profile is recovered:*

$$\lim_{\mathrm{Pe}\to 0} \theta_b(z) = 1 - z. \tag{9.12}$$

Remark 9.2.2. *When the large-*Pe *limit is taken then*

$$\theta_b(z) \sim e^{-\mathrm{Pe}\,z}. \tag{9.13}$$

This means that the temperature field is confined to region of thickness of $O(\mathrm{Pe}^{-1})$ *at the lower surface.*

Both of these extreme cases may be demonstrated easily from Eqs. (9.11), and are confirmed in Figure 9.2, which also shows the detailed manner in which the basic temperature profile varies with the magnitude the Péclet number, Pe.

As Pe increases from zero the upward conduction of heat from the lower surface is counteracted increasingly by the externally-imposed downward advection. Therefore, for very large values of Pe, the layer appears to mimic a region of infinite height because most of the layer is uniformly cold apart from the narrow thermal boundary layer near $z = 0$. Therefore, for $\mathrm{Pe} \gg 1$, we have an *a priori* expectation that instabilities will be confined to this boundary layer which is where the basic temperature gradient is destabilising. In the large-Pe limit, then, the problem essentially becomes independent of the depth of the layer and $1/\mathrm{Pe}$ should be used as an alternative characteristic nondimensional length. With such an approximation we recover the Wooding problem [76]. Hence, if we wished to compare our large-Pe results with those of Wooding, we should rescale the Rayleigh number to the appropriate one for the Wooding problem, namely,

$$\mathrm{Ra}_w = \mathrm{Ra}\mathrm{Pe}^{-1}. \tag{9.14}$$

9.3 Linear instability analysis

We shall now consider the onset of convection. Squire's theorem may be shown easily to hold, and therefore we may confine ourselves to the analysis of two-dimensional perturbations. Let us introduce the stream function ψ such that $u = -\psi_{,z}$ and $w = \psi_{,x}$. Hence, system (9.6) becomes:

$$\begin{cases} \nabla^2\psi = \mathrm{Ra}\,\theta_{,x}, \\ \theta_{,t} + \psi_{,x}\theta_{,z} - \psi_{,z}\theta_{,x} = \nabla^2\theta, \end{cases} \tag{9.15}$$

and the basic solution now takes the form,

$$\psi_b = -\mathrm{Pe}\,x, \qquad \theta_b = g(z). \tag{9.16}$$

By introducing a perturbation $\hat{\psi}, \hat{\theta}$ to (9.16), the non-dimensional system arising from (9.15) is

$$\begin{cases} \nabla^2\psi = \mathrm{Ra}\,\theta_{,x}, \\ \theta_{,t} - \mathrm{Pe}\,\theta_{,z} + g'(z)\psi_{,x} + \psi_{,x}\theta_{,z} - \psi_{,z}\theta_{,x} = \nabla^2\theta, \end{cases} \tag{9.17}$$

where the circumflexes have been dropped for notational convenience and where primes denote ordinary derivatives with respect to z. System (9.17) will be solved subject to the following boundary conditions:

$$\psi = \theta = 0, \quad \text{on } z = 0, 1. \tag{9.18}$$

Let us underline that the perturbation fields are Sobolev functions in $W^{2,2}(V)$ $\forall t \in \mathbb{R}^+$, V being the periodicity cell, and they are periodic in the horizontal direction with period $2\pi/k$.

The determination of the critical threshold for the Rayleigh number begins with a linear stability analysis. The linear system associated with (9.17) is

$$\begin{cases} \nabla^2\psi = \mathrm{Ra}\theta_{,x}, \\ \theta_{,t} - \mathrm{Pe}\,\theta_{,z} + g'(z)\psi_{,x} = \nabla^2\theta. \end{cases} \tag{9.19}$$

Since this system and its boundary conditions are homogeneous with coefficients that are independent of time, it is possible to look for solutions where the spatial dependence may be separated from an exponential time-dependence. Let

$$\varphi(\mathbf{x}, t) = \overline{\varphi}(\mathbf{x})e^{\sigma t} \quad \forall\varphi \in \{\psi, \theta\} \tag{9.20}$$

where σ is the exponential growth rate, so system (9.19) becomes:

$$\begin{cases} \nabla^2\psi = \mathrm{Ra}\theta_{,x}, \\ \sigma\theta - \mathrm{Pe}\,\theta_{,z} + g'(z)\psi_{,x} = \nabla^2\theta. \end{cases} \tag{9.21}$$

Theorem 9.3.1. *The strong form of the principle of exchange of stabilties holds for system* (9.21)-(9.18)*, hence convection can occur only via steady motions.*

Proof. Since the perturbation fields are periodic in the horizontal direction x, (9.21)-(9.18) admits solution of the form:

$$\psi = -i\,\overline{\psi}\,e^{ikx} + c.c., \qquad \theta = \overline{\theta}\,e^{ikx} + c.c., \tag{9.22}$$

where k is the wavenumber and $\overline{\psi}$, $\overline{\theta}$ are complex functions. Hence, system (9.21) becomes (dropping the bars)

$$\begin{cases} (D^2 - k^2)\psi = -\mathrm{Ra}\;k\theta, \\ \sigma\theta = \mathrm{Pe}\;D\theta - g'(z)k\psi + (D^2 - k^2)\theta, \end{cases} \tag{9.23}$$

Equation $(9.23)_1$ is equivalent to

$$\mathrm{Ra}\theta = \frac{D^2 - k^2}{-k}\psi := B^{-1}(\psi) \tag{9.24}$$

i.e.

$$\psi = \mathrm{Ra}B(\theta) \tag{9.25}$$

Using the above, system (9.23) becomes

$$\begin{cases} \psi = \mathrm{Ra}B(\theta), \\ \sigma\theta = \mathrm{Pe}\ D\theta - g'(z)k\mathrm{Ra}B(\theta) + (D^2 - k^2)\theta, \end{cases} \tag{9.26}$$

under the following boundary conditions:

$$\theta(0) = \theta(1) = \psi(0) = \psi(1) = 0. \tag{9.27}$$

The linear operator associated to (9.26) is

$$\mathcal{L} = D^2 - k^2 + \mathrm{Pe}D - g'k\mathrm{Ra}B(\cdot) \tag{9.28}$$

that is not symmetric with respect to the scalar product in $L^2(0,1)$. Therefore, by virtue of a similarity transformation which symmetrizes the operator $\mathcal{L}$, we will show that the principle of exchange of stabilities holds. Let us employ the following transformation

$$\theta = M(z)\varphi := e^{-\frac{\mathrm{Pe}}{2}z}\varphi \tag{9.29}$$

hence,

$$\mathcal{L}\theta = e^{-\frac{\mathrm{Pe}}{2}z}\Big[D^2\varphi - \Big(\frac{\mathrm{Pe}^2}{2} + k^2\Big)\varphi - e^{\frac{\mathrm{Pe}}{2}z}g'k\mathrm{Ra}B(e^{-\frac{\mathrm{Pe}}{2}z}\varphi)\Big] := M\hat{\mathcal{L}}M^{-1}\theta, \tag{9.30}$$

where the operator $\hat{\mathcal{L}}$ is defined as

$$\hat{\mathcal{L}} = D^2 - k^2 - \frac{\mathrm{Pe}^2}{2} - e^{\frac{\mathrm{Pe}}{2}z}g'k\mathrm{Ra}B(\cdot) \tag{9.31}$$

Via the transformation (9.29), we can now focus our attention on the following problem

$$\begin{cases} \psi = \mathrm{Ra}B(e^{-\frac{\mathrm{Pe}}{2}z}\varphi), \\ \sigma\varphi = \hat{\mathcal{L}}\varphi, \end{cases} \tag{9.32}$$

with associated boundary conditions

$$\varphi(0) = \varphi(1) = \psi(0) = \psi(1) = 0. \tag{9.33}$$

The operator $\hat{\mathcal{L}}$ is symmetric - hence its eingenvalues are all real - and the spectrum of $\hat{\mathcal{L}}$ is contained in the spectrum of $\mathcal{L}$ [80]. Moreover, part of the spectrum of $\mathcal{L}$ for which the eigenfunctions are in

$$\{\theta \in L^2(0,1) \mid e^{\frac{\mathrm{Pe}}{2}z}\theta \in L^2(0,1)\}$$

coincides with the spectrum of $\hat{\mathcal{L}}$ with respect to $L^2(0,1)$. Let us consider $\varphi = e^{\frac{\mathrm{Pe}}{2}z}\theta$, with $\theta \in L^2(0,1)$ therefore

$$\|\varphi\|^2_{L^2(0,1)} \leq \|e^{\mathrm{Pe}z}\|_{L^\infty(0,1)}\|\theta\|^2_{L^2(0,1)} < +\infty \tag{9.34}$$

so

$$\varphi \in L^2(0,1),\ \forall\, \theta \in L^2(0,1),$$

this means the spectra of $\mathcal{L}$ and $\hat{\mathcal{L}}$ coincide and the principle of exchange of stabilities holds, i.e. convection can arise only via stationary motions. □

By virtue of theorem 9.3.1, let us assume $\sigma = 0$ at the criticality. Therefore, system (9.21) becomes

$$\begin{cases} \nabla^2\psi - \mathrm{Ra}\theta_{,x} = 0, \\ \nabla^2\theta + \mathrm{Pe}\,\theta_{,z} - g'(z)\psi_{,x} = 0, \end{cases} \tag{9.35}$$

Consequence of theorem 9.3.1 is that $\overline{\psi}$ and $\overline{\theta}$ in (9.22) are real functions. Hence, solutions in (9.22) reduce to

$$\psi = A\ F(z)\sin kx, \qquad \theta = A\ G(z)\cos kx, \tag{9.36}$$

where A is an arbitrary amplitude. Hence, from (9.35) we obtain a boundary value problem consisting of two second order ODEs in z:

$$\begin{cases} F'' - k^2F + \mathrm{Ra}\,kG = 0, \\ G'' - k^2G + \mathrm{Pe}\,G' - kg'F = 0, \end{cases} \tag{9.37}$$

with the boundary conditions:

$$F(0) = 0,\ F(1) = 0,\ G(0) = 0,\ G(1) = 0. \tag{9.38}$$

Nonzero solutions of this ordinary differential eigenvalue problem for Ra were guaranteed by the use of the fifth boundary condition,

$$G'(0) = \text{nonzero constant}, \tag{9.39}$$

which is one of various ways of normalising the eigensolution. This extra condition requires one further ordinary differential equation and, given that Ra is a constant, we may supplement equations (9.37) with

$$\mathrm{Ra}' = 0. \tag{9.40}$$

The fifth order system, (9.37)-(9.40), was solved using the shooting method as described in [81, 82, 83]. To summarise: the system was first reduced to first order form consisting of five ODEs. However, only three initial conditions are given and therefore the values of the two remaining ones ($F'(0)$ and Ra) were found by using a Newton-Raphson iteration scheme which ensures that both the known boundary conditions at $z = 1$ ($F(1) = 0$ and $G(1) = 0$) are satisfied. The classical fourth order Runge-Kutta method was used as the basic solver, and it was found that solutions were generally correct to between five and six decimal places.

The system (9.37)-(9.40) was found to provide a unimodal neutral curve, $\mathrm{Ra}(k)$, with a unique minimum for all values of the Péclet number. The critical Rayleigh number, Ra_c, is defined as being that value which corresponds to the minimum of the neutral curve while the critical wavenumber, k_c, is the corresponding wavenumber where,

$$\mathrm{Ra}_c = \min_{k\in\mathbb{R}^+} \mathrm{Ra}(k) = \mathrm{Ra}(k_c). \tag{9.41}$$

Accurate numerical values of Ra_c and k_c need the system (9.37) to be replaced by a suitable extended system that will fulfil Eq. (9.41). Therefore we solved the following system:

$$\begin{cases} F'' - k^2F + \mathrm{Ra}\,kG = 0, \\ G'' - k^2G + \mathrm{Pe}\,G' - kg'F = 0 \\ \mathrm{Ra}' = 0, \\ F_1'' - k^2F_1 - 2kF + \mathrm{Ra}(G + kG_1) = 0, \\ G_1'' - k^2G_1 - 2kG + \mathrm{Pe}\,G_1' - g'(F + kF_1) = 0, \\ k' = 0, \end{cases} \tag{9.42}$$

where $F_1 = F_{,k},\ G_1 = G_{,k}$. The full set of boundary conditions is,

$$F = G = F_1 = G_1 = 0 \quad \text{for } z = 0, 1 \quad \text{and} \quad G'(0) = 1/\pi,\ G_1'(0) = 0, \tag{9.43}$$

where the specific value used here for $G'(0)$ will be discussed in the following section, while $G_1'(0)$ may take any value.

Figure 9.3 shows the neutral curves for values of the Péclet number varying between $\mathrm{Pe} = 0$ and $\mathrm{Pe} = 10$ with unit increments. These were obtained

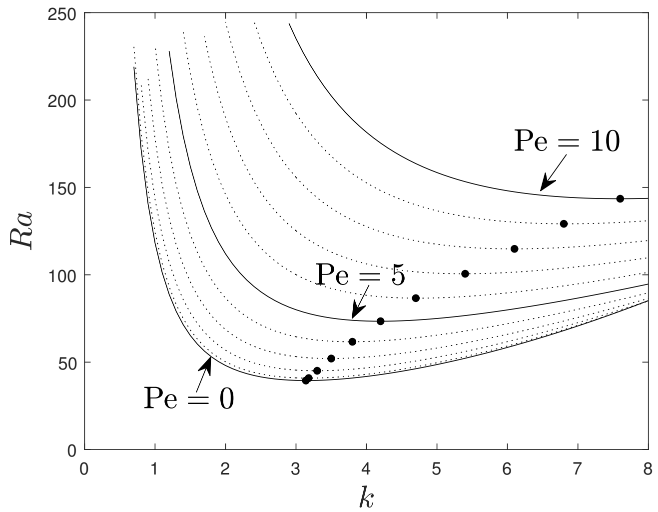

Figure 9.3: Neutral curves Ra(k) for increasing values of Pe. The circles show the location of the minimum, $\mathrm{Ra_c}$ of each curve.

by solving the system (9.37)-(9.40). Also shown as small disks are the critical points (k_c, Ra_c), which were obtained by solving the system (9.42)-(9.43).

When Pe increases from zero, it is immediately apparent that Ra_c increases and thus the system is stabilised increasingly. The corresponding critical wavenumber also increases which means that the wavelength of the convecting pattern decreases. As has already been mentioned, the basic temperature field becomes increasingly confined to the lower part of the layer as Pe increases, and therefore disturbances will be increasingly concentrated there. This is confirmed in Figure 9.4 where we see that locations of the extreme values of both the streamfunction and the isotherms descend as Pe increases. At the moderate value, Pe = 3, the cells still occupy the full cavity but have clearly lost the up/down symmetry that is present when Pe = 0. But when Pe = 10 both the flow and temperature fields are essentially detached from the upper surface, and this becomes increasingly so as Pe increases still further. The width of the convecting cells has now become proportional to the height of the thinning basic thermal boundary layer as we approach the large-Pe asymptotic regime that is the Wooding problem.

Figures 9.5(a) and 9.5(b) show how the critical values of Ra_c and k_c vary as Pe increases. The respective values for the Darcy-Bénard problem are recovered when Pe = 0, while the red dashes show the approach to the Wooding problem as Pe increases for which

$$(k_w, \mathrm{Ra}_w) = (0.7589, 14.3522) \;\Rightarrow\; (k_c, \mathrm{Ra}_c) \sim (0.7589, 14.3522)\mathrm{Pe}, \quad (9.44)$$

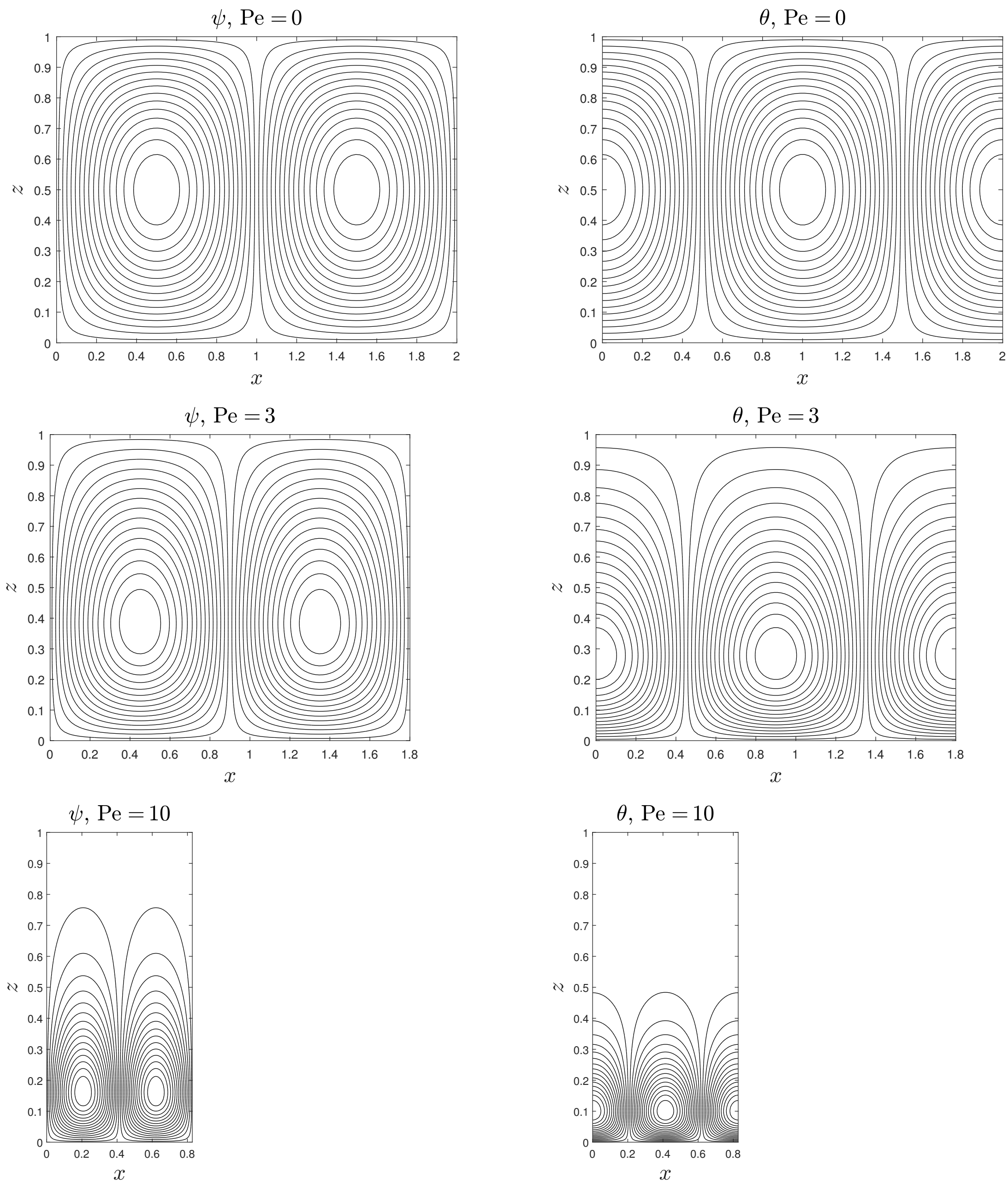

Figure 9.4: Streamlines and isothermal for the quoted values of the Péclet number.

where the numerical data was taken from [84] and confirmed by the present authors.

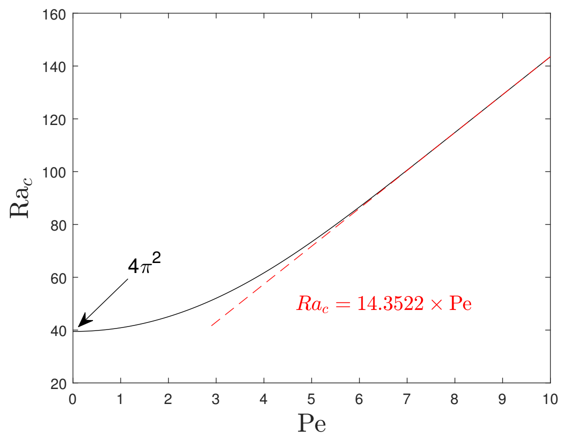

(a)

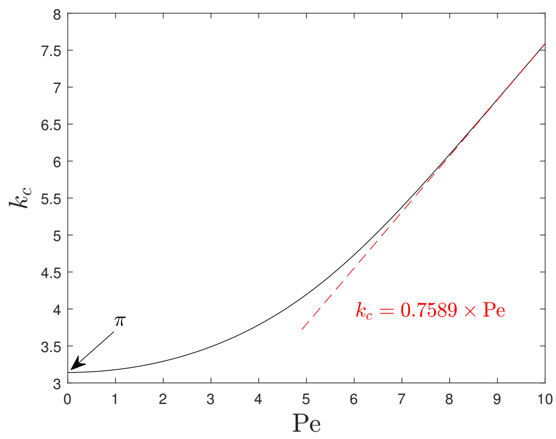

(b)

Figure 9.5: The variation of (a) Ra_c and (b) k_c with the Péclet number. In both cases the dashed red line corresponds to the Wooding problem.

9.4 Weakly nonlinear analysis

It is well-known that the onset of convection for the Darcy-Bénard problem ($\mathrm{Pe} = 0$) is supercritical for all wavenumbers ([85]) and so the primary aim here is to determine whether or not this remains true in the presence of a vertical throughflow. Therefore we shall undertake a weakly nonlinear analysis of the basic steady solution (9.16) close to the onset of convection. Such an analysis allows us to determine the so-called Landau equation which relates the amplitude of the most unstable mode to the deviation of the Rayleigh number from its critical value. The coefficients of the Landau equation will determine whether or not the onset of convection is supercritical or subcritical. Let us introduce a small parameter $\epsilon \ll 1$ and perturb the critical Rayleigh number by an $O(\epsilon^2)$ amount [86], i.e. let

$$\mathrm{Ra} = \mathrm{Ra}_0 + \epsilon^2 \mathrm{Ra}_2 + \ldots \tag{9.45}$$

where Ra_0 is a neutral value of the Rayleigh number arising from the linear analysis. Given the proximity of the Rayleigh number to its critical value we will need to define τ to be a suitably slow time scale, as follows,

$$\tau = \tfrac{1}{2}\epsilon^2 t, \tag{9.46}$$

where the numerical factor was chosen so that the resulting Landau equation will have solely unit coefficients when $\mathrm{Pe} = 0$ and $k = \pi$. Hence system (9.17) becomes,

$$\begin{cases} \nabla^2\psi = (\mathrm{Ra}_0 + \epsilon^2\mathrm{Ra}_2)\theta_{,x}, \\ \nabla^2\theta = \tfrac{1}{2}\epsilon^2\theta_{,\tau} - \mathrm{Pe}\,\theta_{,z} + g'(z)\psi_{,x} + \psi_{,x}\theta_{,z} - \psi_{,z}\theta_{,x}. \end{cases} \tag{9.47}$$

The weakly nonlinear analysis proceeds by expanding the solution of (9.47) as a power series in ϵ [81]:

$$\begin{pmatrix}\psi \\ \theta\end{pmatrix} = \sum_{n=1}^{\infty} \epsilon^n \begin{pmatrix}\psi_n \\ \theta_n\end{pmatrix}. \tag{9.48}$$

The following analysis focuses on the first three orders of approximation arising from the substitution of (9.48) into (9.47).

9.4.1 First order

At the first order of approximation, $O(\epsilon)$, the resulting equations coincide with the linear system (9.35), i.e.

$$\begin{cases} \nabla^2\psi_1 = \mathrm{Ra}_0\theta_{1,x}, \\ \nabla^2\theta_1 = -\mathrm{Pe}\,\theta_{1,z} + g'(z)\psi_{1,x}, \end{cases} \tag{9.49}$$

for which we may choose the following solution

$$\begin{cases} \psi_1 = A(\tau) f_1(z)\sin kx, \\ \theta_1 = A(\tau) g_1(z)\cos kx, \end{cases} \tag{9.50}$$

where $A(\tau)$ is the amplitude of the perturbation which evolves slowly in time. Hence, upon substituting (9.50) in (9.49), we obtain (9.37) which can be solved as already described in Section 9.3.

9.4.2 Second order

At the second order of approximation, $O(\epsilon^2)$, the first self-interaction of the perturbation occurs. System (9.47) reduces to

$$\begin{cases} \nabla^2\psi_2 - \mathrm{Ra}_0\theta_{2,x} = 0, \\ \nabla^2\theta_2 = -\mathrm{Pe}\,\theta_{2,z} + g'(z)\psi_{2,x} + \psi_{1,x}\theta_{1,z} - \psi_{1,z}\theta_{1,x}. \end{cases} \tag{9.51}$$

Since

$$\begin{aligned} \psi_{1,x}\theta_{1,z} - \psi_{1,z}\theta_{1,x} =& A^2k(f_1g_1'\cos^2 kx + f_1'g_1\sin^2 kx) \\ =& \tfrac{1}{2}A^2k\Big[f_1g_1' + f_1'g_1 + (f_1g_1' - f_1'g_1)\cos 2kx\Big] \end{aligned} \tag{9.52}$$

we choose the following form as the solutions for (9.51),

$$\begin{cases} \psi_2 = A^2(\tau)f_2(z)\sin 2kx, \\ \theta_2 = A^2(\tau)g_0(z) + A^2(\tau)g_2(z)\cos 2kx. \end{cases} \tag{9.53}$$

Hence, the resulting system of ODEs is

$$\begin{cases} f_2'' - 4k^2f_2 + \mathrm{Ra}_0 2kg_2 = 0, \\ g_2'' - 4k^2g_2 + \mathrm{Pe}g_2' - 2kg'f_2 = \frac{1}{2}k(f_1g_1' - f_1'g_1), \\ g_0'' + \mathrm{Pe}\,g_0' = \frac{1}{2}k(f_1g_1' + f_1'g_1), \end{cases} \tag{9.54}$$

where each of f_2, g_2 and g_0 are zero at $z = 0, 1$. Generally these equations may be solved easily because the inhomogeneous terms are nonresonant.

9.4.3 Third order

A further self-interaction appears in the $O(\epsilon^3)$ system, which is

$$\begin{cases} \nabla^2\psi_3 = \mathrm{Ra}_0\theta_{3,x} + \mathrm{Ra}_2\theta_{1,x}, \\ \nabla^2\theta_3 = \frac{1}{2}\theta_{1,\tau} - \mathrm{Pe}\,\theta_{3,z} + g'(z)\psi_{3,x} \\ \qquad\qquad +\psi_{1,x}\theta_{2,z} + \psi_{2,x}\theta_{1,z} - \psi_{1,z}\theta_{2,x} - \psi_{2,z}\theta_{1,x}. \end{cases} \tag{9.55}$$

By employing solutions (9.50) and (9.53) and defining the partial differential operators $\mathcal{L}_1$ and $\mathcal{L}_2$ to be such that

$$\begin{aligned} \mathcal{L}_1(\psi_3, \theta_3) &= \nabla^2\psi_3 - \mathrm{Ra}_0\theta_{3,x}, \\ \mathcal{L}_2(\psi_3, \theta_3) &= \nabla^2\theta_3 + \mathrm{Pe}\theta_{3,z} - g'(z)\psi_{3,x}, \end{aligned} \tag{9.56}$$

the resulting system is

$$\begin{cases} \mathcal{L}_1(\psi_3,\theta_3) = & -\,\mathrm{Ra}_2 A k g_1 \sin kx, \\ \mathcal{L}_2(\psi_3,\theta_3) = & \frac{1}{2}A_\tau g_1 \cos kx \\ & \quad + A^3\Big\{\Big[f_1 g_0' + \frac{1}{2}(f_1 g_2' + 2f_2 g_1' + 2f_1' g_2 + f_2' g_1)\Big] k \cos kx \\ & \qquad + \frac{1}{2}\Big[f_1 g_2' + 2f_2 g_1' - 2f_1' g_2 - f_2' g_1\Big] k \cos 3kx\Big\} \end{cases} \tag{9.57}$$

Many of the inhomogeneous terms in (9.57) have the wavenumber k in the x-direction and are therefore resonant because the partial differential operators on the left hand side have eigensolutions with the same horizontal wavenumber. This means that (9.57) cannot be solved unless a solvability condition involving A, A_τ and Ra_2 can be found. In many problems, particularly those which are self-adjoint, it is usually quite straightforward to write down an integral solvability condition for this purpose. The present system is not self-adjoint, but it remains possible to obtain a solvability condition using numerical means. The manner in which we accomplished this may be found in the Appendix to this Chapter, and it means that the quantities $\mathrm{Ra}_2 A$, $A_{,\tau}$ and A^3 need to balance in such a way that they satisfy the Landau equation,

$$c_1 A_{,\tau} = \mathrm{Ra}_2 A - c_2 A^3, \tag{9.58}$$

where the values of c_1 and c_2 are obtained numerically. As a partial check on the accuracy of the present analysis, the value $G'(0) = 1/\pi$ in (9.43) and the 1/2 using for the definition of τ in (9.46) yield $c_1 = c_2 = 1$ when $\mathrm{Pe} = 0$, $k = \pi$ and $\mathrm{Ra} = 4\pi^2$, a result that may be shown analytically. The value, c_1, is found always to be positive; we shall not discuss its value but we note that it is related to the speed at which A varies and it may even be scaled out of Eq. (9.58) by a suitable redefinition of τ. Equation (9.58) admits the steady solutions $A = 0$ and $A = \pm\sqrt{\mathrm{Ra}_2/c_2}$. The former is a stable state when $\mathrm{Ra}_2 < 0$ and an unstable one when $\mathrm{Ra}_2 > 0$; these conclusions are consistent with the linear theory presented earlier. The nonzero solution exists when both Ra_2 and c_2 have the same sign. Therefore positive values of c_2 mean that nonzero solutions arise when $\mathrm{Ra}_2 > 0$ and therefore the onset of convection is supercritical in such cases. This property is shared with the Darcy-Bénard problem. On the other hand, negative values of c_2 means that steady nonzero solutions exist only when $\mathrm{Ra}_2 < 0$, and so the bifurcation is subcritical (see [87, p. 21]). It is already known that the onset of convection is subcritical for the Wooding problem, $\mathrm{Pe} \to \infty$ ([88]). Therefore the simplest *a priori* expectation is that the transition between a supercritical onset and a subcritical one will take place at an intermediate value of Pe, i.e. when

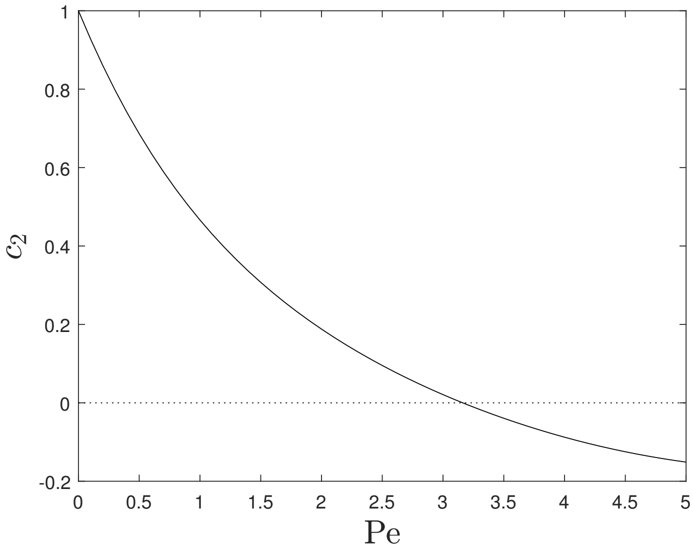

Figure 9.6: Variation of c_2 with Pe when $k = k_c(\mathrm{Pe})$.

the value of c_2 changes sign. The detailed dependence of c_2 on Pe is shown in Figure 9.6, where one may see that c_2 decreases from 1 as Pe increases from zero, and that it changes sign when Pe $= 3.1617$. So far, we have been considering the weakly nonlinear theory at the minimum in the neutral curves, i.e. when $\mathrm{Ra} = \mathrm{Ra}_c$ and $k = k_c$, and therefore Pe $= 3.1617$ marks the global transition between supercritical and subcritical onset subject to that restriction.

We shall now consider what happens at other points on the neutral curves by computing the variation of c_2 along each curve. Figure 9.7 shows a selection of neutral curves where those portions which correspond to a supercritical instability ($c_2 > 0$) are rendered in black, while those which are subcritical ($c_2 < 0$) are rendered in red. Also shown are the neutral pairs, (k_c, Ra_c), as the dotted line. In the figure there are two clear boundaries which demarkate the edge of the region of subcriticality at onset. For convenience, we shall refer to these as the left and right transitional loci.

Immediately, it is clear that all neutral curves, with the exception of when Pe $= 0$, have some portion which corresponds to subcritical instability. Whenever Pe < 3.1617 these sections of the neutral curve do not include the minimum. Therefore the onset of convection in an unbounded domain will be supercritical, but once Pe rises above 3.1617, onset of convection will be subcritical. Clearly, if the domain is bounded horizontally by insulated and impermeable boundaries, then the neutral values of Ra will correspond

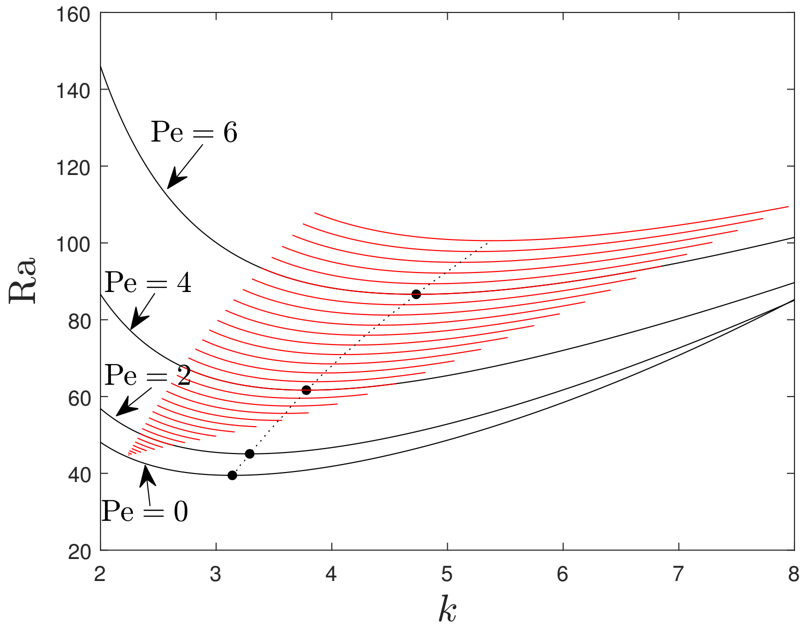

Figure 9.7: Region of subcritical instability as Pe increases.

to a set of discrete values of k. Then the issue of whether onset is supercritical or subcritical will depend on which value of the Rayleigh number is the smallest.

The right hand transitional locus corresponds to when $c_2 = 0$ and this represents a transition from subcriticality to supercriticality as k increases. However, the left hand transitional locus marks the value of k where c_2 has a simple pole. So as the locus is approached from the left $c_2 \to \infty$ but as it is approached from the right then $c_2 \to -\infty$. A detailed examination of the intermediate solutions in the above weakly nonlinear theory shows that the solutions for f_2 and g_2 in (9.54) become infinite in magnitude as this boundary is approached. This marks a new resonance but it is one which involves forcing terms with the wavenumber, $2k$. Indeed, this left hand boundary is precisely where $\mathrm{Ra}(k) = \mathrm{Ra}(2k)$ which is the source of the resonance. Our conclusion for now is that the Landau equation given above is inadequate in this isolated case and the nonlinear dynamics close to onset will involve both wavenumbers as competing solutions. Finally, we note that the left and right transitional loci merge when $\mathrm{Pe} = 0$ which is where we recover the Darcy-Bénard problem. In this case there is no resonance at all because the inhomogeneous terms in (9.54) have an odd symmetry about $z = \frac{1}{2}$ whereas the $O(\epsilon)$ eigensolutions are even. However, it is our intention in a subsequent and future work to break this symmetry weakly by allowing $\mathrm{Pe} = O(\epsilon)$ in magnitude; such a device will relegate the problematical resonance mentioned in the previous paragraph to the $O(\epsilon^3)$ equations and therefore it will be possible to obtain a pair of coupled Landau equations for the amplitudes of the k-mode and the $2k$-mode.

9.5 Main results and future perspective

We studied the onset of convection in a fluid-saturated horizontal porous layer heated from below and under the action of a uniform vertical throughflow. A linear instability analysis has been provided in order to set the context for the subsequent weakly nonlinear analysis and the principle of exchange of stabilities has been proved, hence the instability threshold for the onset of steady convection has been analysed. The main aim of the weakly nonlinear analysis was to establish whether or not the onset of convection is supercritical in all cases and, if not, to determine those circumstances when subcriticality may be expected. Figure 9.7 gives the locus within which the onset of convection is subcritical. We found that the onset of convection at the critical values will always be subcritical once the Péclet number exceeds 3.1617, but that a subcritical onset always arises when $\mathrm{Pe} \neq 0$ but only over ranges of wavenumber that do not contain the critical value.
We have already mentioned one possible extention to the present work where we will consider what happens when $\mathrm{Pe} = O(\epsilon)$.
Another study which will supplement the present work involves undertaking strongly nonlinear computations, one aim for which will be to determine the depth of subcriticality of convective motion. This will enable us to provide a nonlinear stability curves to supplement the present linear stability curves and to compare with energy-based methods. Such an analysis already exists for the Wooding problem in [88] where that author found that nonlinear onset takes place when,

$$\mathrm{Ra}_w = 11.6132 \quad \text{and} \quad k_w = 0.2867, \tag{9.59}$$

which should be compared with the values given in (9.44).

Appendix

Since (9.58) holds also for the stationary case, we can suppress the time derivative term A_τ in system (9.57), obtaining

$$\begin{cases} \mathcal{L}_1(\psi_3,\theta_3) = & -\mathrm{Ra}_2 A k g_1 \sin kx, \\ \mathcal{L}_2(\psi_3,\theta_3) = A^3\Big\{ \Big[f_1 g_0' + \frac{1}{2}(f_1 g_2' + 2 f_2 g_1' + 2 f_1' g_2 + f_2' g_1) \Big] k \cos kx \\ \qquad\qquad + \frac{1}{2}\Big[f_1 g_2' + 2 f_2 g_1' - 2 f_1' g_2 - f_2' g_1 \Big] k \cos 3kx \Big\} \end{cases} \tag{9.60}$$

The resulting system (9.60) admits the following solution

$$\psi_3 = A^3\ f_3(z) \sin kx, \qquad \theta_3 = A^3\ g_3(z) \cos kx, \tag{9.61}$$

Hence, substituting solution (9.61) in (9.60) and dividing both sides of the equations by A^3, we get

$$\begin{cases} f_3'' - k^2 f_3 + \mathrm{Ra}_0 k g_3 = & -\left(\dfrac{\mathrm{Ra}_2}{A^2}\right) k g_1 \sin kx, \\ g_3'' - k^2 g_3 + \mathrm{Pe} g_3' - g'(z) k f_3 = \Big[f_1 g_0' + \frac{1}{2}(f_1 g_2' + 2 f_2 g_1' + 2 f_1' g_2 + f_2' g_1) \Big] k \cos kx \\ \qquad\qquad + \frac{1}{2}\Big[f_1 g_2' + 2 f_2 g_1' - 2 f_1' g_2 - f_2' g_1 \Big] k \cos 3kx \end{cases} \tag{9.62}$$

We then solved system (9.62) as an eigenvalue problem for Ra_2/A^2 from which, and given the form of (9.58), we may now say that

$$c_2 = \frac{\mathrm{Ra}_2}{A^2}. \tag{9.63}$$

A similar device was used to compute c_1.

Conclusions

The onset of convection has been considerably investigated since convective flows are recognised as one of the most prevalent fluid motions in nature, and the mathematical model describing the onset of buoyancy-driven thermal convection is recognised as a powerful tool to model and design man-made materials and engineered systems. In this doctoral thesis, *new stability results* related to the onset of convection in *porous layers* are collected. The focus of the majority of this thesis is on bi-disperse convection, since the mathematical models for *dual porosity materials* are efficient for thermal management problems and to describe the behaviour of high porosity metallic foams, ceramics, engineered tissues, tumors, fractured porous media.
To better model the above materials, we studied *anisotropic* dual porosity materials, finding that anisotropic permeabilities have a remarkable effect on the type of arising convective cells: when a fully anisotropic material is considered, the fluid organizes itself into rolls in the horizontal directions, in particular, for increasing rotation rates of the layer and for increasing values of the anisotropic parameters, we found a transition from convection patterns as rolls along the y-axis (the convective fluid motion occurs in the x and z directions) to rolls in the x-direction (the convective fluid motion occurs in the y and z directions).

Regarding *rotating* layers of bi-disperse porous media, through linear instability and nonlinear stability analyses of the conduction solution, we found a confirmation that the critical Rayleigh number Ra is an increasing function of the Taylor number $\mathcal{T}$ (the dimensionless representation of rotation rates, so it describes Coriolis and centrifugal effects on the onset of convection): rotation has a stabilizing effect on the onset of convection, i.e. increasing rotation rates act to stop the convective heat transfer and delay the onset of convective fluid motion. Besides, when a single component fluid saturating an anisotropic bi-disperse porous rotating layer is considered, we achieved an optimal stability result: the linear instability threshold and the nonlinear stability one coincide, so the linear theory completely captures the onset of convective fluid motions.

Moreover, we found that when dealing with a rotating anisotropic bi-disperse porous medium, convection can arise only as a steady secondary motion, *but* when *inertia effects* are considered too, the convective patterns can eventually set in through oscillatory motions with a definite frequency, meaning that the amplitude of a generic perturbation grows periodically.

As regards *double-diffusive convection* in a rotating bi-disperse porous layer, we considered a binary fluid mixture, i.e. a salt is dissolved at the bottom of the bi-disperse porous layer, this means that there are simultaneous mass and thermal diffusions. Unlike the diffusion of heat, the diffusion of salt can take place only through the fluid phase, so an additional physical effect has to be considered: the Soret effect, that is the mass flux created by a temperature gradient. Later, to further improve the results we found related to rotating anisotropic bi-disperse porous layers, and to further investigate double-diffusive convection, we considered also an anisotropic Brinkman bi-disperse porous medium saturated by a binary fluid mixture.
We found that when a fluid mixture is considered, convection can arise via stationary or oscillatory motions, since the principle of exchange of stabilities holds only under appropriate assumptions on the physical parameters of the problem (i.e. $\epsilon_1 Le \leq 1$). While heating from below has a destabilizing effect on the stability of the thermosolutal conduction solution, we confirmed that rotation and the solute dissolved from below have a stabilizing effect on the onset of convective flows, meaning that the critical steady and oscillatory Rayleigh numbers (Ra_S and Ra_O) are increasing function with respect to the Taylor number $\mathcal{T}$ and the concentration Rayleigh number $\mathcal{C}$.
Moreover, in the isotropic case, we performed a nonlinear stability analysis of thermosolutal conduction solution and we found a *region of subcritical instabilities*, since the linear instability threshold and the global nonlinear stability threshold do not coincide. However, for the Soret number $\mathcal{S}$ that goes to 1, the coincidence between the stationary threshold and the global nonlinear threshold is achieved, even though the dependence of the instability thresholds on the concentration field gets lost. Also, the nonlinear stability threshold Ra_E coincides with the stability threshold obtained when the Soret effect is not taken into account, therefore, if $\mathrm{Ra} < \mathrm{Ra}_E$, the thermal conduction solution is unconditionally stable, regardless of what value $\mathcal{C}$ has and no matter of whether the Soret effect is taken into account or not, hence, the global nonlinear stability threshold is affected only by rotation and the stabilizing effect of the concentration gradient on the onset of convection is not achieved.

We found a *region of subcritical instabilities* also for the Sutton Problem. We considered an horizontal layer of fluid-saturated porous medium bounded by permeable boundaries, and injection of fluid on the top and removal at

the bottom take place, so the layer is subject to a constant downward vertical *throughflow*. The dynamic of the dimensionless system depends on the Péclet number Pe, a non-dimensional number directly proportional to the strength of the throughflow. Via linear instability analysis of the throughflow solution, we proved that the critical Rayleigh number is an increasing function of Pe, so the downward net mass flow has a stabilizing effect on the onset of convection, i.e. the throughflow acts to delay the onset of convective instabilities. Furthermore, we found that the Sutton Problem is a transitioning problem between the Darcy-Bénard Problem and the Wooding Problem: as the Péclet number goes to zero, the problem reduces to the Darcy-Bénard problem — whose convective instabilities are well known to be supercritical — while for very large Péclet number, the problem reduces to the Wooding problem — for which the onset of instability is subcritical. As the Péclet number increases, the temperature field is confined to a region of thickness $O(\mathrm{Pe}^{-1})$ close to the bottom surface, so most of the layer is uniformly cold apart from the thermal boundary layer at the bottom, i.e. for high Pe the flow and temperature fields are essentially detached from the upper surface and the layer appears to mimic a region of infinite height.
Therefore, with the aim of determine for which value of the Péclet number this transition happens, we performed a weakly nonlinear stability analysis of the basic throughflow solution and determined a critical value of Pe beyond which the onset of convection is no longer supercritical.

Finally, the onset of convection in an horizontal layer of porous medium heated from below saturated by an extended-quasi-thermal-incompressible fluid was investigated, with the aim of analysing the thermodynamic consistency of the Oberbeck-Boussinesq approximation and to obtain more thermodynamic consistent stability results. Revising the Oberbeck-Boussinesq approximation, we employed a modified constitutive equation for the fluid density in body force term due to gravity, allowing the fluid to be slightly compressible: the fluid density is assumed as a function of the temperature field and the pressure field. Via the linear instability analysis of the thermal conduction solution, we rigorously determined in closed algebraic form the critical Rayleigh number Ra_L and analysed its behaviour with respect to dimensionless parameter $\widehat{\beta}$ directly proportional to the compressibility factor $\widehat{\beta}$: we proved that Ra_L is a decreasing function with respect to $\widehat{\beta}$, i.e. allowing the fluid to be slightly compressible, the onset of convection is enhanced.

List of Figures

List of Tables

Bibliography

[1] D.A. Nield and A. Bejan. Convection in Porous Media. *5th edn. New York, NY: Springer*, 2017.

[2] B. Straughan. Stability and wave motion in porous media. *Applied Mathematical Sciences, Springer, Cham, Switzerland*, 165, 2008.

[3] A.J. Badday and A.J. Harfash. Chemical reaction effect on convection in bidispersive porous medium. *Transp. Porous Media*, 137:381–397, 2020.

[4] D.A. Nield and A.V. Kuznetsov. The onset of convection in a bidisperse porous medium. *Int. J. Heat Mass Transf.*, 49(17-18):3068–3074, 2006.

[5] J.N. Flavin and S. Rionero. *Qualitative estimates for partial differential equations: an introduction.* CRC Press, Boca Raton, Florida, 1996.

[6] Hadamard J. *Lectures on Cauchy's Problem in linear P.D.E.* 1952.

[7] G.P. Galdi and B. Straughan. Exchange of stabilities, symmetry, and nonlinear stability. *Archive for rational mechanics and analysis*, 89(3):211–228, 1985.

[8] B. Straughan. *The energy method, stability, and nonlinear convection*, volume 91. Springer Science Business Media, 2013.

[9] S.H. Davis. On the principle of exchange of stabilities. *Proc. Roy. Soc. A.*, 310:341–358, 1969.

[10] S. Chandrasekhar. Hydrodynamic and hydromagnetic stability. *Dover Publicationas*, 1981.

[11] H. Bénard. Les tourbillon cellulaires dans une nappe liquide. *Revue Gan. Sci. Pur. Appl.*, 11:1261–1271, 1900.

[12] J.W. (Lord Rayleigh) Strutt. On convection currents in a horizontal layer of fluid, when the higher temperature is on the under side. *Philos. Mag.*, 32:529–546, 1916.

[13] C.W. Horton and F.T. Rogers. Convection currents in a porous medium. *J. Appl. Physics*, 16:367–370, 1945.

[14] E.R. Lapwood. Convection of a fluid in a porous medium. *Math. Proc. Camb. Philos. Soc.*, 44:508–521, 1948.

[15] Z.Q. Chen, P. Cheng, and C.T. Hsu. A theoretical and experimental study on stagnant thermal conductivity of bidispersed porous media. *Int. Comm. Heat Mass Transf.*, 27:601–610, 2000.

[16] B. Straughan. Mathematical aspects of multi–porosity continua. *Springer, Cham, Switzerland*, 2017.

[17] D.A. Nield and A.V. Kuznetsov. A two-velocity temperature model for a bi-dispersed porous medium: forced convection in a channel. *Trans. Porous Media*, 59:325–339, 2005.

[18] D.A. Nield and A.V. Kuznetsov. Heat transfer in bidisperse porous media. *Transport Phenomena in Porous Media III*, pages 34–59, 2005.

[19] G. Imani and K. Hooman. Lattice Boltzmann pore scale simulation of natural convection in a differentially heated enclosure filled with a detached or attached bidisperse porous medium. *Trans. Porous Media*, 116:91–113, 2017.

[20] M. Gentile and B. Straughan. Bidispersive thermal convection with relatively large macropores. *J. Fluid Mech.*, 898, 2020.

[21] F. Capone, R. De Luca, and M. Gentile. Coriolis effect on thermal convection in a rotating bidisperive porous layer. *Proc. R. Soc. A.*, 47620190875, 2020.

[22] F. Capone, R. De Luca, and M. Gentile. Thermal convection in rotating anisotropic bidispersive porous layers. *Mech. Res. Comm.*, page 036106, 2020.

[23] F. Capone and R. De Luca. The effect of the Vadasz number on the onset of thermal convection in rotating bidispersive porous media. *Fluids*, 5(4):173, 2020.

[24] M. Gentile and B. Straughan. Bidispersive vertical convection. *Proc. R. Soc. A.47320170481*, 2017.

[25] M. Gentile and B. Straughan. Bidispersive thermal convection. *Int. J. Heat Mass Transf.*, 114:837–840, 2017.

[26] P. Falsaperla, G. Mulone, and B. Straughan. Bidispersive-inclined convection. *Proc. Roy. Soc. A*, 472(2192):20160480, 2016.

[27] K.N. Moutsopoulos and D.L. Koch. Hydrodynamic and boundary-layer dispersion in bidisperse porous media. *J. Fluid Mech.*, 385:359–379, 1999.

[28] B. Straughan. Convection with local thermal non-equilibrium and microfluidic effects. *Adv Mechanics and Matematics, Springer, Cham, Switzerland*, 32, 2015.

[29] P. Vadasz. Flow and thermal convection in rotating porous media. *Handbook of porous media*, pages 395–440, 2000.

[30] P. Vadasz. Coriolis effect on gravity-driven convection in a rotating porous layer heated from below. *J. Fluid Mech.*, 376:351–375, 1998.

[31] P. Vadasz. Instability and convection in rotating porous media: a review. *Fluids*, 4:1–31, 2019.

[32] P. Vadasz. Fluid flow and heat transfer in rotating porous media. *Springer Brief Thermal Engineering and Applied Sciences (eBook)*, 2016.

[33] F. Capone and R. De Luca. Ultimately boundedness and stability of triply diffusive mixtures in rotating porous layers under the action of Brinkman law. *Int. J. Non-Lin. Mech.*, 47(7):799–805, 2012.

[34] R. De Luca and S. Rionero. Steady and oscillatory convection in rotating fluid layers heated and salted from below. *Int. J. Non-Lin. Mech.*, 78:121–130, 2016.

[35] B. Straughan. Anisotropic bidispersive convection. *Proc. R. Soc. A.*, 475:20190206, 2019.

[36] B. Straughan. Horizontally isotropic double porosity convection. *Proc. R. Soc. A.*, 475:20180672, 2019.

[37] H. Li, H. Guo, Z. Yang, H. Ren, L. Meng, H. Lu, H. Xu, Y. Sun, T. Gao, and H. Zhang. Evaluation of oil production potential in fractured porous media. *Phys. Fluids*, 31:052104, 2019.

[38] F. Capone and M. Gentile. Sharp stability results in LTNE rotating anisotropic porous layer. *Int. J. Therm. Sci.*, 134:661–664, 2018.

[39] O. Kvernvold and P.A. Tyvand. Nonlinear thermal convection in anisotropic porous media. *J. Fluid Mech.*, 90(4):609–624, 1979.

[40] D.A. Nield and A.V. Kuznetsov. The effects of combined horizontal and vertical heterogeneity on the onset of convection in a porous medium with vertical throughflow. *Transp. Porous Media*, 90:465, 2011.

[41] F. Capone, R. De Luca, and G. Massa. Effect of anisotropy on the onset of convection in rotating bi-disperse Brinkman porous media. *Acta Mech.*, 2021.

[42] A.A. Hill. A differential constraint approach to obtain global stability for radiation-induced double-diffusive convection in a porous medium. *Math. Meth. Appl. Sci.*, 32(8):914–921, 2009.

[43] B. Straughan. Global nonlinear stability in porous convection with a thermal non-equilibrium model. *Proc. R. Soc. A.*, 462:409–418, 2006.

[44] F. Capone and S. Rionero. Inertia effect on the onset of convection in rotating porous layers via the "auxiliary system method". *Int. J. Non-Lin. Mech.*, 57:192–200, 2013.

[45] F. Capone and R. De Luca. Porous MHD Convection: Effect of Vadasz inertia term. *Transp. Porous Med.*, 118(3):519–536, 2017.

[46] F. Capone, R. De Luca, and M. Vitiello. Double-diffusive Soret convection phenomenon in porous media: effect of Vadasz inertia term. *Ric. Mat.*, 68(2):581–595, 2019.

[47] B. Straughan. Effect of inertia on double diffusive bidispersive convection. *Int. J. Heat Mass Transf.*, 129:389–396, 2019.

[48] F. Capone and G. Massa. The effects of Vadasz term, anisotropy and rotation on bi-disperse convection. *Int. J. Non-Lin. Mech.*, 135:103749, 2021.

[49] B. Straughan. Bidispersive double diffusive convection. *Int. J. of Heat Mass Transf.*, 126(A):504–508, 2018.

[50] F. Capone, M. Gentile, and G. Massa. The onset of thermal convection in anisotropic and rotating bidisperse porous media. *Z. Angew. Math. Phys.*, 72:169, 2021.

[51] F. Capone, M. Gentile, and A.A. Hill. Double-diffusive penetrative convection simulated via internal heating in an anisotropic porous layer with throughflow. *Int. J. Heat Mass Transf.*, 54(7-8):1622–1626, 2011.

[52] F. Capone and R. De Luca. On the stability-instability of vertical throughflows in double diffusive mixtures saturating rotating porous layers with large pores. *Ric. Mat.*, 63(1):119–148, 2014.

[53] M.S. Malashetty, M.S. Swamy, and W. Sidram. Double diffusive convection in a rotating anisotropic porous layer saturated with viscoelastic fluid. *Int. J. Therm. Sci.*, 50(9):1757–1769, 2011.

[54] H.A. Challoob, A.J. Harfash, and A.J. Harfash. Bidispersive double diffusive convection with relatively large macropores and generalized boundary conditions. *Phys. Fluids*, 33, 2021.

[55] A.J. Badday and A.J. Harfash. Double-diffusive convection in bidispersive porous medium with chemical reaction and magnetic field effects. *Transp. Porous Media*, 139:45–66, 2021.

[56] D.A. Nield and C.T. Simmons. A brief introduction to convection in porous media. *Transp. Porous Media*, 130:237–250, 2019.

[57] M. Eslamian. Advances in thermodiffusion and thermophoresis (Soret effect) in liquid mixtures. *Front. Heat Mass Transf.*, 2(4), 2011.

[58] F. Capone, R. De Luca, and G. Massa. The onset of double diffusive convection in a rotating bi-disperse porous medium. *The European Physical Journal Plus*, 137(9):1–16, 2022.

[59] B. Straughan. Horizontally isotropic bidispersive thermal convection. *Proc. R. Soc. A*, 474:20180018, 2018.

[60] F. Capone, R. De Luca, and G. Massa. The combined effects of rotation and anisotropy on double diffusive bi-disperse convection. *ArXiv*, 2022.

[61] H. Gouin and T. Ruggeri. A consistent thermodynamical model of incompressible media as limit case of quasi-thermal-incompressible materials. *International Journal of Non-Linear Mechanics*, 47(6):688–693, 2012.

[62] T. Ruggeri and M. Sugiyama. *Classical and relativistic rational extended thermodynamics of gases*, volume 197. Springer, 2021.

[63] I. Müller. *Thermodynamics*. Pitman-London, 1985.

[64] H. Gouin, A. Muracchini, and T. Ruggeri. On the Müller paradox for thermal-incompressible media. *Continuum Mechanics and Thermodynamics*, 24(4):505–513, 2012.

[65] A. Oberbeck. Über die wärmeleitung der flüssigkeiten bei berücksichtigung der strömungen infolge von temperaturdifferenzen. *Annalen der Physik*, 243(6):271–292, 1879.

[66] Joseph Boussinesq. Thérie analytique de la chaleur. 2, 1879.

[67] D. R. Lide, editor. *Handbook of Chemistry and Physics.* CRC Press, 2005.

[68] D. R. Lide. *Handbook of Chemistry and Physics.* CRC Press, 2005.

[69] A. Passerini and T. Ruggeri. The Bénard problem for quasi-thermal-incompressible materials: A linear analysis. *International Journal of Non-Linear Mechanics*, 67:178—-185, 2014.

[70] Giuseppe Arnone, Florinda Capone, Roberta De Luca, and Giuliana Massa. Compressibility effect on Darcy porous convection. *arXiv preprint arXiv:2210.08075*, 2022.

[71] A. Corli and A. Passerini. The bénard problem for slightly compressible materials: Existence and linear instability. *Mediterranean Journal of Mathematics*, 16(1):1–24, 2019.

[72] D. Serre. *Matrices.* Springer, New York, 2010.

[73] I.S. Shivakumara. Boundary and inertia effects on convection in porous media with throughflow. *Acta Mech.*, 137:151–165, 1999.

[74] D. A. Nield. Throughflow effects in the Rayleigh-Bénard convective instability problem. *J. of Fluid Mech.*, 185:353–360, 1987.

[75] F.M. Sutton. Onset of convection in a porous channel with net through flow. *Physics of Fluids*, 13(8):1931, 1970.

[76] R.A. Wooding. Rayleigh instability of a thermal boundary layer in flow through a porous medium. *J. Fluid Mech.*, 9(2):183–192, 1960.

[77] G.J.M. Pieters and H.M. Schuttelaars. On the nonlinear dynamics of a saline boundary layer formed by throughflow near the surface of a porous medium. *Physica D: Nonlinear Phenomena*, 237(23):3075–3088, 2008.

[78] B. Florio. The interaction of convection modes in a box of a saturated porous medium. *Journal of Engineering Mathematics*, 86:71–88, 2014.

[79] D. A. S. Rees and A. P. Bassom. The onset of Darcy–Bénard convection in an inclined layer heated from below. *Acta Mech.*, 144:103–118, 2000.

[80] G. J. M. Pieters and C. J. Van Duijn. Transient growth in linearly stable gravity-driven flow in porous media. *European Journal of Mechanics-B/Fluids*, 25(1):83–94, 2006.

[81] D. A. S. Rees and A. Mojtabi. The effect of conducting boundaries on weakly nonlinear Darcy–Bénard convection. *Transp. Porous Media*, 88(1):45–63, 2011.

[82] D. A. S. Rees and A. Barletta. Three-dimensional convective planforms for inclined Darcy–Bénard convection. *Fluids*, 5(2):83, 2020.

[83] N. Banu and D. A. S. Rees. Onset of Darcy–Bénard convection using a thermal non-equilibrium model. *Int. J. Heat Mass Transf.*, 45:2221–2228, 2002.

[84] D. A. S. Rees and A. P. Bassom. The inclined Wooding problem. *Transp. Porous Media*, 125:465–482, 2018.

[85] E. Palm, J. E. Weber, and O. Kvernold. On steady convection in a porous medium. *J. of Fluid Mech.*, 54:153–161, 1972.

[86] B. Bidin and D. A. S. Rees. Pattern selection for Darcy–Bénard convection with local thermal nonequilibrium. *Int. J. of Heat and Mass Transf.*, 153:119539, 2020.

[87] P.G. Drazin. *Introduction to Hydrodynamic Stability*. Cambridge University Press, 2002.

[88] D. A. S. Rees. The onset and nonlinear development of vortex instabilities in a horizontal forced convection boundary layer with uniform surface suction. *Transp. Porous Media*, 77:243–265, 2009.